Neurotoxicity of Acute Intoxication with the Chemical Threat Agent Diisopropylfluorophosphate (DFP) in the Adult and Juvenile Rat Brain

By

EDUARDO AZTLÁN GONZÁLEZ
DISSERTATION

Submitted in partial satisfaction of the requirements for the degree of

DOCTOR OF PHILOSOPHY

In

PHARMACOLOGY AND TOXICOLOGY

In the

OFFICE OF GRADUATE STUDIES

Of the

UNIVERSITY OF CALIFORNIA, DAVIS

Approved:

_____
Dr. Pamela Lein, Chair

_____
Dr. Heike Wulff

_____
Dr. Jill Silverman

_____
Dr. Gene Gurkoff

Committee in Charge
2021

Dedicado a:
Gregoria y Santiago
Olimpia y Francisco
Rosa y Arturo

A mis abuelos y padres, este logro es para ustedes.

Neurotoxicity of Acute Intoxication with the Chemical Threat Agent Diisopropylfluorophosphate (DFP) in the Adult and Juvenile Rat Brain

Abstract

Organophosphate cholinesterase inhibitors (OPs) are a class of neurotoxic chemicals that have been used globally as both pesticides and chemical warfare agents. Most recently, OPs have been used during the Syrian civil war, a political assassination in Asia, and terrorist attacks in Europe. Survivors of high-dose acute OP intoxication can experience convulsions, prolonged seizures, or death if not treated within minutes of exposure. During the months or years that follow, humans who survive acute OP intoxication often experience significant changes in brain structure, general cognition, memory, or electrographic activity. Even those who received standard of care treatment with atropine, oximes, and benzodiazepines may experience chronic neurological deficits or electrographic abnormalities. For this reason, there is an urgent need for more efficacious therapeutics to combat acute OP poisoning. To develop more effective therapeutic strategies, it is critical to better understand how acute OP intoxication impacts the brain and the reasons for the limitations of the current standard of care. A critical question in the field is whether seizure-independent mechanisms contribute to long-term neurological damage following acute OP intoxication, and if so, which mechanisms play a role. Additionally, very few studies have examined the influence of sex and age on the chronic neurological impacts of acute OP intoxication.

This dissertation seeks to address these data gaps using a rat model of acute intoxication with OP threat agent diisopropylfluorophosphate (DFP) as a model. Chapter 2 demonstrates that the current standard of care reduced seizure activity but offered only partial neuroprotection at 3 and 6 months post-intoxication, and failed to protect against chronic microglial activation and midbrain mineralization. Studies described in Chapter 3 leveraged a seizure-resistant subset of rats acutely intoxicated with DFP to determine whether DFP induced neurological damage independent of seizure activity. Seizure-resistant animals showed pronounced neuronal degeneration and mineralization, although these outcomes were not as severe or as persistent as in those animals who experienced seizures. Chapter 5 describes the

development of a juvenile rat model of acute DFP intoxication that addressed potential sex differences and better reflected the diversity of individuals potentially affected by OP intoxication. Juvenile males had more severe seizures, astrogliosis, and aberrant neurogenesis compared to juvenile females, but both sexes experienced persistent microglial activation and cognitive deficits following DFP intoxication. This model also suggested that juveniles were generally more resistant to OP-induced seizures and experienced a later onset of neuroinflammation compared to their adult counterparts.

These findings have important implications for the development of medical countermeasures against OP threat agents. The observation that both benzodiazepine-treated and seizure-resistant animals experienced chronic neuronal degeneration despite having little to no seizure activity suggests that seizure-independent mechanisms contribute to the long-term neurological effects of acute OP intoxication. My findings also suggest that both age and sex are biological variables that influenced OP-induced neurotoxicity, and should, therefore, be important considerations in preclinical assessment of toxicity and therapeutic efficacy. Lastly, the temporal patterns of microglial activation in juvenile animals, as well as the persistence of microglial activation despite antiseizure treatment, point to microglial-mediated neuroinflammation as a likely factor contributing to long-term neurological consequences following acute OP intoxication.

Acknowledgments

To my mentors and colleagues:

Pam, it goes without saying that I could not have completed this milestone without your guidance. Your research skills and relentless pursuit of knowledge are commendable, and I thank you for the important role you played in my growth as a scientist. I have many great memories from my years in the Lein lab, and I will always appreciate your generosity in sharing quality wine and Trader Joe's dark chocolate peanut butter cups with us all. To my other faculty mentors at UC Davis, including Heike Wulff, Jill Silverman, Gene Gurkoff, Danielle Harvey, Michele La Merrill, and Gary Cherr, I am grateful for your mentorship over the years and thank each of you for helping me become a more thoughtful researcher.

I could not have completed this degree without the support of the Lein lab and PTX program. I especially thank all of my co-authors who assisted me with my dissertation work. To the friends I've made in the lab, thank you for the camaraderie, procedure room hangouts, and afternoon drinks that helped me get through long days. I also thank my funding sources, including David Jett and the NINDS, the ARCS Foundation, and the NIH IMSD program, for supporting me throughout graduate school.

This section would not be complete without acknowledging the teachers who made my education enjoyable and instilled in me a desire to learn. In particular, I'd like to thank Ms. Abramson, Mr. Warren, Mr. Spalding, Ms. Solis, Mr. Zappa, and Profesora Dickenson. Without your dedication and patience, I would unlikely be at this point in my education.

To my family and friends:

It's difficult to overstate the role of my parents in my educational journey. To my parents, I'm not sure I will ever be able to thank you enough for your unconditional support. This accomplishment is, without a doubt, dedicated to you and my grandparents. I promise to pay it forward and always remember the sacrifices you made for our family to have these opportunities.

To my siblings and cousins, I have relied on many of you more than you know throughout this process, and I am grateful to have so many people supporting me. Whether it was an intense game night, a trip to Europe, or simply catching up over burritos, you've all helped me recharge and stay grounded. I must give a special shoutout to my sister Cassandra, who is consistently my #1 fan.

To my partner Jonathan, and the best-cats-ever Bella and Sammi, I can't thank you enough for providing the perfect place to come home to every day. Chico, I will always appreciate how fiercely you believe in me. You always know when I need a break, and there is no question that your support helped me get through this program. To Bella and Sammi…*boop*.

Lastly, I must acknowledge the entertainment that kept me smiling throughout graduate school. I thank Stan Lee and the Marvel Cinematic Universe for gifting us the Avengers films, Wanda Maximoff, and short-haired Thor. I also thank the cast of Schitt's Creek, as well as RuPaul and her fierce army of drag queens, for creating such enjoyable content for my friends and I to watch after a long week.

Table of Contents

Chapter 1

Introduction

Based in part on a submission to *Chemical Research in Toxicology* with the following title and authors:

Pathogenic Mechanisms Contributing to the Neurological Damage Associated with Status Epilepticus Triggered by Chemical Threat Agents

Eduardo A. González[*a], Jonas J. Calsbeek[*a], Peter Andrew[a], Jason W. Loxterkamp[a], Dennis R. Carty[a], and Pamela J. Lein[a]

[a]Department of Molecular Biosciences, University of California, Davis, School of Veterinary Medicine, 1089 Veterinary Medicine Drive, Davis, CA 95616, United States

*These authors contributed equally to this manuscript.

Overview of Chemical Threat Agents

Organophosphorus cholinesterase inhibitors (OPs) are used globally as pesticides and are known to cause hundreds of thousands of deaths each year as a result of accidental and intentional poisonings (Eddleston, Buckley et al. 2008, Pereira, Aracava et al. 2014). In addition, OPs have been used as chemical warfare agents, as recently as the 2013 and 2017 chemical attacks in Syria (Vogel 2013, UN 2017), as well as the 2020 chemical attack on a Russian opposition leader (OPCW 2020). It is for these reasons that a number of OPs are listed by the United States Department of Homeland Security as credible chemical threat agents. OP warfare agents are a potent class of OPs that were developed as chemical weapons and have been used by terrorists against civilian populations (Jett and Yeung 2010). They are broadly categorized as G-agents (soman, sarin, tabun, cyclosarin) or V-agents (VX, VE, VG, VM). G-agents are highly volatile and relatively nonpersistent in the environment, while V-agents have low volatility and are highly persistent (Vucinic, Antonijevic et al. 2017). The newly developed novichok agents exhibit volatility and environmental persistence intermediate of G and V agents. Among the OP warfare agents, soman and sarin (**Figure 1-1**) represent two of the most commonly researched chemicals.

Historically, OP warfare agents were the primary class of compounds researched in acute toxicity studies; however, growing interest in the field caused several academic labs to begin similar studies using OP pesticides as surrogate compounds due to the increased safety when testing these compounds in the laboratory environment. There is also extensive literature on acute intoxication with OP pesticides due to accidental exposure or suicide, and these chemicals are now considered credible chemical threat agents (reviewed in Richardson, Fitsanakis et al. 2019). Preclinical models of acute OP pesticide intoxication have been developed using OP

pesticides such as diisopropylfluorophosphate (DFP) or paraoxon (POX), among others, (**Figure 1-1**). These chemicals have been shown to produce comparable behavioral and pathological phenotypes as warfare agents in models of acute intoxication and can be used as a rigorous platform for testing potential therapeutics (Pereira, Aracava et al. 2014).

OP threat agents can trigger convulsions that progress to life threatening *status epilepticus* (SE), a clinical diagnosis characterized by sustained seizure activity (Williamson, Singh et al. 2019). Human survivors of acute OP intoxication present with a variety of neurological dysfunctions ranging from mild to severe decline in memory, affective disorders and chronic epilepsy (Chen, Garcia et al. 2014, Figueiredo, Apland et al. 2018, Jett, Sibrizzi et al. 2020). Preclinical animal models have replicated these findings and demonstrated similar neurological deficits following acute OP intoxication, including electrographic abnormalities, structural brain damage, and cognitive deficits (Guignet and Lein 2019). If treatment of intoxicated individuals is not administered within minutes to hours following intoxication, it is difficult to prevent the initiation of SE or additional pathogenic mechanisms that may result in progressive neurological damage (Jett and Spriggs 2018).

Organophosphate Toxicity and Treatment Challenges

OPs induce seizure activity via inhibition of AChE (Richardson, Fitsanakis et al. 2019), the enzyme that functions to terminate cholinergic transmission by hydrolyzing the excitatory neurotransmitter acetylcholine (ACh; **Figure 1-2**). OPs bind to the serine residue on the active site of AChE to form a covalent bond that is initially reversible. However, a spontaneous hydrolysis reaction occurs and forces a redistribution of electrons that strengthens the covalent bond, causing it to become irreversible (Pope and Brimijoin 2018). The OP-AChE conjugate

then becomes refractory to therapeutic reactivation, making OP intoxication especially difficult to treat (Quinn, Topczewski et al. 2017). This biochemical process is referred to as "aging" and can occur within minutes to hours depending on the OP. As a result of AChE inhibition, ACh accumulates in the synaptic cleft causing excessive cholinergic neurotransmission throughout the central and peripheral nervous systems.

AChE inhibition leads to a physiological cascade often referred to as cholinergic crisis (Williamson, Singh et al. 2019). In the autonomic nervous system, AChE inhibition results in overstimulation of nicotinic and muscarinic cholinergic receptors that function to maintain the body's unconscious physiological processes. This can cause what is clinically referred to as SLUD (salivation, lacrimation, urination, and defecation), muscle weakness, respiratory distress, and bradycardia (Richardson, Fitsanakis et al. 2019). Unregulated ACh also overstimulates cholinergic neurons that innervate skeletal muscle in the somatic nervous system, leading to muscle fasciculations and convulsions (Pereira, Aracava et al. 2014). In the central nervous system (CNS), the buildup of ACh has severe adverse effects on neuronal excitability and signaling, including the downstream release of glutamate, the primary excitatory neurotransmitter in the CNS (Myhrer 2007). This relationship primarily exists in the midbrain, where cholinergic axon terminals can directly innervate glutamatergic neurons (Shin, Adrover et al. 2015). This subset of glutamatergic neurons expresses muscarinic receptors that are sensitive to minor changes in ACh levels, which can result in excessive glutamate release (Shin, Adrover et al. 2015). Severe seizures can be triggered by the overabundance of excitatory neurotransmission in the CNS that progress to SE. This cascade can result in neurological effects that remain active even following detoxification of the compound, further complicating treatment strategies (Tonduli, Testylier et al. 2001).

Current medical countermeasures against acute OP intoxication include a muscarinic receptor antagonist (usually atropine) combined with an oxime reactivator of OP-inhibited cholinesterase, such as pralidoxime chloride (2-PAM). Treatment with atropine and 2-PAM can significantly increase the survival of experimental animals exposed to multiple LD_{50} doses of OP nerve agents. However, the combined treatment regimen does not protect against OP-induced centrally mediated seizure activity (Gordon, Leadbeater et al. 1978, Dirnhuber, French et al. 1979) and is only effective immediately following OP intoxication, especially in the case of nerve agents (Amend, Niessen et al. 2020). Seizures rapidly progress to SE, leading to profound brain damage (Lemercier, Carpentier et al. 1983, McLeod, Singer et al. 1984, McDonough, Jaax et al. 1989). Therefore, concurrent administration of an antiseizure agent is typically used to stop the seizures and attempt to protect the brain against damage. Benzodiazepines (diazepam and midazolam) are the first-line antiseizure treatment for use following chemical-induced seizures (Marrs 2003). In the United States, diazepam has been recently replaced by midazolam as the preferred first line treatment administration (FDA 2018).

Although benzodiazepines may stop OP-induced seizures when administered early after exposure, they are less effective when administered later, and even with early treatment, benzodiazepines are not effective in protecting against OP-induced neuropathology (McDonough, Zoeffel et al. 2000). The refractoriness to benzodiazepines is believed to result from rapid internalization of synaptic $GABA_A$ receptors (Walton and Treiman 1988, Kapur, Stringer et al. 1989), which are the therapeutic targets for these drugs. Moreover, even if $GABA_A$ receptors remain in the synapse, benzodiazepines, particularly at high doses, depress central respiratory drive (Forster, Gardaz et al. 1980) and can have adverse effects on blood pressure (Kitajima, Kanbayashi et al. 2004, Bruun, Cao et al. 2015). Because civilian treatment during a

mass casualty is likely to be delayed for hours (Jett 2016), these observations underscore the urgent need for improved countermeasures to protect the brain following acute intoxication with convulsant threat agents. A better understanding of the mechanisms underlying the progression of OP-induced neurological damage will shed light on therapeutic targets and treatment windows that may provide improved neuroprotection.

Role of Seizures in OP-Induced Neuropathology

Seizure activity is believed to be a primary contributor to OP-induced neuropathology (Figueiredo, Apland et al. 2018). A recent epidemiological study reported that humans exposed to OPs have a 3.57-fold higher risk of developing seizures throughout their lives compared to non-exposed individuals (Chuang, Yang et al. 2019). Antiseizure therapies have been tested for decades with the goal of ultimately mitigating downstream neurological consequences associated with OP intoxication. The cholinergic cascade initiated by AChE inhibition (**Figure 1-2**) presents various cellular and molecular targets to restore balance between excitatory and inhibitory neurotransmission. However, despite numerous efforts to mitigate neurological damage using antiseizure therapies, there are few, if any, studies that demonstrate complete neuroprotection against OPs using solely antiseizure therapeutics. This raises important questions of 1) exactly what role do seizures play in OP-induced neuropathology, and 2) if non-seizure mechanisms are contributing, what might those mechanisms be?

Many studies have reported high seizure variability following OP intoxication, which may provide insights into potential correlations with neuropathology. Humans intoxicated with high-dose OPs can exhibit highly variable seizure behavior, ranging from apparent resistance to severe and prolonged SE (Okumura, Takasu et al. 1996, Peter, Sudarsan et al. 2014). Seizure variability

was also reported in humans who survived the 1995 Tokyo sarin gas attack (Yanagisawa, Morita et al. 2006). Similarly, outbred rat strains have shown variable seizure thresholds comparable to the human condition (Loscher, Ferland et al. 2017). One possible explanation of this variable seizure response to OPs is differences in genetic background, which has been shown to affect susceptibility to chemical-induced seizures in rodents and non-human primates (Lin, Duek et al. 2012, Matson, McCarren et al. 2017, Copping, Adhikari et al. 2019). Given this known variability, further investigation into models of this nature will help inform the role of seizure severity on chronic neurological outcomes following OP intoxication. Preclinical studies have begun to address this question by demonstrating that seizure duration and severity are generally proportional to the extent of neuronal damage following acute OP intoxication (McDonough, Dochterman et al. 1995, McDonough and Shih 1997, Hobson, Rowland et al. 2017). Similarly, therapeutic literature utilizing antiseizure therapies can provide insight as to the causal relationship between seizure severity and chronic neurological outcomes.

Benzodiazepines have demonstrated partial, region-specific neuroprotection with varying effectiveness depending on time of administration following OP intoxication (Shih, McDonough et al. 1999, McDonough, McMonagle et al. 2010, Kuruba, Wu et al. 2018). For example, recent studies demonstrated that treatment with either diazepam or midazolam administered 10 min after a seizurogenic dose of DFP resulted in significant neuroprotection in the hippocampus, amygdala, thalamus, and piriform cortex (Kuruba, Wu et al. 2018, Wu, Kuruba et al. 2018), but this was only demonstrated within days of DFP intoxication and did not address the question of long-term therapeutic efficacy. At 3 days post-treatment, both diazepam and midazolam significantly reduced the number of degenerating neurons, microglial activation, and reactive astrogliosis (Kuruba, Wu et al. 2018, Wu, Kuruba et al. 2018). While early benzodiazepine

therapy can provide neuroprotection at early time points, they are likely ineffective when administered later due to the development of tolerance and refractory SE as synaptic $GABA_A$ receptors are internalized in response to acute SE (Goodkin, Sun et al. 2007, McDonough, McMonagle et al. 2010, Niquet, Baldwin et al. 2016). Additionally, there are no preclinical studies available evaluating whether the short-term neuroprotection by benzodiazepine treatment also extends for weeks to months post-intoxication. For these reasons, it is difficult to gain mechanistic insight from the current benzodiazepine studies alone. Alternative antiseizure therapies are being developed that may be more efficacious and may ultimately provide additional insight into this research question.

Neurosteroids are endogenous neuroactive compounds that are synthesized in the brain and modulate neuronal excitability (Reddy 2010). Like benzodiazepines, they elicit anticonvulsant action by acting as positive modulators of the $GABA_AR$, increasing inhibitory neurotransmission (Miller, Scott et al. 2017). However, many neurosteroids have the advantage of binding to both synaptic and extrasynaptic $GABA_AR$, providing an advantage over benzodiazepines which are limited to synaptic receptors (Rossetti 2018). The endogenous neurosteroids pregnanolone and allopregnanolone have each demonstrated protection against neuropathology in nerve agent rat models (Amitai, Adani et al. 2005), and pregnanolone has also been shown to restore memory function (Lumley, Miller et al. 2019). The synthetic neurosteroid, SGE-516, demonstrated similar therapeutic efficacy against soman intoxication in rats; treatment with SGE-516 20 min post-soman exposure effectively reduced neuronal degeneration in the thalamus, amygdala, piriform cortex at 4 h post-intoxication (Althaus, McCarren et al. 2017). More recently, a novel K_v7 modulator, retigabine, administered with midazolam at 40 min post-intoxication attenuated seizures and partially reduced neuronal degeneration 24 h post-DFP or soman exposure (Barker,

Spampanato et al. 2021). While these studies demonstrate a positive correlation between seizure severity and neuropathology, the majority only provide neuroprotection in select brain regions. Additionally, most studies only evaluate short-term neuropathology and fail to address chronic neurological consequences. Follow-up studies should confirm these data gaps and address alternative mechanisms that may also be contributing to chronic neurological damage. Although many of these mechanisms are still being elucidated, it has been proposed that neuroinflammation, oxidative stress, and calcium dysregulation are likely contributors to OP-induced neurological damage, particularly at late time-points.

Additional Mechanisms Underlying OP-Induced Neurological Damage

Neuroinflammation

Neuroinflammation describes the cellular and molecular changes involved in immune activation within the nervous system in response to an insult or injury (Guignet and Lein 2018). Inflammatory processes are highly implicated in seizures and the development of epilepsy (Vezzani, Balosso et al. 2019), and human epileptic patients present with robust neuroinflammatory responses characterized by glial cell activation and elevated expression of inflammatory mediators (Choi, Nordli et al. 2009, Vezzani, Balosso et al. 2019). As of yet, no human studies have investigated the relationship between OPs and neuroinflammation in the context of acute intoxication. A recent PET imaging study, however, identified elevated levels of the neuroinflammatory marker translocator protein (TSPO) in patients with OP-associated Gulf War Illness (Alshelh, Albrecht et al. 2020), supporting the biological plausibility of neuroinflammation following acute OP intoxication.

Despite a scarcity of human data, a wealth of preclinical research documents OP-induced neuroinflammation, suggesting a pivotal role for neuroinflammation in OP-associated neurological damage, regardless of agent. While OP models differ in the precise profile of inflammatory processes, the overall response is proinflammatory, emerging in hours and progressing over a course of days to months following the initial intoxication event (Collombet, Four et al. 2007, Hobson, Rowland et al. 2019, Yang, Bruun et al. 2019, Guignet, Dhakal et al. 2020). The elicited neuroinflammatory phenotype is characterized by activation of microglial and astrocyte populations and increased expression of inflammatory mediators with distinct spatiotemporal distribution patterns in the brain.

In a variety of seizure models, these same inflammatory processes and molecular mediators promote neurodegeneration and enhance neuronal excitability (Vezzani and Viviani 2015, Vezzani, Balosso et al. 2019). Neuroinflammation following OP exposure corresponds temporally with the development of chronic adverse outcomes (Guignet and Lein 2019, Guignet, Dhakal et al. 2020), suggesting the involvement of inflammatory responses in the manifestation of cognitive and behavioral deficits and epileptogenic processes. Moreover, regions with the most intense and persistent neuroinflammatory responses (hippocampus, amygdala, and piriform cortex) have consistently been tied to functional abnormalities associated with acute OP intoxication (Okeefe and Nadel 1979, de Lanerolle, Kim et al. 1989, Vogt, Hyman et al. 1990, Davis and Whalen 2001, LeDoux 2003, Curia, Longo et al. 2008, Vaughan and Jackson 2014). This spatial correlation further suggests a contribution of neuroinflammation to these deficits.

Neuroinflammation can influence excitatory tone in the CNS through modulation of neurotransmission and ion homeostasis, and can also induce changes in brain architecture and neuronal health (Guignet and Lein 2018). These processes are critically tied to cognition, affect,

and seizure development (Kwon, Luikart et al. 2006, Morgan and Soltesz 2008, Femenia, Gomez-Galan et al. 2012, Liao, Zhang et al. 2014, Cathomas, Stegen et al. 2015). Inflammatory cytokines modulate neurotransmission, with several of them potentiating excitatory neurotransmitter systems. For example, IL-1β signaling stimulates phosphorylation of N-methyl-D-aspartate (NMDA) receptors, augmenting NMDA-dependent calcium currents, raising intracellular calcium concentrations, and promoting seizure activity (Viviani, Bartesaghi et al. 2003, Yang, Liu et al. 2005, Balosso, Maroso et al. 2008, Kawasaki, Zhang et al. 2008). Similarly, damage-associated molecular pattern signaling, such as through the high-mobility group box-1 (HMGB-1)/toll-like receptor 4 (TLR4) axis, promotes seizure activity via potentiation of glutamate (NMDA) receptor subunit epsilon-2 (NR2B) (Maroso, Balosso et al. 2010). Moreover, surface α-amino-3-hydroxy-5-methyl-4-isoxazolepropionic acid (AMPA) receptor expression is increased by TNFα (Beattie, Stellwagen et al. 2002, Leonoudakis, Braithwaite et al. 2004, Stellwagen, Beattie et al. 2005).

A number of investigators have found that therapies that reduce neuroinflammation improved chronic outcomes following acute OP intoxication. Direct targeting of canonical inflammatory processes suggests a complex relationship between neuroinflammation and chronic sequelae of acute OP intoxication. Delayed inhibition of the PGE2 receptor 2 subtype (EP2) provided protection against OP-induced neurodegeneration and neuroinflammation (Rojas, Ganesh et al. 2015) while improving cognitive function in the novel object recognition test (Rojas, Ganesh et al. 2016). Importantly, this treatment did not alter OP-induced SE, indicating that efficacy is independent of acute seizure response. Alternatively, enhancement of regulatory T cell function attenuated neurodegeneration and glial activation in the weeks following OP intoxication but failed to attenuate learning deficits (Finkelstein, Kunis et al. 2012). Administration of the

neurotrophic cytokines fibroblast growth factor 2 (FGF2) and epidermal growth factor (EGF) following soman intoxication did not improve performance in the Morris Water Maze and T Maze, but did improve performance in the elevated plus maze and fear conditioning tests (Collombet, Béracochéa et al. 2011).

While not directly anti-inflammatory, iNOS inhibition suppressed neuroinflammation and neurodegeneration while attenuating SRS development following DFP intoxication (Putra, Sharma et al. 2019). This treatment, however, failed to improve cognitive deficits following acute OP intoxication. Alternatively, naltrexone, an opioid receptor antagonist with anti-inflammatory properties, attenuated OP-associated cognitive deficits, but investigators did not correlate these improvements with modulation of neuroinflammatory processes (Brewster, Lugo et al. 2013). The anesthetic urethane, while offering comparable seizure control to diazepam, is significantly better at reducing neuroinflammation, neurodegeneration, and the development of SRS than diazepam (Rojas, Wang et al. 2018). While these data support the hypothesis that neuroinflammation is associated with the chronic neurologic consequences of acute OP intoxication, they do not explicitly demonstrate a causal relationship. Additionally, it must be considered whether the effects observed using such therapies are due to anti-inflammatory properties or whether additional mechanisms are at play.

The lack of therapeutic congruence using anti-inflammatory agents has made it challenging to provide a cohesive characterization of neuroinflammation following acute OP intoxication. One possible explanation is that the relative role of neuroinflammation may change over time such that differences in the timing of therapeutic administration could dramatically impact treatment outcomes (Guignet and Lein 2018). It has been proposed that the neurotoxic/neuroprotective contribution of neuroinflammatory processes may shift following OP

neurological insult (Collombet 2011, Banks and Lein 2012). Indeed, in other neuroinflammatory models, the neuroprotective versus neurotoxic potential of glial cells shifts depending on the time since the insult (Rice, Spangenberg et al. 2015, Szalay, Martinecz et al. 2016, Jin, Shi et al. 2017, Rice, Pham et al. 2017, Lloyd, Davies et al. 2019), and this has recently been demonstrated in response to DFP as well (Maupu, Enderlin et al. 2021). However, additional investigation is needed to evaluate this relationship more completely.

To conclude, a growing body of research implicates neuroinflammatory processes in OP-associated neurological outcomes. Following acute OP intoxication, neuroinflammation correlates temporally with the development of neurological deficits and abnormalities, and spatially with brain regions that control those impaired functions. While the greater neuroinflammation field has identified mechanistic connections between neuroinflammatory processes and sequelae associated with acute OP intoxication, a causal relationship has yet to be demonstrated in models of acute OP intoxication. A number of studies suggest the therapeutic potential of reducing neuroinflammation to improve OP-associated chronic outcomes. Only a handful of studies, however, have explicitly targeted inflammatory pathways for therapeutic benefit following acute OP intoxication, and more investigation is needed to characterize the relationship between neuroinflammation and chronic outcomes. Regardless, accumulating evidence identifies neuroinflammation as a critical dimension of OP-associated neuropathology that contributes to chronic impairment following acute intoxication.

Oxidative Stress

Oxidative stress is a physiological response that occurs when there is an imbalance between pro-oxidant species and antioxidant defense mechanisms (Sánchez-Rodríguez and Mendoza-Núñez 2019). This imbalance results in increased levels of reactive oxygen species (ROS) and

reactive nitrogen species (RNS), each of which can compromise the function of cellular macromolecules, including proteins, lipids, and nucleic acids (Sánchez-Rodríguez and Mendoza-Núñez 2019). These interactions can ultimately contribute to cell death and, therefore, represent important components of many disease states. The variety of clinical and preclinical studies implicating oxidative damage in chronic neurological diseases provides important rationale for their potential role in OP-induced brain damage. While limited studies have addressed this question in the context of acute OP intoxication, other disease models provide convincing evidence of this relationship. In particular, oxidative stress is implicated in neurodegenerative diseases such as Alzheimer's disease (AD) and Parkinson's disease (PD) (Singh, Kukreti et al. 2019).

In AD patients, strong correlations are observed between overall neurological health and oxidative damage, particularly in brain regions associated with cognitive function such as the hippocampus and neocortex (reviewed in Huang, Zhang et al. 2016). A clinical study of ~4,000 AD patients aged 45–69 found serum levels of reactive oxygen metabolites to be inversely associated with global cognition and verbal fluency (Horvat, Kubinova et al. 2016). These associations are also observed in preclinical animal models. A recent study in superoxide dismutase-1 (SOD1) knockout mice found that SOD1 deficiency not only increased oxidative stress markers, but also increased neuroinflammatory markers and impaired cognitive function (Logan, Royce et al. 2019). Similarly, PD patients demonstrate high levels of oxidative stress in the brain, and experimental evidence has linked this to neuronal degeneration and downstream health effects (reviewed in Dias, Junn et al. 2013). Although fairly strong associations have been observed between oxidative brain damage and neurological health, the mechanistic link to long-

term cognitive deficits requires further elucidation, particularly in response to acute OP intoxication.

A controlled study of humans exposed acutely to OPs reported significant levels of oxidative stress biomarkers in the blood (Ranjbar, Solhi et al. 2005). Preclinical studies demonstrate that acute OP intoxication can markedly disrupt neuronal mitochondrial homeostasis, resulting in the production of reactive oxygen species (ROS), lipid peroxidation, and oxidation of DNA and proteins (Pearson and Patel 2016). More specifically, several studies have reported impaired antioxidant capacity and increased oxidative cellular damage in the brain during the first few days (Brocardo, Pandolfo et al. 2005, Tüzmen, Candan et al. 2007, Liang, Pearson-Smith et al. 2019) and weeks (Putra, Gage et al. 2020) following acute OP intoxication. Although the brain regions reported to exhibit oxidative damage are variable, it is clear that the hippocampus and regions of the cortex are among the most affected (Brocardo, Pandolfo et al. 2005, Pearson and Patel 2016, Liang, Pearson-Smith et al. 2019). This regional pattern, which points largely to brain regions associated with cognitive function, provides further support for a role of oxidative damage in OP-induced neurological deficits. However, despite the strong evidence of oxidative damage at early time-points post-intoxication, the role and presence of oxidative damage at chronic time points are much less clear.

Given the importance of chronic neurological health in human survivors of OP intoxication, it is critical to understand the spatial and temporal profiles of neuropathology well past the time of intoxication. Recent DFP models have reported oxidative stress in the brain up to 12 weeks post-intoxication in the hippocampus, thalamus, and cortical regions, suggesting that oxidative stress is a persistent phenotype in the brain (Guignet, Dhakal et al. 2020, Putra, Sharma et al. 2020). While it remains unclear whether oxidative damage is linked to cognitive deficits

following OP intoxication, studies have proposed mechanisms that may link the two. ROS in the brain is thought to directly cause mitochondrial dysfunction, resulting in impaired oxidative phosphorylation and further ROS generation that ultimately promotes cellular degeneration (Naughton and Terry 2018). Another proposed mechanism driving this relationship is synaptic dysfunction, which has been shown in various *in vivo* and *in vitro* AD models to be exacerbated by oxidative stress in the brain (Tönnies and Trushina 2017). Although the relationship between oxidative stress and synaptic dysfunction has not specifically been addressed in OP models, the biological plausibility for this relationship to exist is high.

Therapeutic data has also implicated oxidative stress in the development of OP-induced neurological outcomes, particularly on endpoints measured at early time points post-intoxication. Omega-3 fatty acids have both antioxidant and anti-inflammatory properties (Pan, Hu et al. 2012), and have demonstrated neuroprotective efficacy in OP models. When combined with diazepam in a soman rat model, α-linolenic acid (LIN) treatment (30 min post-soman) resulted in increased NF-κB levels, decreased neuronal degeneration, and decreased neuronal necrosis in the hippocampus, amygdala, and piriform cortex at 1 day post-intoxication (Pan, Hu et al. 2012). A follow-up study in this model showed that LIN treatment increased brain-derived neurotrophic factor (BDNF) and neurogenesis levels at 10 d and improved memory function at 21 d (Piermartiri, Pan et al. 2015). The inducible nitric oxide synthase (iNOS) inhibitor 1400W, which prevents the production of nitric oxide, also implicated oxidative stress in the pathogenesis of chronic effects of OP-induced SE. 1400W reduced oxidative stress, neurodegeneration, and neuroinflammation in the amygdala, hippocampus, thalamus, and piriform cortex at 1 and 7 d post-exposure in a rat model of acute DFP intoxication (Putra, Sharma et al. 2019). Similarly, rats treated with repeated doses of the NADPH oxidase inhibitor diapocynin following acute

DFP intoxication showed significant reductions in neurodegeneration and neuroinflammation in the hippocampus and piriform cortex at 6 weeks post-intoxication (Putra, Gage et al. 2020). These findings suggest a pathologic role of oxidative stress in the progression of neurologic consequences following acute OP intoxication and justify further exploration into this therapeutic approach. Studies using this strategy are limited, and further studies would be helpful to better understand the mechanistic relationship between oxidative stress and chronic neurological outcomes.

It is clear from the neurodegeneration literature that oxidative stress plays a role in neuronal cell death, and likely contributes, at least in part, to chronic neurological deficits. In the context of OP intoxication, however, this relationship is less clearly defined. It is clear that oxidative stress in the brain is a prominent response observed in the days following OP intoxication, particularly in brain regions associated with cognitive function. However, both the patterns of oxidative stress at later time points post-intoxication, as well as the causal link between oxidative damage and cognitive dysfunction, require further elucidation. Despite some early successes with antioxidant therapies, a deeper understanding of chronic oxidative stress in OP patients will better inform the use of antioxidants as a medical countermeasure.

Calcium Dysregulation

Calcium signaling is critical to a variety of cellular processes, including neuronal growth, exocytosis, synapse development, and cognitive function (Kumar 2020). In the event of excess calcium signaling, unregulated release of intracellular calcium by ryanodine receptors can result in neuronal injury and altered synaptic plasticity (Deshpande, Blair et al. 2016). It has recently become clear that calcium signaling is altered in the aging brain, and calcium channels generally become deregulated as cognitive function begins to decline (Chandran, Kumar et al. 2019).

Recent literature has proposed dysregulated calcium signaling as a mechanism contributing to age-related cognitive decline. More specifically, several preclinical studies have found associations between aberrant calcium signaling and decreased synaptic plasticity in the hippocampus, a critical brain region for learning and memory function (Kumar 2020). In the context of OPs, it has been proposed that prolonged calcium dysregulation is a key driver of OP-induced cognitive impairment via pathological changes in synaptic connectivity (Phillips and Deshpande 2020). Although these associations are strong, further experimentation is required to determine whether this relationship is truly causal.

While relatively few studies have evaluated the role of calcium in OP models, there is recent evidence of calcium dysregulation in the brain following OP-induced seizures (Deshpande, Carter et al. 2010, Deshpande, Blair et al. 2016, Deshpande, Blair et al. 2016). The cholinergic crisis induced by acute OP intoxication leads to coactivation of glutamatergic networks in the brain and the downstream release of glutamate (**Figure 1-2**). Excessive glutamate levels in the brain overstimulate excitatory AMPA, NMDA, and kainate receptors, exacerbating cholinergic excitotoxicity and allowing pathologically high levels of calcium to enter the neurons (Manev, Favaron et al. 1989). A preclinical study evaluating calcium activity in neurons isolated from OP-intoxicated rats demonstrated a sustained elevation of intracellular calcium in hippocampal neurons, which lasted for up to 1 month post-intoxication and was primarily mediated by NMDA receptors (Deshpande, Carter et al. 2010). While preclinical studies have not rigorously examined any relationships between calcium dysregulation and neurological outcomes following acute OP intoxication, limited therapeutic data in OP models has begun to implicate calcium dysregulation in the development of neurological damage. Dantrolene, an inhibitor of the calcium-releasing ryanodine receptor, blocks the release of stored calcium from the endoplasmic

reticulum, thereby reducing hyperexcitability driven by calcium-induced calcium release (CICR) (Krause, Gerbershagen et al. 2004). When dantrolene was administered in a rat model of paroxon-induced SE, decreases in neurodegeneration coincided with reduced neuronal calcium concentrations at 2 d post-intoxication (Deshpande, Blair et al. 2016).

Although evidence from one lab suggests that calcium signaling is altered following high-dose OP intoxication, little data is available to demonstrate a mechanistic role in chronic neurological health following acute OP intoxication. Nonetheless, the relationship between calcium function and synaptic plasticity certainly represents a potential mechanism in the pathogenesis of long-term cognitive deficits associated with acute OP intoxication. Additionally, while the neuroprotective efficacy of calcium stabilizing therapeutics shows promise, it is still unknown whether these therapeutics will show efficacy at chronic time points post-OP intoxication. Understanding the long-term temporal profile of calcium alterations in the OP-intoxicated brain will likely shed light onto the effective use of calcium stabilizers.

Influence of Sex and Age on OP-Induced Neurotoxicity

One of the many challenges associated with developing more effective medical countermeasures against chemical threat agents is the diversity of individuals potentially affected by these compounds, particularly in the event of a civilian mass casualty. Current preclinical research is focused primarily on the adult brain. Thus, whether children represent a potentially vulnerable subpopulation has not been rigorously addressed in the context of acute OP intoxication. The potential for children to exhibit differential susceptibility is suggested by a significant literature indicating that children are more susceptible than adults to the neurotoxic effects of environmentally relevant OP levels (Bouchard, Chevrier et al. 2011, Muñoz-Quezada,

Lucero et al. 2013, Gonzalez-Alzaga, Lacasana et al. 2014). Moreover, a recent study suggests that juvenile rats at varying stages of neurodevelopment are differentially susceptible to the proconvulsant activity of OP chemical threat agents (Scholl, Miller-Smith et al. 2018). However, there are no published studies addressing the important question of whether acute intoxication with these compounds during postnatal neurodevelopment has lasting neuropathological or neurobehavioral consequences. There is also a lack of data to indicate whether the juvenile brain responds to therapeutics in the same manner as the adult brain following acute OP intoxication.

Prenatal neurodevelopment is a particularly sensitive window that often results in diverse neurological deficits in children exposed to OPs, including problems with motor function and attention (Gonzalez-Alzaga, Lacasana et al. 2014), social behavior (Wang, Zhang et al. 2017, Sagiv, Harris et al. 2018), and general cognition (Engel, Bradman et al. 2016, Sapbamrer and Hongsibsong 2019). This is understandable given the critical neurodevelopmental processes occurring in the brain during the prenatal period, such as progenitor cell differentiation, neuronal maturation and migration, immune development, synaptogenesis, and establishment of the blood-brain barrier (reviewed in Semple, Blomgren et al. 2013). Adolescent males (12-17 years) chronically exposed to OPs as pesticide applicators demonstrated a positive correlation between chlorpyrifos exposure and cognitive deficits (Rohlman, Ismail et al. 2016). However, susceptibility to the neurotoxic effects OPs requires further elucidation during early postnatal and juvenile neurodevelopment in terms of severity, timing, and functional outcomes. By 2-3 years of age (~21 days in rodents), the human brain is largely developed and is at ~90% of its adult weight (Giedd, Blumenthal et al. 1999). Despite this, the brain continues to undergo important developmental processes throughout the postnatal period, many of which may have implications for motor and cognitive function. Among these processes are alterations in neurotransmitter and

receptor composition (Romijn, Hofman et al. 1991), structural maturation of cortical regions (Tsujimoto 2008), ongoing neuronal myelination (Baloch, Verma et al. 2008), and synaptic pruning and cognitive refinement (Schafer, Lehrman et al. 2012). These biological processes increase susceptibility of juvenile individuals to OP-induced neurological deficits (Semple, Blomgren et al. 2013).

While the preclinical literature evaluating juvenile sensitivity to high-dose OP intoxication is relatively scarce, recent studies have begun to address this question. A direct investigation of age-dependent seizure activity and brain damage revealed that the OPs sarin, VX, and DFP all elicited age-specific outcomes in postnatal rats (Scholl, Miller-Smith et al. 2018). Juvenile rats were found to develop more severe seizures and neurodegeneration with increasing age, and P28 was identified as the most susceptible juvenile age tested (P14, P21, and P28). While the long-term effects of OP chemical threat agents have not been studied in juvenile animals, other chemical-induced seizure models provide strong evidence of chronic neurological deficits following developmental intoxication. For example, it has been reported that juveniles intoxicated with pentylenetetrazol experienced a significantly lower seizure threshold later in adulthood (Kouis, Mikroulis et al. 2014). Similarly, preclinical studies demonstrated that postnatal seizure induction with pilocarpine can cause both behavioral changes and reduced hippocampal volume in adulthood (Labbate, da Silva et al. 2014). It is likely that acute DFP intoxication during postnatal neurodevelopment will also induce lasting neuropathological and/or behavioral consequences in adulthood, but this question has yet to be addressed. Additionally, it is unclear which pathogenic mechanisms may be contributing to the development of chronic neurological consequences following developmental OP intoxication.

Altered neurogenesis has been associated with both seizures and OP exposure. In the absence of seizures, chronic OP exposures can inhibit neurogenesis over time (Wang, Ohishi et al. 2013). Conversely, the induction of SE is known to induce abnormal neuronal growth and promote neurogenesis in adult epilepsy models (Parent, Jessberger et al. 2007, Jiruska, Shtaya et al. 2013). Recent studies using pilocarpine have shown increased neurogenesis following chemical-induced seizures as well in both juvenile and adult rats (Wu, Hu et al. 2019, Velazco-Cercas, Beltran-Parrazal et al. 2020). It has been proposed that both increases and decreases in neurogenesis may be detrimental and can possibly contribute to cognitive decline following seizure induction (Rotheneichner, Marschallinger et al. 2013). These findings raise questions as to whether acute DFP intoxication during postnatal neurodevelopment can induce changes in neurogenesis, and if so, whether these changes are associated with functional neurological consequences.

Neuroinflammation has unique functions during neurodevelopment that may be critical to the onset of neurological deficits following OP intoxication. Microglia are key drivers of synaptic pruning, a neurodevelopmental process that refines cognitive function via the elimination of weak or redundant synapses (Wilton, Dissing-Olesen et al. 2019). Because this process does not begin until ~P35 (Semple, Blomgren et al. 2013), an insult to microglia prior to this age has the potential to disrupt the pruning process. It has been hypothesized that aberrant synaptic pruning by microglia contributes to long-term neurological deficits following seizures (reviewed in Andoh, Ikegaya et al. 2019). In addition to their role in pruning, epilepsy models have demonstrated that seizure-induced neurogenesis is mediated by microglia (Eyo, Murugan et al. 2017, Mo, Eyo et al. 2019). Further supporting this hypothesis is a recent publication demonstrating that pharmacological inhibition of neuroinflammation using minocycline

prevented aberrant neurogenesis following pilocarpine-induced SE (Zhu, Yao et al. 2020). However, the patterns of neuroinflammation and neurogenesis following acute OP intoxication of the developing brain have yet to be studied, especially at late time-points post-intoxication. Addressing this data gap will not only provide important information regarding the spatiotemporal patterns of damage in the developing brain, but may also provide therapeutic insight as to the potential role of neuroinflammation and/or neurodegeneration in OP-induced cognitive outcomes.

In addition to age, sex is an important biological variable in determining neurotoxicologic outcome, particularly in the context of OP intoxication. A systematic review of epidemiological studies found that the effects of chronic, low-dose OP exposure are highly sex-specific, with males often demonstrating greater sensitivity to OP toxicity than females (Comfort and Re 2017). Clinical studies have reported sex-specific effects of chronic OP exposure on hormone levels (Qin, Zhang et al. 2020), language comprehension tasks (Sagiv, Bruno et al. 2019), and IQ scores (Ntantu Nkinsa, Muckle et al. 2020). For these reasons, preclinical studies have begun to consider sex as an important biological variable influencing OP neurotoxicology studies. Chemical-induced seizure models have confirmed sex-specific effects. A recent study using the nerve agent soman identified that females have higher mortality rates than males following an acute seizurogenic dose of soman (Kundrick, Marrero-Rosado et al. 2020). Similarly, a model of pilocarpine-induced SE reported a clear sex difference in seizure activity, with fewer females experiencing SE than their male counterparts (Scharfman and MacLusky 2014). Perhaps the most relevant to this dissertation is the recent study evaluating sex differences in an adult DFP neurotoxicity model, in which it was found that DFP females experienced less severe seizure activity and neuropathology compared to DFP males (Gage, Golden et al. 2020).

While it has become clear that OPs can elicit sex-specific neurotoxic effects, several research questions remain regarding this issue. The specific influence of sex on OP intoxication during neurodevelopment, which itself is complex and sexually dimorphic, requires further elucidation. Additionally, given that OPs themselves can have unique neurotoxic effects (Pope 1999), future research is needed to determine whether DFP has sex-specific consequences during neurodevelopment, and, if so, whether these consequences persist into young adulthood. Lastly, more research is needed to better understand the mechanisms underlying sex differences in OP-induced neurotoxicity, particularly in seizure models.

In the case of chemical-induced seizure models, sexually dimorphic receptor composition of the brain throughout development is likely a key driver of sex-specific responses. Both excitatory (glutamatergic and cholinergic) and inhibitory (GABAergic) receptors in the brain exhibit sex-specific expression patterns (Akman, Moshé et al. 2014, Scharfman and MacLusky 2014). During neurodevelopment, males express higher levels of the excitatory glutamate receptors NR1, NR2A, and GluR1 than age-matched females (Hsu, Hsieh et al. 2000, Bian, Zhu et al. 2012, Damborsky and Winzer-Serhan 2012). Adult and juvenile males also express higher levels of cholinergic receptors throughout the brain (Potier, Sénécal et al. 2005), which may explain the increased sensitivity to seizures induced by pentylenetetrazol. Also in line with this finding is the observation that females express greater levels of $GABA_A$ receptors than males throughout postnatal neurodevelopment (Ravizza, Friedman et al. 2003, Li, Huguenard et al. 2007, Chudomel, Herman et al. 2009). Although sex hormones are often considered as a mechanism underlying sex differences, their relatively low expression during rodent neurodevelopment (Bell 2018) and the strong case for receptor differences make it unlikely that hormones are primary drivers of sex differences in OP seizure models. In support of this, a recent study reported that

estrous stage in adult rats has no effect on the seizurogenic effects of DFP (Gage, Golden et al. 2020). This body of literature describing sex-specific effects of OPs provides important rational for investigating whether DPF causes sex-specific neuropathology during susceptible windows of neurodevelopment. It is clear that the complexity of neurological damage following acute OP-induced SE is influenced by many factors, including age, sex, time post-intoxication, and timing of therapeutic administration. Given this complexity, as well as the abundance of pathogenic mechanisms that may contribute to sustained neurological damage, it is apparent that further research is needed to better elucidate how acute OP intoxication triggers chronic neurological deficits.

Dissertation Overview

The data presented in this dissertation address a number of critical data gaps in the field of medical countermeasures for acute OP intoxication. Preclinical studies assessing the current standard of care provide little data regarding the efficacy of benzodiazepine treatment against long-term neuropathology following OP-induced seizures. The recent replacement of diazepam with midazolam as an anticonvulsant raises questions as to whether midazolam is superior to diazepam in protecting against the chronic neurologic sequelae associated with acute OP intoxication. To develop neurotherapeutics better than benzodiazepines, it is necessary to understand the precise role of seizures in long-term neuropathology. It is still unclear whether OPs, including DFP, cause chronic neurological damage via neurotoxic effects independent of seizure activity. Answers to these questions will facilitate the development of more efficacious countermeasures. There are also gaps in the availability of diverse models for evaluating chemical toxicity and therapeutic efficacy. The majority of available models prioritize adult male

subjects and fail to study young or female individuals. More diverse animal models are needed to promote therapeutic testing in understudied populations.

The goal of chapter 2 is to increase understanding of the efficacy of the standard of care benzodiazepines midazolam and diazepam in protecting against chronic neurologic effects following acute DFP intoxication. While numerous studies have evaluated their short-term efficacy, few have assessed their neuroprotective potential for months post OP-intoxication. For this reason, we compared neurodegeneration, neuroinflammation, and mineralization between animals that received a vehicle injection, DFP, DFP + midazolam, or DFP + diazepam. The data presented in chapter 2 highlight the persistence of DFP-induced neuropathology and the minimal neuroprotection provided by either benzodiazepine, suggesting a need for alternative or adjunct therapeutics.

To confirm the need for alternative therapeutic targets, chapter 3 seeks to better elucidate the role of seizures in DFP-induced neuropathology. Understanding the respective contributions of SE versus the chemical DFP itself will allow for better prioritization of therapeutic targets for preclinical researchers. To address these questions, we took advantage of a population of rats apparently resistant to DFP-induced seizures (low-responders) observed over years in the Lein lab. This small subset of animals is apparently resistant to DFP-induced seizures despite having significant uptake of DFP into the brain. By comparing this low-responding population to our typical high-responding population, we were able to determine whether DFP itself still caused neurological damage independent of SE. Those data show that DFP low-responders display significant neurodegeneration, although it is less severe than DFP high-responders, confirming the suspected contribution of non-seizure damage mechanisms.

Lastly, chapter 4 seeks to determine the influence of age and sex on the response to acute OP intoxication by evaluating acute seizures responses, chronic neuropathology, and neurobehavior in developing male and female rats acutely intoxicated with DFP. Better understanding each of these endpoints will not only inform us whether sex-differences exist following acute DFP intoxication, but also provide a model to the broader research community that can be used to test lead therapeutic candidates.

Overall, the following data chapters enhance our understanding of both the acute and chronic neurotoxicity induced by acute high-dose DFP exposures, and contributes to the body of literature describing chemical threats and medical countermeasures. Chapter 2 expands on our understanding of standard of care benzodiazepines by highlighting their limitations for neuroprotection. Chapter 3 provides useful mechanistic insight for therapeutic development by demonstrating that controlling seizure activity alone is unlikely to full protect against the chronic neurotoxic effects of acute OP intoxication. Chapter 4 presents a juvenile DFP model that provides novel information on the sex-specific effects of DFP intoxication during neurodevelopment and identifies neurogenesis as a potential mechanism underlying chronic neurologic deficits in this model. This model also serves as a platform that can be used to evaluate therapeutic efficacy in understudied subpopulations, including young individuals and females. Taken together, these studies contribute to our understanding of OP threat agents and provide information to inform the development of improved countermeasures.

Figures and Figure Legends

Figure 1-1

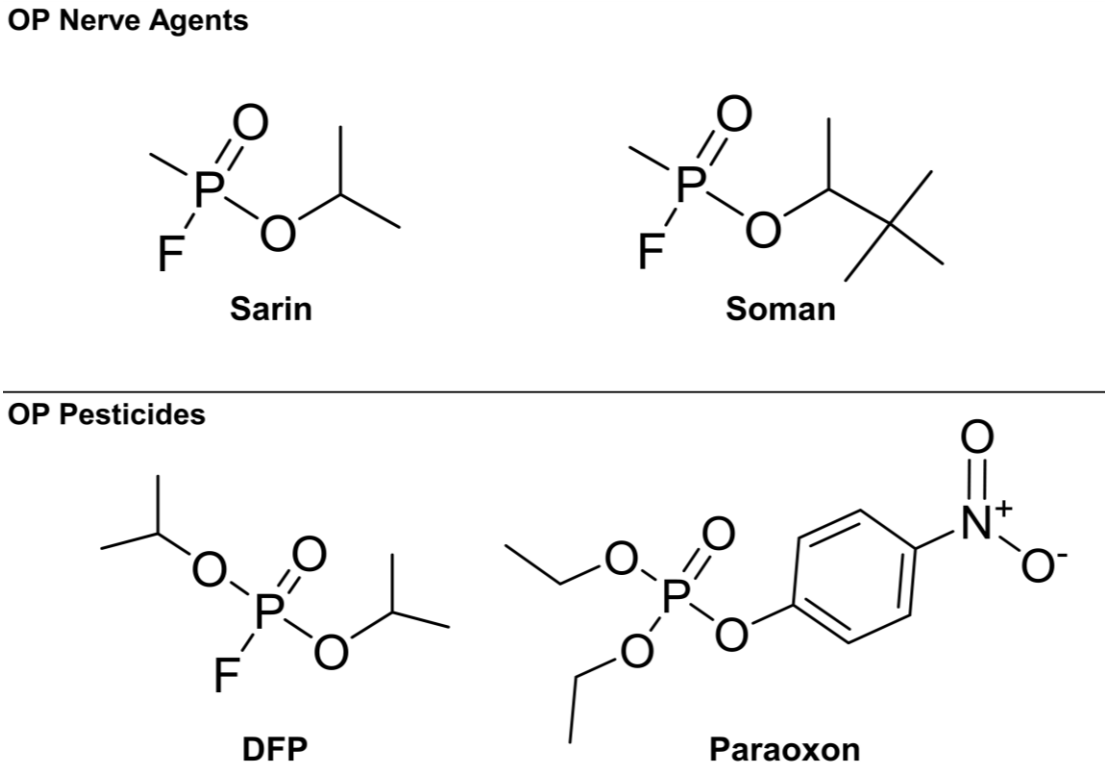

Figure 1-1. Chemical structures of common OP pesticides and nerve agents.

Figure 1-2.

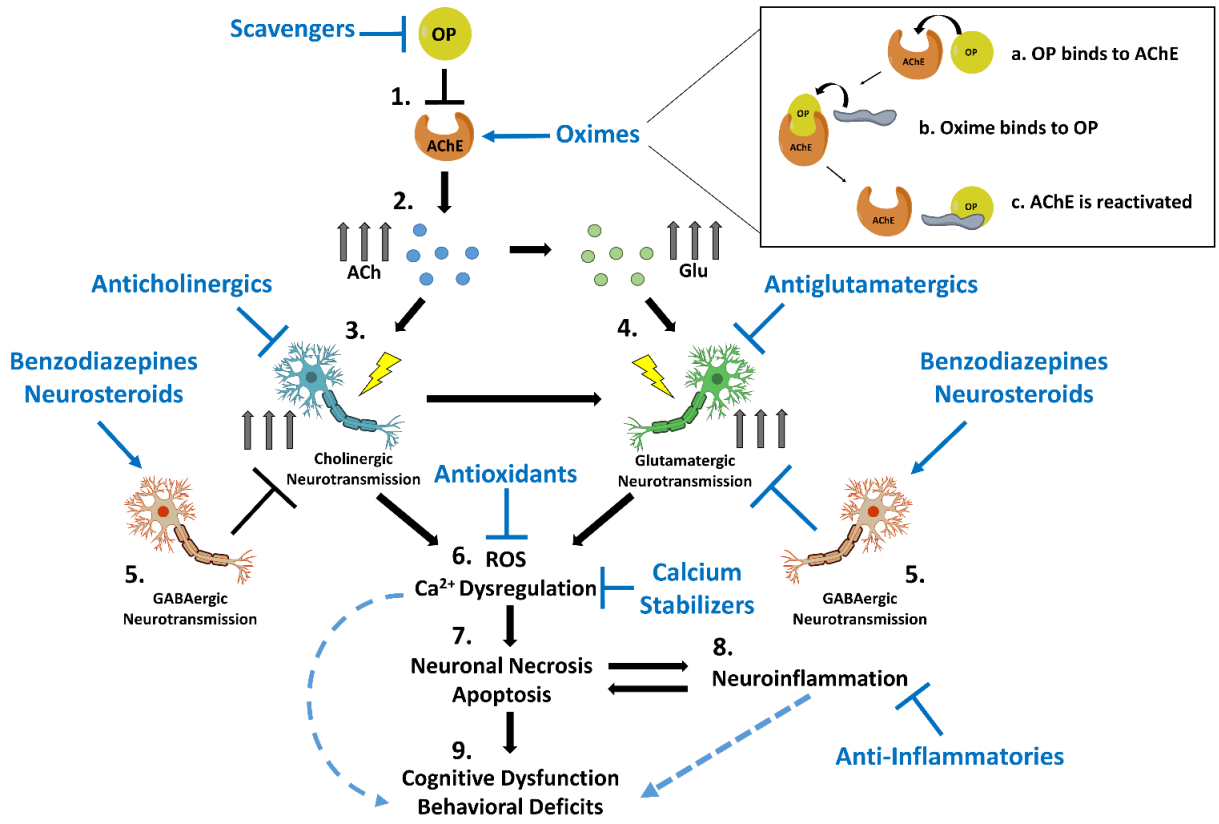
Scavengers
OP
1.
AChE
Oximes
2.
ACh
Glu
Anticholinergics
Antiglutamatergics
3.
4.
Benzodiazepines
Neurosteroids
Benzodiazepines
Neurosteroids
Cholinergic
Neurotransmission
Antioxidants
Glutamatergic
Neurotransmission
5.
GABAergic
Neurotransmission
6. ROS
Ca2+ Dysregulation
Calcium
Stabilizers
5.
GABAergic
Neurotransmission
7.
Neuronal Necrosis
Apoptosis
8.
Neuroinflammation
9.
Cognitive Dysfunction
Behavioral Deficits
Anti-Inflammatories
a. OP binds to AChE
b. Oxime binds to OP
c. AChE is reactivated

Figure 1-2. Mechanisms of OP-induced neuropathology and molecular targets for therapeutic intervention (blue). OPs inhibit acetylcholinesterase (AChE – orange) [1], preventing hydrolysis of the neurotransmitter acetylcholine (Ach – blue dots) [2]. Increased cholinergic neurotransmission [3] leads to increased glutamatergic neurotransmission [4], both of which are dampened by inhibitory GABAergic neurotransmission [5]. Excessive release of glutamate (Glu – green dots) can result in excitotoxicity, which is characterized by elevated levels of reactive oxygen species (ROS) and Ca^{2+} dysregulation [6]. Excitotoxicity is associated with apoptosis and neuronal necrosis [7], which can elicit robust neuroinflammatory responses [8]. Apoptosis, neuronal necrosis and persistent neuroinflammation are implicated in the pathogenesis of behavioral deficits and cognitive dysfunction [9]. Each of these events are targets for therapeutic compounds being explored as candidates for terminating OP-induced status epilepticus and/or mitigating the delayed neurological deficits associated with acute OP intoxication.

References

Akman, O., S. L. Moshé and A. S. Galanopoulou (2014). "Sex-specific consequences of early life seizures." Neurobiology of disease **72 Pt B**(Pt B): 153-166.

Alshelh, Z., D. S. Albrecht, C. Bergan, O. Akeju, D. J. Clauw, L. Conboy, R. R. Edwards, M. Kim, Y. C. Lee, E. Protsenko, V. Napadow, K. Sullivan and M. L. Loggia (2020). "In-vivo imaging of neuroinflammation in veterans with Gulf War illness." Brain, Behavior, and Immunity.

Althaus, A. L., H. S. McCarren, A. Alqazzaz, C. Jackson, J. H. McDonough, C. D. Smith, E. Hoffman, R. S. Hammond, A. J. Robichaud and J. J. Doherty (2017). "The synthetic neuroactive steroid SGE-516 reduces status epilepticus and neuronal cell death in a rat model of soman intoxication." Epilepsy Behav **68**: 22-30.

Amend, N., K. V. Niessen, T. Seeger, T. Wille, F. Worek and H. Thiermann (2020). "Diagnostics and treatment of nerve agent poisoning-current status and future developments." Ann N Y Acad Sci **1479**(1): 13-28.

Amitai, G., R. Adani, E. Fishbein, H. Meshulam, I. Laish and S. Dachir (2005). "Bifunctional compounds eliciting anti-inflammatory and anti-cholinesterase activity as potential treatment of nerve and blister chemical agents poisoning." Journal of Applied Toxicology **26**(1): 81-87.

Andoh, M., Y. Ikegaya and R. Koyama (2019). "Synaptic Pruning by Microglia in Epilepsy." J Clin Med **8**(12).

Baloch, S., R. Verma, H. Huang, P. Khurd, S. Clark, P. Yarowsky, T. Abel, S. Mori and C. Davatzikos (2008). "Quantification of Brain Maturation and Growth Patterns in C57BL/6J Mice via Computational Neuroanatomy of Diffusion Tensor Images." Cerebral Cortex **19**(3): 675-687.

Balosso, S., M. Maroso, M. Sanchez-Alavez, T. Ravizza, A. Frasca, T. Bartfai and A. Vezzani (2008). "A novel non-transcriptional pathway mediates the proconvulsive effects of interleukin-1beta." Brain **131**(Pt 12): 3256-3265.

Banks, C. N. and P. J. Lein (2012). "A review of experimental evidence linking neurotoxic organophosphorus compounds and inflammation." Neurotoxicology **33**(3): 575-584.

Barker, B. S., J. Spampanato, H. S. McCarren, K. Berger, C. E. Jackson, D. T. Yeung, F. E. Dudek and J. H. McDonough (2021). "The K(v)7 Modulator, Retigabine, is an Efficacious Antiseizure Drug for Delayed Treatment of Organophosphate-induced Status Epilepticus." Neuroscience **463**: 143-158.

Beattie, E. C., D. Stellwagen, W. Morishita, J. C. Bresnahan, K. H. Byeong, M. Von Zastrow, M. S. Beattie and R. C. Malenka (2002). "Control of synaptic strength by glial TNFα." Science **295**: 2282-2285.

Bell, M. R. (2018). "Comparing Postnatal Development of Gonadal Hormones and Associated Social Behaviors in Rats, Mice, and Humans." Endocrinology **159**(7): 2596-2613.

Bian, C., K. Zhu, Q. Guo, Y. Xiong, W. Cai and J. Zhang (2012). "Sex differences and synchronous development of steroid receptor coactivator-1 and synaptic proteins in the hippocampus of postnatal female and male C57BL/6 mice." Steroids **77**(1-2): 149-156.

Bouchard, M. F., J. Chevrier, K. G. Harley, K. Kogut, M. Vedar, N. Calderon, C. Trujillo, C. Johnson, A. Bradman, D. B. Barr and B. Eskenazi (2011). "Prenatal exposure to organophosphate pesticides and IQ in 7-year-old children." Environ Health Perspect **119**(8): 1189-1195.

Brewster, A. L., J. N. Lugo, V. V. Patil, W. L. Lee, Y. Qian, F. Vanegas and A. E. Anderson (2013). "Rapamycin Reverses Status Epilepticus-Induced Memory Deficits and Dendritic Damage." PLoS ONE **8**(3).

Brocardo, P. S., P. Pandolfo, R. N. Takahashi, A. L. Rodrigues and A. L. Dafre (2005). "Antioxidant defenses and lipid peroxidation in the cerebral cortex and hippocampus following acute exposure to malathion and/or zinc chloride." Toxicology **207**(2): 283-291.

Bruun, D. A., Z. Cao, B. Inceoglu, S. T. Vito, A. T. Austin, S. Hulsizer, B. D. Hammock, D. J. Tancredi, M. A. Rogawski, I. N. Pessah and P. J. Lein (2015). "Combined treatment with diazepam and allopregnanolone reverses tetramethylenedisulfotetramine (TETS)-induced calcium dysregulation in cultured neurons and protects TETS-intoxicated mice against lethal seizures." Neuropharmacology **95**: 332-342.

Cathomas, F., M. Stegen, H. Sigrist, L. Schmid, E. Seifritz, M. Gassmann, B. Bettler and C. R. Pryce (2015). "Altered emotionality and neuronal excitability in mice lacking KCTD12, an auxiliary subunit of GABAB receptors associated with mood disorders." Translational Psychiatry **5**(2): e510-e510.

Chandran, R., M. Kumar, L. Kesavan, R. S. Jacob, S. Gunasekaran, S. Lakshmi, C. Sadasivan and R. V. Omkumar (2019). "Cellular calcium signaling in the aging brain." J Chem Neuroanat **95**: 95-114.

Chen, Y., G. E. Garcia, W. Huang and S. Constantini (2014). "The involvement of secondary neuronal damage in the development of neuropsychiatric disorders following brain insults." Front Neurol **5**: 22.

Choi, J., D. R. Nordli, T. D. Alden, A. DiPatri, L. Laux, K. Kelley, J. Rosenow, S. U. Schuele, V. Rajaram and S. Koh (2009). "Cellular injury and neuroinflammation in children with chronic intractable epilepsy." Journal of Neuroinflammation **6**: 38.

Chuang, C. S., K. W. Yang, C. M. Yen, C. L. Lin and C. H. Kao (2019). "Risk of Seizures in Patients with Organophosphate Poisoning: A Nationwide Population-Based Study." Int J Environ Res Public Health **16**(17).

Chudomel, O., H. Herman, K. Nair, S. L. Moshé and A. S. Galanopoulou (2009). "Age- and gender-related differences in GABAA receptor-mediated postsynaptic currents in GABAergic neurons of the substantia nigra reticulata in the rat." Neuroscience **163**(1): 155-167.

Collombet, J.-M. (2011). "Nerve agent intoxication: Recent neuropathophysiological findings and subsequent impact on medical management prospects." Toxicology and Applied Pharmacology **255**(3): 229-241.

Collombet, J.-M., E. Four, W. Fauquette, M.-F. Burckhart, C. Masqueliez, D. Bernabé, D. Baubichon and G. Lallement (2007). "Soman poisoning induces delayed astrogliotic scar and angiogenesis in damaged mouse brain areas." NeuroToxicology **28**: 38-48.

Collombet, J. M., D. Béracochéa, P. Liscia, C. Piérard, G. Lallement and P. Filliat (2011). "Long-term effects of cytokine treatment on cognitive behavioral recovery and neuronal regeneration in soman-poisoned mice." Behavioural Brain Research **221**(1): 261-270.

Comfort, N. and D. B. Re (2017). "Sex-Specific Neurotoxic Effects of Organophosphate Pesticides Across the Life Course." Current environmental health reports **4**(4): 392-404.

Copping, N. A., A. Adhikari, S. P. Petkova and J. L. Silverman (2019). "Genetic backgrounds have unique seizure response profiles and behavioral outcomes following convulsant administration." Epilepsy Behav **101**(Pt A): 106547.

Curia, G., D. Longo, G. Biagini, R. S. Jones and M. Avoli (2008). "The pilocarpine model of temporal lobe epilepsy." J Neurosci Methods **172**(2): 143-157.

Damborsky, J. C. and U. H. Winzer-Serhan (2012). "Effects of sex and chronic neonatal nicotine treatment on $Na^{2+}/K^{+}/Cl^{-}$ co-transporter 1, K^{+}/Cl^{-} co-transporter 2, brain-derived neurotrophic factor, NMDA receptor subunit 2A and NMDA receptor subunit 2B mRNA expression in the postnatal rat hippocampus." Neuroscience **225**: 105-117.

Davis, M. and P. J. Whalen (2001). "The amygdala: vigilance and emotion." Mol Psychiatry **6**(1): 13-34.

de Lanerolle, N. C., J. H. Kim, R. J. Robbins and D. D. Spencer (1989). "Hippocampal interneuron loss and plasticity in human temporal lobe epilepsy." Brain Res **495**(2): 387-395.

Deshpande, L. S., R. E. Blair, B. A. Huang, K. F. Phillips and R. J. DeLorenzo (2016). "Pharmacological blockade of the calcium plateau provides neuroprotection following organophosphate paraoxon induced status epilepticus in rats." Neurotoxicology and teratology **56**: 81-86.

Deshpande, L. S., R. E. Blair, K. F. Phillips and R. J. DeLorenzo (2016). "Role of the calcium plateau in neuronal injury and behavioral morbidities following organophosphate intoxication." Annals of the New York Academy of Sciences **1374**(1): 176-183.

Deshpande, L. S., D. S. Carter, R. E. Blair and R. J. DeLorenzo (2010). "Development of a prolonged calcium plateau in hippocampal neurons in rats surviving status epilepticus induced by the organophosphate diisopropylfluorophosphate." Toxicol Sci **116**(2): 623-631.

Dias, V., E. Junn and M. M. Mouradian (2013). "The role of oxidative stress in Parkinson's disease." Journal of Parkinson's disease **3**(4): 461-491.

Dirnhuber, P., M. C. French, D. M. Green, L. Leadbeater and J. A. Stratton (1979). "The protection of primates against soman poisoning by pretreatment with pyridostigmine." J Pharm Pharmacol **31**(5): 295-299.

Eddleston, M., N. A. Buckley, P. Eyer and A. H. Dawson (2008). "Management of acute organophosphorus pesticide poisoning." Lancet **371**(9612): 597-607.

Engel, S. M., A. Bradman, M. S. Wolff, V. A. Rauh, K. G. Harley, J. H. Yang, L. A. Hoepner, D. B. Barr, K. Yolton, M. G. Vedar, Y. Xu, R. W. Hornung, J. G. Wetmur, J. Chen, N. T. Holland, F. P. Perera, R. M. Whyatt, B. P. Lanphear and B. Eskenazi (2016). "Prenatal Organophosphorus Pesticide Exposure and Child Neurodevelopment at 24 Months: An Analysis of Four Birth Cohorts." Environ Health Perspect **124**(6): 822-830.

Eyo, U. B., M. Murugan and L. J. Wu (2017). "Microglia-Neuron Communication in Epilepsy." Glia **65**(1): 5-18.

FDA (2018). "Center For Drug Evalutaion And Research- Midazolam Review." Food and Drug Administration **Application 209566Orig1s000**.

Femenia, T., M. Gomez-Galan, M. Lindskog and S. Magara (2012). "Dysfunctional hippocampal activity affects emotion and cognition in mood disorders." Brain Res **1476**: 58-70.

Figueiredo, T. H., J. P. Apland, M. F. M. Braga and A. M. Marini (2018). "Acute and long-term consequences of exposure to organophosphate nerve agents in humans." Epilepsia **59**(S2): 92-99.

Finkelstein, A., G. Kunis, T. Berkutzki, A. Ronen, A. Krivoy, E. Yoles, D. Last, Y. Mardor, K. Van Shura, E. McFarland, B. A. Capacio, C. Eisner, M. Gonzales, D. Gregorowicz, A. Eisenkraft, J. H. McDonough and M. Schwartz (2012). "Immunomodulation by poly-YE reduces organophosphate-induced brain damage." Brain, Behavior, and Immunity **26**(1): 159-169.

Forster, A., J. P. Gardaz, P. M. Suter and M. Gemperle (1980). "Respiratory depression by midazolam and diazepam." Anesthesiology **53**(6): 494-497.

Gage, M., M. Golden, M. Putra, S. Sharma and T. Thippeswamy (2020). "Sex as a biological variable in the rat model of diisopropylfluorophosphate-induced long-term neurotoxicity." Ann N Y Acad Sci **1479**(1): 44-64.

Giedd, J. N., J. Blumenthal, N. O. Jeffries, F. X. Castellanos, H. Liu, A. Zijdenbos, T. Paus, A. C. Evans and J. L. Rapoport (1999). "Brain development during childhood and adolescence: a longitudinal MRI study." Nat Neurosci **2**(10): 861-863.

Gonzalez-Alzaga, B., M. Lacasana, C. Aguilar-Garduno, M. Rodriguez-Barranco, F. Ballester, M. Rebagliato and A. F. Hernandez (2014). "A systematic review of neurodevelopmental effects of prenatal and postnatal organophosphate pesticide exposure." Toxicol Lett **230**(2): 104-121.

Goodkin, H. P., C. Sun, J. L. Yeh, P. S. Mangan and J. Kapur (2007). "GABA(A) receptor internalization during seizures." Epilepsia **48 Suppl 5**: 109-113.

Gordon, J. J., L. Leadbeater and M. P. Maidment (1978). "The protection of animals against organophosphate poisoning by pretreatment with a carbamate." Toxicol Appl Pharmacol **43**(1): 207-216.

Guignet, M., K. Dhakal, B. M. Flannery, B. A. Hobson, D. Zolkowska, A. Dhir, D. A. Bruun, S. Li, A. Wahab, D. J. Harvey, J. L. Silverman, M. A. Rogawski and P. J. Lein (2020). "Persistent behavior deficits, neuroinflammation, and oxidative stress in a rat model of acute organophosphate intoxication." Neurobiology of disease **133**: 104431-104431.

Guignet, M., K. Dhakal, B. M. Flannery, B. A. Hobson, D. Zolkowska, A. Dhir, D. A. Bruun, S. Li, A. Wahab, D. J. Harvey, J. L. Silverman, M. A. Rogawski and P. J. Lein (2020). "Persistent behavior deficits, neuroinflammation, and oxidative stress in a rat model of acute organophosphate intoxication." Neurobiol Dis **133**: 104431.

Guignet, M. and P. J. Lein (2018). Organophosphates. Advances in Neurotoxicology: Role of Inflammation in Environmental Neurotoxicity. M. Aschner and L. G. Costa. Oxford, UK, Elsevier, Ltd. **3:** 35-79.

Guignet, M. and P. J. Lein (2019). Neuroinflammation in organophosphate-induced neurotoxicity, Academic Press. **3:** 35-79.

Hobson, B. A., D. J. Rowland, S. Sisó, M. A. Guignet, Z. T. Harmany, S. B. Bandara, N. Saito, D. J. Harvey, D. A. Bruun, J. R. Garbow, A. J. Chaudhari and P. J. Lein (2019). "TSPO PET Using [18F]PBR111 Reveals Persistent Neuroinflammation Following Acute Diisopropylfluorophosphate Intoxication in the Rat." Toxicological Sciences **170**(2): 330-344.

Hobson, B. A., D. J. Rowland, S. Supasai, D. J. Harvey, P. J. Lein and J. R. Garbow (2017). "A magnetic resonance imaging study of early brain injury in a rat model of acute DFP intoxication." Neurotoxicology.

Horvat, P., R. Kubinova, A. Pajak, A. Tamosiunas, B. Schöttker, H. Pikhart, A. Peasey, M. Kozela, E. Jansen, A. Singh-Manoux and M. Bobak (2016). "Blood-Based Oxidative Stress Markers and Cognitive Performance in Early Old Age: The HAPIEE Study." Dementia and geriatric cognitive disorders **42**(5-6): 297-309.

Hsu, C., Y. L. Hsieh, R. C. Yang and H. K. Hsu (2000). "Blockage of N-methyl-D-aspartate receptors decreases testosterone levels and enhances postnatal neuronal apoptosis in the preoptic area of male rats." Neuroendocrinology **71**(5): 301-307.

Huang, W.-J., X. Zhang and W.-W. Chen (2016). "Role of oxidative stress in Alzheimer's disease." Biomedical reports **4**(5): 519-522.

Jett, D. A. (2016). "The NIH Countermeasures Against Chemical Threats Program: overview and special challenges." Annals of the New York Academy of Sciences **1374**(1): 5-9.

Jett, D. A., C. A. Sibrizzi, R. B. Blain, P. A. Hartman, P. J. Lein, K. W. Taylor and A. A. Rooney (2020). "A national toxicology program systematic review of the evidence for long-term effects after acute exposure to sarin nerve agent." Crit Rev Toxicol **50**(6): 474-490.

Jett, D. A. and S. M. Spriggs (2018). "Translational research on chemical nerve agents." Neurobiol Dis.

Jett, D. A. and D. T. Yeung (2010). "The CounterACT Research Network: basic mechanisms and practical applications." Proc Am Thorac Soc **7**(4): 254-256.

Jin, W.-N., S. X.-Y. Shi, Z. Li, M. Li, K. Wood, R. J. Gonzales and Q. Liu (2017). "Depletion of microglia exacerbates postischemic inflammation and brain injury." Journal of cerebral blood flow and metabolism : official journal of the International Society of Cerebral Blood Flow and Metabolism **37**(6): 2224-2236.

Jiruska, P., A. B. Y. Shtaya, D. M. S. Bodansky, W.-C. Chang, W. P. Gray and J. G. R. Jefferys (2013). "Dentate gyrus progenitor cell proliferation after the onset of spontaneous seizures in the tetanus toxin model of temporal lobe epilepsy." Neurobiology of Disease **54**: 492-498.

Kapur, J., J. L. Stringer and E. W. Lothman (1989). "Evidence that repetitive seizures in the hippocampus cause a lasting reduction of GABAergic inhibition." J Neurophysiol **61**(2): 417-426.

Kawasaki, Y., L. Zhang, J. K. Cheng and R. R. Ji (2008). "Cytokine mechanisms of central sensitization: Distinct and overlapping role of interleukin-1β, interleukin-6, and tumor necrosis factor-α in regulating synaptic and neuronal activity in the superficial spinal cord." Journal of Neuroscience **28**(20): 5189-5194.

Kitajima, T., T. Kanbayashi, Y. Saito, Y. Takahashi, Y. Ogawa, T. Sugiyama, Y. Kaneko, R. Aizawa and T. Shimizu (2004). "Diazepam reduces both arterial blood pressure and muscle sympathetic nerve activity in human." Neurosci Lett **355**(1-2): 77-80.

Kouis, P., A. Mikroulis and C. Psarropoulou (2014). "A single episode of juvenile status epilepticus reduces the threshold to adult seizures in a stimulus-specific way." Epilepsy Res **108**(9): 1564-1571.

Krause, T., M. U. Gerbershagen, M. Fiege, R. Weisshorn and F. Wappler (2004). "Dantrolene--a review of its pharmacology, therapeutic use and new developments." Anaesthesia **59**(4): 364-373.

Kumar, A. (2020). "Calcium Signaling During Brain Aging and Its Influence on the Hippocampal Synaptic Plasticity." Adv Exp Med Biol **1131**: 985-1012.

Kundrick, E., B. Marrero-Rosado, M. Stone, C. Schultz, K. Walker, R. B. Lee-Stubbs, M. de Araujo Furtado and L. A. Lumley (2020). "Delayed midazolam dose effects against soman in male and female plasma carboxylesterase knockout mice." Ann N Y Acad Sci **1479**(1): 94-107.

Kuruba, R., X. Wu and D. S. Reddy (2018). "Benzodiazepine-refractory status epilepticus, neuroinflammation, and interneuron neurodegeneration after acute organophosphate intoxication." Biochim Biophys Acta Mol Basis Dis **1864**(9 Pt B): 2845-2858.

Kwon, C. H., B. W. Luikart, C. M. Powell, J. Zhou, S. A. Matheny, W. Zhang, Y. Li, S. J. Baker and L. F. Parada (2006). "Pten Regulates Neuronal Arborization and Social Interaction in Mice." Neuron **50**(3): 377-388.

Labbate, G. P., A. V. da Silva and R. C. Barbosa-Silva (2014). "Effect of severe neonatal seizures on prepulse inhibition and hippocampal volume of rats tested in early adulthood." Neurosci Lett **568**: 62-66.

LeDoux, J. (2003). "The emotional brain, fear, and the amygdala." Cell Mol Neurobiol **23**(4-5): 727-738.

Lemercier, G., P. Carpentier, H. Sentenac-Roumanou and P. Morelis (1983). "Histological and histochemical changes in the central nervous system of the rat poisoned by an irreversible anticholinesterase organophosphorus compound." Acta Neuropathol **61**(2): 123-129.

Leonoudakis, D., S. P. Braithwaite, M. S. Beattie, E. C. Beattie and D. D. Leonoudakis (2004). "TNFα-induced AMPA-receptor trafficking in CNS neurons; relevance to excitotoxicity?" Neuron Glia Biology **1**: 263-273.

Li, H., J. R. Huguenard and R. S. Fisher (2007). "Gender and age differences in expression of GABAA receptor subunits in rat somatosensory thalamus and cortex in an absence epilepsy model." Neurobiol Dis **25**(3): 623-630.

Liang, L.-P., J. N. Pearson-Smith, J. Huang, B. J. Day and M. Patel (2019). "Neuroprotective effects of a catalytic antioxidant in a rat nerve agent model." Redox Biology **20**: 275-284.

Liao, W., Z. Zhang, D. Mantini, Q. Xu, G.-J. Ji, H. Zhang, J. Wang, Z. Wang, G. Chen, L. Tian, Q. Jiao, Y.-F. Zang, G. Lu, W. Liao, Á. H. G-J Ji Á Zhang Á J Wang Á Y-F Zang, W. H. Liao Á G-J Ji Á Zhang Á J Wang Á Y-F Zang, W. Z. Liao Á Zhang Á Q Xu Á Z Wang Á Q Jiao Á G Lu, D. Mantini, G. j. Ji, G. Chen and L. Tian (2014). "Dynamical intrinsic functional architecture of the brain during absence seizures." Brain Struct Funct **219**: 2001-2015.

Lin, T., O. Duek, A. Dori and O. Kofman (2012). "Differential long term effects of early diisopropylfluorophosphate exposure in Balb/C and C57Bl/J6 mice." Int J Dev Neurosci **30**(2): 113-120.

Lloyd, A. F., C. L. Davies, R. K. Holloway, Y. Labrak, G. Ireland, D. Carradori, A. Dillenburg, E. Borger, D. Soong, J. C. Richardson, T. Kuhlmann, A. Williams, J. W. Pollard, A. des Rieux, J. Priller and V. E. Miron (2019). "Central nervous system regeneration is driven by microglia necroptosis and repopulation." Nature Neuroscience **22**(7): 1046-1052.

Logan, S., G. H. Royce, D. Owen, J. Farley, M. Ranjo-Bishop, W. E. Sonntag and S. S. Deepa (2019). "Accelerated decline in cognition in a mouse model of increased oxidative stress." GeroScience **41**(5): 591-607.

Loscher, W., R. J. Ferland and T. N. Ferraro (2017). "The relevance of inter- and intrastrain differences in mice and rats and their implications for models of seizures and epilepsy." Epilepsy Behav **73**: 214-235.

Lumley, L., D. Miller, W. T. Muse, B. Marrero-Rosado, M. de Araujo Furtado, M. Stone, J. McGuire and C. Whalley (2019). "Neurosteroid and benzodiazepine combination therapy reduces status epilepticus and long-term effects of whole-body sarin exposure in rats." Epilepsia Open **4**(3): 382-396.

Manev, H., M. Favaron, A. Guidotti and E. Costa (1989). "Delayed increase of Ca2+ influx elicited by glutamate: role in neuronal death." Molecular Pharmacology **36**(1): 106.

Maroso, M., S. Balosso, T. Ravizza, J. Liu, E. Aronica, A. M. Iyer, C. Rossetti, M. Molteni, M. Casalgrandi, A. A. Manfredi, M. E. Bianchi and A. Vezzani (2010). "Toll-like receptor 4 and high-mobility group box-1 are involved in ictogenesis and can be targeted to reduce seizures." Nature Medicine.

Marrs, T. C. (2003). "Diazepam in the treatment of organophosphorus ester pesticide poisoning." Toxicol Rev **22**(2): 75-81.

Matson, L. M., H. S. McCarren, C. L. Cadieux, D. M. Cerasoli and J. H. McDonough (2017). "The role of genetic background in susceptibility to chemical warfare nerve agents across rodent and non-human primate models." Toxicology **393**: 51-61.

Maupu, C., J. Enderlin, A. Igert, M. Oger, S. Auvin, R. Hassan-Abdi, N. Soussi-Yanicostas, X. Brazzolotto, F. Nachon, G. Dal Bo and N. Dupuis (2021). "Diisopropylfluorophosphate-induced status epilepticus drives complex glial cell phenotypes in adult male mice." Neurobiol Dis **152**: 105276.

McDonough, J. H., Jr., L. W. Dochterman, C. D. Smith and T. M. Shih (1995). "Protection against nerve agent-induced neuropathology, but not cardiac pathology, is associated with the anticonvulsant action of drug treatment." Neurotoxicology **16**(1): 123-132.

McDonough, J. H., Jr., N. K. Jaax, R. A. Crowley, M. Z. Mays and H. E. Modrow (1989). "Atropine and/or diazepam therapy protects against soman-induced neural and cardiac pathology." Fundam Appl Toxicol **13**(2): 256-276.

McDonough, J. H., Jr. and T. M. Shih (1997). "Neuropharmacological mechanisms of nerve agent-induced seizure and neuropathology." Neurosci Biobehav Rev **21**(5): 559-579.

McDonough, J. H., Jr., L. D. Zoeffel, J. McMonagle, T. L. Copeland, C. D. Smith and T. M. Shih (2000). "Anticonvulsant treatment of nerve agent seizures: anticholinergics versus diazepam in soman-intoxicated guinea pigs." Epilepsy Res **38**(1): 1-14.

McDonough, J. H., J. D. McMonagle and T. M. Shih (2010). "Time-dependent reduction in the anticonvulsant effectiveness of diazepam against soman-induced seizures in guinea pigs." Drug Chem Toxicol **33**(3): 279-283.

McLeod, C. G., Jr., A. W. Singer and D. G. Harrington (1984). "Acute neuropathology in soman poisoned rats." Neurotoxicology **5**(2): 53-57.

Miller, P. S., S. Scott, S. Masiulis, L. De Colibus, E. Pardon, J. Steyaert and A. R. Aricescu (2017). "Structural basis for GABAA receptor potentiation by neurosteroids." Nat Struct Mol Biol **24**(11): 986-992.

Mo, M., U. B. Eyo, M. Xie, J. Peng, D. B. Bosco, A. D. Umpierre, X. Zhu, D. S. Tian, P. Xu and L. J. Wu (2019). "Microglial P2Y12 Receptor Regulates Seizure-Induced Neurogenesis and Immature Neuronal Projections." J Neurosci **39**(47): 9453-9464.

Morgan, R. J. and I. Soltesz (2008). "Nonrandom connectivity of the epileptic dentate gyrus predicts a major role for neuronal hubs in seizures." Proceedings of the National Academy of Sciences of the United States of America **105**(16): 6179-6184.

Muñoz-Quezada, M. T., B. A. Lucero, D. B. Barr, K. Steenland, K. Levy, P. B. Ryan, V. Iglesias, S. Alvarado, C. Concha, E. Rojas and C. Vega (2013). "Neurodevelopmental effects in children associated with exposure to organophosphate pesticides: A systematic review." Neurotoxicology **39**: 158-168.

Myhrer, T. (2007). "Neuronal structures involved in the induction and propagation of seizures caused by nerve agents: implications for medical treatment." Toxicology **239**(1-2): 1-14.

Naughton, S. X. and A. V. Terry, Jr. (2018). "Neurotoxicity in acute and repeated organophosphate exposure." Toxicology **408**: 101-112.

Niquet, J., R. Baldwin, L. Suchomelova, L. Lumley, D. Naylor, R. Eavey and C. G. Wasterlain (2016). "Benzodiazepine-refractory status epilepticus: pathophysiology and principles of treatment." Ann N Y Acad Sci **1378**(1): 166-173.

Ntantu Nkinsa, P., G. Muckle, P. Ayotte, B. P. Lanphear, T. E. Arbuckle, W. D. Fraser and M. F. Bouchard (2020). "Organophosphate pesticides exposure during fetal development and IQ scores in 3 and 4-year old Canadian children." Environ Res **190**: 110023.

Okeefe, J. and L. Nadel (1979). "The Cognitive Map as a Hippocampus." Behavioral and Brain Sciences **2**(4): 520-528.

Okumura, T., N. Takasu, S. Ishimatsu, S. Miyanoki, A. Mitsuhashi, K. Kumada, K. Tanaka and S. Hinohara (1996). "Report on 640 Victims of the Tokyo Subway Sarin Attack." Annals of Emergency Medicine **28**(2): 129-135.

OPCW (2020). "OPCW Issues Report on Technical Assistance Requested by Germany." Organisation for the Prohibition of Chemical Weapons.

Pan, H., X.-z. Hu, D. M. Jacobowitz, C. Chen, J. McDonough, K. Van Shura, M. Lyman and A. M. Marini (2012). "Alpha-linolenic acid is a potent neuroprotective agent against soman-induced neuropathology." NeuroToxicology **33**(5): 1219-1229.

Parent, J. M., S. Jessberger, F. H. Gage and C. Gong (2007). "Is neurogenesis reparative after status epilepticus?" Epilepsia **48**(s8): 69-71.

Pearson, J. N. and M. Patel (2016). "The role of oxidative stress in organophosphate and nerve agent toxicity." Annals of the New York Academy of Sciences **1378**(1): 17-24.

Pereira, E. F., Y. Aracava, L. J. DeTolla, Jr., E. J. Beecham, G. W. Basinger, Jr., E. J. Wakayama and E. X. Albuquerque (2014). "Animal models that best reproduce the clinical manifestations of human intoxication with organophosphorus compounds." J Pharmacol Exp Ther **350**(2): 313-321.

Pereira, E. F. R., Y. Aracava, L. J. DeTolla, E. J. Beecham, G. W. Basinger, E. J. Wakayama and E. X. Albuquerque (2014). "Animal Models That Best Reproduce the Clinical Manifestations of Human Intoxication with Organophosphorus Compounds." The Journal of Pharmacology and Experimental Therapeutics **350**(2): 313-321.

Peter, J. V., T. I. Sudarsan and J. L. Moran (2014). "Clinical features of organophosphate poisoning: A review of different classification systems and approaches." Indian J Crit Care Med **18**(11): 735-745.

Phillips, K. F. and L. S. Deshpande (2020). "Calcium Hypothesis of Gulf War Illness: Role of Calcium Ions in Neurological Morbidities in a DFP-Based Rat Model for Gulf War Illness." Neurosci Insights **15**: 2633105520979841.

Piermartiri, T. C. B., H. Pan, J. Chen, J. McDonough, N. Grunberg, J. P. Apland and A. M. Marini (2015). "Alpha-Linolenic Acid-Induced Increase in Neurogenesis is a Key Factor in the Improvement in the Passive Avoidance Task After Soman Exposure." NeuroMolecular Medicine **17**(3): 251-269.

Pope, C. N. (1999). "Organophosphorus pesticides: do they all have the same mechanism of toxicity?" J Toxicol Environ Health B Crit Rev **2**(2): 161-181.

Pope, C. N. and S. Brimijoin (2018). "Cholinesterases and the fine line between poison and remedy." Biochem Pharmacol.

Potier, S., J. Sénécal, J. G. Chabot, C. Psarropoulou and L. Descarries (2005). "A pentylenetetrazole-induced generalized seizure in early life enhances the efficacy of muscarinic receptor coupling to G-protein in hippocampus and neocortex of adult rat." Eur J Neurosci **21**(7): 1828-1836.

Putra, M., M. Gage, S. Sharma, C. Gardner, G. Gasser, V. Anantharam and T. Thippeswamy (2020). "Diapocynin, an NADPH oxidase inhibitor, counteracts diisopropylfluorophosphate-induced long-term neurotoxicity in the rat model." Ann N Y Acad Sci **1479**(1): 75-93.

Putra, M., M. Gage, S. Sharma, C. Gardner, G. Gasser, V. Anantharam and T. Thippeswamy (2020). "Diapocynin, an NADPH oxidase inhibitor, counteracts diisopropylfluorophosphate-induced long-term neurotoxicity in the rat model." Ann N Y Acad Sci.

Putra, M., S. Sharma, M. Gage, G. Gasser, A. Hinojo-Perez, A. Olson, A. Gregory-Flores, S. Puttachary, C. Wang, V. Anantharam and T. Thippeswamy (2019). "Inducible nitric oxide synthase inhibitor, 1400W, mitigates DFP-induced long-term neurotoxicity in the rat model." Neurobiology of Disease: 104443-104443.

Putra, M., S. Sharma, M. Gage, G. Gasser, A. Hinojo-Perez, A. Olson, A. Gregory-Flores, S. Puttachary, C. Wang, V. Anantharam and T. Thippeswamy (2019). "Inducible nitric oxide synthase inhibitor, 1400W, mitigates DFP-induced long-term neurotoxicity in the rat model." Neurobiol Dis.

Putra, M., S. Sharma, M. Gage, G. Gasser, A. Hinojo-Perez, A. Olson, A. Gregory-Flores, S. Puttachary, C. Wang, V. Anantharam and T. Thippeswamy (2020). "Inducible nitric oxide synthase inhibitor, 1400W, mitigates DFP-induced long-term neurotoxicity in the rat model." Neurobiol Dis **133**: 104443.

Qin, K., Y. Zhang, Y. Wang, R. Shi, R. Pan, Q. Yao, Y. Tian and Y. Gao (2020). "Prenatal organophosphate pesticide exposure and reproductive hormones in cord blood in Shandong, China." Int J Hyg Environ Health **225**: 113479.

Quinn, D. M., J. Topczewski, N. Yasapala and A. Lodge (2017). "Why is Aged Acetylcholinesterase So Difficult to Reactivate?" Molecules **22**(9).

Ranjbar, A., H. Solhi, F. J. Mashayekhi, A. Susanabdi, A. Rezaie and M. Abdollahi (2005). "Oxidative stress in acute human poisoning with organophosphorus insecticides; a case control study." Environ Toxicol Pharmacol **20**(1): 88-91.

Ravizza, T., L. K. Friedman, S. L. Moshé and J. Velísková (2003). "Sex differences in GABA(A)ergic system in rat substantia nigra pars reticulata." Int J Dev Neurosci **21**(5): 245-254.

Reddy, D. S. (2010). "Neurosteroids: endogenous role in the human brain and therapeutic potentials." Progress in brain research **186**: 113-137.

Rice, R. A., J. Pham, R. J. Lee, A. R. Najafi, B. L. West and K. N. Green (2017). "Microglial repopulation resolves inflammation and promotes brain recovery after injury." Glia **65**(6): 931-944.

Rice, R. A., E. E. Spangenberg, H. Yamate-Morgan, R. J. Lee, R. P. S. Arora, M. X. Hernandez, A. J. Tenner, B. L. West and K. N. Green (2015). "Elimination of microglia improves functional outcomes following extensive neuronal loss in the hippocampus." Journal of Neuroscience **35**(27): 9977-9989.

Richardson, J. R., V. Fitsanakis, R. H. S. Westerink and A. G. Kanthasamy (2019). "Neurotoxicity of pesticides." Acta Neuropathol **138**(3): 343-362.

Rohlman, D. S., A. A. Ismail, G. A. Rasoul, M. R. Bonner, O. Hendy, K. Mara, K. Wang and J. R. Olson (2016). "A 10-month prospective study of organophosphorus pesticide exposure and neurobehavioral performance among adolescents in Egypt." Cortex **74**: 383-395.

Rojas, A., T. Ganesh, N. Lelutiu, P. Gueorguieva and R. Dingledine (2015). "Inhibition of the prostaglandin EP2 receptor is neuroprotective and accelerates functional recovery in a rat model of organophosphorus induced status epilepticus." Neuropharmacology **93**: 15-27.

Rojas, A., T. Ganesh, Z. Manji, T. O'Neill and R. Dingledine (2016). "Inhibition of the prostaglandin E2 receptor EP2 prevents status epilepticus-induced deficits in the novel object recognition task in rats." Neuropharmacology **110**: 419-430.

Rojas, A., W. Wang, A. Glover, Z. Manji, Y. Fu and R. Dingledine (2018). "Beneficial Outcome of Urethane Treatment Following Status Epilepticus in a Rat Organophosphorus Toxicity Model." eNeuro **5**(2).

Romijn, H. J., M. A. Hofman and A. Gramsbergen (1991). "At what age is the developing cerebral cortex of the rat comparable to that of the full-term newborn human baby?" Early Human Development **26**(1): 61-67.

Rossetti, A. O. (2018). "Place of neurosteroids in the treatment of status epilepticus." Epilepsia **59**(S2): 216-219.

Rotheneichner, P., J. Marschallinger, S. Couillard-Despres and L. Aigner (2013). "Neurogenesis and neuronal regeneration in status epilepticus." Epilepsia **54**(s6): 40-42.

Sagiv, S. K., J. L. Bruno, J. M. Baker, V. Palzes, K. Kogut, S. Rauch, R. Gunier, A. M. Mora, A. L. Reiss and B. Eskenazi (2019). "Prenatal exposure to organophosphate pesticides and functional neuroimaging in adolescents living in proximity to pesticide application." Proc Natl Acad Sci U S A **116**(37): 18347-18356.

Sagiv, S. K., M. H. Harris, R. B. Gunier, K. R. Kogut, K. G. Harley, J. Deardorff, A. Bradman, N. Holland and B. Eskenazi (2018). "Prenatal Organophosphate Pesticide Exposure and Traits Related to Autism Spectrum Disorders in a Population Living in Proximity to Agriculture." Environ Health Perspect **126**(4): 047012.

Sánchez-Rodríguez, M. A. and V. M. Mendoza-Núñez (2019). "Oxidative Stress Indexes for Diagnosis of Health or Disease in Humans." Oxidative medicine and cellular longevity **2019**: 4128152-4128152.

Sapbamrer, R. and S. Hongsibsong (2019). "Effects of prenatal and postnatal exposure to organophosphate pesticides on child neurodevelopment in different age groups: a systematic review." Environ Sci Pollut Res Int **26**(18): 18267-18290.

Schafer, D. P., E. K. Lehrman, A. G. Kautzman, R. Koyama, A. R. Mardinly, R. Yamasaki, R. M. Ransohoff, M. E. Greenberg, B. A. Barres and B. Stevens (2012). "Microglia sculpt postnatal neural circuits in an activity and complement-dependent manner." Neuron **74**(4): 691-705.

Scharfman, H. E. and N. J. MacLusky (2014). "Sex differences in the neurobiology of epilepsy: a preclinical perspective." Neurobiol Dis **72 Pt B**: 180-192.

Scholl, E. A., S. M. Miller-Smith, S. L. Bealer, M. J. Lehmkuhle, J. J. Ekstrand, F. E. Dudek and J. H. McDonough (2018). "Age-dependent behaviors, seizure severity and neuronal damage in response to nerve agents or the organophosphate DFP in immature and adult rats." Neurotoxicology **66**: 10-21.

Semple, B. D., K. Blomgren, K. Gimlin, D. M. Ferriero and L. J. Noble-Haeusslein (2013). "Brain development in rodents and humans: Identifying benchmarks of maturation and vulnerability to injury across species." Progress in neurobiology **0**: 1-16.

Semple, B. D., K. Blomgren, K. Gimlin, D. M. Ferriero and L. J. Noble-Haeusslein (2013). "Brain development in rodents and humans: Identifying benchmarks of maturation and vulnerability to injury across species." Prog Neurobiol **106-107**: 1-16.

Shih, T., J. H. McDonough, Jr. and I. Koplovitz (1999). "Anticonvulsants for soman-induced seizure activity." J Biomed Sci **6**(2): 86-96.

Shin, J. H., M. F. Adrover, J. Wess and V. A. Alvarez (2015). "Muscarinic regulation of dopamine and glutamate transmission in the nucleus accumbens." Proc Natl Acad Sci U S A **112**(26): 8124-8129.

Singh, A., R. Kukreti, L. Saso and S. Kukreti (2019). "Oxidative Stress: A Key Modulator in Neurodegenerative Diseases." Molecules (Basel, Switzerland) **24**(8): 1583.

Stellwagen, D., E. C. Beattie, J. Y. Seo and R. C. Malenka (2005). "Differential regulation of AMPA receptor and GABA receptor trafficking by tumor necrosis factor-α." Journal of Neuroscience **25**(12): 3219-3228.

Szalay, G., B. Martinecz, N. Lénárt, Z. Környei, B. Orsolits, L. Judák, E. Császár, R. Fekete, B. L. West, G. Katona, B. Rózsa and Á. Dénes (2016). "Microglia protect against brain injury and their selective elimination dysregulates neuronal network activity after stroke." Nature Communications **7**: 1-13.

Tonduli, L. S., G. Testylier, C. Masqueliez, G. Lallement and P. Monmaur (2001). "Effects of Huperzine used as pre-treatment against soman-induced seizures." Neurotoxicology **22**(1): 29-37.

Tönnies, E. and E. Trushina (2017). "Oxidative Stress, Synaptic Dysfunction, and Alzheimer's Disease." Journal of Alzheimer's disease : JAD **57**(4): 1105-1121.

Tsujimoto, S. (2008). "The Prefrontal Cortex: Functional Neural Development During Early Childhood." The Neuroscientist **14**(4): 345-358.

Tüzmen, M. N., N. Candan and E. Kaya (2007). "The evaluation of altered antioxidative defense mechanism and acetylcholinesterase activity in rat brain exposed to chlorpyrifos, deltamethrin, and their combination." Toxicol Mech Methods **17**(9): 535-540.

UN (2017). Report of the Independent International Commission of Inquiry on the Syrian Arab Republic United Nations General Assembly: Human Rights Council.

Vaughan, D. N. and G. D. Jackson (2014). "The piriform cortex and human focal epilepsy." Front Neurol **5**: 259.

Velazco-Cercas, E., L. Beltran-Parrazal, C. Morgado-Valle and M. L. López-Meraz (2020). "Status Epilepticus Increases Cell Proliferation and Neurogenesis in the Developing Rat Cerebellum." Cerebellum **19**(1): 48-57.

Vezzani, A., S. Balosso and T. Ravizza (2019). "Neuroinflammatory pathways as treatment targets and biomarkers in epilepsy." Nature Reviews Neurology **15**: 459-472.

Vezzani, A. and B. Viviani (2015). "Neuromodulatory properties of inflammatory cytokines and their impact on neuronal excitability." Neuropharmacology **96**: 70-82.

Viviani, B., S. Bartesaghi, F. Gardoni, A. Vezzani, M. M. Behrens, T. Bartfai, M. Binaglia, E. Corsini, M. Di Luca, C. L. Galli and M. Marinovich (2003). "Interleukin-1β enhances NMDA receptor-mediated intracellular calcium increase through activation of the Src family of kinases." Journal of Neuroscience **23**: 8692-8700.

Vogel, L. (2013). "WHO releases guidelines for treating chemical warfare victims after possible Syria attacks." CMAJ : Canadian Medical Association Journal **185**(14): E665-E665.

Vogt, L. J. K., B. T. Hyman, G. W. Van Hoesen and A. R. Damasio (1990). "Pathological alterations in the amygdala in Alzheimer's disease." Neuroscience **37**: 377-385.

Vucinic, S., B. Antonijevic, A. M. Tsatsakis, L. Vassilopoulou, A. O. Docea, A. E. Nosyrev, B. N. Izotov, H. Thiermann, N. Drakoulis and D. Brkic (2017). "Environmental exposure to organophosphorus nerve agents." Environmental Toxicology and Pharmacology **56**: 163-171.

Walton, N. Y. and D. M. Treiman (1988). "Response of status epilepticus induced by lithium and pilocarpine to treatment with diazepam." Exp Neurol **101**(2): 267-275.

Wang, L., T. Ohishi, H. Akane, A. Shiraki, M. Itahashi, K. Mitsumori and M. Shibutani (2013). "Reversible effect of developmental exposure to chlorpyrifos on late-stage neurogenesis in the hippocampal dentate gyrus in mouse offspring." Reproductive Toxicology **38**: 25-36.

Wang, Y., Y. Zhang, L. Ji, Y. Hu, J. Zhang, C. Wang, G. Ding, L. Chen, M. Kamijima, J. Ueyama, Y. Gao and Y. Tian (2017). "Prenatal and postnatal exposure to organophosphate pesticides and childhood neurodevelopment in Shandong, China." Environ Int **108**: 119-126.

Williamson, J., T. Singh and J. Kapur (2019). "Neurobiology of organophosphate-induced seizures." Epilepsy Behav **101**(Pt B): 106426.

Wilton, D. K., L. Dissing-Olesen and B. Stevens (2019). "Neuron-Glia Signaling in Synapse Elimination." Annu Rev Neurosci **42**: 107-127.

Wu, P., Y. Hu, X. J. Li, M. Cheng and L. Jiang (2019). "Sodium valproate suppresses abnormal neurogenesis induced by convulsive status epilepticus." Neural Regen Res **14**(3): 480-484.

Wu, X., R. Kuruba and D. S. Reddy (2018). "Midazolam-Resistant Seizures and Brain Injury after Acute Intoxication of Diisopropylfluorophosphate, an Organophosphate Pesticide and Surrogate for Nerve Agents." J Pharmacol Exp Ther **367**(2): 302-321.

Yanagisawa, N., H. Morita and T. Nakajima (2006). "Sarin experiences in Japan: Acute toxicity and long-term effects." Journal of the Neurological Sciences **249**(1): 76-85.

Yang, J., D. A. Bruun, C. Wang, D. Wan, C. B. McReynolds, K. Phu, B. Inceoglu, P. J. Lein and B. D. Hammock (2019). "Lipidomes of brain from rats acutely intoxicated with diisopropylfluorophosphate identifies potential therapeutic targets." Toxicology and Applied Pharmacology **382**: 114749.

Yang, S., Z. W. Liu, L. Wen, H. F. Qiao, W. X. Zhou and Y. X. Zhang (2005). "Interleukin-1β enhances NMDA receptor-mediated current but inhibits excitatory synaptic transmission." Brain Research **1034**(1-2): 172-179.

Zhu, X., Y. Yao, J. Yang, Q. Ge, D. Niu, X. Liu, C. Zhang, G. Gan, A. Zhang and H. Yao (2020). "Seizure-induced neuroinflammation contributes to ectopic neurogenesis and aggressive behavior in pilocarpine-induced status epilepticus mice." Neuropharmacology **170**: 108044.

Chapter 2

Acute Administration of Diazepam or Midazolam Minimally Alters Long-Term Neuropathological Effects in the Rat Brain Following Acute Intoxication with Diisopropylfluorophosphate

Based on a publication in *European Journal of Pharmacology* (accepted September 2020) under the same title with the following authors:

Suangsuda Supasai[a,b]*, Eduardo A. González[a]*, Douglas J. Rowland[c], Brad Hobson[a, c], Donald A. Bruun[a], Michelle A. Guignet[a], Sergio Soares[c], Vikrant Singh[d], Heike Wulff[d], Naomi Saito[e], Danielle J. Harvey[e], and Pamela J. Lein[a]

[a]Department of Molecular Biosciences, University of California, Davis, School of Veterinary Medicine, Davis, CA 95616, USA (supasai.suangsuda@gmail.com; azgonzalez@ucdavis.edu; bahobson@ucdavis.edu; dabruun@ucdavis.edu; mguignet@ucdavis.edu; pjlein@ucdavis.edu); [b]Department of Molecular Tropical Medicine and Genetics, Faculty of Tropical Medicine, Mahidol University, Bangkok 10400, Thailand (suangsuda.sup@mahidol.edu); [c]Center for Molecular and Genomic Imaging, University of California, Davis, College of Engineering, Davis, CA 95616, USA (djrowland@ucdavis.edu; bahobson@ucdavis.edu; srpsoares@ucdavis.edu); [d]Department of Pharmacology, University of California, Davis, School of Medicine, Davis, CA 95616, USA (vssingh@ucdavis.edu; hwulff@ucdavis.edu); [e]Department of Public Health Sciences, University of California, Davis, School of Medicine, Davis, CA 95616, USA (nhsaito@ucdavis.edu; djharvey@ucdavis.edu).

*These authors contributed equally to this manuscript.

Abstract

Acute intoxication with organophosphorus cholinesterase inhibitors (OPs) can trigger seizures that rapidly progress to life-threatening status epilepticus. Diazepam, long considered the standard of care for treating OP-induced seizures, is being replaced by midazolam. Whether midazolam is more effective than diazepam in mitigating the persistent effects of acute OP intoxication has not been rigorously evaluated. We compared the efficacy of diazepam vs. midazolam in preventing persistent neuropathology in adult male Sprague-Dawley rats acutely intoxicated with the OP diisopropylfluorophosphate (DFP). Subjects were administered pyridostigmine bromide (0.1 mg/kg, *i.p.*) 30 min prior to injection with DFP (4 mg/kg, *s.c.*) or vehicle (saline) followed 1 min later by atropine sulfate (2 mg/kg, *i.m.*) and pralidoxime (25 mg/kg, *i.m.*), and 40 min later by diazepam (5 mg/kg, *i.p.*), midazolam (0.73 mg/kg, *i.m.*), or vehicle. At 3 and 6 months post-exposure, neurodegeneration, reactive astrogliosis, microglial activation, and oxidative stress were assessed in multiple brain regions using quantitative immunohistochemistry. Brain mineralization was evaluated by *in vivo* micro-computed tomography (micro-CT). Acute DFP intoxication caused persistent neurodegeneration, neuroinflammation, and brain mineralization. Midazolam transiently mitigated neurodegeneration, and both benzodiazepines partially protected against reactive astrogliosis in a brain region-specific manner. Neither benzodiazepine attenuated microglial activation or brain mineralization. These findings indicate that neither benzodiazepine effectively protects against persistent neuropathological changes, and suggest that midazolam is not significantly better than diazepam. Overall, this study highlights the need for improved neuroprotective strategies for treating humans in the event of a chemical emergency involving OPs.

Keywords: benzodiazepines, diazepam, micro-CT, midazolam, neuroinflammation, organophosphate neurotoxicity

Abbreviations

DFP = diisopropylfluorophosphate; GFAP = glial fibrillary acidic protein; IBA-1 = ionized calcium-binding adapter molecule 1; micro-CT = micro-computed tomography; OP = organophosphorus cholinesterase inhibitors; PBS = phosphate-buffered saline; ROI = region of interest

Introduction

Organophosphorus cholinesterase inhibitors (OPs) are used as both pesticides and chemical threat agents. These compounds cause hundreds of thousands of death each year as a result of accidental exposures and suicides, and terrorist use of OPs remains a serious threat (Eddleston, Buckley et al. 2008, Patel, Ramasundarahettige et al. 2012, Pereira, Aracava et al. 2014). Inhibition of acetylcholinesterase by OPs causes cholinergic overexcitation at both central and peripheral synapses (Pope, Karanth et al. 2005). In both humans and animals, this cholinergic crisis can trigger seizures that rapidly progress to life threatening *status epilepticus* (de Araujo Furtado, Rossetti et al. 2012). Humans who survive OP-induced *status epilepticus* often develop persistent neurological impairments, including structural brain damage, cognitive deficits, and epilepsy (Yamasue, Abe et al. 2007, Loh, Swanberg et al. 2010, Chen 2012).

Current standard of care for treatment of OP poisoning includes atropine to block peripheral cholinergic symptoms, an oxime to reactivate acetylcholinesterase and a benzodiazepine to terminate seizures. In the United States, and other countries, midazolam is replacing diazepam as the standard of care for treating OP-induced seizures. Midazolam is superior to diazepam in terminating seizures in animal models of OP-induced *status epilepticus* (McDonough, McMonagle et al. 1999, McMullan, Sasson et al. 2010). Based on these findings and data from the Rapid Anticonvulsant Medication Prior to Arrival Trial (RAMPART) study, a double-blind clinical trial that evaluated the efficacy of midazolam as an emergency anticonvulsant (Silbergleit, Lowenstein et al. 2011, Silbergleit, Lowenstein et al. 2013), the United States Food and Drug Administration (US FDA) determined that midazolam is superior to either diazepam or the benzodiazepine lorazepam for the treatment of OP-induced seizures, largely due to increased bioavailability following *i.m.* administration (FDA 2018).

Improved seizure termination following acute OP intoxication is thought to improve neurological outcomes in exposed individuals (McDonough, McMonagle et al. 1999, Jett 2016). However, whether midazolam provides enhanced neuroprotection relative to diazepam when administered at a delayed time after acute OP intoxication, as would be the case in a mass civilian casualty or suicide attempts involving OPs, has not been rigorously evaluated. Therefore, the goal of this study was to compare post-OP exposure treatment with diazepam vs. midazolam on persistent neuropathology in a rat model of acute intoxication with the OP, diisopropylfluorophosphate (DFP). Adult male rats acutely intoxicated with DFP exhibit persistent human-relevant neuropathology, behavioral deficits, and electroencephalographic abnormalities (Deshpande, Carter et al. 2010, Pouliot, Bealer et al. 2016, Liang, Pearson-Smith et al. 2017, Siso, Hobson et al. 2017, Guignet, Dhakal et al. 2019).

Methods and Materials

Animals and Husbandry

All animals were maintained in facilities fully accredited by AAALAC International. Studies were performed under protocols approved by the UC Davis Institutional Animal Care and Use Committee (IACUC protocol #20165) with attention to minimizing pain and suffering. Animal experiments strictly adhered to ARRIVE guidelines and the National Institutes of Health guide for the care and use of laboratory animals. Adult (7-8 wk) male Sprague-Dawley rats (250-280g; Charles River Laboratories, Hollister, CA, USA) were individually housed in standard plastic cages with absorbent corn cob bedding and a 12 h light/dark cycle and controlled environment (22 ± 2 °C, 40-50% humidity). This species was chosen as it is a well-established model for

evaluating acute DFP intoxication (Pessah, Rogawski et al. 2016). Rodent chow (2018 Tekland global 18% protein rodent diet; Envigo, Huntingdon, UK) and water were provided *ad libitum.*

Study design

The data reported here are a subset of the data generated from a single study designed to assess the efficacy of diazepam and midazolam on the chronic effects of DFP-induced *status epilepticus*. All animals in the study were monitored for seizure activity during the first 4 hours post-DFP injection (**Figure 2-1A**). In the subsequent days to weeks to months, these animals were evaluated by magnetic resonance (MR) and positron emission tomography (PET) imaging with each animal experiencing up to three separate imaging sessions. The data from these *in vivo* imaging studies are described in a separate manuscript (Hobson et al., under review). At 3 and 6 months post-exposure, the brains of a subset of these animals were also scanned using micro-computed tomography (micro-CT) prior to euthanizing the animals to collect brains for neuropathologic analyses. For seizure monitoring, vehicle and DFP alone groups consisted of 14 animals each, while diazepam and midazolam groups consisted of 10 animals each (**Figure 2-1B**). Due to the complexity of the study and limitations on the number of animals that could be imaged in a single day, animals in this study were injected across multiple days. All animals were injected in the morning, and injections on any given morning included animals from each experimental group. Following the acute seizure analysis, 3 randomly chosen animals were removed from the diazepam and midazolam groups for separate analyses not included in this study; thus 7 animals from each of these two groups were assessed for neuropathologic responses at later time points.

Pharmacokinetic Analysis of Diazepam and Midazolam

Adult male rats not injected with DFP were used to evaluate the pharmacokinetics of diazepam and midazolam. Brain and plasma concentrations were evaluated at 10 min, 30 min, 1 h, 4 h, 12 h, and 24 h post-administration by ultra-performance liquid chromatography-mass spectrometry (UPLC-MS) as previously described (Ulu, Inceoglu et al. 2016). Midazolam was analyzed by the selective reaction monitoring (SRM) transition of its positively charged quasi-molecular ion 326.08 (M+1)+ into product ions of 223.05, 249.04 & 291.05 m/z. Diazepam was analyzed by the SRM transition of its positively charged quasi-molecular ion 285.08 (M+1)+ into product ions of 227.99, 193.03 & 154.04 m/z. Adult rats were injected with either diazepam (USP grade; Hospira Inc., Lake Forest, IL, USA; 5 mg/kg, *i.p.*) or midazolam (USP grade; Hospira Inc.; 0.73 mg/kg, *i.m.*). Diazepam provided in ChemPacks is intended to be administered *i.m*. However, diazepam is known to have very poor *i.m.* bioavailability (Reddy and Reddy 2015, Ulu, Inceoglu et al. 2016); therefore, diazepam was injected *i.p.* at 5 mg/kg, a dose that reaches therapeutic concentrations in the brain (Ulu, Inceoglu et al. 2016). Diazepam administered *i.p*. at $\geq$5 mg/kg is used by multiple laboratories in animal models of acute OP intoxication (Auta, Costa et al. 2004, Zhang, Todorovic et al. 2017, Matson, Dunn et al. 2019). A single autoinjector provided in the ChemPack for human use contains 10 mg midazolam, which based on allometric scaling (Nair and Jacob 2016) is approximately 0.73 mg/kg midazolam in the adult rat.

DFP Exposure and Seizure Monitoring

Animals were pretreated with pyridostigmine bromide (0.1 mg/kg *i.p.*; TCI America, Portland, USA; >98% purity), a reversible cholinesterase inhibitor, in sterile saline 30 min prior to DFP injection to minimize peripheral cholinergic symptoms (Kim, Hur et al. 1999). DFP (Sigma Chemical Company, St Louis, MO, USA) was prepared 5 min before administration in ice-cold

sterile phosphate-buffered saline (PBS, 3.6 mM Na_2HPO_4, 1.4 mM NaH_2PO_4, 150 mM NaCl; pH 7.2). DFP stocks were evaluated for purity using ^{1}H-, ^{13}C, ^{19}F, and ^{31}P-NMR methods (Gao, Naughton et al. 2016) and determined to be 90 ± 7% pure. Upon arrival, DFP aliquots were stored at -80 °C, a condition that maintains chemical stability for over 1 year (Heiss, Zehnder et al. 2016). Rats were injected between the shoulder blades with DFP at 4 mg/kg *s.c.*, a dosing paradigm previously shown to induce *status epilepticus* (Guignet, Dhakal et al. 2019) in 80-90% of DFP-injected animals (González, Rindy et al. 2020). Animals were then given a combined *i.m.* inner thigh injection of 2 mg/kg atropine-sulfate (Sigma; >97% purity) and 25 mg/kg pralidoxime (Sigma; >99% purity) in sterile saline (0.9% NaCl) within 1 min following DFP injection to increase survival. Atropine sulfate blocks peripheral muscarinic cholinergic receptors and pralidoxime reactivates peripheral acetylcholinesterase to minimize mortality in the DFP model from overstimulation of the parasympathetic nervous system (Bruun, Guignet et al. 2019). Vehicle control animals were similarly treated with atropine sulfate and pralidoxime but were injected with 300 µl ice-cold sterile saline *s.c.* in place of DFP. At 40 min post-DFP exposure, animals were administered diazepam, midazolam, or an equal volume (~300 µl) of saline vehicle (*i.p.* or *i.m.*) with *i.m*. injections administered to the inner thigh of the hind leg.

Immediately following injection, all animals were monitored for seizure behavior for 4 h and the severity of seizure behavior scored using a seizure behavior scale established for use in rat models of acute OP intoxication (Deshpande, Carter et al. 2010). Two experimenters without knowledge of experimental group independently monitored animals in real-time, and scores from both experimenters were averaged for each observation. The scores for each animal were averaged over time to obtain an individual average seizure score. At 40 min post-DFP administration, DFP animals were further randomized into one of three groups: DFP alone, DFP + diazepam (referred

to as the diazepam group), or DFP + midazolam (referred to as the midazolam group). Only animals with consecutive seizure scores of $\geq$3 were selected for these groups to ensure that all animals used in the study experienced DFP-induced *status epilepticus* (Deshpande, Carter et al. 2010, Phelan, Shwe et al. 2015). At the end of the 4 h observation period animals were injected *s.c.* with 10 ml 5% dextrose in 0.9% isotonic saline (Baxter International, Deerfield, IL, USA) prior to being returned to their home cages. Animals were provided access to moistened chow until they resumed consumption of solid chow. In the subsequent days to weeks to months, these animals were evaluated by magnetic resonance (MR) and positron emission tomography (PET) imaging with each animal experiencing up to three separate imaging sessions. The data from these *in vivo* imaging studies are described in a separate manuscript (Hobson et al., under review). At 3 or 6 months post-exposure, subjects were anesthetized with isoflurane/O_2 (Piramal Healthcare, Bethlehem, Pennsylvania) using 2.0%–3.0% vol/vol to induce and 1.0%–2.0% vol/vol to maintain anesthesia for micro-CT imaging. Animals were then euthanized with 4% isoflurane and transcardially perfused using a Masterflex peristaltic pump (Cole Parmer, Vernon Hills, IL, USA) and 100 ml cold PBS at a flow rate of 15 ml/min. A subset of animals underwent micro-CT imaging at both 3 and 6 months post-DFP prior to euthanasia. Sample sizes for each endpoint were determined using a two-tailed power analysis, with effect size calculated using previously generated preliminary data.

Micro-CT Imaging

At 3 and 6 months post-DFP intoxication, the brains of living animals were imaged with an Inveon Multi-Modality CT scanner (Siemens Healthineers, Munich, Germany) at the University of California, Davis Center for Molecular and Genomic Imaging. A subset of animals underwent micro-CT imaging at both 3 and 6 months post-DFP prior to euthanasia. Sample sizes for each

endpoint were determined using a two-tailed power analysis, with effect size calculated using previously generated preliminary data. Animals were anesthetized with isoflurane/O_2 (Piramal Healthcare, Bethlehem, PA, USA) using 2.0-3.0% isoflurane v/v to induce and 1.0-2.0% isoflurane v/v to maintain anesthesia. Once anesthetized, animals were stereotactically restrained in custom beds for imaging in the CT scanner. Voltage and beam current were set to 80kVp and 425 µA, respectively. A 0.5-mm aluminum filter was used to harden the beam. The detector was set to image at 4096 x 2048 using bin 2 with a low magnification resulting in a voxel size of 48.26 µm. Projections were taken over 360^o in 1^o steps with a 1000-ms exposure time. Scans were reconstructed using a Feldkamp algorithm (Yamamoto, Suzuki et al. 2007) with Shepp-Logan filter into 16 bit values. A subset of animals were images at both 3 and 6 months, generating larger sample sizes at the 3 month time point relative to the 6 month time point.

Images were analyzed using Amira software version 6.5.0 (Thermo Fisher Scientific). ROIs for the medial and dorsolateral thalamus were drawn on previously acquired T2w images using the magnetic lasso tool (Amira software). A small number of animals (0-1 per experimental group) were excluded due to image artifacts that confounded quantitative analysis. All image analysis was performed completely blinded to group and time point. A non-local means filter was applied to all micro-CT scans to decrease the noise in the images while maintaining image clarity (Chen, Arad et al. 2018). Micro-CT scans were manually aligned with MR scans for anatomical reference. An intensity threshold (intensity value $\geq$ 450) was applied to micro-CT scans to isolate areas of mineralization as individual ROIs in the brain. Quantitative data was only obtained from the automatically calculated three-dimensional mineral deposits. The volumes of the medial thalamus, dorsolateral thalamus, and mineralization ROIs were exported from Amira. The percent mineralization was calculated and used to conduct statistical analysis.

Two-dimensional cross-sections were selected from each group to visually represent mineralization from the raw micro-CT images.

Neuropathologic analyses

At 3 months post-DFP, approximately half of all animals were randomly selected for euthanasia to collect brains for neuropathologic analyses. The remaining animals were euthanized at 6 months post-DFP. FluoroJade-C staining was performed as previously described (Hobson, Rowland et al. 2017). Briefly, following euthanasia, brains were harvested and immediately cut into 2-mm coronal sections starting at bregma point 0 and post-fixed in 4% paraformaldehyde solution (Sigma) in PBS for 24 h at 4 °C. Brain sections were then equilibrated in 30% w/v sucrose (Thermo Fisher Healthcare, Waltham, MA, USA) in PBS at 4 °C overnight, embedded in OCT medium (Thermo Fisher Healthcare), and then cryosectioned into 10-µm slices onto Superfrost Plus slides (Thermo Fisher Healthcare). Sections were then dehydrated in 70% ethanol, incubated in 0.06% potassium permanganate w/v (Sigma) in distilled water for 10 min, incubated in distilled water for 2 min, and incubated in 0.0001% w/v FluoroJade-C (Cat #AG325; Millipore, Billerica, MA, USA) in 0.1% v/v acetic acid (Acros Organics, Geel, Belgium) in distilled water for 10 min. The FluoroJade-C solution contained a 1:50,000 dilution of DAPI (Invitrogen, Carlsbad, CA, USA). Slides were dried at 50 °C for 5 min, cleared in chemical grade xylene (Fisher Chemical, Waltham, MA, USA) for 1 min, and mounted in 50 µl of Permount (Thermo Fisher Scientific, Waltham, MA).

For immunohistochemistry, sections were processed for antigen retrieval using a 10 mM sodium citrate solution (pH 6.0) in distilled water for 20 min at 90 ^{o}C followed by 3 washes in PBS for 10 min. Sections were then blocked in a blocking solution of PBS containing 10% w/v goat serum (Vector Laboratories, Burlingame, CA, USA), 1% w/v bovine serum albumin

(Sigma), and 0.03% w/v Triton X-100 (Thermo Fisher Scientific) for 1 h at room temperature, followed by incubation with primary antibodies in blocking solution at 4 ^{o}C overnight. The primary antibodies used in this study were mouse anti-glial fibrillary acidic protein (GFAP, 1:1000, Cell Signaling Technology, Danvers, MA, USA; Cat# 3670, RRID:AB_561049), rabbit anti-S100 calcium-binding protein β (S100β, 1:500, Abcam, Cambridge, UK; Cat# ab14688, RRID:AB_2184443), rabbit anti-ionized calcium-binding adapter molecule 1 (IBA-1, 1:1000, Wako Laboratory Chemicals, Richmond, VA, USA; Cat# 019-19741, RRID:AB_839504), mouse anti-CD68 (1:200, Serotec, Hercules, CA, USA; Cat# MCA341R, RRID:AB_2291300), mouse anti-NeuN (1:1000, Millipore; Cat# MAB377, RRID:AB_2298772), and rabbit anti-3-nitrotyrosine (1:200, Millipore; Cat# 06-284, RRID:AB_310089). Sections were triple-washed in PBS followed by 0.03% w/v Triton X-100 in PBS for 10 min and then incubated in secondary antibody in blocking solution for 90 min at room temperature in complete darkness. The secondary antibody used for IBA-1 was Alexa Fluor 568-conjugated goat anti-rabbit IgG (1:500, Life Technologies, Carlsbad, CA, USA; Cat# A-21069, RRID:AB_2535730); for CD68, Alexa Fluor 488-conjugated goat anti-mouse IgG (1:500, Life Technologies; Cat# A-11001, RRID:AB_2534069); for GFAP and NeuN, Alexa Fluor 568-conjugated goat anti-mouse IgG_1 (γ1) (1:1000, Life Technologies; Cat# A-21124, RRID:AB_2535766); and for 3-NT and S100β, Alexa Fluor 488-conjugated goat anti-rabbit IgG (1:500, Life Technologies; Cat# A-11034, RRID:AB_2576217). Following incubation in secondary antibody, sections were triple-washed with PBS followed by 0.03% w/v Triton X-100 in PBS for 10 min before cover slipping using ProLong Gold Antifade Mountant with DAPI (Invitrogen). Negative controls were incubated with blocking buffer containing no primary antibody and subsequently stained using identical protocols.

Fluorescent immunoreactivity was visualized using an ImageXpress XL High-Content Imaging System at 20X magnification (Molecular Devices, Sunnyvale, CA, USA). Images were acquired from the amygdala, hippocampus (CA1, CA3, and dentate gyrus), piriform cortex, and somatosensory cortex between -3.6-mm to -4.2-mm posterior to bregma and the dorsolateral thalamus between -3.0-mm to -3.6-mm posterior to bregma. A rat brain atlas was used to verify that homologous bregma ranges were assessed between animals (Kruger, Saporta et al. 1995). A small number of animals (0-1 per experimental group) were excluded due to poor image quality that confounded statistical analyses.

Fluorescent immunostaining was quantified as previously described (Guignet, Dhakal et al. 2019). Briefly, for dual staining of IBA-1/CD68 and NeuN/3-nitrotyrosine, immunopositive cells were quantified in two consecutive sections using the Multi-Wavelength Cell Sorting Journal within the Custom Module Editor of the MetaXpress High-Content Image Acquisition and Analysis software (version 5.3, Molecular Devices) combined with a Matlab script (Matlab 2014b, The Mathworks Inc., Natick, MA, USA) for Otsu's method background subtraction (Otsu 1979) to identify the percentage of IBA-1 or NeuN positive cells that also expressed CD68 or 3-nitrotyrosine, respectively. For GFAP and S100β staining, the area of immunofluorescence respective to the total area of the ROI was analyzed separately following normalization to a background-subtracted image and binarization using ImageJ (version 1.48, National Institutes of Health, Bethesda, MD, USA). Positive staining was identified as fluorescence intensity that, at a minimum, was twice that of the background fluorescence levels observed in negative control images. To preclude bias, all image acquisition and analyses were performed by a single experimenter without knowledge of exposure group or time point.

Data and Statistical Analysis

Time-weighted seizure scores were calculated for each individual animal to account for time as a variable. Once a score was obtained for each individual animal, a one-way ANOVA with post-hoc Kruskal-Wallis test to calculate statistical differences between treatment groups. For neuropathology measures, primary outcomes of interest included the total number of FluoroJade-C stained cells, percentage of IBA-1+ cells, percentage of IBA-1+ that also co-expressed CD68, percentage of NeuN+ cells that were also immunoreactive for 3-nitrotyrosine, percentage of total cells that were NeuN+, percent area of GFAP immunoreactivity, and percent area of S100β immunoreactivity in seven brain regions for each animal. Percent mineralization, measured by micro-CT as described above, was also available for two brain regions for each animal. Raw data points for each neuropathologic outcome are shown in supplemental figures 3-S1-8.

Mixed-effect regression models, including animal-specific random effects, were used to assess differences between exposure groups by region and time point. Exploratory analysis indicated that a natural logarithmic transformation was needed for all outcomes, except percentage of NeuN+ cells, to stabilize the variance and meet the underlying assumptions of normality for the mixed effects models. Due to observed zeroes for these outcomes, all values were shifted by 0.5 prior to taking the natural logarithm. Primary factors included in the statistical analyses were exposure group (vehicle, DFP, diazepam, midazolam), brain region (which for immunohistochemistry outcomes included the thalamus, dentate gyrus, CA1, CA3, amygdala, somatosensory cortex, piriform cortex; but for micro-CT outcome included the medial thalamus, dorsolateral thalamus), and time point (3 or 6 months post-DFP). Interactions between these variables were also considered. Akaike information criterion was used for model selection to identify the best model for each outcome. Specific contrasts were constructed to test groups of

interest (DFP vs. vehicle, midazolam vs. DFP, diazepam vs. DFP, and diazepam vs. midazolam) and examined using Wald tests. Within an outcome, Benjamini-Hochberg False Discovery Rate (Benjamini and Hochberg 1995) was used to correct for multiple comparisons between groups; therefore, a false discovery rate-adjusted p-value<0.05 was considered statistically significant.

Results for all log-transformed outcomes are presented as geometric mean ratios. These ratios may be interpreted as fold changes, so that a ratio of 1.5 corresponds to a 50% increase and a ratio of 0.5 corresponds to a 50% decrease. Point estimates of the ratios and the 95% confidence intervals are presented in the figures. When the confidence interval includes 1, there is no statistical evidence of a difference between groups. However, when the confidence interval does not include 1, the estimated effect is significant at the 5% level ($p \leq 0.05$). Results for the non-transformed outcome are presented as average differences between groups along with the 95% confidence interval. All analyses were conducted using SAS (version 9.4, SAS Institute, Inc., Cary, NC, USA), and graphics were created in R (version 3.1.0, R Core Team, Vienna, Austria).

Results

Benzodiazepine pharmacokinetics and effects on DFP-induced seizure behavior

Naïve adult male rats were administered diazepam (5 mg/kg, *i.p.*) or MDZ (0.73 mg/kg, *i.m.*) and euthanized at varying times post-administration to collect serum and brain samples (**Figure 2-2A**). Peak concentrations of diazepam were reached within the first hour post-administration and were ~3-fold higher in the brain than the plasma. The brain to plasma ratio for diazepam was ~3.5. Peak concentrations of midazolam were reached at 10 min and were only slightly higher in brain tissue compared to plasma. Brain levels of midazolam remained slightly higher than

plasma until 4 h when both concentrations fell below 10 nM. The greatest difference between brain and plasma concentrations of midazolam was observed at 40 min when brain levels were almost 2-fold higher than plasma levels. The brain to plasma ratio was ~1.2-2.1. Direct comparison showed higher brain concentrations of midazolam than diazepam at 10 and 30 min, but comparable concentrations at all other time points. Midazolam and diazepam were effectively eliminated and no longer pharmacologically active by 4 h in both brain and plasma. These pharmacokinetic profiles are consistent with prior literature for both diazepam (Fenyk-Melody, Shen et al. 2004, Ulu, Inceoglu et al. 2016) and midazolam (Arendt, Greenblatt et al. 1987, Miyamoto, Matsueda et al. 2015) and suggest that midazolam enters the brain more rapidly and at higher concentrations than diazepam.

To assess the relative efficacy of diazepam vs. midazolam in terminating OP-induced seizures, seizure behavior was scored in vehicle and DFP-exposed animals for 4 h post-injection using an established seizure behavior scale (**Figure 2-2B**). DFP animals demonstrated seizure behavior within 6-8 minutes following DFP administration and continued seizing for the duration of the 4 h monitoring period. For the first 2.5 hours, DFP animals maintained severe seizure scores (≥ 3) that then began to decline slightly. Animals treated with diazepam at 40 min post-DFP intoxication showed markedly reduced seizure scores within 20 min of diazepam administration. For the last 2 hours of seizure monitoring, diazepam-treated animals showed seizure scores of ~2, which are below the threshold of clonic seizures that are thought to be consistent with *status epilepticus* (Deshpande, Carter et al. 2010, Phelan, Shwe et al. 2015). Similarly, midazolam-treated animals showed decreased seizure behavior within 20 min and also maintained seizure scores of ~2 through the rest of the seizure monitoring period. Although both

diazepam and midazolam attenuated seizure behavior, neither benzodiazepine reduced seizure behavior to baseline levels observed in vehicle control animals.

Seizure scores collected at individual time points post-injection for each individual animal were averaged to obtain an average seizure score over the 4 h period for that animal. Average seizure scores for each group confirmed that DFP animals experienced significant seizure behavior, as previous studies indicate that prolonged seizure scores of ≥ 3 are consistent with *status epilepticus* (Deshpande, Carter et al. 2010, Phelan, Shwe et al. 2015). These data also confirmed that post-exposure treatment with either diazepam or midazolam significantly attenuated, but did not completely block, DFP-induced seizure behavior. Importantly, there were no significant differences in average seizure scores between DFP + diazepam and DFP + midazolam animals.

Neurodegeneration is transiently reduced by midazolam

FluoroJade-C staining was used to visualize degenerating or recently degenerated neurons (Schmued, Stowers et al. 2005) in multiple brain regions, including the CA1, CA3 and dentate gyrus of the hippocampus, the amygdala, piriform and somatosensory cortex, and the thalamus at 3 and 6 months after acute intoxication with DFP (**Figure 2-3A**). The number of FluoroJade-C-labeled cells differed between groups by time point ($F(3, 204)=3.82$, $p=0.01$) but not by brain region. Therefore, estimates of group differences at each time point were averaged across brain regions. At both 3 ($t(204)=3.78$, $p=0.0002$) and 6 months ($t(204)=6.44$, $p<0.0001$), DFP animals had a significantly increased number of FluoroJade-C-labeled cells relative to vehicle animals in all brain regions (**Figure 2-3B**). While there was a trend towards significance at 3 months, diazepam-treated DFP animals did not have significantly decreased FluoroJade-C labeling at 3 or 6 months. At 3 months, midazolam significantly decreased FluoroJade-C labeling ($t(204)=-2.38$,

p=0.018); however, by 6 months, there was no significant difference between DFP animals that did not receive benzodiazepine vs. DFP animals that were treated with midazolam. The difference between DFP and vehicle animals remained significant after false discovery rate correction. There were no differences between diazepam and midazolam-treated DFP animals at either time point.

Midazolam reduces reactive astrogliosis in more brain regions than diazepam

Reactive astrogliosis was measured using GFAP (**Figure 2-4A**) and S100β (**Figure 2-5A**) immunoreactivity to capture unique populations of astrocytes (reviewed in Holst, Brochner et al. 2019). The difference between groups in percent area of GFAP immunoreactivity varied by brain region ($F(18,188)=4.04$, $p<0.0001$) but not by time point. Thus, estimates of group differences by brain region were averaged across time points. The percent area of GFAP immunoreactivity was significantly increased in DFP compared to vehicle animals in all seven brain regions examined (**Figure 2-4B**, $p<0.005$). In the initial mixed-effect comparison, DFP animals treated with diazepam had significantly reduced GFAP expression in the hippocampal CA1 subregion ($t(188)=-2.11$, $p=0.036$) and somatosensory cortex ($t(188)=-2.04$, $p=0.043$) compared to DFP animals that did not receive any benzodiazepine, but these differences did not remain significant after false discovery rate correction. Treatment with midazolam significantly decreased GFAP expression in the CA1 ($t(188)=-4.01$, $p<0.0001$), CA3 ($t(188)=-2.37$, $p=0.019$), and dentate gyrus ($t(188)=-2.48$, $p=0.014$) subregions of the hippocampus, as well as in the somatosensory cortex ($t(188)=-4.41$, $p<0.0001$) and thalamus ($t(188)=-2.36$, $p=0.019$) compared to DFP animals that did not receive any benzodiazepine, and these all remained significant after false discovery rate correction. There were no differences between diazepam or midazolam-treated DFP animals.

The percent area of S100β immunoreactivity also differed by brain region ($F(18,182)=5.95$, $p<0.0001$) but not by time point. The percent area of S100β immunoreactivity was significantly greater in DFP than vehicle animals in all brain regions studied, although the difference in the hippocampal CA3 and dentate gyrus did not remain significant after false discovery rate correction (**Figure 2-5B**). Diazepam decreased S100β expression in the hippocampal CA1 ($t(182)=-2.14$, $p=0.033$), dentate gyrus ($t(182)=-2.86$, $p=0.0047$) and somatosensory cortex ($t(182)=-3.16$, $p=0.0018$), although the difference in the CA1 did not remain significant after false discovery rate correction. Midazolam decreased S100β expression in the hippocampal CA1 ($t(182)=-2.66$, $p=0.0086$), somatosensory cortex ($t(182)=-4.56$, $p<0.0001$), and thalamus ($t(182)=-5.12$, $p<0.0001$), all of which remained significant after false discovery rate correction. DFP animals treated with diazepam had significantly increased S100β expression in the thalamus compared to DFP animals treated with midazolam ($t(182)=4.55$, $p<0.0001$), which remained significant after false discovery rate correction.

Neither midazolam nor diazepam reduces microglial activation

Microglial activation was measured as the percentage of cells within the field that were immunopositive for IBA-1 and by the percentage of IBA-1 immunopositive cells that were phagocytic, as identified by co-labelling for CD68 (**Figure 2-6A**). The differences between groups in percentage of IBA-1 immunopositive cells did not differ by brain region or time point (**Figure 2-6B**). DFP animals had a higher percentage of IBA-1 immunopositive cells than vehicle animals ($t(32)=2.12$, $p=0.04$), but this difference did not remain significant after false discovery rate correction. There was a significant difference between groups in the percentage of IBA-1 immunopositive cells that co-expressed CD68 ($F(3,32)=9.95$, $p<0.0001$), and this difference was similar across brain regions and time points. DFP animals showed an increased

percentage of CD68-labeled IBA-1 immunopositive cells compared to vehicle animals ($t(32)=5.34$, $p<0.0001$) that remained significant after false discovery rate correction. However, there were no differences between DFP animals treated with diazepam or midazolam compared to DFP animals not treated with any benzodiazepine. Furthermore, there was no difference between diazepam and midazolam-treated DFP animals.

DFP-induced oxidative stress returns to baseline levels by 6 months post-intoxication

Previous studies have shown that biomarkers of oxidative stress increase in the rat brain following acute DFP intoxication (Pearson and Patel 2016) and persist up to 2 months post-intoxication (Guignet, Dhakal et al. 2019). Here, co-localization of 3-nitrotyrosine and NeuN immunoreactivity was used to determine whether oxidative stress in neurons persists at 3 and 6 months post-DFP exposure. The expression of 3-nitrotyrosine was normalized to the number of neurons (NeuN) (**Figure 2-7A**). While there were no significant differences in the number of NeuN+ cells between treatment groups, there was a trend towards decreased neuronal numbers in DFP animals relative to vehicle (**Figure 2-7B**). Similarly, there was no significant difference between groups in the number of cells co-labeled for 3-nitrotyrosine and NeuN, but there was a strong trend towards increased expression in DFP animals relative to vehicle.

3.6 Diazepam is more effective than midazolam in mitigating mineralization in the medial thalamus

Acute OP intoxication produces pronounced calcium dysregulation (reviewed in Deshpande, Blair et al. 2016), thus, we used *in vivo* micro-CT imaging to monitor the formation and presence of mineral inclusions in the medial and dorsolateral thalamus of DFP-intoxicated rats at 3 and 6 months (**Figure 2-8A and 2-8B**). Two-dimensional cross-sections of microCT images (color) overlaid on anatomical MRI images (grayscale) show focal areas of mineralization in the 48-

micron thick slice (**Figure 2-8A**). The difference in percent mineralization between groups, which was quantified from three-dimensional reconstructions of mineralized areas, varied by both time point and brain region. DFP animals had a higher percent mineralization than vehicle animals at both time points and both brain regions (**Figure 2-8C**, $p<0.05$). Diazepam decreased mineralization in the medial, but not dorsolateral, thalamus at both 3 ($t(50)=-2.97$, $p=0.0045$) and 6 months ($t(50)=-2.44$, $p=0.018$). Midazolam decreased mineralization in the medial thalamus at 6, but not 3, months ($t(50)=-2.41$, $p=0.02$); midazolam had no significant protective effect on mineralization in the dorsolateral thalamus at either time point. Diazepam-treated DFP animals had a lower percent of mineralization than midazolam-treated DFP animals in the medial thalamus ($t(50)=-2.76$, $p=0.0081$) at 3 months but not at 6 months. All differences remained significant after false discovery rate correction.

Discussion

Previous work has demonstrated that DFP-induced *status epilepticus* triggers neuroinflammation in the days to weeks following acute intoxication (Liu, Li et al. 2012, Li, Lein et al. 2015, Flannery, Bruun et al. 2016, Wu, Kuruba et al. 2018). Here we show that robust neuroinflammation persists at 3 and 6 months post-DFP intoxication, as evidenced by increased expression of IBA-1, CD68, GFAP, and S100β. We previously demonstrated that neuroinflammation measured by IBA-1 immunoreactivity was more severe at 1 month than 2 months post-DFP (Siso, Hobson et al. 2017, Guignet, Dhakal et al. 2020). The present findings demonstrate that IBA-1 immunoreactivity does not decrease with time but rather remains elevated in the brain at least until 6 months post-DFP. While IBA-1 is a marker of microglia, it also labels monocytes and macrophages (Ito, Imai et al. 1998), which may migrate from the

periphery to contribute to the inflammatory response in the brain. Thus, the elevated IBA-1 immunoreactivity we observe at 3 and 6 months post-exposure may indicate not only microgliosis, but also infiltration of peripheral immune cells into the brain. In contrast, reactive astrogliosis is relatively consistent in the brain with limited temporal or regional variability up to 2 months post-exposure (Siso, Hobson et al. 2017, Guignet, Dhakal et al. 2020), peaking later than either microgliosis or neuronal degeneration (Siso, Hobson et al. 2017). Consistent with these earlier reports, we saw relatively uniform GFAP reactivity across all seven brain regions that persisted at 3 and 6 months post-DFP exposure.

While our earlier study found that DFP-induced neurodegeneration declined to background levels by 2 months post-exposure (Siso, Hobson et al. 2017), here, we observed significant neurodegeneration at 3 and 6 months post-exposure in all seven brain regions examined. The increase in neurodegeneration at 3 and 6 months may contribute to the persistent microgliosis observed at these later time points. The delayed neurodegeneration observed in the DFP-intoxicated brain may be due in part to spontaneous recurrent seizures that develop in >80% of animals that survive OP-induced *status epilepticus* (de Araujo Furtado, Lumley et al. 2010, Guignet, Dhakal et al. 2020). Given the extensive literature implicating neuroinflammation in the pathogenesis of impaired cognition and epilepsy (reviewed in Guignet and Lein 2018), our data suggest a feed-forward model in which neuroinflammation promotes persistent electrographic and neurological deficits in the months following acute OP intoxication (Flannery, Bruun et al. 2016, Guignet, Dhakal et al. 2020), which in turn sustains the neuroinflammatory response. While neuroinflammation has yet to be causally linked to either the chronic cognitive deficits or electrographic abnormalities associated with acute OP intoxication, several studies have shown that anti-inflammatory compounds protect against some aspects of OP-induced neurological

damage (Finkelstein, Kunis et al. 2012, Li, Lein et al. 2012, Pan, Piermartiri et al. 2015, Piermartiri, Pan et al. 2015). These observations, together with our findings of persistent neuroinflammation, support neuroimmune modulation as a viable therapeutic strategy for protecting against OP-induced persistent neurological consequences.

Robust increases in the expression of biomarkers of oxidative stress have been documented in the hours and days immediately following acute DFP intoxication (Zaja-Milatovic, Gupta et al. 2009, López-Granero, Cañadas et al. 2013, Liang, Pearson-Smith et al. 2017, Chaubey, Alam et al. 2019). We previously observed oxidative stress in the rat brain at both 1 and 2 months post-DFP intoxication (Guignet, Dhakal et al. 2020). However, here, we observed low to negligible levels of 3-NT at 3 and 6 months post-exposure. The absence of oxidative stress despite persistent neuroinflammation is surprising given the typically close relationship between these activities (reviewed in Guignet and Lein 2018). One caveat of our study is that only one biomarker of oxidative stress was used, thus, follow-up studies evaluating additional markers of oxidative stress at these later time points would be useful to further understand the temporal profile of oxidative damage in this model.

A novel finding of this study was the significant mineralization in the thalamus of DFP-intoxicated animals detected by micro-CT imaging at both 3 and 6 months post-exposure. While this technique does not identify the chemical composition of mineral deposits, calcium is a primary constituent of mineral deposits detected by micro-CT and calcium deposits frequently occur in the thalamus (Valdes Hernandez Mdel, Maconick et al. 2012). Additionally, *status epilepticus* and the associated glutamatergic excitotoxicity have been shown to increase intracellular calcium concentrations to pathogenic levels (reviewed in Deshpande, Blair et al. 2016, Maher, van Leyen et al. 2018). Although calcium is likely a primary component of the

mineral deposits we observed, iron, copper, and manganese have also been identified as significant components of mineralized areas in damaged brain tissue (Valdes Hernandez Mdel, Maconick et al. 2012). Follow-up studies evaluating the chemical composition of mineral deposits are needed to better understand this aspect of the chronic pathophysiology of acute DFP intoxication.

To the best of our knowledge, this is the first report of mineral deposits in the brain of acute OP-intoxicated animals. Although the functional consequences of cerebral mineral deposits are poorly understood, calcium dyshomeostasis is associated with altered neuronal activity and impaired cognition (Kirkland, Sarlo et al. 2018, Lerdkrai, Asavapanumas et al. 2018, Muller, Ahumada-Castro et al. 2018). Additionally, mineral deposits occur naturally in the aging brain, contributing to age-related cognitive decline (reviewed in Youssef, Capucchio et al. 2016). The presence of persistent mineral deposits in the brains of DFP-intoxicated animals suggest the intriguing possibility that acute DFP intoxication accelerates the onset and/or progression of aging phenotypes. Our findings also support the possibility that stabilizing calcium levels will protect against chronic OP-induced neuropathology. Indeed, the calcium-stabilizing compound dantrolene was recently shown to protect against OP-induced neurodegeneration at 2 d post-intoxication (Deshpande, Blair et al. 2016). While additional research is required to evaluate the causal relationship between calcium dysregulation and neurological function following acute OP intoxication, our data suggest that monitoring mineralization by micro-CT may be a non-invasive, longitudinal biomarker of neuropathology.

Our results demonstrate that diazepam and midazolam partially mitigate the long-term neuropathological consequences of acute DFP intoxication. While these benzodiazepines reduced acute seizure behavior to comparable levels, at 3 months post-DFP exposure, midazolam

conferred protection against neurodegeneration whereas diazepam did not, but diazepam protected against mineralization while midazolam did not. However, neither drug significantly reduced neurodegeneration at 6 months, and both were only partially protective against mineralization at 6 months. Neither midazolam nor diazepam reduced microglial activation at 3 or 6 months post-DFP. While both compounds reduced reactive astrogliosis, midazolam reduced both GFAP and S100β immunoreactivity, whereas diazepam only reduced S100β expression. Additionally, midazolam protected against neuroinflammation in more brain regions than diazepam. Interestingly, neither benzodiazepine was effective in protecting against DFP-induced astrogliosis in the piriform cortex or amygdala. $GABA_A$ receptor subunits are heterogeneously distributed in the brain (Mennini and Gobbi 1990, Nutt 2006); thus, regional differences in the $GABA_A$ subunit composition likely contribute to the region-specific neuroprotection observed in the brain of DFP animals treated with benzodiazepines. The α5 subunit is reported to play an important role in the inhibitory response to benzodiazepines (Etherington, Mihalik et al. 2017), and expression of the α5 subunit is very low in the amygdala and piriform cortex (Pirker, Schwarzer et al. 2000). While benzodiazepines bind primarily to synaptic $GABA_A$ receptors, the α5 subunit is highly expressed in both synaptic and extrasynaptic receptors. Should this subunit play a role in neuroprotection following OP intoxication, compounds that target extrasynaptic $GABA_A$ receptors, such as neurosteroids, may confer additional neuroprotection.

Benzodiazepine administration within 10 min after acute DFP intoxication has been reported to protect the brain against acute neuropathology (Kuruba, Wu et al. 2018, Wu, Kuruba et al. 2018). However, delaying benzodiazepine treatment more than 10 min post-exposure offers only partial neuroprotection in the days following OP intoxication (Gilat, Kadar et al. 2005, Kuruba, Wu et al. 2018, Wu, Kuruba et al. 2018, Spampanato, Pouliot et al. 2019). Our data extend these

previous studies by demonstrating that delayed administration of benzodiazepines also fails to provide neuroprotection at months post-exposure, and by showing that neither benzodiazepine provides a neuroprotective advantage relative to the other. Unfortunately, many victims of acute OP intoxication will not receive immediate medical attention (Jett and Spriggs 2020). This sobering fact coupled with our findings that neither diazepam nor midazolam offers complete neuroprotection at 3 or 6 months post-DFP intoxication when administered at 40 min post-OP intoxication suggest the urgent need for neuroprotective therapeutics to complement the current standard of care.

Acknowledgements

We thank Dr. Suzette Smiley-Jewell (UC Davis CounterACT Center) for her assistance in editing this manuscript. This work was supported by the CounterACT Program, National Institutes of Health (NIH) Office of the Director and the National Institute of Neurological Disorders and Stroke (NINDS) [grant number U54 NS079202], predoctoral fellowships to E.A.G from the NINDS [grant number F31 NS110522], the NIH Initiative for Maximizing Student Development [grant number R25 GM5676520], and the ARCS Foundation, and predoctoral fellowships to B.A.H. and M.G. from the National Institute of General Medical Sciences [grant number T32 GM099608] and the David and Dana Loury Foundation. This project used core facilities supported by the UC Davis MIND Institute Intellectual and Developmental Disabilities Research Center (U54 HD079125). The sponsors were not involved in the study design, in the collection, analysis, or interpretation of data, in the writing of the report, or in the decision to submit the paper for publication.

Figures and Figure Legends

Figure 2-1

A.

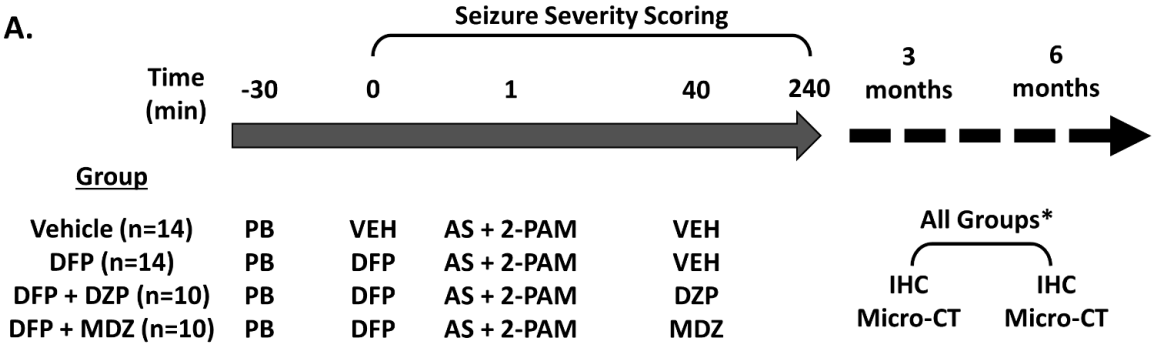

B.

Summary of sample sizes.

Endpoint(s) Evaluated	Sample Size (3 months)	Sample Size (6 months)	Figure
Fluoro-Jade C (FJC)	6 VEH, DFP 3 DZP, MDZ	8 VEH, DFP 4 DZP, MDZ	3
Immunohistochemistry[#]	6 VEH, DFP 3 DZP, MDZ	8 VEH, DFP 4 DZP, MDZ	4-7
Micro-CT	4 VEH, 12 DFP 6 DZP, 5 MDZ	7 VEH, 8 DFP 4 DZP, 4 MDZ	8

Figure 2-1. Experimental paradigm. (A) Adult male Sprague Dawley rats were pretreated with pyridostigmine bromide (PB) at 0.1 mg/kg (*i.p.*), and then randomly assigned to vehicle (VEH), DFP, DFP + diazepam (DZP) or DFP + midazolam (MDZ) groups. Vehicle (saline) or DFP (4 mg/kg, *s.c.*) were administered 30 min after pyridostigmine bromide, and followed 1 min later by *i.m.* injections of atropine sulfate (AS, 2 mg/kg) and pralidoxime (2-PAM, 25 mg/kg). At 40 min after DFP injection, vehicle (saline), diazepam (5 mg/kg, *i.p.*), or midazolam (0.73 mg/kg, *i.m.*) were administered, and animals were monitored for seizure activity for 4 h. At 3 and 6 months post-exposure, animals were imaged using *in vivo* micro-CT prior to euthanasia for neuropathologic assessments, including FluoroJade-C staining and immunohistochemical (IHC) analyses of neuroinflammation. *Three animals were removed from each of the diazepam and midazolam groups for separate analyses not included in this study; thus only 7 animals from these groups moved forward for IHC and micro-CT assessment at 3 and 6 months. (B) Summary of sample sizes used for outcome measures at 3 and 6 months post-exposure. A total of 14 vehicle, 14 DFP, 7 diazepam and 7 midazolam animals were available after the acute seizure analyses. At 3 months post-exposure, 4 vehicle, 12 DFP, 6 diazepam and 5 midazolam animals were successfully imaged using micro-CT, and 6 vehicle, 6 DFP, 3 diazepam and 3 midazolam were randomly selected to be euthanized to collect brains for histological analyses, leaving 8 vehicle, 8 DFP, 4 diazepam and 4 midazolam animals for the 6 month time point. For the micro-CT studies at 6 months, 7 vehicle, 8 DFP, 4 diazepam and 4 midazolam animals were successfully imaged. Following micro-CT imaging, 8 vehicle, 8 DFP, 4 diazepam and 4 midazolam animals were euthanized to collect their brains for histological analyses.
[#]Information from both time points were combined across groups for statistical analysis.

Figure 2-2

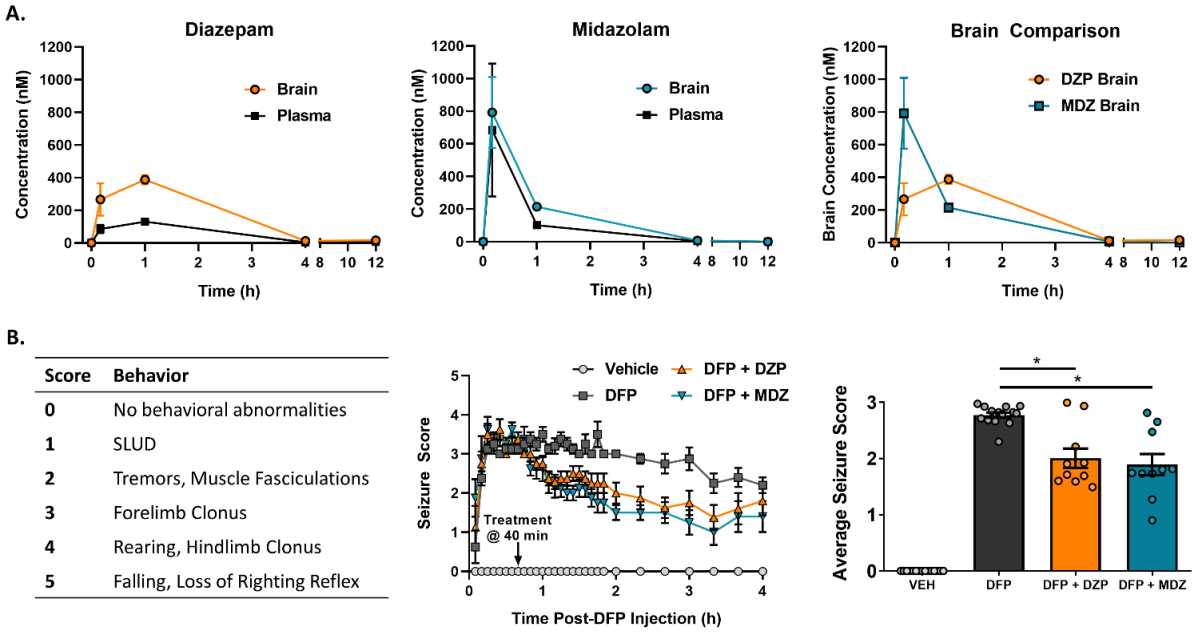
A.
Diazepam
Midazolam
Brain Comparison
Concentration (nM)
Brain Concentration (nM)
Time (h)
Brain
Plasma
DZP Brain
MDZ Brain
B.
Score
Behavior
0
No behavioral abnormalities
1
SLUD
2
Tremors, Muscle Fasciculations
3
Forelimb Clonus
4
Rearing, Hindlimb Clonus
5
Falling, Loss of Righting Reflex
Vehicle
DFP
DFP + DZP
DFP + MDZ
Seizure Score
Treatment
@ 40 min
Time Post-DFP Injection (h)
Average Seizure Score
VEH
DFP
DFP + DZP
DFP + MDZ

Figure 2-2. Benzodiazepine pharmacokinetics and pharmacodynamics. (A) Total diazepam (5 mg/kg, *i.p.*) and midazolam (0.73 mg/kg, *i.m.*) concentrations were measured in the brain and serum of naïve adult male rats at varying times post-administration. Data are presented as the mean ± SD (n=3-4 animals/time point). (B) Effect of diazepam and midazolam on DFP-induced seizure behavior. A modified Racine scale was used to score seizure behavior at 5 min intervals from 0-120 min post-DFP, and at 20-min intervals from 120-240 min post-DFP (≥ 10 observations per animal). The average seizure score was calculated as the time-weighted average of the animal's individual seizure scores across the 4 h of observation. Data presented as the mean ± SEM (n = 10-14 animals/group). *$p<0.05$ by one-way ANOVA with post-hoc Kruskal-Wallis test.

Figure 2-3

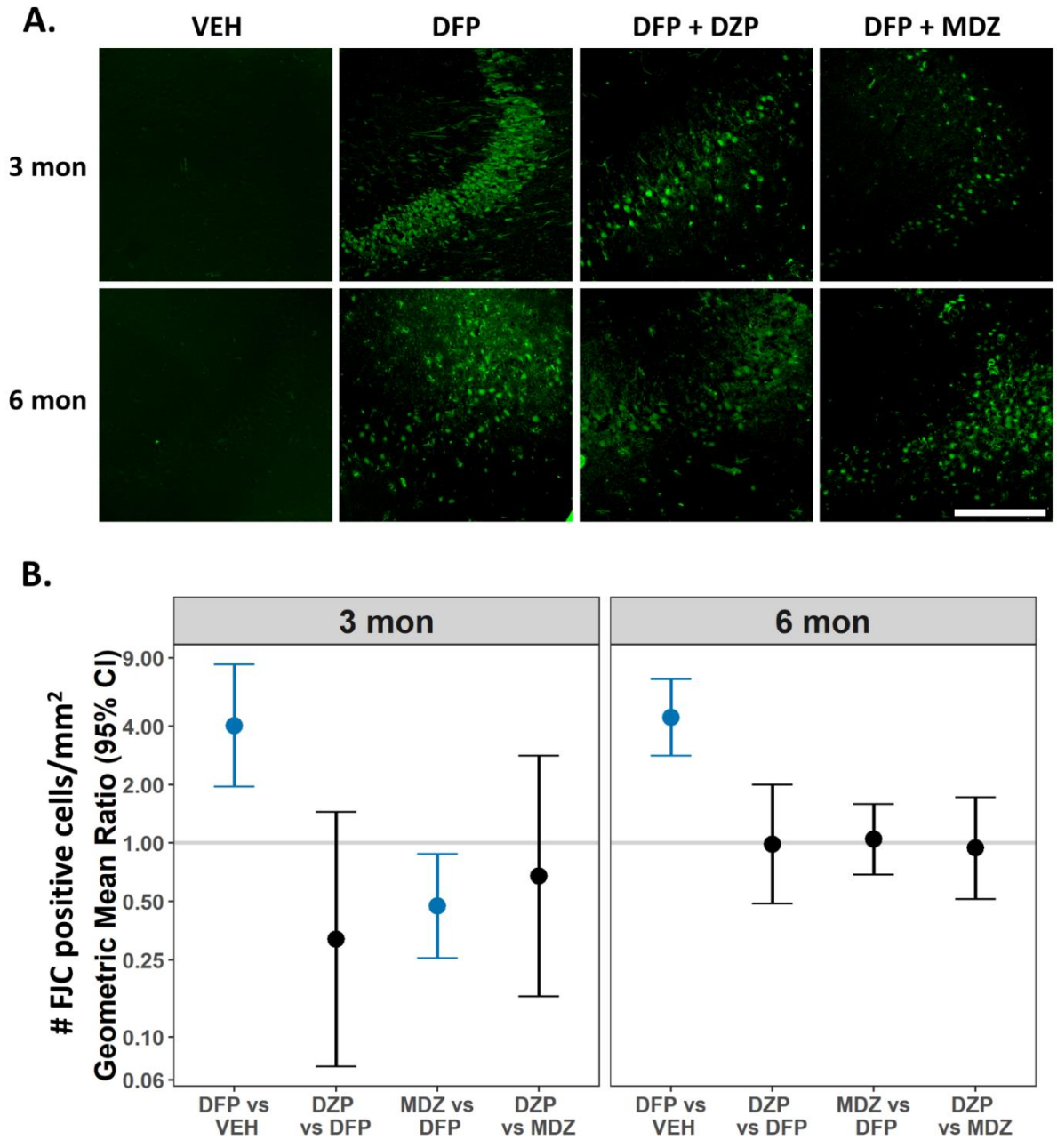
A.
VEH
DFP
DFP + DZP
DFP + MDZ
3 mon
6 mon
B.
3 mon
6 mon
FJC positive cells/mm²
Geometric Mean Ratio (95% CI)
9.00
4.00
2.00
1.00
0.50
0.25
0.10
0.06
DFP vs VEH
DZP vs DFP
MDZ vs DFP
DZP vs MDZ
DFP vs VEH
DZP vs DFP
MDZ vs DFP
DZP vs MDZ

Figure 2-3. DFP causes persistent neurodegeneration that persists at 6 months post-exposure even with benzodiazepine therapy. (A) Representative photomicrographs of FluoroJade C (FJC) staining in the CA1 subregion of the hippocampus at 3 and 6 months post-DFP exposure. Bar = 200 μm. (B) The number of FJC-labeled cells was quantified in seven brain regions (amygdala, CA1, CA3, and dentate gyrus of the hippocampus, piriform and somatosensory cortex, and thalamus) at 3 and 6 months post-DFP exposure. Estimates of exposure or treatment effects at each time point were averaged across brain regions as the group differences in number of FJC+ cells did not differ significantly between brain regions. Data are presented as the geometric mean ratio with 95% confidence interval (n = 5-6 vehicle, 5-8 DFP, 2-4 diazepam, 3-4 midazolam animals per time point). Confidence intervals that do not include 1.00 are colored blue and indicate a significant difference between groups at $p<0.05$. Raw data used to generate this figure are provided in the supplemental material (Fig. 3-S1).

Figure 2-4

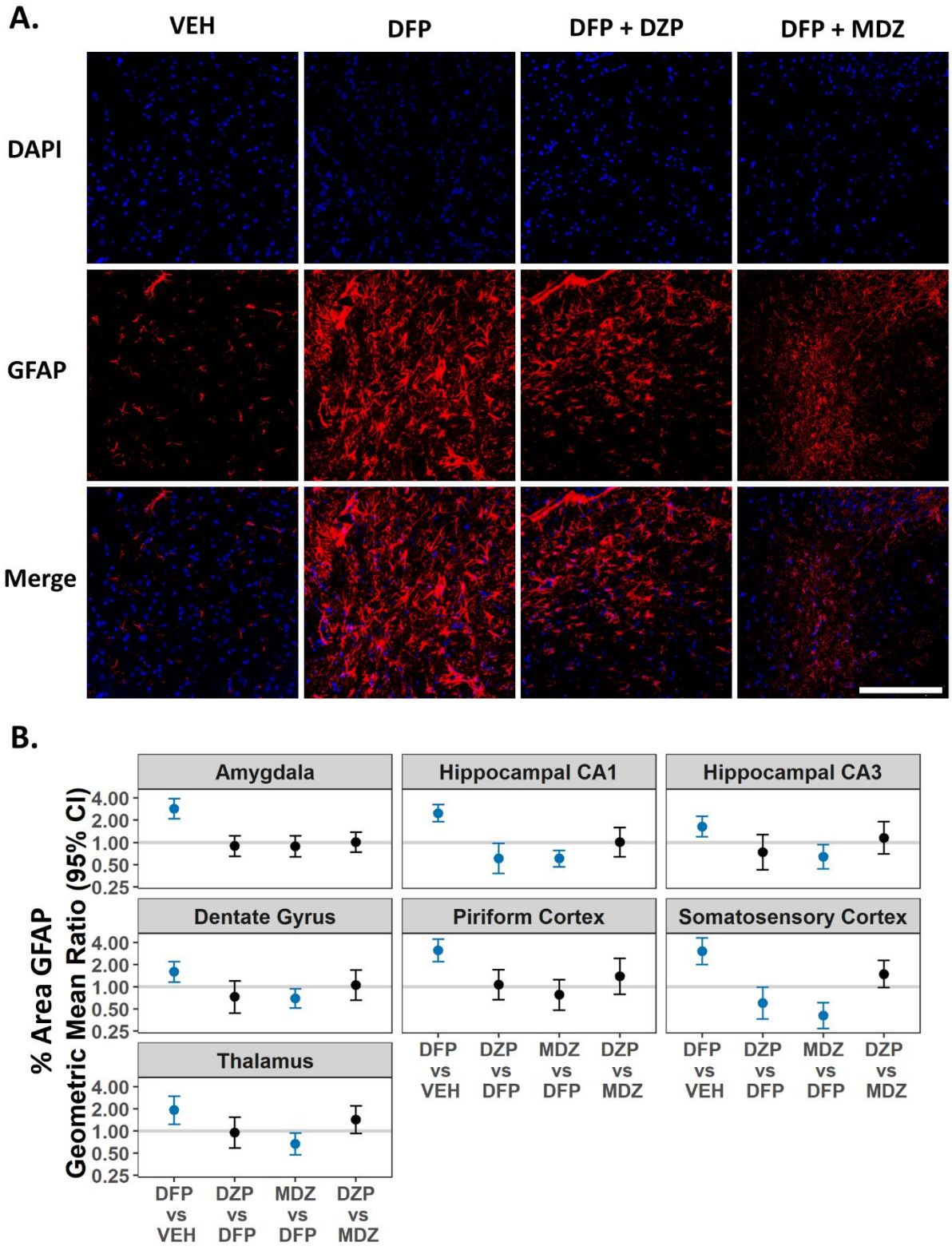
A.
VEH
DFP
DFP + DZP
DFP + MDZ
DAPI
GFAP
Merge
B.
% Area GFAP
Geometric Mean Ratio (95% CI)
Amygdala
Hippocampal CA1
Hippocampal CA3
Dentate Gyrus
Piriform Cortex
Somatosensory Cortex
Thalamus
4.00
2.00
1.00
0.50
0.25
DFP vs VEH
DZP vs DFP
MDZ vs DFP
DZP vs MDZ

Figure 2-4. Midazolam but not diazepam attenuates GFAP upregulation in some but not all brain regions. (A) Representative photomicrographs of GFAP immunoreactivity (reactive astrocytes, red) in the thalamus at 6 months post-exposure. Sections were counterstained with DAPI (blue) to label cell nuclei. Bar = 200 μm. (B) The percent area of GFAP immunoreactivity was quantified in seven brain regions at 3 and 6 months post-DFP exposure. Estimates of exposure or treatment effects by brain region were averaged across time points as group differences did not differ significantly between time points. Data are presented as the geometric mean ratio with 95% confidence intervals (n = 11 vehicle, 13 DFP, 6 diazepam, 7 midazolam animals combined across time points). Confidence intervals that do not include 1.00 are colored blue and indicate a significant difference between groups at $p<0.05$. Raw data used to generate this figure are provided in the supplemental material (Fig. 3-S2).

Figure 2-5

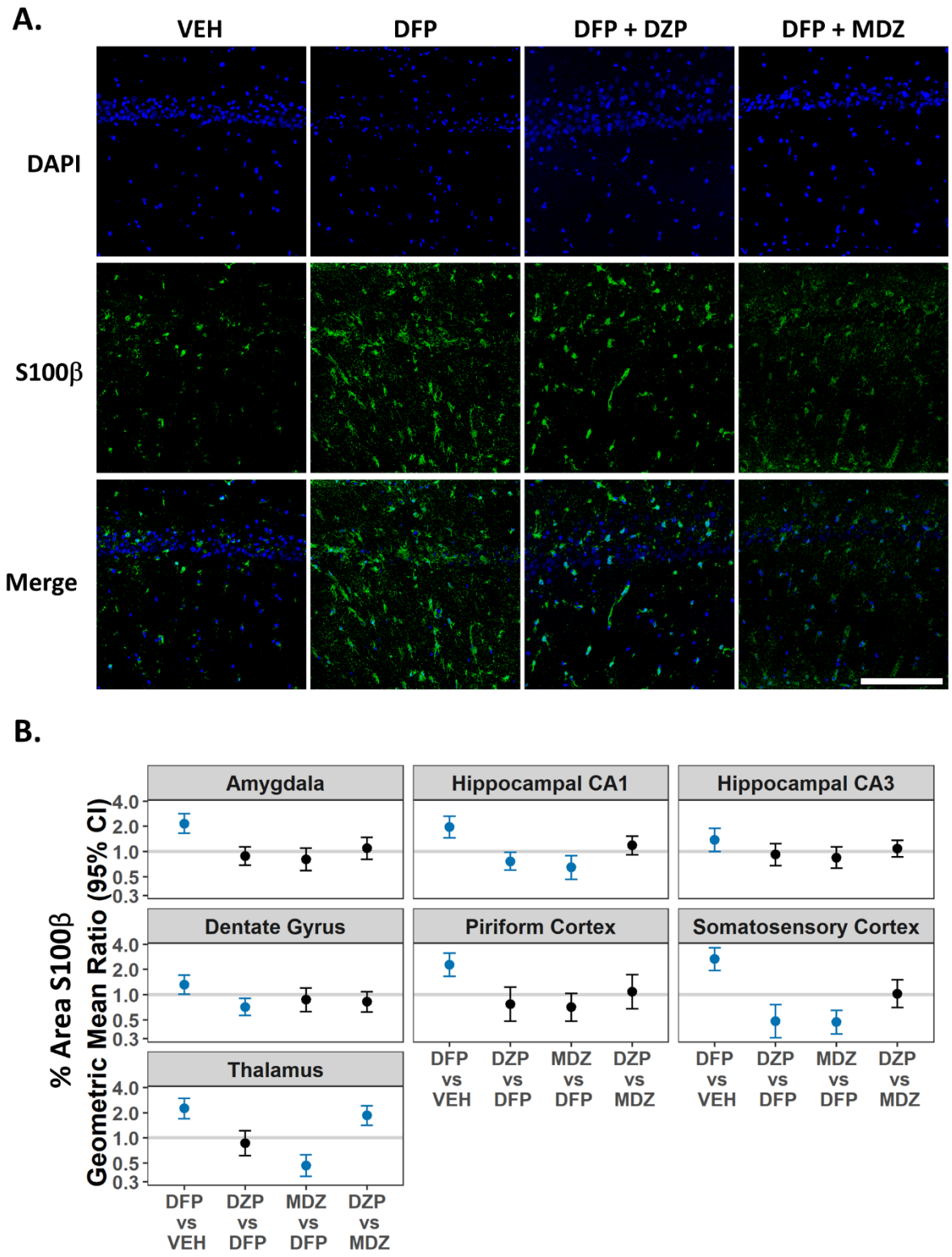
A.
VEH
DFP
DFP + DZP
DFP + MDZ
DAPI
S100β
Merge
B.
% Area S100β
Geometric Mean Ratio (95% CI)
Amygdala
Hippocampal CA1
Hippocampal CA3
Dentate Gyrus
Piriform Cortex
Somatosensory Cortex
Thalamus
4.0
2.0
1.0
0.5
0.3
DFP vs VEH
DZP vs DFP
MDZ vs DFP
DZP vs MDZ

Figure 2-5. Diazepam and midazolam reduce S100β immunoreactivity in a region-specific manner. (A) Representative photomicrographs of S100β immunoreactivity (astrocytes, green) in the CA3 subregion of the hippocampus at 6 months post-exposure. Sections were counterstained with DAPI (blue) to label cell nuclei. Bar = 200 μm. (B) The percent area of S100β immunoreactivity was quantified in seven brain regions at 3 and 6 months post-DFP exposure. Estimates of exposure or treatment effects by brain region were averaged across time point as group differences did not differ significantly between time points. Data are presented as the geometric mean ratio with 95% confidence intervals (n = 11 vehicle, 13 DFP, 6 diazepam, 7 midazolam animals combined across time points). Confidence intervals that do not include 1.00 are colored blue and indicate a significant difference between groups at $p<0.05$. Raw data used to generate this figure are provided in the supplemental material (Fig. 3-S3).

Figure 2-6

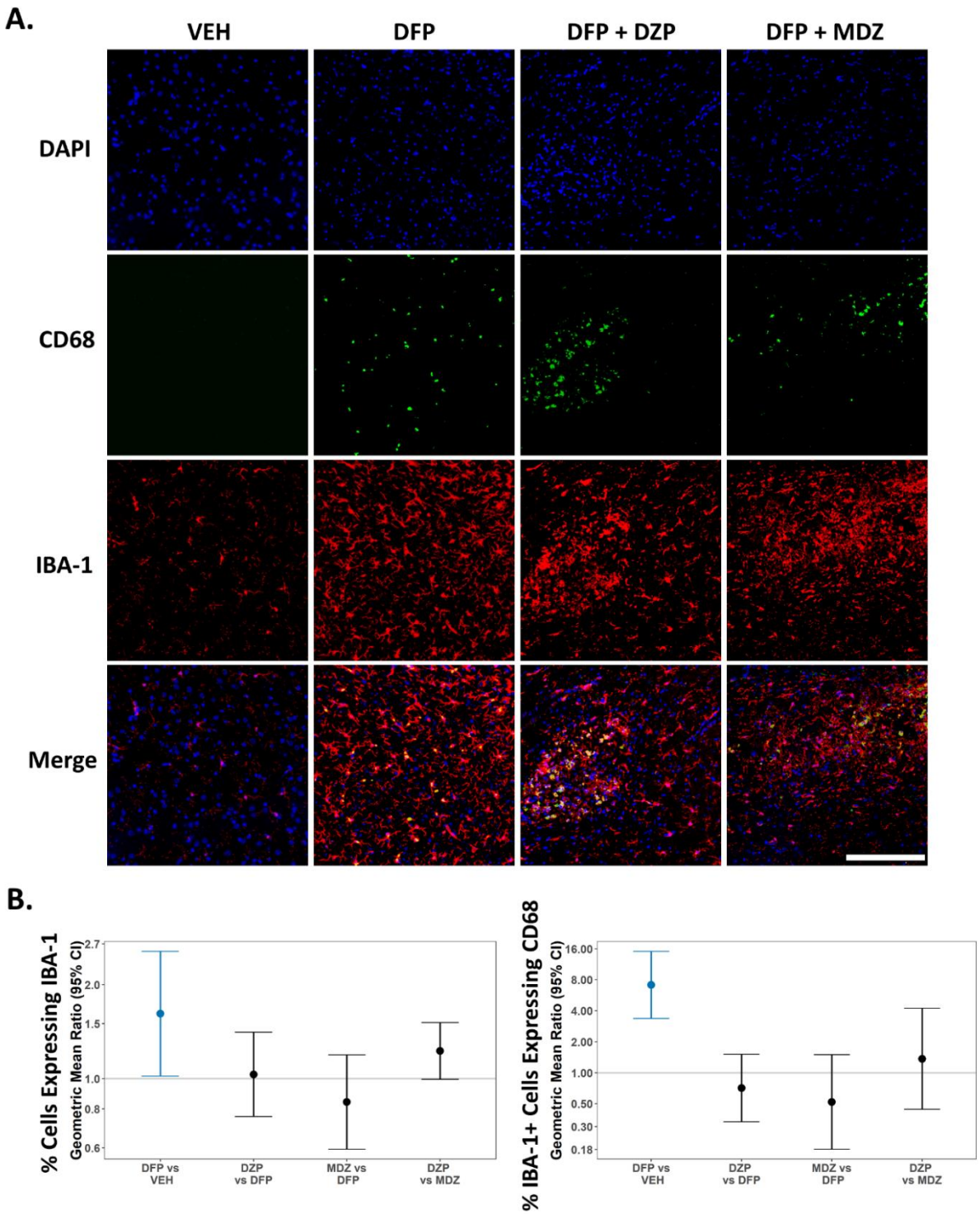
A.
VEH
DFP
DFP + DZP
DFP + MDZ
DAPI
CD68
IBA-1
Merge
B.
% Cells Expressing IBA-1
Geometric Mean Ratio (95% CI)
2.7
2.0
1.5
1.0
0.8
0.6
DFP vs VEH
DZP vs DFP
MDZ vs DFP
DZP vs MDZ
% IBA-1+ Cells Expressing CD68
Geometric Mean Ratio (95% CI)
16.00
8.00
4.00
2.00
1.00
0.50
0.30
0.18
DFP vs VEH
DZP vs DFP
MDZ vs DFP
DZP vs MDZ

Figure 2-6. Neither diazepam nor midazolam reduce persistent microglial activation. (A) Representative photomicrographs of IBA-1 (microglia; red) and CD68 (phagocytic microglia; green) immunoreactivity in the thalamus at 6 months post-exposure. Sections were counterstained with DAPI (blue) to label cell nuclei. Bar = 200 µm. (B) The percent of total cells that were IBA-1 immunopositive and the percent of IBA-1 immunopositive cells that were immunoreactive for CD68 were quantified in seven brain regions (amygdala, CA1, CA3 and dentate gyrus of the hippocampus, piriform and somatosensory cortex, and thalamus) at 3 and 6 months post-DFP exposure. Estimates of exposure or treatment effects were averaged across brain regions and time points as these did not differ significantly by brain region or time point. Data are presented as the geometric mean ratio with 95% confidence intervals (n = 11 vehicle, 13 DFP, 6 diazepam, 7 midazolam animals combined across time points). Confidence intervals that do not include 1.00 are colored blue and indicate a significant difference between groups at $p<0.05$. Raw data used to generate this figure are provided in the supplemental material (Fig. 3-S4 and 3-S5).

Figure 2-7

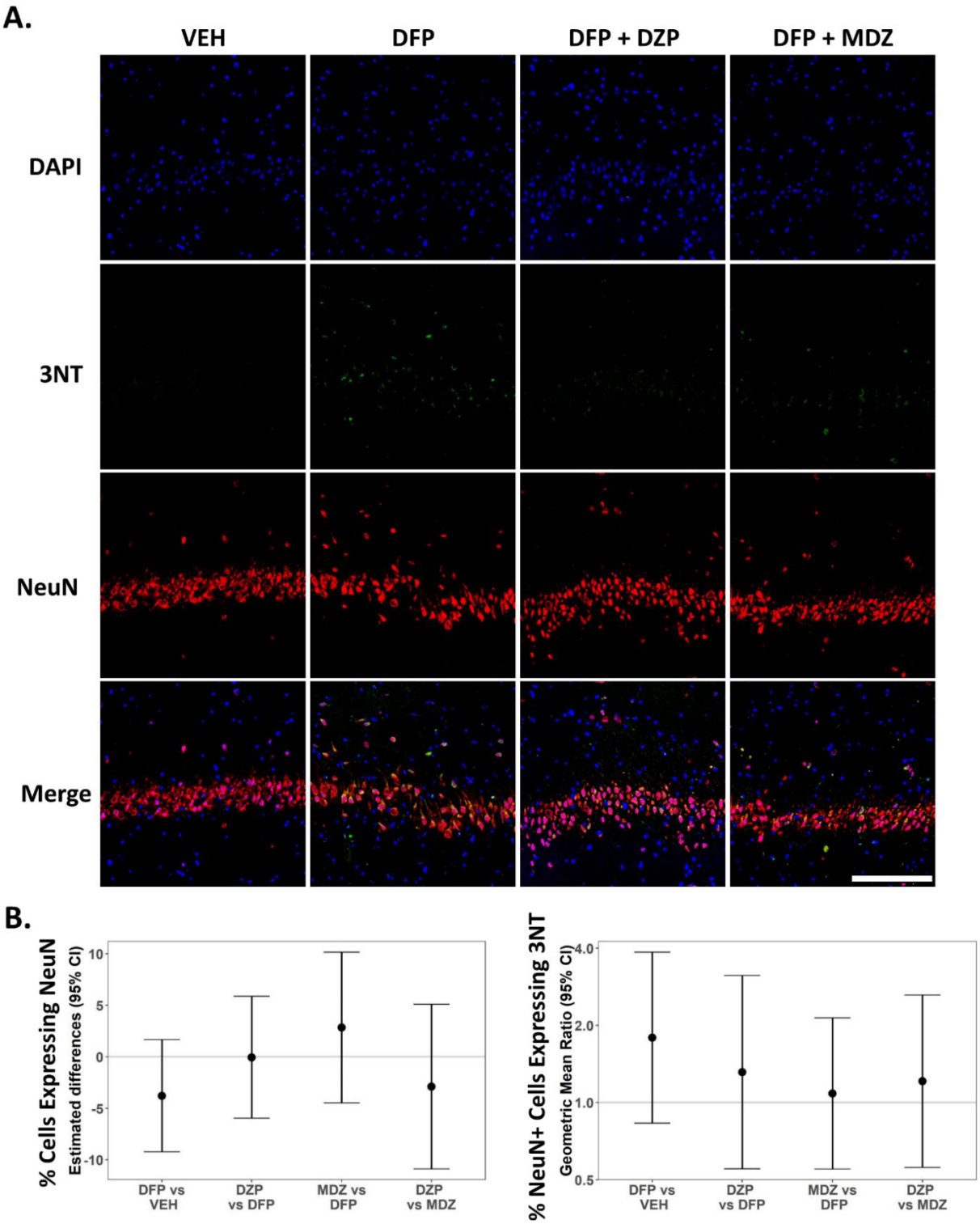
A.
VEH
DFP
DFP + DZP
DFP + MDZ
DAPI
3NT
NeuN
Merge
B.
% Cells Expressing NeuN
Estimated differences (95% CI)
10
5
0
-5
-10
DFP vs VEH
DZP vs DFP
MDZ vs DFP
DZP vs MDZ
% NeuN+ Cells Expressing 3NT
Geometric Mean Ratio (95% CI)
4.0
2.0
1.0
0.5
DFP vs VEH
DZP vs DFP
MDZ vs DFP
DZP vs MDZ

Figure 2-7. Biomarkers of oxidative stress are not significantly elevated in the brain of DFP-intoxicated animals at 3 or 6 months post-DFP exposure. (A) Representative photomicrographs of NeuN (neurons; red) and 3-nitrotyrosine (oxidative damage; green) immunoreactivity in the CA3 subregion of the hippocampus at 6 months post-exposure. Sections were counterstained with DAPI (blue) to label cell nuclei. Bar = 200 μm. (B) The percent of total cells that were immunopositive for NeuN and the percent of NeuN immunopositive cells that expressed 3-nitrotyrosine were quantified in seven brain regions (amygdala, CA1, CA3 and dentate gyrus of the hippocampus, piriform and somatosensory cortex, and thalamus) at 3 and 6 months post-DFP. Estimates of exposure or treatment effects were averaged across brain regions and time points as these did not differ significantly by brain region or time point. Data represented as geometric mean ratio (percent of NeuN immunopositive cells that expressed 3-nitrotyrosine) or estimated differences between groups (percent of total cells that were immunopositive for NeuN) with 95% confidence intervals (n = 11 vehicle, 13 DFP, 6 diazepam, 7 midazolam animals combined across time points). Confidence intervals entirely above 1 (percent of NeuN immunopositive cells that expressed 3-NT) or 0 (percent of total cells that were immunopositive for NeuN) are colored blue satisfy $p<0.05$. Raw data used to generate this figure are provided in the supplemental material (Fig. 3-S6 and 3-S7).

Figure 2-8

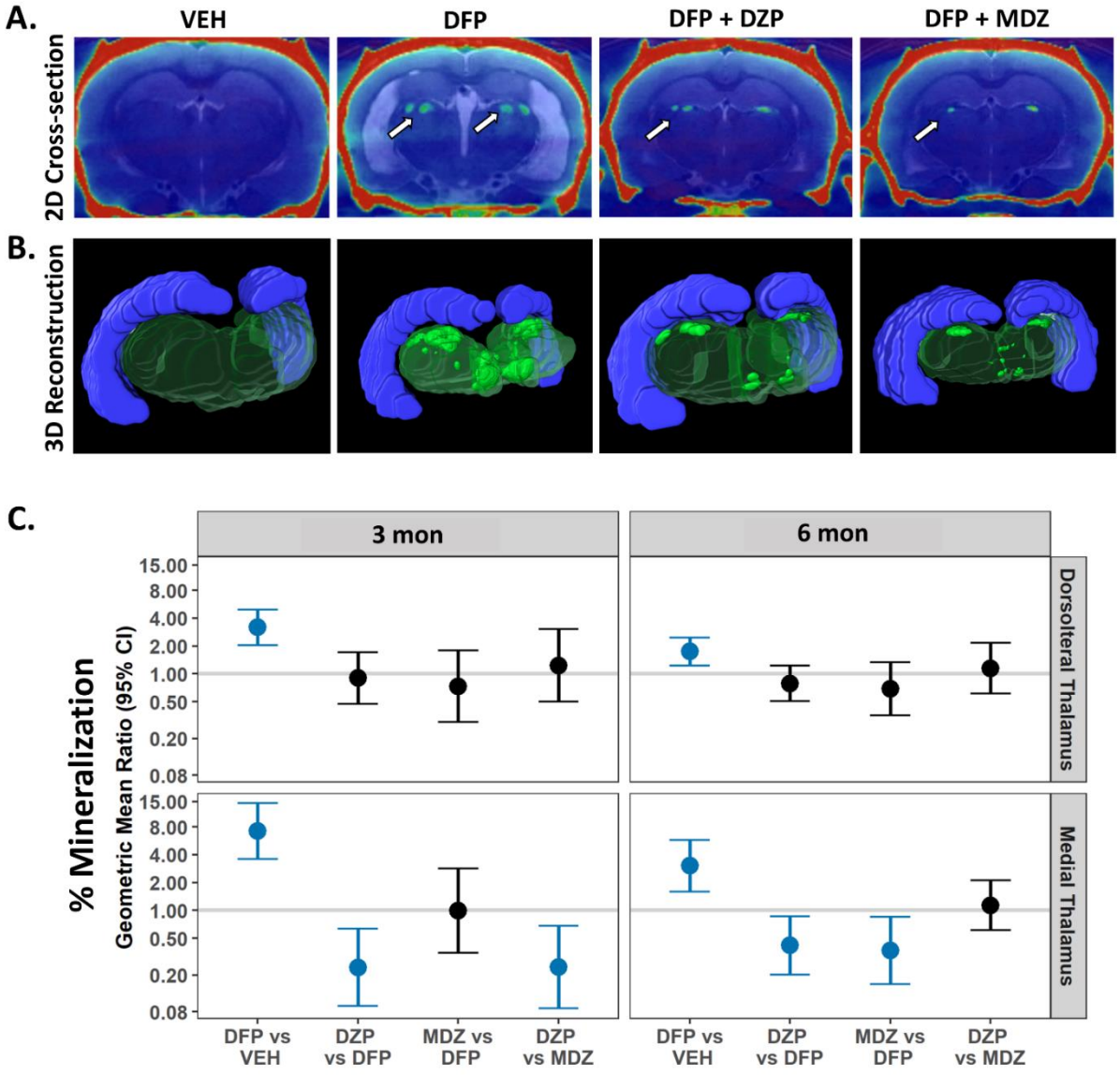
A.
VEH
DFP
DFP + DZP
DFP + MDZ
2D Cross-section
B.
3D Reconstruction
C.
3 mon
6 mon
% Mineralization
Geometric Mean Ratio (95% CI)
15.00
8.00
4.00
2.00
1.00
0.50
0.20
0.08
Dorsolteral Thalamus
Medial Thalamus
DFP vs VEH
DZP vs DFP
MDZ vs DFP
DZP vs MDZ

Figure 2-8. Neither diazepam nor midazolam protect against delayed DFP-induced mineralization in the brain. (A) Representative micro-CT output images overlaid on anatomical MR images at 6 months post-exposure. Mineralized areas are shown in green, and arrows point to representative mineral deposits. (B) Reconstructed three-dimensional micro-CT images showing the hippocampus (solid blue), thalamus (transparent green), and mineralized area (solid green) at 6 months post-exposure. (C) Quantitative analyses comparing the percent area of mineralization in the dorsolateral (top) and medial (bottom) thalamus at 3 and 6 months post-exposure. Data are presented as the geometric mean ratio with 95% confidence intervals (n = 4-7 vehicle, 8-12 DFP, 4-7 diazepam, 4-7 midazolam animals per time point; note that a subset of animals were imaged at both 3 and 6 months). Confidence intervals that do not include 1.00 are colored blue and indicate a significant difference between groups at $P<0.05$. Raw data used to generate this figure are provided in the supplemental material (Fig. 3-S8).

Supplemental Data

Figure 2-S1

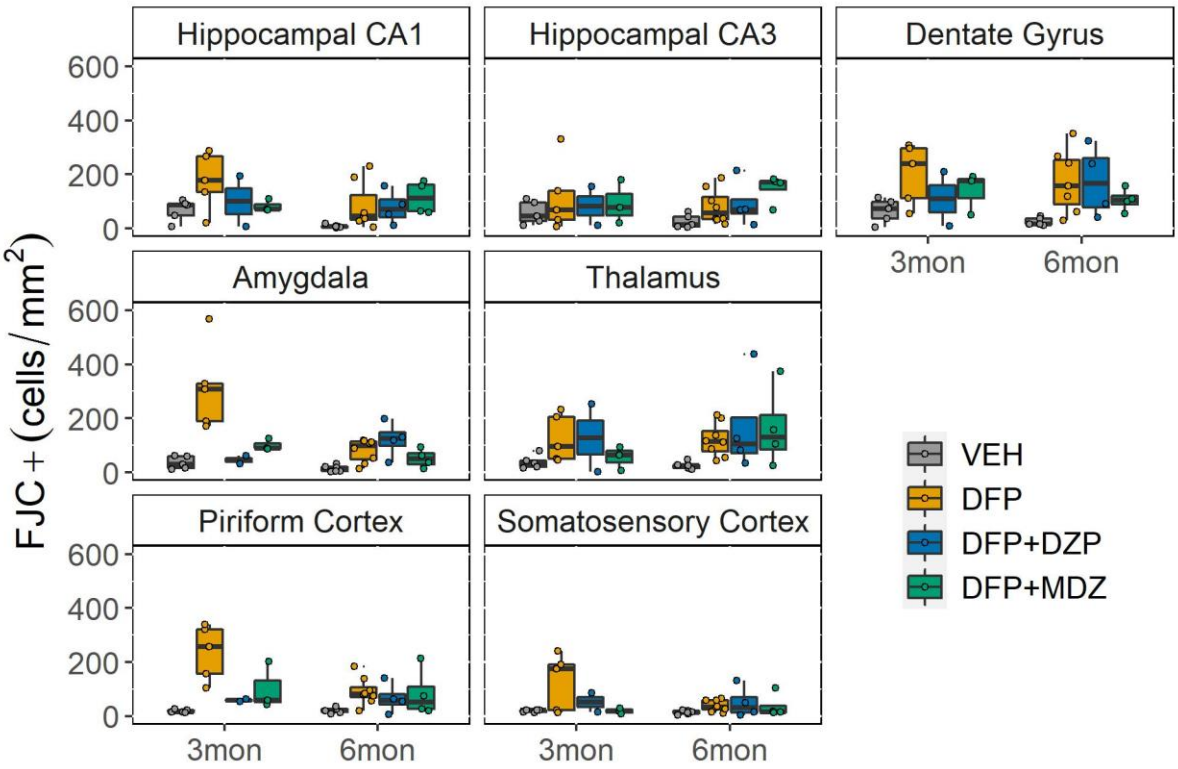

Figure 2-S1. Raw data of FJC staining (positive cells/mm^2) in 7 major brain regions at both 3 and 6 months post-DFP. Each circle represents an individual animal. Edges of the boxes reflect the 25th and 75th percentiles of the raw data, while the horizontal line within the box reflects the median value. Whiskers extend to the last data point within 1.5 times the length of the box (75th -25th percentiles) of the edges of the box. Statistical differences between groups are shown in the main figures of the article. VEH=vehicle; DZP=diazepam; MDZ=midazolam.

Figure 2-S2

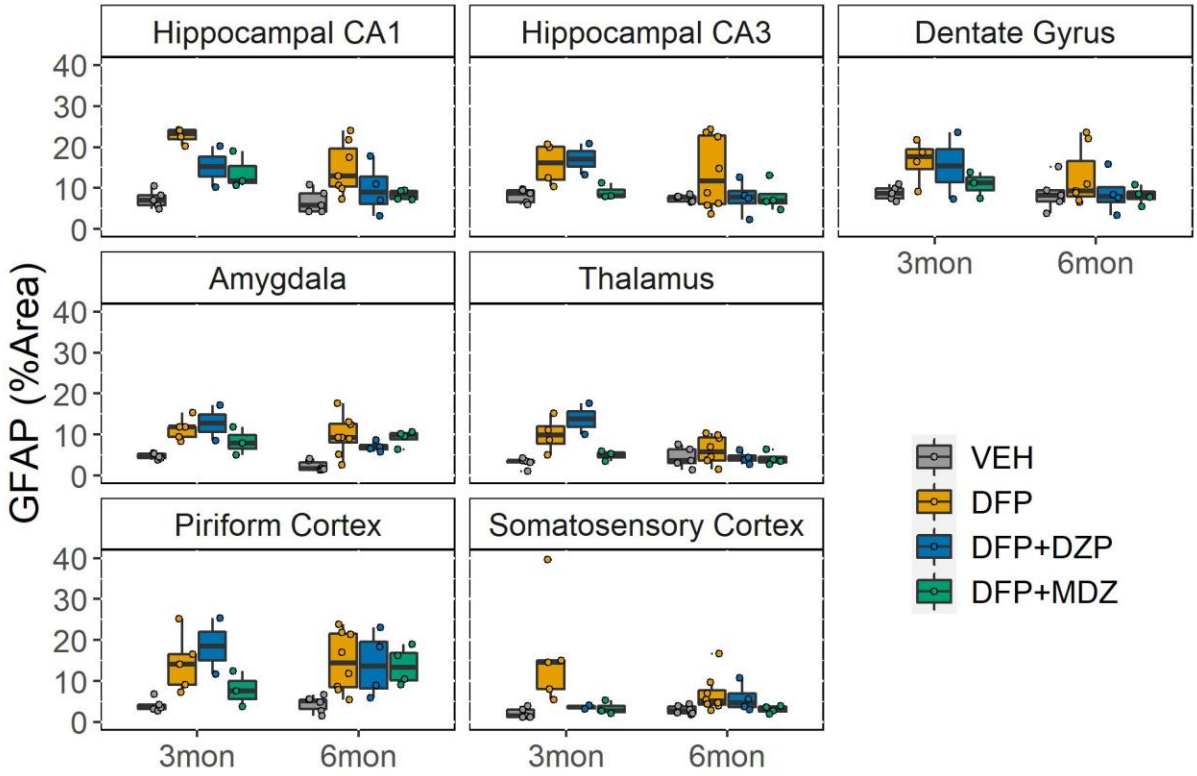
Hippocampal CA1
Hippocampal CA3
Dentate Gyrus
Amygdala
Thalamus
Piriform Cortex
Somatosensory Cortex
GFAP (%Area)
0
10
20
30
40
3mon
6mon
VEH
DFP
DFP+DZP
DFP+MDZ

Figure 2-S2. Raw data of GFAP immunoreactivity (% area) in 7 major brain regions at both 3 and 6 months post-DFP. Each circle represents an individual animal. Edges of the boxes reflect the 25th and 75th percentiles of the raw data, while the horizontal line within the box reflects the median value. Whiskers extend to the last data point within 1.5 times the length of the box (75th -25th percentiles) of the edges of the box. Statistical differences between groups are shown in the main figures of the article. VEH=vehicle; DZP=diazepam; MDZ=midazolam.

Figure 2-S3

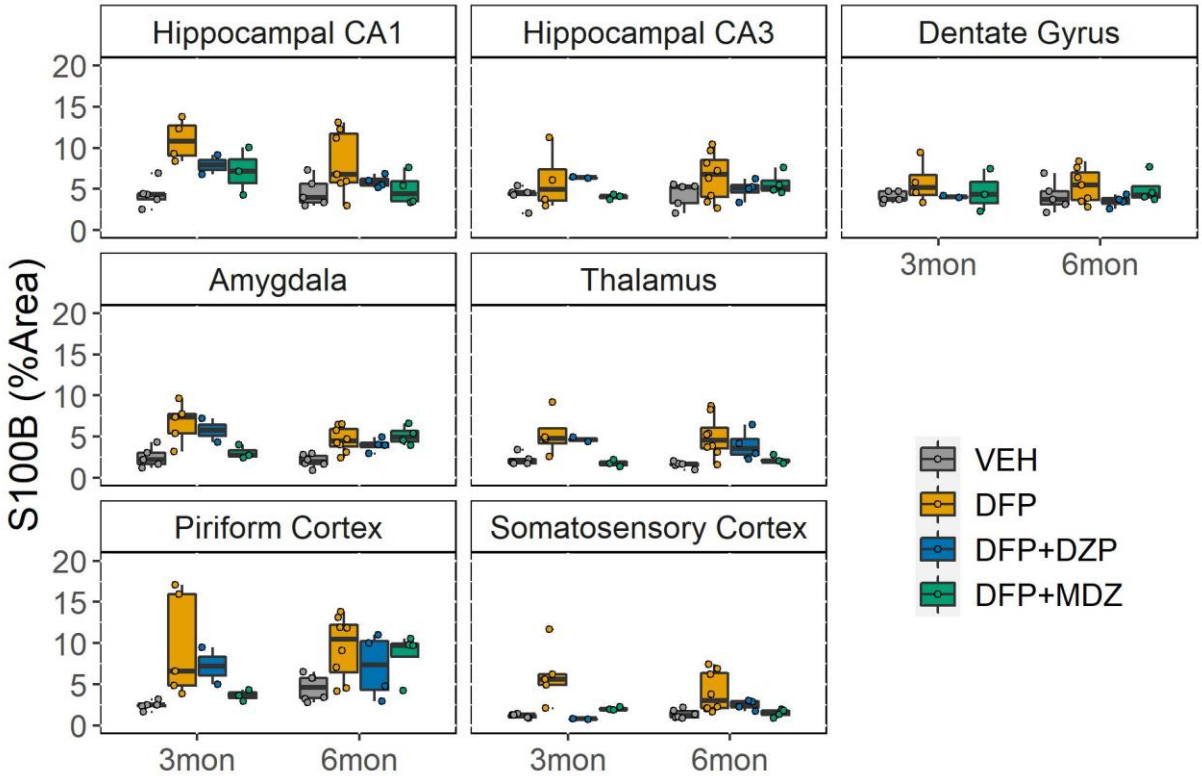
Hippocampal CA1
Hippocampal CA3
Dentate Gyrus
Amygdala
Thalamus
Piriform Cortex
Somatosensory Cortex
S100B (%Area)
0
5
10
15
20
3mon
6mon
VEH
DFP
DFP+DZP
DFP+MDZ

Figure 2-S3. Raw data of S100β immunoreactivity (% area) in 7 major brain regions at both 3 and 6 months post-DFP. Each circle represents an individual animal. Edges of the boxes reflect the 25th and 75th percentiles of the raw data, while the horizontal line within the box reflects the median value. Whiskers extend to the last data point within 1.5 times the length of the box (75th -25th percentiles) of the edges of the box. Statistical differences between groups are shown in the main figures of the article. VEH=vehicle; DZP=diazepam; MDZ=midazolam.

Figure 2-S4

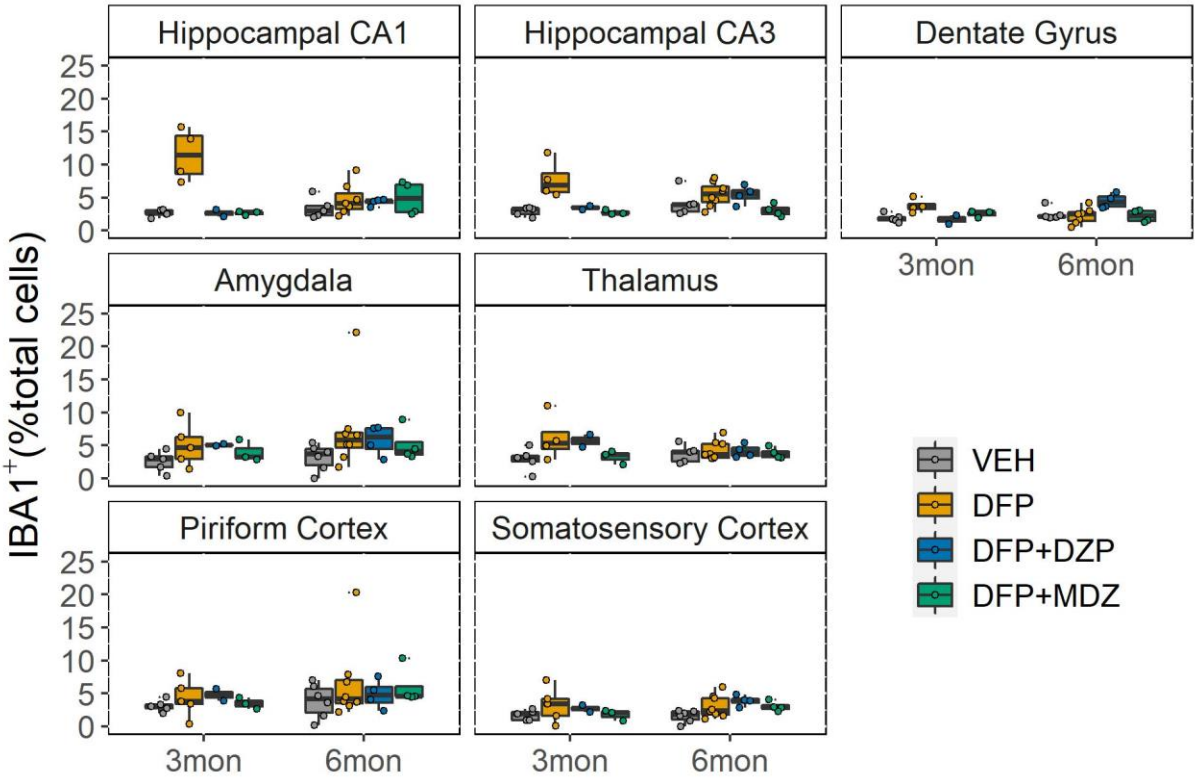
Hippocampal CA1
Hippocampal CA3
Dentate Gyrus
Amygdala
Thalamus
Piriform Cortex
Somatosensory Cortex
IBA1+(%total cells)
0
5
10
15
20
25
3mon
6mon
VEH
DFP
DFP+DZP
DFP+MDZ

Figure 2-S4. Raw data of IBA-1 immunoreactivity (% of total cells) in 7 major brain regions at both 3 and 6 months post-DFP. Each circle represents an individual animal. Edges of the boxes reflect the 25^{th} and 75^{th} percentiles of the raw data, while the horizontal line within the box reflects the median value. Whiskers extend to the last data point within 1.5 times the length of the box (75^{th} -25^{th} percentiles) of the edges of the box. Statistical differences between groups are shown in the main figures of the article. VEH=vehicle; DZP=diazepam; MDZ=midazolam.

Figure 2-S5

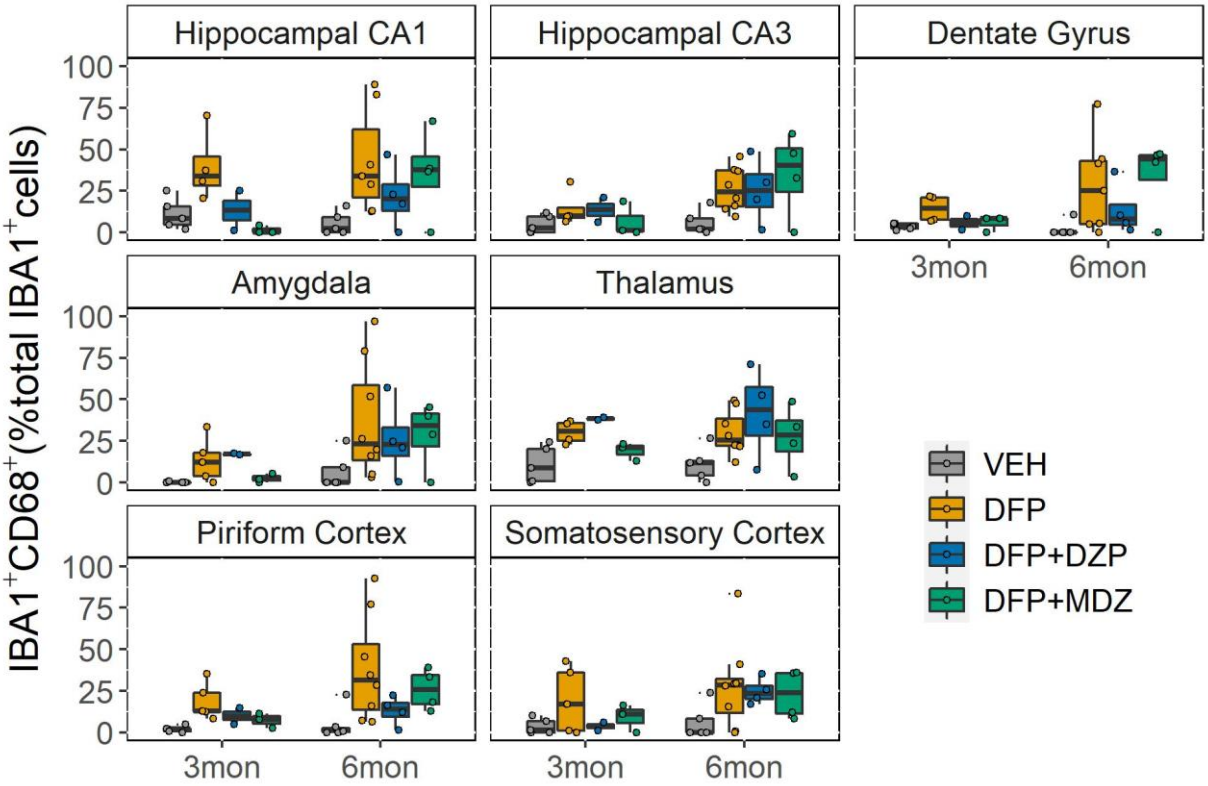
Hippocampal CA1
Hippocampal CA3
Dentate Gyrus
Amygdala
Thalamus
Piriform Cortex
Somatosensory Cortex
IBA1+CD68+(%total IBA1+cells)
100
75
50
25
0
3mon
6mon
VEH
DFP
DFP+DZP
DFP+MDZ

Figure 2-S5. Raw data of IBA-1/CD68 immunoreactivity (% of total IBA-1+ cells) in 7 major brain regions at both 3 and 6 months post-DFP. Each circle represents an individual animal. Edges of the boxes reflect the 25^{th} and 75^{th} percentiles of the raw data, while the horizontal line within the box reflects the median value. Whiskers extend to the last data point within 1.5 times the length of the box (75^{th} -25^{th} percentiles) of the edges of the box. Statistical differences between groups are shown in the main figures of the article. VEH=vehicle; DZP=diazepam; MDZ=midazolam.

Figure 2-S6

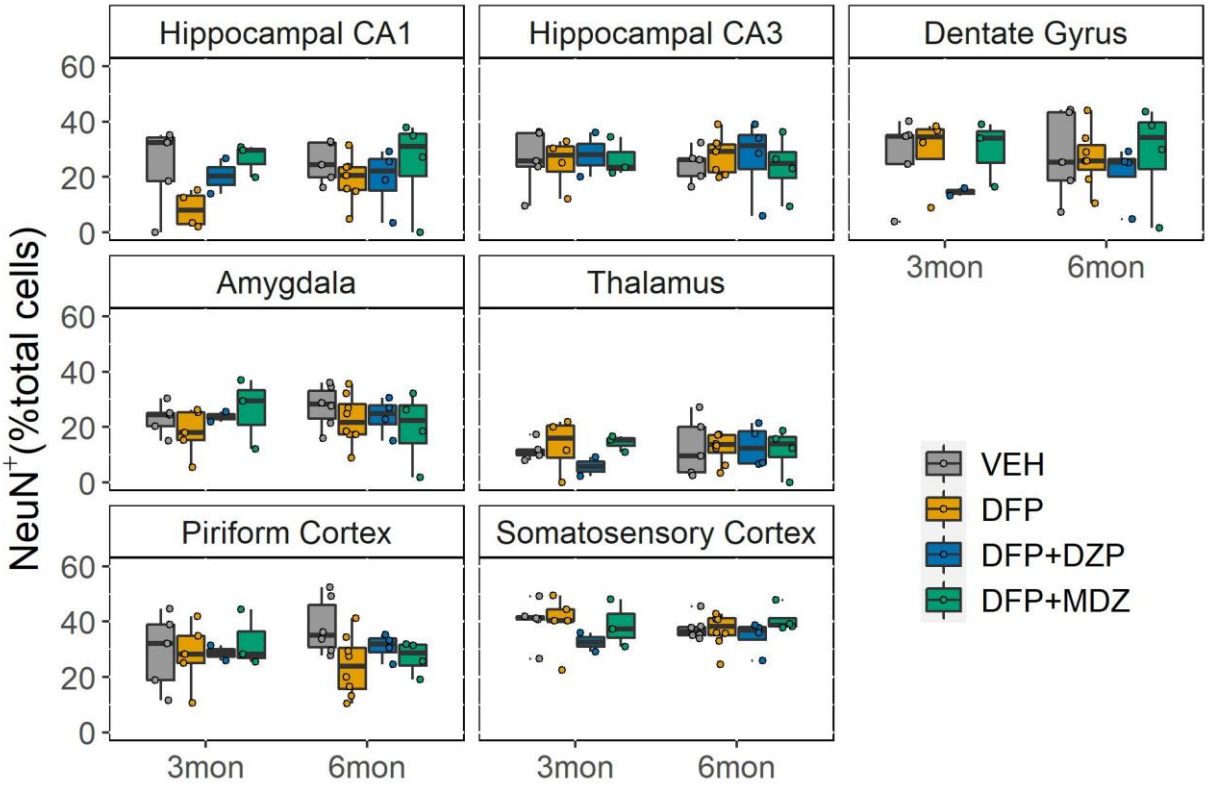
Hippocampal CA1
Hippocampal CA3
Dentate Gyrus
Amygdala
Thalamus
Piriform Cortex
Somatosensory Cortex
NeuN+(%total cells)
0
20
40
60
3mon
6mon
VEH
DFP
DFP+DZP
DFP+MDZ

Figure 2-S6. Raw data of NeuN immunoreactivity (% of total cells) in 7 major brain regions at both 3 and 6 months post-DFP. Each circle represents an individual animal. Edges of the boxes reflect the 25^{th} and 75^{th} percentiles of the raw data, while the horizontal line within the box reflects the median value. Whiskers extend to the last data point within 1.5 times the length of the box (75^{th} -25^{th} percentiles) of the edges of the box. Statistical differences between groups are shown in the main figures of the article. VEH=vehicle; DZP=diazepam; MDZ=midazolam.

Figure 2-S7

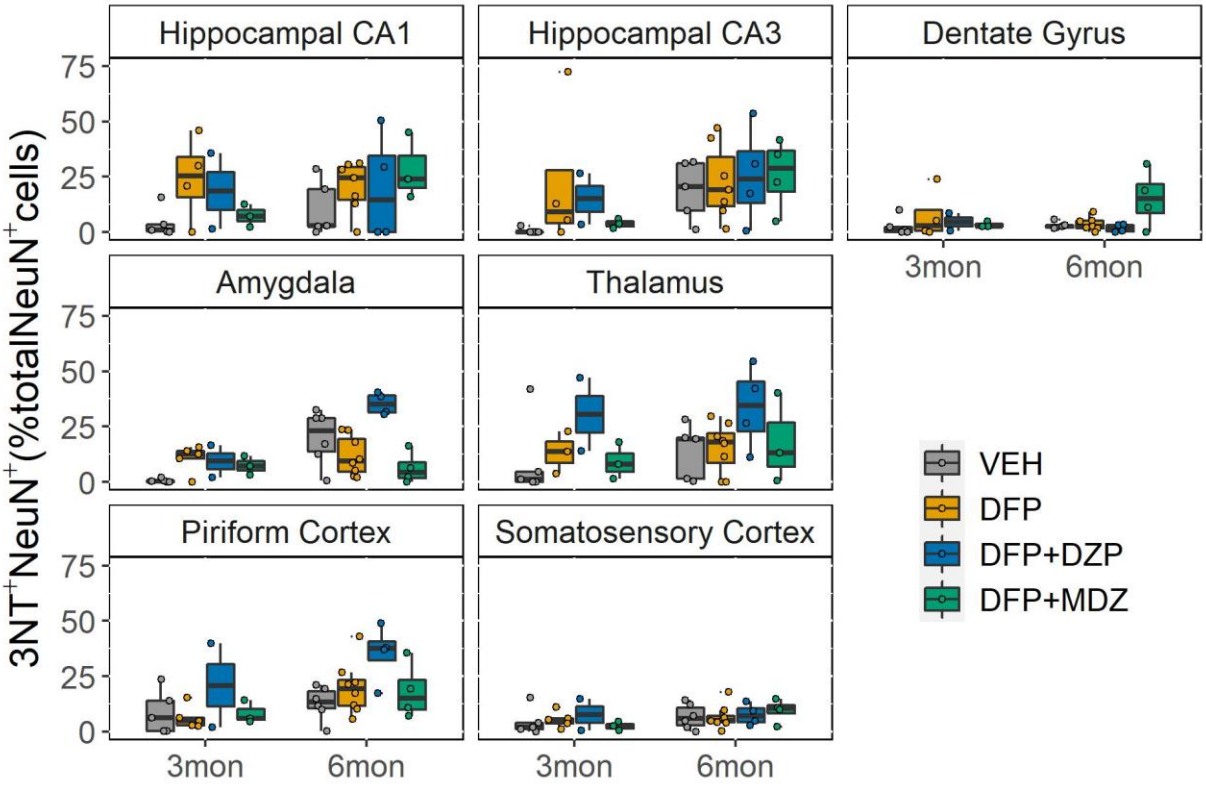
Hippocampal CA1
Hippocampal CA3
Dentate Gyrus
Amygdala
Thalamus
Piriform Cortex
Somatosensory Cortex
3NT+NeuN+(%totalNeuN+cells)
75
50
25
0
3mon
6mon
VEH
DFP
DFP+DZP
DFP+MDZ

Figure 2-S7. Raw data of NeuN/3NT immunoreactivity (% of total NeuN+ cells) in 7 major brain regions at both 3 and 6 months post-DFP. Each circle represents an individual animal. Edges of the boxes reflect the 25th and 75th percentiles of the raw data, while the horizontal line within the box reflects the median value. Whiskers extend to the last data point within 1.5 times the length of the box (75th -25th percentiles) of the edges of the box. Statistical differences between groups are shown in the main figures of the article. VEH=vehicle; DZP=diazepam; MDZ=midazolam.

Figure 2-S8

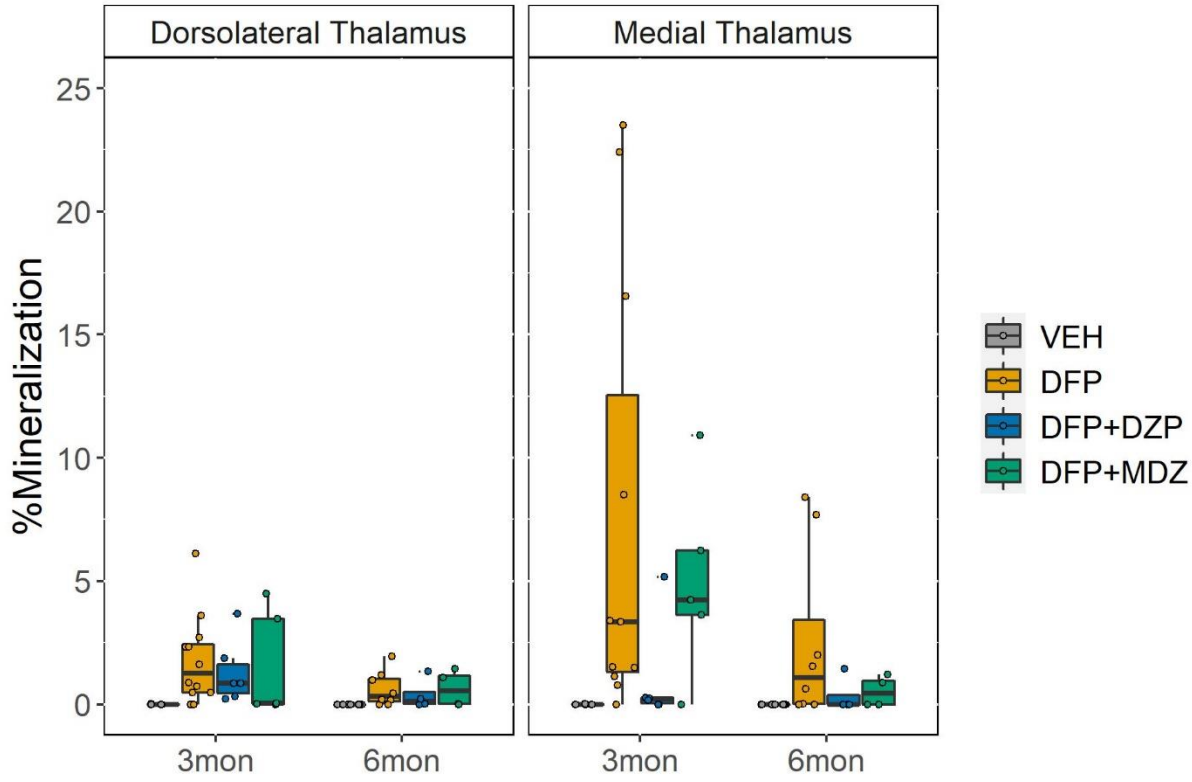
Dorsolateral Thalamus
Medial Thalamus
%Mineralization
25
20
15
10
5
0
3mon
6mon
3mon
6mon
VEH
DFP
DFP+DZP
DFP+MDZ

Figure 2-S8. Raw micro-CT data showing % mineralization in the dorsolateral and medial thalamus at both 3 and 6 months post-DFP. Each circle represents an individual animal. Edges of the boxes reflect the 25^{th} and 75^{th} percentiles of the raw data, while the horizontal line within the box reflects the median value. Whiskers extend to the last data point within 1.5 times the length of the box (75^{th} -25^{th} percentiles) of the edges of the box. Statistical differences between groups are shown in the main figures of the article. VEH=vehicle; DZP=diazepam; MDZ=midazolam.

References

Arendt, R. M., D. J. Greenblatt, D. C. Liebisch, M. D. Luu and S. M. Paul (1987). "Determinants of benzodiazepine brain uptake: lipophilicity versus binding affinity." Psychopharmacology (Berl) **93**(1): 72-76.

Auta, J., E. Costa, J. Davis and A. Guidotti (2004). "Imidazenil: a potent and safe protective agent against diisopropyl fluorophosphate toxicity." Neuropharmacology **46**(3): 397-403.

Benjamini, Y. and Y. Hochberg (1995). "Controlling the False Discovery Rate: A Practical and Powerful Approach to Multiple Testing." Journal of the Royal Statistical Society. Series B (Methodological) **57**(1): 289-300.

Bruun, D. A., M. Guignet, D. J. Harvey and P. J. Lein (2019). "Pretreatment with pyridostigmine bromide has no effect on seizure behavior or 24 hour survival in the rat model of acute diisopropylfluorophosphate intoxication." Neurotoxicology **73**: 81-84.

Chaubey, K., S. I. Alam, C. K. Waghmare, L. Singh, N. Srivastava and B. K. Bhattacharya (2019). "Differential proteome analysis of rat plasma after diisopropyl fluorophosphate (DFP) intoxication, a surrogate of nerve agent sarin." Chemico-Biological Interactions **298**: 66-71.

Chen, K. C., A. Arad, Z. M. Song and D. Croaker (2018). "High-definition neural visualization of rodent brain using micro-CT scanning and non-local-means processing." BMC Med Imaging **18**(1): 38.

Chen, Y. (2012). "Organophosphate-induced brain damage: mechanisms, neuropsychiatric and neurological consequences, and potential therapeutic strategies." Neurotoxicology **33**(3): 391-400.

de Araujo Furtado, M., L. A. Lumley, C. Robison, L. C. Tong, S. Lichtenstein and D. L. Yourick (2010). "Spontaneous recurrent seizures after status epilepticus induced by soman in Sprague-Dawley rats." Epilepsia **51**(8): 1503-1510.

de Araujo Furtado, M., F. Rossetti, S. Chanda and D. Yourick (2012). "Exposure to nerve agents: from status epilepticus to neuroinflammation, brain damage, neurogenesis and epilepsy." Neurotoxicology **33**(6): 1476-1490.

Deshpande, L. S., R. E. Blair, B. A. Huang, K. F. Phillips and R. J. DeLorenzo (2016). "Pharmacological blockade of the calcium plateau provides neuroprotection following organophosphate paraoxon induced status epilepticus in rats." Neurotoxicology and teratology **56**: 81-86.

Deshpande, L. S., R. E. Blair, K. F. Phillips and R. J. DeLorenzo (2016). "Role of the calcium plateau in neuronal injury and behavioral morbidities following organophosphate intoxication." Annals of the New York Academy of Sciences **1374**(1): 176-183.

Deshpande, L. S., D. S. Carter, R. E. Blair and R. J. DeLorenzo (2010). "Development of a prolonged calcium plateau in hippocampal neurons in rats surviving status epilepticus induced by the organophosphate diisopropylfluorophosphate." Toxicol Sci **116**(2): 623-631.

Eddleston, M., N. A. Buckley, P. Eyer and A. H. Dawson (2008). "Management of acute organophosphorus pesticide poisoning." Lancet **371**(9612): 597-607.

Etherington, L.-A., B. Mihalik, A. Pálvölgyi, I. Ling, K. Pallagi, S. Kertész, P. Varga, B. G. Gunn, A. R. Brown, M. R. Livesey, O. Monteiro, D. Belelli, J. Barkóczy, M. Spedding, I. Gacsályi, F. A. Antoni and J. J. Lambert (2017). "Selective inhibition of extra-synaptic α5-GABAA receptors by S44819, a new therapeutic agent." Neuropharmacology **125**: 353-364.

FDA (2018). "Center For Drug Evalutaion And Research- Midazolam Review." Food and Drug Administration **Application 209566Orig1s000**.

Fenyk-Melody, J. E., X. Shen, Q. Peng, W. Pikounis, L. Colwell, J. Pivnichny, L. C. Anderson and C. S. Tamvakopoulos (2004). "Comparison of the effects of perfusion in determining brain penetration (brain-to-plasma ratios) of small molecules in rats." Comp Med **54**(4): 378-381.

Finkelstein, A., G. Kunis, T. Berkutzki, A. Ronen, A. Krivoy, E. Yoles, D. Last, Y. Mardor, K. Van Shura, E. McFarland, B. A. Capacio, C. Eisner, M. Gonzales, D. Gregorowicz, A. Eisenkraft, J. H. McDonough and M. Schwartz (2012). "Immunomodulation by poly-YE reduces organophosphate-induced brain damage." Brain, Behavior, and Immunity **26**(1): 159-169.

Flannery, B. M., D. A. Bruun, D. J. Rowland, C. N. Banks, A. T. Austin, D. L. Kukis, Y. Li, B. D. Ford, D. J. Tancredi, J. L. Silverman, S. R. Cherry and P. J. Lein (2016). "Persistent neuroinflammation and cognitive impairment in a rat model of acute diisopropylfluorophosphate intoxication." J Neuroinflammation **13**(1): 267.

Gao, J., S. X. Naughton, H. Wulff, V. Singh, W. D. Beck, J. Magrane, B. Thomas, N. A. Kaidery, C. M. Hernandez and A. V. Terry, Jr. (2016). "Diisopropylfluorophosphate Impairs the Transport of Membrane-Bound Organelles in Rat Cortical Axons." J Pharmacol Exp Ther **356**(3): 645-655.

Gilat, E., T. Kadar, A. Levy, I. Rabinovitz, G. Cohen, Y. Kapon, R. Sahar and R. Brandeis (2005). "Anticonvulsant treatment of sarin-induced seizures with nasal midazolam: An electrographic, behavioral, and histological study in freely moving rats." Toxicology and Applied Pharmacology **209**(1): 74-85.

González, E. A., A. C. Rindy, M. A. Guignet, J. J. Calsbeek, D. A. Bruun, A. Dhir, P. Andrew, N. Saito, D. J. Rowland, D. J. Harvey, M. A. Rogawski and P. J. Lein (2020). "The chemical convulsant diisopropylfluorophosphate (DFP) causes persistent neuropathology in adult male rats independent of seizure activity." Arch Toxicol **94**(6): 2149-2162.

Guignet, M., K. Dhakal, B. M. Flannery, B. A. Hobson, D. Zolkowska, A. Dhir, D. A. Bruun, S. Li, A. Wahab, D. J. Harvey, J. L. Silverman, M. A. Rogawski and P. J. Lein (2019). "Persistent behavior deficits, neuroinflammation, and oxidative stress in a rat model of acute organophosphate intoxication." Neurobiol Dis.

Guignet, M., K. Dhakal, B. M. Flannery, B. A. Hobson, D. Zolkowska, A. Dhir, D. A. Bruun, S. Li, A. Wahab, D. J. Harvey, J. L. Silverman, M. A. Rogawski and P. J. Lein (2020). "Persistent behavior deficits, neuroinflammation, and oxidative stress in a rat model of acute organophosphate intoxication." Neurobiol Dis **133**: 104431.

Guignet, M. and P. J. Lein (2018). Organophosphates. Advances in Neurotoxicology: Role of Inflammation in Environmental Neurotoxicity. M. Aschner and L. G. Costa. Oxford, UK, Elsevier**:** 35-79.

Heiss, D. R., D. W. Zehnder, D. A. Jett, G. E. Platoff, D. T. Yeung and B. N. Brewer (2016). "Synthesis and Storage Stability of Diisopropylfluorophosphate." Journal of Chemistry **2016**: 5.

Hobson, B. A., D. J. Rowland, S. Supasai, D. J. Harvey, P. J. Lein and J. R. Garbow (2017). "A magnetic resonance imaging study of early brain injury in a rat model of acute DFP intoxication." Neurotoxicology.

Holst, C. B., C. B. Brochner, K. Vitting-Seerup and K. Mollgard (2019). "Astrogliogenesis in human fetal brain: complex spatiotemporal immunoreactivity patterns of GFAP, S100, AQP4 and YKL-40." J Anat.

Ito, D., Y. Imai, K. Ohsawa, K. Nakajima, Y. Fukuuchi and S. Kohsaka (1998). "Microglia-specific localisation of a novel calcium binding protein, Iba1." Brain Res Mol Brain Res **57**(1): 1-9.

Jett, D. A. (2016). "The NIH Countermeasures Against Chemical Threats Program: overview and special challenges." Annals of the New York Academy of Sciences **1374**(1): 5-9.

Jett, D. A. and S. M. Spriggs (2020). "Translational research on chemical nerve agents." Neurobiol Dis **133**: 104335.

Kim, Y. B., G. H. Hur, S. Shin, D. E. Sok, J. K. Kang and Y. S. Lee (1999). "Organophosphate-induced brain injuries: delayed apoptosis mediated by nitric oxide." Environ Toxicol Pharmacol **7**(2): 147-152.

Kirkland, A. E., G. L. Sarlo and K. F. Holton (2018). "The Role of Magnesium in Neurological Disorders." Nutrients **10**(6): 730.

Kruger, L., S. Saporta and L. W. Swanson (1995). Photographic atlas of the rat brain: the cell and fiber architecture illustrated in three planes with stereotaxic coordinates. Cambridge, Cambridge University Press.

Kuruba, R., X. Wu and D. S. Reddy (2018). "Benzodiazepine-refractory status epilepticus, neuroinflammation, and interneuron neurodegeneration after acute organophosphate intoxication." Biochimica et Biophysica Acta (BBA) - Molecular Basis of Disease **1864**(9, Part B): 2845-2858.

Lerdkrai, C., N. Asavapanumas, B. Brawek, Y. Kovalchuk, N. Mojtahedi, M. Olmedillas Del Moral and O. Garaschuk (2018). "Intracellular Ca(2+) stores control in vivo neuronal

hyperactivity in a mouse model of Alzheimer's disease." Proc Natl Acad Sci U S A **115**(6): E1279-e1288.

Li, Y., P. J. Lein, G. D. Ford, C. Liu, K. C. Stovall, T. E. White, D. A. Bruun, T. Tewolde, A. S. Gates, T. J. Distel, M. C. Surles-Zeigler and B. D. Ford (2015). "Neuregulin-1 inhibits neuroinflammatory responses in a rat model of organophosphate-nerve agent-induced delayed neuronal injury." J Neuroinflammation **12**: 64.

Li, Y., P. J. Lein, C. Liu, D. A. Bruun, C. Giulivi, G. D. Ford, T. Tewolde, C. Ross-Inta and B. D. Ford (2012). "Neuregulin-1 is neuroprotective in a rat model of organophosphate-induced delayed neuronal injury." Toxicology and applied pharmacology **262**(2): 194-204.

Liang, L. P., J. N. Pearson-Smith, J. Huang, P. McElroy, B. J. Day and M. Patel (2017). "Neuroprotective Effects of AEOL10150 in a Rat Organophosphate Model." Toxicol Sci.

Liu, C., Y. Li, P. J. Lein and B. D. Ford (2012). "Spatiotemporal patterns of GFAP upregulation in rat brain following acute intoxication with diisopropylfluorophosphate (DFP)." Curr Neurobiol **3**(2): 90-97.

Loh, Y., M. M. Swanberg, M. V. Ingram and J. Newmark (2010). "Case report: Long-term cognitive sequelae of sarin exposure." NeuroToxicology **31**(2): 244-246.

López-Granero, C., F. Cañadas, D. Cardona, Y. Yu, E. Giménez, R. Lozano, D. S. Avila, M. Aschner and F. Sánchez-Santed (2013). "Chlorpyrifos-, diisopropylphosphorofluoridate-, and parathion-induced behavioral and oxidative stress effects: are they mediated by analogous mechanisms of action?" Toxicological sciences : an official journal of the Society of Toxicology **131**(1): 206-216.

Maher, P., K. van Leyen, P. N. Dey, B. Honrath, A. Dolga and A. Methner (2018). "The role of Ca(2+) in cell death caused by oxidative glutamate toxicity and ferroptosis." Cell Calcium **70**: 47-55.

Matson, L., E. Dunn, K. Haines, S. Miller-Smith, R. Lee-Stubbs, K. Whitten, C. Ardinger, H. McCarren and J. McDonough (2019). "Evaluation of first-line anticonvulsants to treat nerve agent-induced seizures and prevent neuropathology in adult and pediatric rats." Neurotoxicology **74**: 203-208.

McDonough, J. H., Jr., J. McMonagle, T. Copeland, D. Zoeffel and T. M. Shih (1999). "Comparative evaluation of benzodiazepines for control of soman-induced seizures." Arch Toxicol **73**(8-9): 473-478.

McMullan, J., C. Sasson, A. Pancioli and R. Silbergleit (2010). "Midazolam versus diazepam for the treatment of status epilepticus in children and young adults: a meta-analysis." Acad Emerg Med **17**(6): 575-582.

Mennini, T. and M. Gobbi (1990). "Regional distribution of low-affinity GABA receptors coupled to benzodiazepine receptor subtypes in rat brain: an autoradiographic evaluation." Eur J Pharmacol **189**(2-3): 143-148.

Miyamoto, H., S. Matsueda, A. Moritsuka, K. Shimokawa, H. Hirata, M. Nakashima, H. Sasaki, S. Fumoto and K. Nishida (2015). "Evaluation of hypothermia on the in vitro metabolism and binding and in vivo disposition of midazolam in rats." Biopharm Drug Dispos **36**(7): 481-489.

Muller, M., U. Ahumada-Castro, M. Sanhueza, C. Gonzalez-Billault, F. A. Court and C. Cardenas (2018). "Mitochondria and Calcium Regulation as Basis of Neurodegeneration Associated With Aging." Front Neurosci **12**: 470.

Nair, A. B. and S. Jacob (2016). "A simple practice guide for dose conversion between animals and human." Journal of basic and clinical pharmacy **7**(2): 27-31.

Nutt, D. (2006). "GABAA receptors: subtypes, regional distribution, and function." J Clin Sleep Med **2**(2): S7-11.

Otsu, N. (1979). "A Threshold Selection Method from Gray-Level Histograms." IEEE Transactions on Systems, Man, and Cybernetics **9**(1): 62-66.

Pan, H., T. C. B. Piermartiri, J. Chen, J. McDonough, C. Oppel, W. Driwech, K. Winter, E. McFarland, K. Black, T. Figueiredo, N. Grunberg and A. M. Marini (2015). "Repeated systemic administration of the nutraceutical alpha-linolenic acid exerts neuroprotective efficacy, an antidepressant effect and improves cognitive performance when given after soman exposure." NeuroToxicology **51**: 38-50.

Patel, V., C. Ramasundarahettige, L. Vijayakumar, J. S. Thakur, V. Gajalakshmi, G. Gururaj, W. Suraweera and P. Jha (2012). "Suicide mortality in India: a nationally representative survey." Lancet **379**(9834): 2343-2351.

Pearson, J. N. and M. Patel (2016). "The role of oxidative stress in organophosphate and nerve agent toxicity." Ann N Y Acad Sci **1378**(1): 17-24.

Pereira, E. F., Y. Aracava, L. J. DeTolla, Jr., E. J. Beecham, G. W. Basinger, Jr., E. J. Wakayama and E. X. Albuquerque (2014). "Animal models that best reproduce the clinical manifestations of human intoxication with organophosphorus compounds." J Pharmacol Exp Ther **350**(2): 313-321.

Pessah, I. N., M. A. Rogawski, D. J. Tancredi, H. Wulff, D. Zolkowska, D. A. Bruun, B. D. Hammock and P. J. Lein (2016). "Models to identify treatments for the acute and persistent effects of seizure-inducing chemical threat agents." Ann N Y Acad Sci **1378**(1): 124-136.

Phelan, K. D., U. T. Shwe, D. K. Williams, L. J. Greenfield and F. Zheng (2015). "Pilocarpine-induced status epilepticus in mice: A comparison of spectral analysis of electroencephalogram and behavioral grading using the Racine scale." Epilepsy Res **117**: 90-96.

Piermartiri, T. C. B., H. Pan, J. Chen, J. McDonough, N. Grunberg, J. P. Apland and A. M. Marini (2015). "Alpha-Linolenic Acid-Induced Increase in Neurogenesis is a Key Factor in the Improvement in the Passive Avoidance Task After Soman Exposure." NeuroMolecular Medicine **17**(3): 251-269.

Pirker, S., C. Schwarzer, A. Wieselthaler, W. Sieghart and G. Sperk (2000). "GABA(A) receptors: immunocytochemical distribution of 13 subunits in the adult rat brain." Neuroscience **101**(4): 815-850.

Pope, C., S. Karanth and J. Liu (2005). "Pharmacology and toxicology of cholinesterase inhibitors: uses and misuses of a common mechanism of action." Environmental Toxicology and Pharmacology **19**(3): 433-446.

Pouliot, W., S. L. Bealer, B. Roach and F. E. Dudek (2016). "A rodent model of human organophosphate exposure producing status epilepticus and neuropathology." Neurotoxicology **56**: 196-203.

Reddy, S. D. and D. S. Reddy (2015). "Midazolam as an anticonvulsant antidote for organophosphate intoxication--A pharmacotherapeutic appraisal." Epilepsia **56**(6): 813-821.

Schmued, L. C., C. C. Stowers, A. C. Scallet and L. Xu (2005). "Fluoro-Jade C results in ultra high resolution and contrast labeling of degenerating neurons." Brain Res **1035**(1): 24-31.

Silbergleit, R., D. Lowenstein, V. Durkalski and R. Conwit (2011). "RAMPART (Rapid Anticonvulsant Medication Prior to Arrival Trial): a double-blind randomized clinical trial of the efficacy of intramuscular midazolam versus intravenous lorazepam in the prehospital treatment of status epilepticus by paramedics." Epilepsia **52 Suppl 8**: 45-47.

Silbergleit, R., D. Lowenstein, V. Durkalski and R. Conwit (2013). "Lessons from the RAMPART study--and which is the best route of administration of benzodiazepines in status epilepticus." Epilepsia **54 Suppl 6**: 74-77.

Siso, S., B. A. Hobson, D. J. Harvey, D. A. Bruun, D. J. Rowland, J. R. Garbow and P. J. Lein (2017). "Editor's Highlight: Spatiotemporal Progression and Remission of Lesions in the Rat Brain Following Acute Intoxication With Diisopropylfluorophosphate." Toxicol Sci **157**(2): 330-341.

Spampanato, J., W. Pouliot, S. L. Bealer, B. Roach and F. E. Dudek (2019). "Antiseizure and neuroprotective effects of delayed treatment with midazolam in a rodent model of organophosphate exposure." Epilepsia **60**(7): 1387-1398.

Ulu, A., B. Inceoglu, J. Yang, V. Singh, S. Vito, H. Wulff and B. D. Hammock (2016). "Inhibition of soluble epoxide hydrolase as a novel approach to high dose diazepam induced hypotension." J Clin Toxicol **6**(3).

Valdes Hernandez Mdel, C., L. C. Maconick, E. M. Tan and J. M. Wardlaw (2012). "Identification of mineral deposits in the brain on radiological images: a systematic review." Eur Radiol **22**(11): 2371-2381.

Wu, X., R. Kuruba and D. S. Reddy (2018). "Midazolam-Resistant Seizures and Brain Injury after Acute Intoxication of Diisopropylfluorophosphate, an Organophosphate Pesticide and Surrogate for Nerve Agents." J Pharmacol Exp Ther **367**(2): 302-321.

Yamamoto, S., M. Suzuki, K. Kohara, G. Iinuma and N. Moriyama (2007). "Technical aspects of X-ray micro-computed tomography: initial experience of 27-microm resolution using Feldkamp cone-beam reconstruction." Nihon Hoshasen Gijutsu Gakkai Zasshi **63**(2): 257-260.

Yamasue, H., O. Abe, K. Kasai, M. Suga, A. Iwanami, H. Yamada, M. Tochigi, T. Ohtani, M. A. Rogers, T. Sasaki, S. Aoki, T. Kato and N. Kato (2007). "Human brain structural change related to acute single exposure to sarin." Annals of Neurology **61**(1): 37-46.

Youssef, S. A., M. T. Capucchio, J. E. Rofina, J. K. Chambers, K. Uchida, H. Nakayama and E. Head (2016). "Pathology of the Aging Brain in Domestic and Laboratory Animals, and Animal Models of Human Neurodegenerative Diseases." Vet Pathol **53**(2): 327-348.

Zaja-Milatovic, S., R. C. Gupta, M. Aschner and D. Milatovic (2009). "Protection of DFP-induced oxidative damage and neurodegeneration by antioxidants and NMDA receptor antagonist." Toxicol Appl Pharmacol **240**(2): 124-131.

Zhang, T., M. S. Todorovic, J. Williamson and J. Kapur (2017). "Flupirtine and diazepam combination terminates established status epilepticus: results in three rodent models." Ann Clin Transl Neurol **4**(12): 888-896.

Chapter 3

The Chemical Convulsant Diisopropylfluorophosphate (DFP) Causes Persistent Neuropathology in Adult Male Rats Independent of Seizure Activity

Based on a publication in *Archives of Toxicology* (accepted April 2020) under the same title with the following authors:

Eduardo A. González[a*], Alexa C. Rindy[a*], Michelle A. Guignet[a], Jonas J. Calsbeek[a], Donald A. Bruun[a], Ashish Dhir[b], Peter Andrew[a], Naomi Saito[c], Douglas J. Rowland[d], Danielle J. Harvey[c], Michael A. Rogawski[b], and Pamela J. Lein[a]

[a]Department of Molecular Biosciences, University of California, Davis, School of Veterinary Medicine, 1089 Veterinary Medicine Drive, Davis, CA 95616, United States; [b]Department of Neurology, University of California, Davis, School of Medicine, 4860 Y Street, Sacramento, CA 95817, United States; [c]Department of Public Health Sciences, University of California, Davis, School of Medicine, One Shields Avenue, Davis, CA 95616, United States; [d]Center for Molecular and Genomic Imaging, University of California, Davis, College of Engineering, 451 Health Sciences Drive, Davis, CA 95616, United States.

*These authors contributed equally to this manuscript.

Abstract

Organophosphate (OP) threat agents can trigger seizures that progress to *status epilepticus*, resulting in persistent neuropathology and cognitive deficits in humans and preclinical models. However, it remains unclear whether patients who do not show overt seizure behavior will develop neurological consequences. Therefore, this study compared two subpopulations of rats with a low versus high seizure responses to diisopropylfluorophosphate (DFP) to evaluate whether acute OP intoxication causes persistent neuropathology in non-seizing individuals. Adult male Sprague-Dawley rats administered DFP (4 mg/kg, sc), atropine sulfate (2 mg/kg, im), and pralidoxime (25 mg/kg, im) were monitored for seizure activity for 4 h post-exposure. Animals were separated into groups with low vs. high seizure activity based on behavioral criteria and electroencephalogram (EEG) recordings. Cholinesterase activity was evaluated by Ellman assay and neuropathology at 1, 2, 4, and 60 d post-exposure by Fluoro-Jade C (FJC) staining and micro-CT imaging. DFP significantly inhibited cholinesterase activity in the cortex, hippocampus, and amygdala to the same extent in low and high responders. FJC staining revealed significant neurodegeneration in DFP low responders albeit this response was delayed, less persistent, and decreased in magnitude compared to DFP high responders. Micro-CT scans at 60 d revealed significant mineralization that was not significantly different between low vs. high DFP responders. These findings highlight the importance of considering non-seizing patients for medical care in the event of a chemical emergency. They also suggest that OP intoxication may induce neurological damage via seizure-independent mechanisms, which if identified, might provide insight into novel therapeutic targets.

Key Words*:* Diisopropylfluorophosphate, micro-CT, neurodegeneration, organophosphate neurotoxicity, *status epilepticus*

Abbreviations

AChE, acetylcholinesterase; AS, atropine-sulfate; BChE, butyrylcholinesterase; ChE, cholinesterase; CT, computed tomography; DFP, diisopropylfluorophosphate; EEG, electroencephalogram; FJC, Fluoro-Jade C; im, intramuscular; ip, intraperitoneal; OP, organophosphate; 2-PAM, pralidoxime; PBS, phosphate-buffered saline; ROI, region of interest; sc, subcutaneous; SE, status epilepticus; T2w, T2-weighted; VEH, vehicle

Introduction

Organophosphate (OP) nerve agents have been used as chemical threat agents in Tokyo and Syria (Okumura, Hisaoka et al. 2005, Thiermann, Worek et al. 2013), and OP poisonings have been estimated to cause hundreds of thousands of deaths annually throughout the world (Gunnell, Eddleston et al. 2007). OPs cause acute neurotoxicity by inhibiting acetylcholinesterase (AChE), which can trigger seizures that progress to *status epilepticus* (SE), respiratory failure, and death (reviewed in de Araujo Furtado, Rossetti et al. 2012). Clinical and epidemiological data suggest that humans who survive OP-induced SE exhibit persistent neurological deficits, such as structural brain damage, electroencephalographic abnormalities, cognitive deficits, and affective disorders (reviewed in Chen 2012). However, it has been observed that seizure behavior in humans acutely intoxicated with OPs is variable, ranging from the complete absence of apparent seizure activity to SE (Okumura, Takasu et al. 1996, Peter, Sudarsan et al. 2014). For example, victims of the Tokyo subway sarin attack exhibited differential susceptibility to cholinergic symptoms and seizure induction following acute exposure (Yanagisawa, Morita et al. 2006). While preclinical studies demonstrate that the severity and extent of brain damage following acute OP intoxication are proportional to seizure duration (McDonough, Dochterman et al. 1995, Hobson, Rowland et al. 2017), it remains unclear to what extent intoxicated individuals who do not seize are susceptible to neurological damage.

Acute intoxication with the OP threat agent, diisopropylfluorophosphate (DFP), causes SE in experimental animals (Li, Lein et al. 2011, Todorovic, Cowan et al. 2012) that results in acute and persistent neuropathology that parallels the neuropathology observed in humans following acute OP intoxication (Flannery, Bruun et al. 2016, Siso, Hobson et al. 2017, Guignet, Dhakal et

al. 2019). However, over the past 10 years, we have observed that 10-15% of adult male Sprague-Dawley rats exhibit minimal to no seizure behavior when injected with a dose of DFP that typically triggers prolonged seizure activity in rats of the same strain, sex, weight, and age. These observations are consistent with previous reports of variable sensitivity to DFP toxicity in Sprague-Dawley rats (Russell, Overstreet et al. 1982), and of non-seizing animals in rodent models of acute intoxication with soman (Prager, Aroniadou-Anderjaska et al. 2013) or sarin (Te, Spradling-Reeves et al. 2015, Lewine, Weber et al. 2018).

A subpopulation of rats that is apparently resistant to DFP-induced seizures represents a unique model for determining whether acute OP intoxication can induce neurological damage in non-seizing individuals. Here, we leveraged this subpopulation to compare seizure behavior, electrographic seizure activity, AChE activity, and neuropathology in rats that respond to acute DFP intoxication with robust seizure behavior vs. those that exhibit minimal seizure behavior. Our findings suggest that DFP can cause persistent neurological damage independent of severe seizure activity. In addition, our results indicate that while seizure activity influences the spatiotemporal profile and magnitude of the neuropathologic response to acute OP intoxication, it is not the sole determinant of persistent OP neurotoxicity. These data suggest that therapeutic strategies focused solely on terminating seizure activity will likely not fully protect the brain against long-term neurological damage. Understanding seizure-independent mechanisms of damage will likely provide novel therapeutic insights for mitigating adverse neurological outcomes in all exposed individuals in a chemical emergency involving OPs.

Materials and Methods

Animals and husbandry

Animals were maintained in facilities fully accredited by AAALAC International, and all studies were performed with regard for alleviation of pain and suffering under protocols approved by the UC Davis Institutional Animal Care and Use Committee (IACUC protocol numbers 20122 and 20165). All animal experiments were conducted in accordance with the ARRIVE guidelines and the National Institutes of Health guide for the care and use of laboratory animals (NIH publication No. 8023, revised 1978). All surgical procedures were performed under the UC Davis IACUC guidelines for rodent survival surgery. Adult male Sprague-Dawley rats (~8 weeks old, 250-280 g; Charles River Laboratories, Hollister, CA, USA) were housed individually in standard plastic cages under controlled environmental conditions (22 ± 2^0C, 40-50% humidity) with a normal 12 h light/dark cycle. Food and water were provided *ad libitum.*

Animal Selection

For ~10 years, the Lein lab has been regularly conducting experiments with rats acutely intoxicated with DFP. Over the first few years, we began to notice that a small percentage of animals did not exhibit robust seizure behavior following injection with DFP. To determine the approximate frequency of DFP low responders, historical seizure data from several cohorts (combined total of 62 animals) were evaluated retrospectively. Due to the low incidence of DFP low responders, the animals reported here were removed from various cohorts over a period of ~4 years. This was done primarily because of ethical concerns associated with generating a single large animal cohort to study only a small subset of animals. When a DFP low responder was identified in an ongoing study, a DFP high responder and vehicle control were randomly selected from the same cohort to control for differences across cohorts. The animals removed

from the original cohort for this study were analyzed exclusively for the present study. Therefore, none of the animals reported herein have been analyzed in another study nor has data from these animals been previously published. Animals were selected over a 4-year period until sample sizes for each endpoint reached the number needed to reliably detect group differences as determined by power analysis (e.g. geometric mean ratios of 2.0+ under two-sided testing with alpha=5%). As described in **Table 3-1**, unique cohorts of animals were collected for electroencephalographic (EEG) recordings because electrode implantation is a confound for histological analyses. Another unique cohort was used for micro-computed tomography (micro-CT) because it was performed at a late time point and required a higher sample size as determined by power analysis.

Dosing paradigm

Upon arrival in the laboratory, DFP (Sigma Chemical Company, St Louis, MO, USA) was aliquoted and stored at -80°C. Under these storage conditions, DFP remains stable for over one year (Heiss, Zehnder et al. 2016). The purity of each lot of DFP was determined in-house using ^{1}H-, ^{13}C, ^{19}F and ^{31}P-NMR methods, as previously described (Gao, Naughton et al. 2016), and found to be approximately 90 ± 7%. For all experiments, DFP was diluted with ice-cold sterile phosphate-buffered saline (PBS, 3.6 mM Na_2HPO_4, 1.4 mM NaH_2PO_4, 150 mM NaCl; pH 7.2) five min before administration. Unanesthetized rats were injected sc in the subscapular region with 300 µl DFP at 4 mg/kg, a dose shown to induce *status epilepticus* in adult male Sprague Dawley rats (Flannery, Bruun et al. 2016, Guignet, Dhakal et al. 2019). To increase survival following DFP exposure, animals were injected im with 2 mg/kg atropine sulfate (Sigma) and 25 mg/kg pralidoxime (2-PAM; Sigma) in sterile isotonic saline (0.9% NaCl) within 1 min after DFP injection (**Fig. 3-1A**). Certificate of analysis provided by the manufacturers confirmed the purity

of atropine sulfate (>97%, lot #BCBM6966V) and 2-PAM (>99%, lot #MKCG3184). These drugs effectively block peripheral cholinergic toxicity, thereby reducing mortality (Bruun, Guignet et al. 2019). Vehicle (VEH) control animals were injected sc with 300 µl ice-cold sterile PBS in place of DFP but were similarly treated with atropine and 2-PAM. A random number generator was used to assign animals to experimental groups. Once returned to their home cage, rats were given access to moistened chow for 3-5 days or until they resumed consumption of solid chow. All experiments were performed in at least three independent cohorts.

Behavioral seizure scoring

To identify animals with "high" versus "low" seizure activity, seizure behavior was scored every 5 min during the first 120 min after DFP injection and then every 20 min from 120 – 240 min post-DFP injection using an established seizure behavior scale (Deshpande, Carter et al. 2010) as previously described (Guignet, Dhakal et al. 2019). The seizure scores for each individual animal were averaged over the first 4 h post-injection to determine the "average seizure score". An average seizure score of 2.5 was used as the threshold to separate animals that exhibited behavior consistent with *status epilepticus* (referred to as "DFP high responders") and animals that did not exhibit behavior consistent with *status epilepticus* (referred to as "DFP low responders").

EEG recordings

In an independent cohort of animals not used for biochemical or histological analyses, both DFP low and high responders (6-7 per group) were monitored for 1 h post-DFP to determine whether behavioral seizures correlated with electrographic seizure activity. A tethered EEG system was used for these short-term electrographic experiments as previously described (Guignet, Dhakal et al. 2019). Briefly, 60 mg/kg ketamine and 0.5 mg/kg dexmedetomidine were injected ip

to anesthetize animals and stabilize them in a stereotaxic apparatus (Kopf Instruments, Tujunga, CA, USA). Six recording screws were implanted epidurally and connected to a 6-pin rat implant (Pinnacle 8239-SE3, Pinnacle Technology, Lawrence, KS, USA). Animals were allowed a minimum of 7 d to recover from surgery before undergoing further procedures. EEG recordings were acquired for ~10 min prior to DFP injection (baseline period) and for 1 h post-DFP injection using the Pinnacle 8401 Data Conditioning & Acquisition System (Pinnacle Technology). These data were reviewed using Sirenia Seizure Pro software (Pinnacle Technology) and quantitated using NeuroScore™ (version 3.3.9, Data Sciences International, St. Paul, MN, USA). EEG data were filtered using a band-pass filter of 20-70 Hz to reduce noise, as previously described (Pouliot, Bealer et al. 2016), and analyzed using epoch durations of 1 s. Spike amplitude was quantified for each time period using root mean squared (RMS) values automatically extracted from the band-pass filtered EEG traces. In order to calculate spike frequency, the average amplitude of the baseline period was calculated for each animal (~20 μV in most animals). Peaks that reached >2x baseline amplitude were identified as paroxysmal and therefore quantified. The spike frequency (RMS) and spike amplitude (number of peaks/s above baseline) were quantified and averaged over the 1 h recording period.

To determine whether DFP low responders exhibit delayed electrographic abnormalities, a different cohort of animals (3-4 per group) was implanted with cortical electrodes to wirelessly monitor electrographic activity for 24 h following acute DFP intoxication. Animals were deeply anesthetized with isoflurane (1-3%) in medical grade oxygen (flow rate=1L/min) for the entire duration of the surgical procedure. Fur was shaved from the surgical site before stabilizing the head in a stereotaxic apparatus (Stoelting, Wood Dale, IL, USA). Altalube™ ophthalmic ointment (Altaire Pharmaceuticals Inc, Riverhead, NY, USA) was applied to the eyes to prevent them from

drying out during the procedure. A complete aseptic surgical scrub of the skin was performed using three alternating rounds of betadine scrub (Purdue Products, Stamford, CT, USA) and 70% isopropyl alcohol wipes (Covidien Plc, Dublin, Ireland) before creating an approximate 1.5-inch incision that extended from between the eyes to the base of the skull. Four head mount screws were implanted at the following coordinates relative to Bregma: 2 mm anterior, 7mm posterior, and 1.5 mm laterally on each side of the sagittal skull suture. Sterile F20-EET telemetry devices (Data Sciences International) were inserted between the skin and muscle layer along the flank of the animal, and the recording wires were extended to the skull and secured around the head mount screws. The screws and leads were secured using dental cement (Stoelting). The incision site was sutured (Ethicon, Bridgewater, NJ, USA) over the head mount, and animals were given separate injections of 5% dextrose in sterile saline (1 mL, sc, Baxter Healthcare, Deerfield, IL, USA) and Meloxicam (4 mg/kg, sc, Vet One, Boise, ID, USA) before being removed from anesthesia and allowed to recover on a heating pad. Animals were administered two additional doses of Meloxicam (4 mg/kg, sc, once daily for 48 h) and allowed to recover for 14 d before being administered DFP.

One day prior to injection with DFP, animals were placed in their home cages on wireless PhysioTel® Receivers (Model RPC1, Data Sciences International). Baseline electrographic activity (Ponemah software version 5.32, Data Sciences International) coupled with video monitoring (Noldus media recorder, version 2.6, Wageningen, Netherlands) was recorded for a full 24 h to capture normal wake and sleep EEG patterns in freely moving animals. On the day of DFP injections, animals were given either a single dose of DFP or VEH (PBS), and video EEG activity was recorded during the first 24 hours after DFP administration. Seizure activity was determined as spike wave discharges with an amplitude at least twice that of background activity

in awake animals with at least 100 Hz frequency and duration of at least 5 s. All seizures were automatically detected using NeuroScore™ (version 3.3.9, Data Sciences International) and manually validated by a trained investigator.

Cholinesterase assays

At 1 and 4 d post-DFP exposure, animals were anesthetized with 4-5% isoflurane in medical grade oxygen (Western Medical Supply, Arcadia, CA, USA) and euthanized by perfusion with cold PBS (15 mL/min) using a Masterflex peristaltic pump (Cole Parmer, Vernon Hills, IL, USA). Brains were rapidly harvested and brain regions rapidly dissected on ice. The cortex, hippocampus, and amygdala of each animal were snap frozen on dry ice and stored at -80°C. The Ellman assay (Ellman, Courtney et al. 1961) was used to measure cholinesterase activity in each brain region using 5,5'-dithio-bis(2-nitrobenzoic acid) (DTNB, Sigma) as the colorimetric reagent and acetylthiocholine iodide (ASChI, Sigma) as the AChE substrate. All samples were homogenized in lysis buffer (0.1 M phosphate buffer, pH 8.0 with 0.1% Triton) using a Polytron PT 1200 E and centrifuged for 1 min at 13,400 x g. Supernatant was collected and plated in triplicate in a 96-well plate for analysis. Blank wells contained an equal volume of buffer with DTNB. After equilibration with DTNB for 5 min, the reaction was started with the addition of ASChI. ASChI hydrolysis was quantified by measuring changes in absorbance at 405 nm over 15 min using the Synergy H1 Hybrid Plate Reader with Gen5 2.0 software (BioTek Instruments, Winooski VT, USA). All samples were run in the absence and presence of the butyrylcholinesterase (BChE) inhibitor tetraisopropyl pyrophosphoramide (100 µM) to measure total ChE versus AChE specific activity, respectively. ChE activity was normalized against total protein concentration determined using the BCA assay according to the manufacturer's directions (Pierce, Rockford, IL, USA).

Fluoro-Jade C staining

At 1, 2, 4, and 60 d post-DFP exposure, animals were anesthetized with 4-5% isoflurane in medical grade oxygen and perfused with cold PBS (15 mL/min) using a Masterflex peristaltic pump (n=6-10/group). Brains were quickly harvested, cut into 2 mm thick coronal sections starting at Bregma point 0 and post-fixed in cold 4% (w/v) paraformaldehyde (Sigma) in PBS (pH 7.4) for 24 h. Coronal sections were removed from fixative, cryoprotected in 30% (w/v) sucrose (Fisher, Houston, TX, USA) in PBS overnight at 4°C, and then embedded in OCT medium (Fisher) in plastic cryomolds and stored at -80°C until sectioned. Frozen blocks were cryosectioned into 10 µm thick coronal sections, which were mounted on Superfrost Plus microscope slides (Fisher) and stored at -80°C until stained. Fluoro-Jade C (FJC; Cat. #AG325, Lot #2301303, Millipore, Billerica, MA, USA) labeling was performed according to the manufacturer's protocol with minor modifications. Briefly, after 30 min of drying at 50°C, sections were rinsed with 70% ethanol and incubated for 10 min on a shaker table in a solution of 0.06% (w/v) potassium permanganate (Sigma) in distilled water followed by 2 min in distilled water. Sections were then incubated for 10 min in a freshly prepared solution of 0.0001% FJC in 0.1% (v/v) acetic acid (Acros Organics, Geel, Belgium) in distilled water containing a 1:50,000 dilution of DAPI (Invitrogen, Carlsbad, CA, USA). The slides were dried completely at 50°C and then dipped in xylene (Fisher) for 1 min. The slides were mounted in Permount (Fisher), cover slipped, dried overnight, and stored at 4°C until imaged.

Images were automatically acquired at 20X magnification using the ImageXpress high content imaging system (Molecular Devices, Sunnyvale, CA, USA). The number of FJC-labeled cells per unit area was automatically quantified in the somatosensory cortex, hippocampus, piriform cortex, and thalamus using the Cell Counter plugin for the ImageJ image analysis

software (version 1.50i, http://imagej.nih.gov/ij). Input parameters for determining cell size and circularity were 50 µm-150 µm diameter and 0.3-1.0 circularity, respectively. Four brain sections with Bregma ranging from -2 to -5 mm were analyzed per animal. FJC-labeled cells were counted in three regions per section, and the number of cells was averaged across sections in each brain region per animal. The number of FJC-labeled cells was quantified as the number of positively-labelled cells per 1.0 mm^2. Image acquisition and analysis were performed by an investigator blinded to experimental group.

Micro-CT imaging

Animal brains were imaged *in vivo* at the UC Davis Center for Molecular and Genomic Imaging using an Inveon MM CT scanner (Siemens Preclinical Solutions, Malvern, PA, USA). Animals were anesthetized with isoflurane/O_2 (Piramal Healthcare, Bethlehem, PA, USA) using 2.0-3.0% (vol/vol) to induce and 1.0-2.0% (vol/vol) to maintain anesthesia. Once animals were completely anesthetized, as determined by a complete absence of toe squeeze reflex, they were stereotactically restrained within the CT scanner on custom restraint beds. CT scan parameters were performed as previously described (Supasai et al., under review). Scans were digitally reconstructed using a Fledkamp algorithm with Shepp-Logan filter into 16 bit values.

Micro-CT scan images were analyzed using Amira software (version 6.5.0, ThermoFisher) as previously described (Supasai et al., under review). Briefly, regions of interest (ROIs) were drawn around the dorsolateral and medial thalamus on previously acquired T2-weighted (T2w) magnetic resonance images. Micro-CT scans were "de-noised", manually aligned to T2w images, and an intensity threshold was applied to isolate areas of mineralization. ROI volumes were exported from Amira for the dorsolateral thalamus, medial thalamus, and mineral deposits. All analyses were conducted by a single experimenter without any knowledge of exposure group

and time point. The percent mineralization was calculated for each ROI, and three-dimensional reconstructions of the mineralized areas in both the dorsolateral and medial thalamus were combined to visualize mineral deposits throughout the thalamus. While this technique provides clear visualization of mineralized tissues, microCT does not provide identification of the chemical composition of mineral deposits.

Statistical analysis

Primary outcomes included measures of total ChE, AChE, and number of FJC-labeled cells across multiple regions of the brain for three groups of animals (VEH, DFP low responders, and DFP high responders). The ChE measures were obtained for the cortex, hippocampus, and amygdala. The number of FJC-labeled cells was measured across the somatosensory cortex, hippocampus, piriform cortex, and thalamus. Mixed-effects regression models, including animal-specific random effects, were used to assess the differences between the groups across the brain regions. Because time was another factor of interest, groups were further split by day (ChE: days 1, 4; FJC labeling: days 1, 2, 4, 60). Exploratory analysis indicated that a natural logarithmic transformation was needed for all outcomes to stabilize the variance and meet the underlying assumptions of the mixed-effects models. Due to zeros in the FJC-labeling experiments, all FJC values were shifted by 5 prior to the log-transformation. Days, group, and brain region were all variables of interest in the models. Interactions between these variables were also considered. Akaike information criterion was used for model selection, and Wald tests were used for comparing groups in each brain region by time point.

Micro-CT data were available for 23 animals for two regions (medial and dorsolateral thalamus). Mixed-effects regression models, including animal-specific random effects, were used to assess differences between groups. Exploratory analysis indicated that a natural logarithmic

transformation was needed for percent mineralization to stabilize the variance and meet the underlying assumptions of the mixed-effects models. Due to observed zeroes for this outcome, all values were shifted by 0.5 prior to taking the natural logarithm. Primary factors of interest included group (VEH, DFP low responders, and DFP high responders) and region (medial and dorsolateral thalamus). An interaction between these variables was also considered. Akaike information criterion was used for model selection to identify the best model. Specific contrasts were constructed for all pairwise comparisons between groups and examined using Wald tests.

FJC and micro-CT results are presented as geometric mean ratios. These ratios may be interpreted as fold changes, so that a ratio of 1.5 corresponds to a 50% increase and a ratio of 0.5 corresponds to a 50% decrease. Point estimates of the ratios and the 95% confidence intervals are presented in the figures. When the confidence interval includes 1, there is no statistical evidence of a difference between groups. However, when the confidence interval does not include 1, the estimated effect is significant at the 5% level. All analyses were conducted using SAS version 9.4, and graphics were created in R version 3.1.0.

Results

DFP low responders do not exhibit seizure-like behavior or electrographic activity

Historic data in the Lein laboratory suggests that ~13% of adult male Sprague Dawley rats exposed to a DFP dosing paradigm that typically generates robust seizures (**Fig. 3-1A**) do not respond with seizure-like behavior (**Fig. 3-1B**). To determine whether animals that do not show overt seizure behavior develop neurological consequences, we selected DFP low responders as they arose in ongoing studies in the lab for further study. A vehicle control and DFP high responder was randomly selected from each cohort of animals from which DFP low responders

were obtained, resulting in 16 animals per group collected over a 2-year period. To identify DFP low vs. high responders, we used a modified Racine scale [(Deshpande, Carter et al. 2010); also see **Fig. 3-1C**] to assess seizure behavior (**Fig. 3-1D**). The mean ± SE of the average seizure score across all DFP low responders was 1.7 ± 0.3. Notably, none of the animals in this group exhibited seizure behavior scores above 2.5 throughout the first 4 h post-exposure. The mean ± SE of the average seizure score across all DFP high responders was 3.1 ± 0.2. Vehicle controls (animals not exposed to DFP) did not exhibit any seizure behavior or any signs of cholinergic toxicity, thus, their mean seizure score was 0.

To confirm the absence of seizure activity in DFP low responders, a separate cohort of animals was implanted with intracortical electrodes to record EEG activity during the first 60 min post-DFP. EEG recordings showed comparable baseline activity between DFP high and low responders (**Fig. 3-2A**). However, following acute DFP intoxication, the EEG of DFP high responders was consistent with SE, while the EEG of DFP low responders did not appear different from baseline. Quantification of spike amplitude and frequency confirmed there was no significant difference between baseline EEG in high vs. low responders (**Fig 3-2B**). Following DFP administration, high responders showed significantly greater spike amplitude and frequency than DFP low responders. Correlation analysis of all DFP animals (including both high and low responders) revealed that behavioral seizure scores are strongly correlated with EEG measures (**Fig 3-2C**), including spike amplitude (left; Spearman r=0.780, p=0.002) and spike frequency (right; Spearman r=0.835, p=0.0006).

To determine whether DFP low responders develop delayed seizure activity, EEG recordings were collected from both DFP high and low responders over the first 24 h post-injection (**Fig. 3-3A**). DFP high responders showed ~60 min of total seizure activity compared to 0 min in DFP

low responders (**Fig. 3-3B**). Both DFP high and low responders showed comparable baseline electrographic activity for ~2 h prior to DFP injection. (**Fig. 3-3C**). EEG traces over the 24 h recording period showed peak seizure activity in DFP high responders at 30 min, with paroxysmal spike activity at 6 h post-exposure. Although there was a dramatic reduction in seizure activity in the DFP high responders by 12 h, abnormal spike activity was observed throughout the 24 h period. In contrast, DFP low responders had minimal deviation from baseline EEG activity throughout the 24 h recording period (**Fig 3-3C**).

Both DFP high and low responders show significant cholinesterase inhibition

One possible explanation for the lack of seizure activity in DFP low responders relative to DFP high responders is differences in DFP metabolism and uptake in the brain. To address this possibility, cholinesterase activity was measured in the cortex, hippocampus, and amygdala at 1 and 4 d post-exposure. Relative to VEH animals, DFP low responders had significantly decreased activity of total ChE and AChE in all brain regions at both time points (**Fig. 3-4**). Similarly, total ChE and AChE activities were significantly decreased in all brain regions of DFP high responders at both time points compared to VEH animals. Comparative analysis suggests that total ChE and AChE activities were similarly inhibited in DFP low and high responders in all brain regions examined, suggesting no differences in DFP metabolism or brain uptake between the two groups.

Acute DFP intoxication triggers neuronal degeneration in DFP low and high responders

FJC staining was performed at both early (1, 2, and 4 d) and late (60 d) times post-DFP injection to evaluate neurodegeneration in brain regions previously found to be significantly affected by acute DFP intoxication, specifically, the somatosensory cortex, hippocampus, piriform cortex, and thalamus (Hobson, Rowland et al. 2017, Siso, Hobson et al. 2017).

Representative photomicrographs of FJC staining in the somatosensory cortex of VEH, DFP low responders, and DFP high responders (**Fig. 3-5A)** reveal negligible FJC staining in VEH animals at any time point, and significantly increased FJC staining in DFP high responders as early as 1 d post-exposure that persists at 60 d post-exposure. An increase in FJC-labeled cells was also evident in the somatosensory cortex of DFP low responders, although this appeared to be delayed and of lower magnitude compared to the DFP high responders.

Quantitative assessment of the number of FJC-labeled cells in the somatosensory cortex, hippocampus, piriform cortex, and thalamus as a function of time post-exposure confirmed these observations (**Fig. 3-5B)**. The number of FJC-labeled cells in DFP low responders did not differ from VEH animals in any brain region at 1 d post-exposure, except for a slight increase in the piriform cortex ($p=0.03$). However, on days 2 and 4 post-exposure, DFP low responders had significantly increased numbers of FJC-labeled cells in all four brain regions relative to VEH. By day 60 post-exposure, FJC staining in DFP low responders was not significantly different from that in VEH in any brain regions, except the piriform cortex. In contrast, relative to VEH, DFP high responders had significantly increased numbers of FJC-labeled cells in all four brain regions at 1, 2, and 4 d post-exposure. By day 60 post-exposure, significantly elevated FJC staining was only apparent in the somatosensory cortex of the DFP high responders ($p=0.002$). The number of FJC-labeled cells was significantly greater in DFP high responders relative to DFP low responders in all four brain regions on days 1 and 2 post-exposure. This difference persisted on days 4 and 60 post-exposure in the somatosensory cortex, but not in the hippocampus, piriform cortex, or thalamus.

DFP low and high responders show significant mineralization in the thalamus at 60 d post-exposure

Calcium dysregulation is known to occur following acute OP intoxication (Deshpande, Blair et al. 2016), and calcification in the brain is associated with numerous neurologic conditions, including chemical-induced *status epilepticus* (Gayoso, Al-Majdalawi et al. 2003, Aggarwal, Li et al. 2018). Therefore, micro-CT was used to assess mineralization in the brain of DFP rats. Significant mineralization was detected in both the medial thalamus and dorsolateral thalamus of DFP low and high responders at 60 d post-DFP exposure (**Fig. 3-6A, 3-6B**). Quantification of the percent mineralization within the region of interest confirmed significantly increased mineralization in the thalamus of both DFP low and high responders compared to VEH animals (**Fig. 3-6C**). However, there was no significant difference in the percent area of mineralization in the thalamus of DFP high vs. low responders. Correlational analysis of all DFP-intoxicated animals (low and high responders) failed to find a correlation between average seizure score and percent area of mineralization (Spearmen r=0.189, p=0.43) (**Fig. 3-6D**).

Discussion

Previous reports have demonstrated that repeated exposure to lower doses of DFP (400 µg/kg) that do not trigger seizures can cause neuronal injury and behavioral changes in a rodent model (Phillips and Deshpande 2016). Here, we extend these observations by demonstrating that a single exposure to DFP at a dose that elicits robust SE in the majority of exposed animals can also cause neurological damage independent of seizure activity. Our findings highlight the importance of considering neuropathological consequences in both seizing and non-seizing individuals following acute OP intoxication.

As summarized in **Table 3-2**, DFP low responders show little to no seizure activity, despite >80% inhibition of brain AChE, which is well above the threshold of >65% AChE inhibition

presumed to be necessary for seizure initiation (Tonduli, Testylier et al. 2001). We confirmed the lack of seizure activity in the DFP low responder subpopulation over the first 24 hours post-exposure using both behavioral and EEG criteria. Consistent with previous reports of rats acutely intoxicated with DFP (Deshpande, Carter et al. 2010, Guignet, Dhakal et al. 2019) or soman (Prager, Aroniadou-Anderjaska et al. 2013), animals that did not exhibit seizure behavior were also negative for electrographic seizure activity. The level of AChE inhibition observed in three different brain regions associated with seizure initiation and propagation was comparable in DFP low vs. high responders, suggesting that the differential seizure responses are not due to differences in DFP distribution in the brain. It seems unlikely that AChE was significantly inhibited in DFP low responders in a brain region we did not examine because DFP is lipid soluble and rapidly penetrates all regions of the brain (Martin 1985). Moreover, it has been previously reported that acute intoxication of rats with a seizurogenic dose of DFP results in similar levels of AChE inhibition across multiple brain regions (Ferchmin, Andino et al. 2014).

While our study did not delineate mechanism(s) contributing to the seizure resistance of the DFP low responders, our observations are consistent with a report demonstrating that Sprague-Dawley rats, which are an outbred strain, exhibit more variable seizure thresholds than inbred rat strains (Loscher, Ferland et al. 2017). Indeed, previous studies have established that genetic background influences individual susceptibility to chemical convulsants in mice, rats, and non-human primates (Lin, Duek et al. 2012, Matson, McCarren et al. 2017, Copping, Adhikari et al. 2019). Genetic mutations in α4 and β2 neuronal nicotinic acetylcholine receptor subunits are implicated as determinants of seizure susceptibility in rodent models, and mutations in the Kir4.1 gene, *Kcnj10*, have been linked to both rodent and human forms of epilepsy (Loscher, Ferland et al. 2017). Whether these mutations contribute to the differential susceptibility of DFP low vs.

high responder subpopulations is a testable hypothesis. Alternatively, it may be that DFP low responders are differentially responsive to the protective effects of atropine and/or oxime. However, that seems unlikely because both compounds are poorly brain penetrant and primarily protect against lethality by mitigating peripheral cholinergic symptoms (Bruun, Guignet et al. 2019). A previous transcriptomic analysis of brains from seizing vs. non-seizing animals in a rat model of acute sarin intoxication identified increased expression of anti-inflammatory and apoptotic genes in the brains of non-seizing animals, suggesting that seizure resistance may be linked to differential activation of these pathways (Te, Spradling-Reeves et al. 2015).

While the DFP low responders were resistant to OP-induced seizures, this did not translate into protection against the neuropathological consequences associated with acute OP intoxication. The spatiotemporal pattern of neurodegeneration observed in the DFP high responders is consistent with previous studies of acute DFP (Li, Lein et al. 2011, Siso, Hobson et al. 2017) and soman (McDonough and Shih 1997) intoxication. Also consistent with prior literature (Tanaka, Graham et al. 1996, McDonough and Shih 1997), the extent of neurodegeneration was positively correlated with seizure severity as reflected by the fact that DFP high responders exhibited earlier onset and greater magnitude of neurodegeneration compared to DFP low responders across all the brain regions and post-exposure times that were examined. Collectively, these finding suggest that while there is a positive correlation between seizure severity and the extent of neuronal damage, seizure activity is not the sole pathogenic mechanism responsible for neurodegeneration following acute OP intoxication.

The mechanism(s) contributing to neurodegeneration independent of sustained seizure activity in the DFP low responders remain unknown. In the rat model of acute soman intoxication, the resolution of neurodegeneration coincides temporally with the recovery of

AChE (Prager, Aroniadou-Anderjaska et al. 2014), suggesting the possibility that persistent AChE inhibition contributes to the neurodegeneration observed in DFP low responders. However, the onset of neurodegeneration in the DFP low responders was delayed relative to the DFP high responders despite the fact that AChE inhibition was comparable in terms of both the level and timing of inhibition. This suggests that mechanisms other than or in addition to AChE inhibition are driving the neuropathology observed in the DFP low responders. Reports that OPs interact with multiple molecular targets in addition to AChE (reviewed in (Terry 2012) support this possibility.

Additional alternative mechanisms include neuroinflammation, (Banks and Lein 2012, Guignet and Lein 2019), oxidative stress, and disruption of axonal transport (Zaja-Milatovic, Gupta et al. 2009, Terry 2012, Naughton and Terry 2018), all of which can be induced by exposure to OPs at levels that do not trigger seizures. Another possible mechanism suggested by the micro-CT data from this study is calcium dyshomeostasis. Calcium is a major constituent of mineralized regions in the brain commonly detected in the thalamus under various chronic neurological conditions (Valdes Hernandez Mdel, Maconick et al. 2012). Published data supports the hypothesis that calcium dyshomeostasis not only mediates acute excitotoxic neuronal injury, but also contributes to several comorbidities observed in survivors of acute OP intoxication, including cognitive dysfunction and acquired epilepsy (Deshpande, Blair et al. 2016). Thus, it has been proposed that calcium-stabilizing drugs may be effective neuroprotectants following acute OP intoxication (Deshpande, Blair et al. 2016). Our data demonstrating significant mineralization in the brains of non-seizing animals acutely intoxicated with DFP suggests that calcium-stabilizing drugs may be useful in treating not only OP-intoxicated individuals with SE but also those with minimal evidence of seizure activity.

In summary, our findings suggest that even if seizures do not occur, neuroprotective therapeutics may still be needed for individuals acutely intoxicated with OPs. Further study of animals that do not exhibit seizures in response to acute OP intoxication may identify mechanisms that confer resistance to OP-induced seizures and seizure-independent mechanisms that contribute to OP-induced neuropathology thereby providing insight into novel therapeutic targets.

Acknowledgements

We thank Dr. Suzette Smiley-Jewell (UC Davis CounterACT Center) for her assistance in editing this manuscript. This work was supported by the CounterACT Program, National Institutes of Health Office of the Director and the National Institute of Neurological Disorders and Stroke [grant number U54 NS079202], predoctoral fellowships to E.A.G from the National Institute of Neurological Disorders and Stroke [grant number F31 NS110522] and the National Institutes of Health Initiative for Maximizing Student Development [grant number R25 GM5676520], and predoctoral fellowships to M.G. from the National Institute of General Medical Sciences [grant number T32 GM099608], and the David and Dana Loury Foundation. This project used core facilities supported by the UC Davis MIND Institute Intellectual and Developmental Disabilities Research Center (U54 HD079125).

Figures and Figure Legends

Table 3-1. Summary of animal cohorts.

Cohort	Endpoint(s) Evaluated	Sample Size	Figure
Historical	Frequency of DFP low responders	62 DFP rats	1b
1	Seizure behavior	16/group	1d
	Cholinesterase (ChE) activity	4-6/group used for ChE	4
	FluoroJade-C (FJC)	6-10/group used for FJC	5
2	Acute EEG (1 h post-DFP)	6-7/group	2
3	Long-term EEG (24 h post-DFP)	3-4/group	3
4	Micro-CT	3 vehicle 6 DFP low responders 14 DFP high responders	6

ChE = cholinesterase, EEG = electroencephalogram, FJC = FluoroJade C

Table 3-2. Summary of major findings.

Group	Avg. Seizure Score	EEG Activity	Cholinesterase Inhibition	FJC Staining	Brain Mineralization
Vehicle	0	−	−	−	−
DFP Low	1.7	−	+++	++ (Delayed)	+++
DFP High	3.1	↑↑↑	+++	+++ (Rapid)	+++

EEG=electroencephalogram, FJC= FluoroJade C, DFP Low=low responder, DFP High=high responder

Figure 3-1

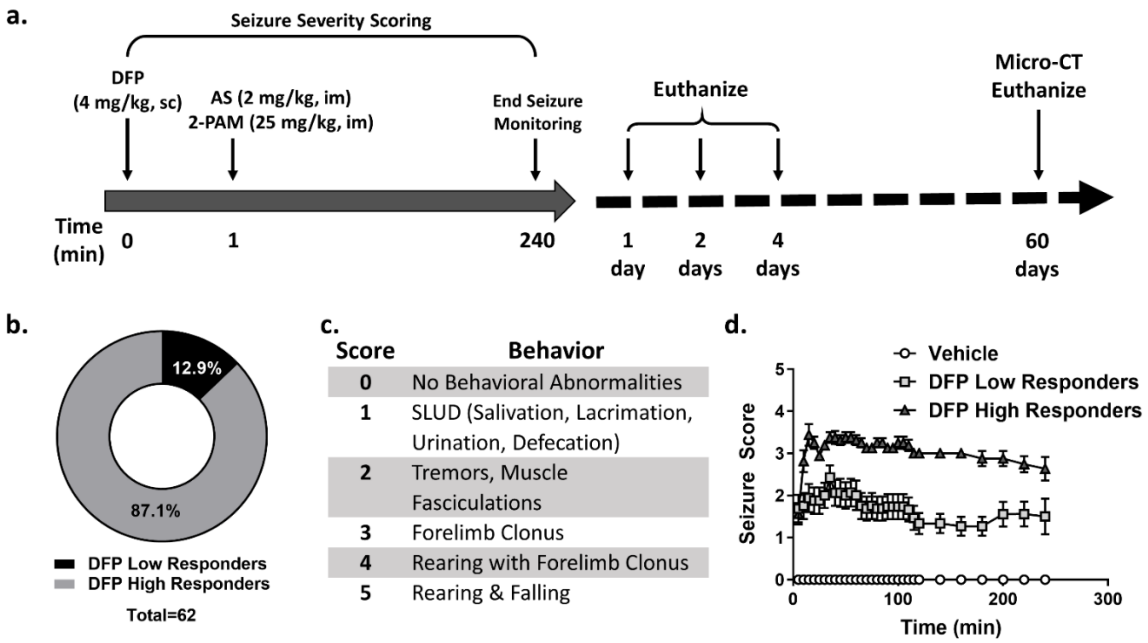
a.
Seizure Severity Scoring
DFP
(4 mg/kg, sc)
AS (2 mg/kg, im)
2-PAM (25 mg/kg, im)
End Seizure
Monitoring
Euthanize
Micro-CT
Euthanize
Time
(min)
0
1
240
1
day
2
days
4
days
60
days
b.
12.9%
87.1%
DFP Low Responders
DFP High Responders
Total=62
c.
Score
Behavior
0
No Behavioral Abnormalities
1
SLUD (Salivation, Lacrimation, Urination, Defecation)
2
Tremors, Muscle Fasciculations
3
Forelimb Clonus
4
Rearing with Forelimb Clonus
5
Rearing & Falling
d.
Vehicle
DFP Low Responders
DFP High Responders
Seizure Score
Time (min)

Figure 3-1. The rat model of acute DFP intoxication and seizure behavior of DFP low versus high responders. (**a**) Schematic illustrating the dosing paradigm used to trigger DFP-induced seizures in adult male Sprague Dawley rats and time-line of data collection. (**b**) Percentage of DFP low vs. high responders in previous studies in the Lein lab. Of 62 DFP-intoxicated rats, 54 were high responders and 8 were low responders. (**c**) Scale used to score seizure behavior in DFP-intoxicated rats. Rats with an average seizure score of ≤ 2.5 were identified as "DFP low responders". (**d**) Temporal profile of seizure scores in VEH, DFP low responders, and DFP high responders. Data presented as mean ± SE (n=16 animals/group).

Figure 3-2

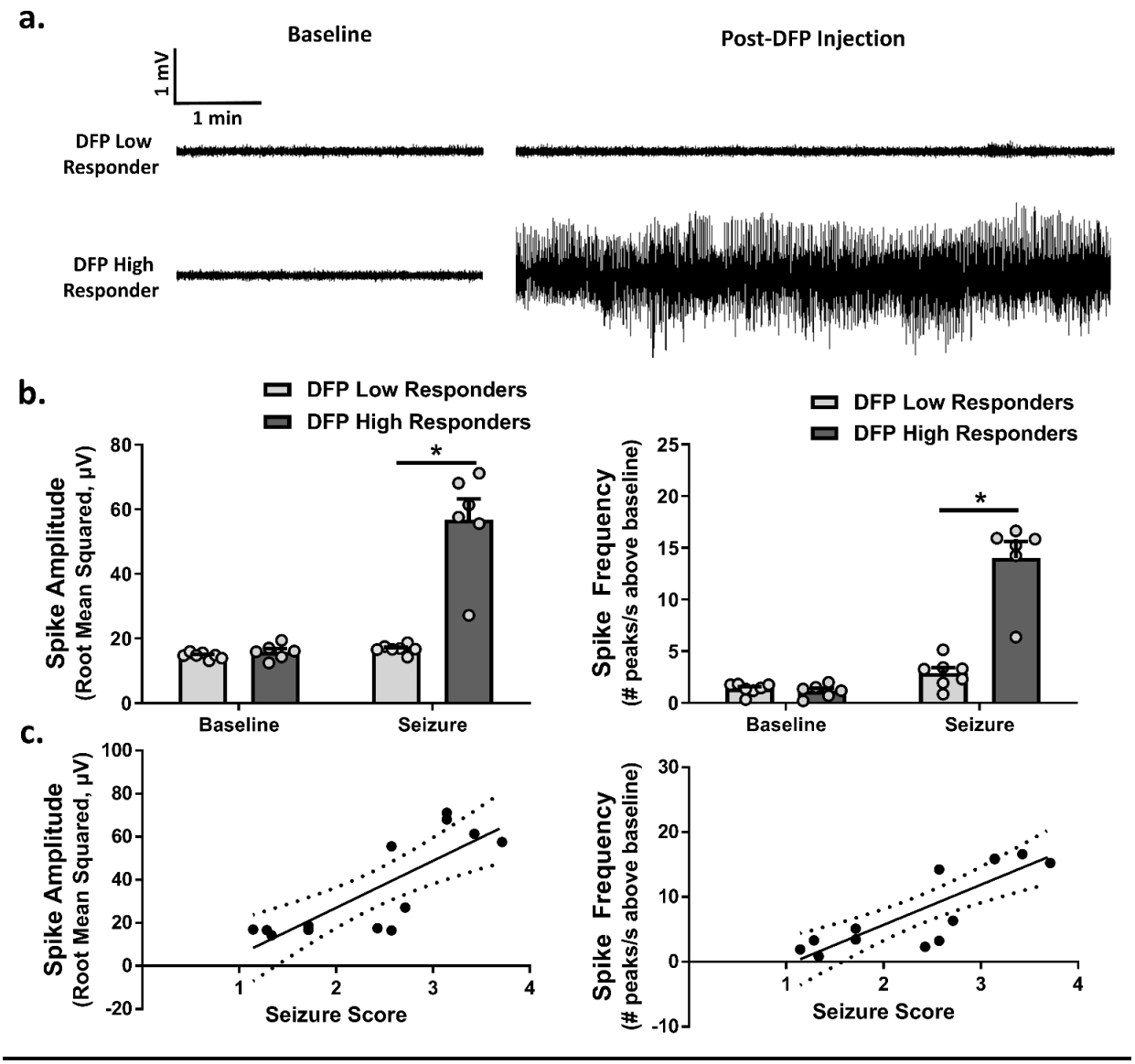
a.
Baseline
Post-DFP Injection
1 mV
1 min
DFP Low Responder
DFP High Responder
b.
DFP Low Responders
DFP High Responders
Spike Amplitude (Root Mean Squared, µV)
Baseline
Seizure
Spike Frequency (# peaks/s above baseline)
c.
Seizure Score

Figure 3-2. Behavioral seizure scores correlate with electrographic activity during the first 60 min post-DFP. (**a**) Representative EEG traces in high and low responding animals before DFP injection (baseline period) and within the first 60 min post-intoxication. (**b**) Quantitative assessment of spike amplitude and spike frequency in both DFP high and low responding animals at baseline and within the first 60 min post-DFP intoxication. Group data are shown with bars representing the mean ± standard error of the mean (n=6-7 animals/group). *Significantly different at $p < 0.05$. (**c**) Correlation analysis between seizure score and spike amplitude (left; Spearman r=0.780, p=0.002) and between seizure score and spike frequency (right; Spearman r=0.835, p=0.0006).

Figure 3-3

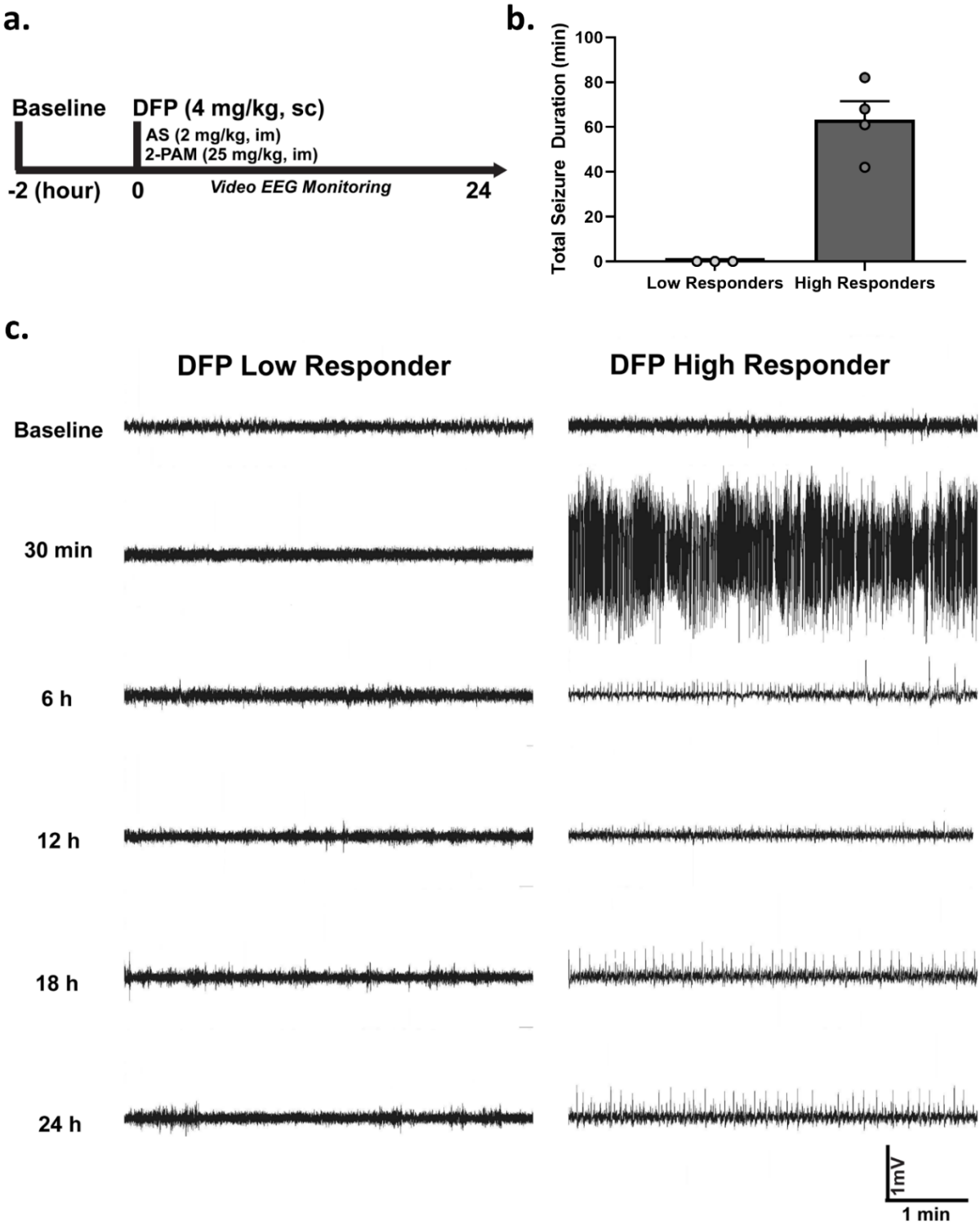
a.
Baseline
DFP (4 mg/kg, sc)
AS (2 mg/kg, im)
2-PAM (25 mg/kg, im)
-2 (hour)
0
Video EEG Monitoring
24
b.
Total Seizure Duration (min)
100
80
60
40
20
0
Low Responders
High Responders
c.
DFP Low Responder
DFP High Responder
Baseline
30 min
6 h
12 h
18 h
24 h
1mV
1 min

Figure 3-3. DFP low responders show no electrographic evidence of seizure activity during the first 24 h post-intoxication. (**a**) Experimental timeline for evaluation of seizure activity in EEG-implanted animals during the first 24 h following DFP intoxication. (**b**) Quantitative assessment of the total duration of electrographic seizure activity (min) during the first 24 h post-DFP in high responding (dark gray; n=4) and low responding (light gray; n=3) animals. Data presented as mean ± SD; p = 0.0571 as determined by Mann Whitney test. (**c**) Representative EEG traces in high responding (left) and low responding (right) DFP animals at baseline, 30 min, 6 h, 12 h, 18 h and 24 h post intoxication.

Figure 3-4

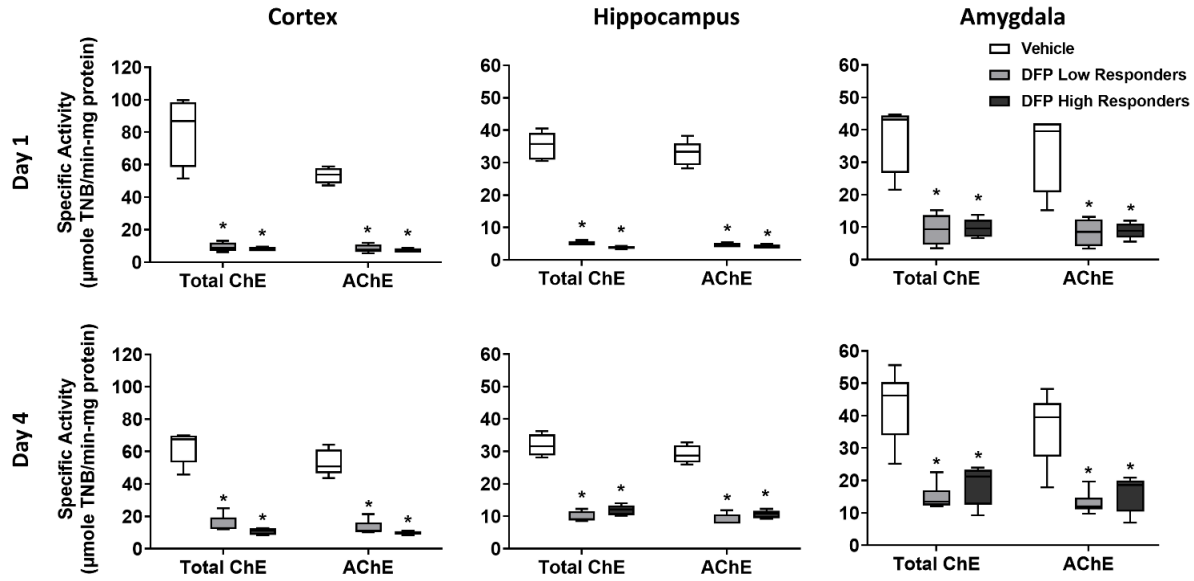
Cortex
Hippocampus
Amygdala
Vehicle
DFP Low Responders
DFP High Responders
Day 1
Day 4
Specific Activity
(µmole TNB/min-mg protein)
Total ChE
AChE

Figure 3-4. Cholinesterase activity in the brain is significantly and similarly inhibited in low and high responding DFP animals. The specific activity of total cholinesterase (total ChE) and acetylcholinesterase (AChE) was measured in cortical, hippocampal, and amygdalar tissue at 1 d and 4 d post-DFP injection. Group data are shown with boxes representing the 25-75 percentile; horizontal lines in the boxes, the median; and whiskers, the maximum and minimum values (n=4-6 VEH, 5-8 DFP animals). *Significantly different from vehicle at $p < 0.05$.

Figure 3-5

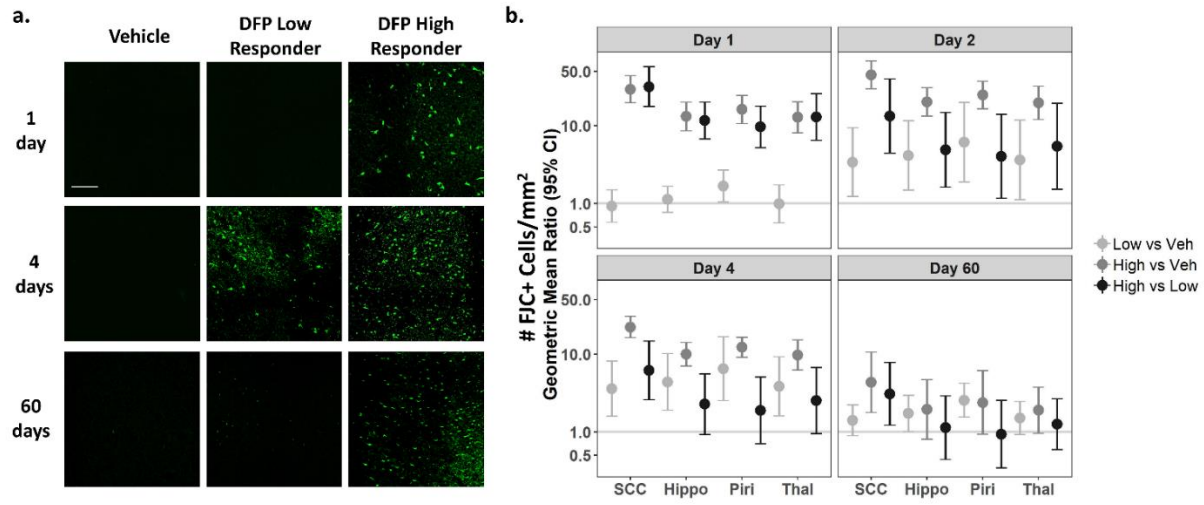
a.
Vehicle
DFP Low Responder
DFP High Responder
1 day
4 days
60 days
b.
Day 1
Day 2
Day 4
Day 60
FJC+ Cells/mm²
Geometric Mean Ratio (95% CI)
50.0
10.0
1.0
0.5
SCC
Hippo
Piri
Thal
Low vs Veh
High vs Veh
High vs Low

Figure 3-5. Low and high responding DFP animals exhibit significant neurodegeneration in multiple brain regions. (**a**) Representative photomicrographs of FluoroJade C (FJC) staining in the somatosensory cortex of vehicle controls, DFP low responders, and DFP high responders at 1, 4, and 60 d post-exposure. Bar = 100 µm. (**b**) The number of FJC-labeled cells was quantified in the somatosensory cortex (SSC), hippocampus (Hippo), piriform cortex (Piri), and thalamus (Thal) of vehicle controls (VEH), DFP low responders, and DFP high responders at 1, 2, 4, and 60 d post-DFP injection. Data shown as the geometric mean ratio with 95% confidence intervals. Confidence intervals entirely above 1 indicate a significant difference between the two groups being compared at $p < 0.05$ (n=6-10 animals/group).

Figure 3-6

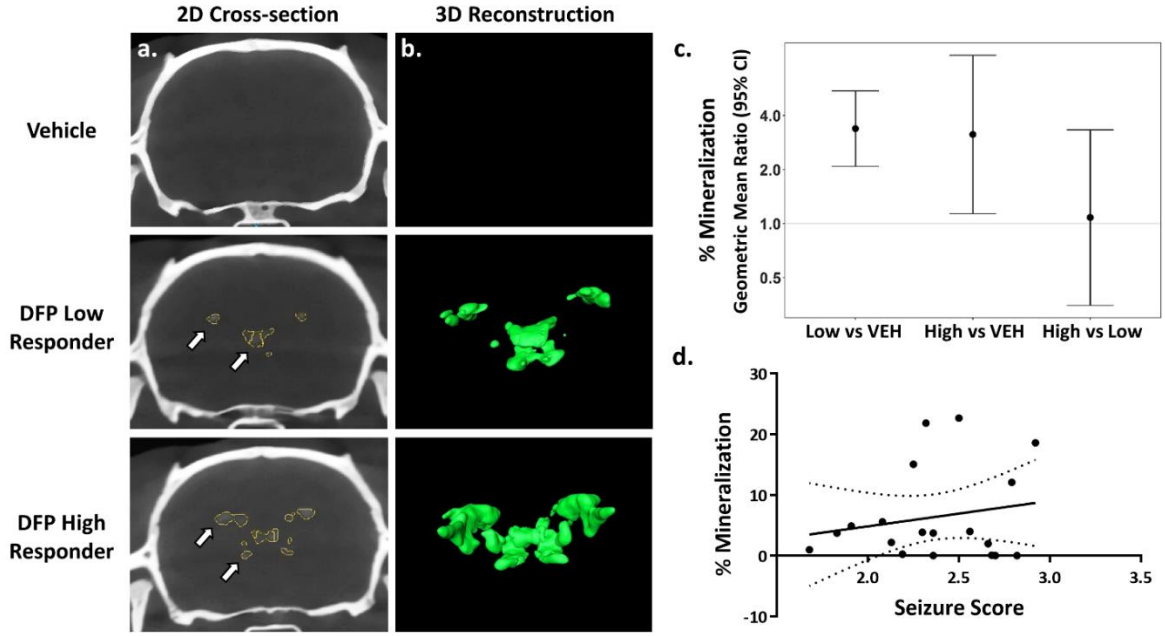
2D Cross-section
3D Reconstruction
a.
b.
Vehicle
DFP Low Responder
DFP High Responder
c.
% Mineralization Geometric Mean Ratio (95% CI)
4.0
2.0
1.0
0.5
Low vs VEH
High vs VEH
High vs Low
d.
% Mineralization
30
20
10
0
-10
2.0
2.5
3.0
3.5
Seizure Score

Figure 3-6. DFP low and high responders have significant mineralization in the thalamus at 60 days post-exposure. (**a**) Representative two-dimensional (2-D) whole brain micro-CT output images. Mineralized areas were automatically detected (yellow outline). Arrows point to representative mineral deposits. (**b**) 3-D micro-CT images generated from the 2-D output images showing mineral deposits (green) in the brains of vehicle, DFP low responding, and DFP high responding animals. (**c**) Quantification of the percent mineralized area relative to total brain region volume in the medial thalamus and dorsolateral thalamus of vehicle (VEH), DFP low responding, and DFP high responding animals. Statistical significance between groups did not vary by brain region, so all reported differences apply to both the medial thalamus and dorsolateral thalamus. Data are represented as the geometric mean ratio with 95% confidence intervals. Confidence intervals entirely above 1 indicate a significant difference between the two groups being compared at $p < 0.05$ (n=3 VEH, 6-14 DFP animals). (**d**) Correlation analysis between seizure score and percent mineralization in the brain. Spearman r=0.189, p=0.43.

References

Aggarwal, M., X. Li, O. Grohn and A. Sierra (2018). "Nuclei-specific deposits of iron and calcium in the rat thalamus after status epilepticus revealed with quantitative susceptibility mapping (QSM)." J Magn Reson Imaging **47**(2): 554-564.

Banks, C. N. and P. J. Lein (2012). "A review of experimental evidence linking neurotoxic organophosphorus compounds and inflammation." Neurotoxicology **33**(3): 575-584.

Bruun, D. A., M. Guignet, D. J. Harvey and P. J. Lein (2019). "Pretreatment with pyridostigmine bromide has no effect on seizure behavior or 24 hour survival in the rat model of acute diisopropylfluorophosphate intoxication." Neurotoxicology **73**: 81-84.

Chen, Y. (2012). "Organophosphate-induced brain damage: mechanisms, neuropsychiatric and neurological consequences, and potential therapeutic strategies." Neurotoxicology **33**(3): 391-400.

Copping, N. A., A. Adhikari, S. P. Petkova and J. L. Silverman (2019). "Genetic backgrounds have unique seizure response profiles and behavioral outcomes following convulsant administration." Epilepsy Behav **101**(Pt A): 106547.

de Araujo Furtado, M., F. Rossetti, S. Chanda and D. Yourick (2012). "Exposure to nerve agents: from status epilepticus to neuroinflammation, brain damage, neurogenesis and epilepsy." Neurotoxicology **33**(6): 1476-1490.

Deshpande, L. S., R. E. Blair, K. F. Phillips and R. J. DeLorenzo (2016). "Role of the calcium plateau in neuronal injury and behavioral morbidities following organophosphate intoxication." Ann N Y Acad Sci **1374**(1): 176-183.

Deshpande, L. S., D. S. Carter, R. E. Blair and R. J. DeLorenzo (2010). "Development of a prolonged calcium plateau in hippocampal neurons in rats surviving status epilepticus induced by the organophosphate diisopropylfluorophosphate." Toxicol Sci **116**(2): 623-631.

Ellman, G. L., K. D. Courtney, V. Andres, Jr. and R. M. Feather-Stone (1961). "A new and rapid colorimetric determination of acetylcholinesterase activity." Biochem Pharmacol **7**: 88-95.

Ferchmin, P. A., M. Andino, R. Reyes Salaman, J. Alves, J. Velez-Roman, B. Cuadrado, M. Carrasco, W. Torres-Rivera, A. Segarra, A. H. Martins, J. E. Lee and V. A. Eterovic (2014). "4R-cembranoid protects against diisopropylfluorophosphate-mediated neurodegeneration." Neurotoxicology **44**: 80-90.

Flannery, B. M., D. A. Bruun, D. J. Rowland, C. N. Banks, A. T. Austin, D. L. Kukis, Y. Li, B. D. Ford, D. J. Tancredi, J. L. Silverman, S. R. Cherry and P. J. Lein (2016). "Persistent neuroinflammation and cognitive impairment in a rat model of acute diisopropylfluorophosphate intoxication." J Neuroinflammation **13**(1): 267.

Gao, J., S. X. Naughton, H. Wulff, V. Singh, W. D. Beck, J. Magrane, B. Thomas, N. A. Kaidery, C. M. Hernandez and A. V. Terry, Jr. (2016). "Diisopropylfluorophosphate Impairs the

Transport of Membrane-Bound Organelles in Rat Cortical Axons." J Pharmacol Exp Ther **356**(3): 645-655.

Gayoso, M. J., A. Al-Majdalawi, M. Garrosa, B. Calvo and L. Diaz-Flores (2003). "Selective calcification of rat brain lesions caused by systemic administration of kainic acid." Histol Histopathol **18**(3): 855-869.

Guignet, M., K. Dhakal, B. M. Flannery, B. A. Hobson, D. Zolkowska, A. Dhir, D. A. Bruun, S. Li, A. Wahab, D. J. Harvey, J. L. Silverman, M. A. Rogawski and P. J. Lein (2019). "Persistent behavior deficits, neuroinflammation, and oxidative stress in a rat model of acute organophosphate intoxication." Neurobiol Dis.

Guignet, M. and P. J. Lein (2019). Organophopshates. Advances in Neurotoxicology: Role of Inflammation in Environmental Neurotoxicity. M. Aschner and L. G. Costa. Cambridge, MA, Academic Press. **3:** 35-79.

Gunnell, D., M. Eddleston, M. R. Phillips and F. Konradsen (2007). "The global distribution of fatal pesticide self-poisoning: Systematic review." BMC Public Health **7**(1): 357.

Heiss, D. R., D. W. Zehnder, D. A. Jett, G. E. Platoff, D. T. Yeung and B. N. Brewer (2016). "Synthesis and Storage Stability of Diisopropylfluorophosphate." Journal of Chemistry **2016**: 5.

Hobson, B. A., D. J. Rowland, S. Supasai, D. J. Harvey, P. J. Lein and J. R. Garbow (2017). "A magnetic resonance imaging study of early brain injury in a rat model of acute DFP intoxication." Neurotoxicology.

Lewine, J. D., W. Weber, A. Gigliotti, J. D. McDonald, M. Doyle-Eisele, N. Bangera, K. Paulson, C. Magcalas, D. A. Hamilton, E. Garcia, R. Raulli and J. Laney (2018). "Addition of ketamine to standard-of-care countermeasures for acute organophosphate poisoning improves neurobiological outcomes." Neurotoxicology **69**: 37-46.

Li, Y., P. J. Lein, C. Liu, D. A. Bruun, T. Tewolde, G. Ford and B. D. Ford (2011). "Spatiotemporal pattern of neuronal injury induced by DFP in rats: a model for delayed neuronal cell death following acute OP intoxication." Toxicol Appl Pharmacol **253**(3): 261-269.

Lin, T., O. Duek, A. Dori and O. Kofman (2012). "Differential long term effects of early diisopropylfluorophosphate exposure in Balb/C and C57Bl/J6 mice." Int J Dev Neurosci **30**(2): 113-120.

Loscher, W., R. J. Ferland and T. N. Ferraro (2017). "The relevance of inter- and intrastrain differences in mice and rats and their implications for models of seizures and epilepsy." Epilepsy Behav **73**: 214-235.

Martin, B. R. (1985). "Biodisposition of [3H]diisopropylfluorophosphate in mice." Toxicol Appl Pharmacol **77**(2): 275-284.

Matson, L. M., H. S. McCarren, C. L. Cadieux, D. M. Cerasoli and J. H. McDonough (2017). "The role of genetic background in susceptibility to chemical warfare nerve agents across rodent and non-human primate models." Toxicology **393**: 51-61.

McDonough, J. H., Jr., L. W. Dochterman, C. D. Smith and T. M. Shih (1995). "Protection against nerve agent-induced neuropathology, but not cardiac pathology, is associated with the anticonvulsant action of drug treatment." Neurotoxicology **16**(1): 123-132.

McDonough, J. H., Jr. and T. M. Shih (1997). "Neuropharmacological mechanisms of nerve agent-induced seizure and neuropathology." Neurosci Biobehav Rev **21**(5): 559-579.

Naughton, S. X. and A. V. Terry, Jr. (2018). "Neurotoxicity in acute and repeated organophosphate exposure." Toxicology **408**: 101-112.

Okumura, T., T. Hisaoka, T. Naito, H. Isonuma, S. Okumura, K. Miura, H. Maekawa, S. Ishimatsu, N. Takasu and K. Suzuki (2005). "Acute and chronic effects of sarin exposure from the Tokyo subway incident." Environ Toxicol Pharmacol **19**(3): 447-450.

Okumura, T., N. Takasu, S. Ishimatsu, S. Miyanoki, A. Mitsuhashi, K. Kumada, K. Tanaka and S. Hinohara (1996). "Report on 640 Victims of the Tokyo Subway Sarin Attack." Annals of Emergency Medicine **28**(2): 129-135.

Peter, J. V., T. I. Sudarsan and J. L. Moran (2014). "Clinical features of organophosphate poisoning: A review of different classification systems and approaches." Indian J Crit Care Med **18**(11): 735-745.

Phillips, K. F. and L. S. Deshpande (2016). "Repeated low-dose organophosphate DFP exposure leads to the development of depression and cognitive impairment in a rat model of Gulf War Illness." Neurotoxicology **52**: 127-133.

Pouliot, W., S. L. Bealer, B. Roach and F. E. Dudek (2016). "A rodent model of human organophosphate exposure producing status epilepticus and neuropathology." Neurotoxicology **56**: 196-203.

Prager, E. M., V. Aroniadou-Anderjaska, C. P. Almeida-Suhett, T. H. Figueiredo, J. P. Apland and M. F. Braga (2013). "Acetylcholinesterase inhibition in the basolateral amygdala plays a key role in the induction of status epilepticus after soman exposure." Neurotoxicology **38**: 84-90.

Prager, E. M., V. Aroniadou-Anderjaska, C. P. Almeida-Suhett, T. H. Figueiredo, J. P. Apland, F. Rossetti, C. H. Olsen and M. F. Braga (2014). "The recovery of acetylcholinesterase activity and the progression of neuropathological and pathophysiological alterations in the rat basolateral amygdala after soman-induced status epilepticus: relation to anxiety-like behavior." Neuropharmacology **81**: 64-74.

Russell, R. W., D. H. Overstreet, M. Messenger and S. C. Helps (1982). "Selective breeding for sensitivity to DFP: Generalization of effects beyond criterion variables." Pharmacology Biochemistry and Behavior **17**(5): 885-891.

Siso, S., B. A. Hobson, D. J. Harvey, D. A. Bruun, D. J. Rowland, J. R. Garbow and P. J. Lein (2017). "Editor's Highlight: Spatiotemporal Progression and Remission of Lesions in the Rat Brain Following Acute Intoxication With Diisopropylfluorophosphate." Toxicol Sci **157**(2): 330-341.

Tanaka, K., S. H. Graham and R. P. Simon (1996). "The role of excitatory neurotransmitters in seizure-induced neuronal injury in rats." Brain Res **737**(1-2): 59-63.

Te, J. A., K. D. Spradling-Reeves, J. F. Dillman, 3rd and A. Wallqvist (2015). "Neuroprotective mechanisms activated in non-seizing rats exposed to sarin." Brain Res **1618**: 136-148.

Terry, A. V., Jr. (2012). "Functional consequences of repeated organophosphate exposure: potential non-cholinergic mechanisms." Pharmacol Ther **134**(3): 355-365.

Thiermann, H., F. Worek and K. Kehe (2013). "Limitations and challenges in treatment of acute chemical warfare agent poisoning." Chem Biol Interact **206**(3): 435-443.

Todorovic, M. S., M. L. Cowan, C. A. Balint, C. Sun and J. Kapur (2012). "Characterization of status epilepticus induced by two organophosphates in rats." Epilepsy Res **101**(3): 268-276.

Tonduli, L. S., G. Testylier, C. Masqueliez, G. Lallement and P. Monmaur (2001). "Effects of Huperzine used as pre-treatment against soman-induced seizures." Neurotoxicology **22**(1): 29-37.

Valdes Hernandez Mdel, C., L. C. Maconick, E. M. Tan and J. M. Wardlaw (2012). "Identification of mineral deposits in the brain on radiological images: a systematic review." Eur Radiol **22**(11): 2371-2381.

Yanagisawa, N., H. Morita and T. Nakajima (2006). "Sarin experiences in Japan: Acute toxicity and long-term effects." Journal of the Neurological Sciences **249**(1): 76-85.

Zaja-Milatovic, S., R. C. Gupta, M. Aschner and D. Milatovic (2009). "Protection of DFP-induced oxidative damage and neurodegeneration by antioxidants and NMDA receptor antagonist." Toxicol Appl Pharmacol **240**(2): 124-131.

Chapter 4

Diisopropylfluorophosphate (DFP)-Induced Seizures Cause Sex-Specific Neuropathology and Cognitive Deficits in Juvenile Rats

Based on a manuscript for submission to *Current Research in Toxicology* under the same title with the following authors:

Eduardo A. González[a], Jonas J. Calsbeek[a], Yi-Hua Tsai[a], Mei-Yun Tang[a], Joan Vu[a], Elizabeth Berg[b], Peter Andrew[a], Danielle J. Harvey[c], Suangsuda Supasai[a,d], Jill L. Silverman[b], and Pamela J. Lein[a]

[a]Department of Molecular Biosciences, University of California, Davis, School of Veterinary Medicine, 1089 Veterinary Medicine Drive, Davis, CA 95616, USA; [b]Department of Psychiatry, University of California, Davis, School of Medicine, Sacramento, CA 95817; [c]Department of Public Health Sciences, University of California, Davis, School of Medicine, Davis, CA 95616, USA; [d]Department of Molecular Tropical Medicine and Genetics, Faculty of Tropical Medicine, Mahidol University, Bangkok 10400, Thailand.

Abstract

Preclinical efforts to develop improved medical countermeasures against the highly lethal organophosphate (OPs) chemical threat agents have largely focused on adult male models. However, OP-induced neurotoxicity is known to differ between juveniles and adults, as well as between males and females. Therefore, the goal of this project was to develop a juvenile model of acute OP intoxication to better understand the role of sex and age on long-term neurological deficits. Postnatal day 28 Sprague-Dawley male and female rats were acutely intoxicated with the OP diisopropylfluorophosphate (DFP; 3.4 mg/kg, s.c.) or an equal volume (~80 µl) of vehicle (saline, s.c.) followed by atropine sulfate (0.1 mg/kg, i.m.) and 2-PAM (25 mg/kg, i.m.) to prevent death from peripheral toxic effects. DFP distribution to the brain was assessed by measuring acetylcholinesterase (AChE) activity in cortical tissue at 1 day post-exposure; seizures were assessed using both behavioral criteria and electroencephalographic (EEG) recordings collected during the first 4 hours post-exposure. At 1, 7, and 28 d post-intoxication, animals were evaluated histologically for markers of neurodegeneration and neuroinflammation. At 1 month post-DFP, animals were analyzed for motor function, learning and memory, and hippocampal neurogenesis. Males experienced more severe seizure behavior throughout the 4 h monitoring period following DFP than females, but EEG recordings confirmed the presence of seizure activity in females despite lower behavioral scores. While both sexes experienced significant neuronal degeneration, males showed earlier onset and more severe astrogliosis compared to females. In contrast, both sexes showed persistent microglial activation in all examined brain regions. DFP induced pronounced memory deficits in both sexes using each assay. Sex-specific effects of DFP were also found in hippocampal neurogenesis, which was only altered in DFP males. These findings demonstrate that acute DFP intoxication triggers seizures in juvenile rats,

and that neurotoxic outcomes in juvenile rats vary by sex. The spatiotemporal patterns of neurological damage suggest that microglial activation may be a more important factor than astrogliosis or neurogenesis in the pathogenesis of cognitive deficits in juveniles following acute OP intoxication.

Key Words: neurodegeneration, neurodevelopment, neuroinflammation, neurotoxicity, organophosphate, sex differences

Abbreviations:

AChE, acetylcholinesterase; AS, atropine-sulfate; BChE, butyrylcholinesterase; ChE, cholinesterase; CT, computed tomography; DFP, diisopropylfluorophosphate; EEG, electroencephalogram; FJC, Fluoro-Jade C; im, intramuscular; ip, intraperitoneal; OP, organophosphate; 2-PAM, pralidoxime; PBS, phosphate-buffered saline; ROI, region of interest; sc, subcutaneous; SE, status epilepticus; T2w, T2-weighted; VEH, vehicle

Highlights

- Acute DFP intoxication caused persistent sex-specific brain damage in juvenile rats
- Seizure behavior and neuroinflammation were more severe in males than females
- Both sexes experienced cognitive deficits at 1 month post-DFP intoxication
- Acute DFP intoxication increased hippocampal neurogenesis in males but not females
- Microglial activation may be a critical driver of OP-induced cognitive deficits

Introduction

Organophosphorus cholinesterase inhibitors (OPs) are widely used pesticides that cause hundreds of thousands of deaths each year as a result of accidental and intentional poisonings (Pereira, Aracava et al. 2014, Mew, Padmanathan et al. 2017) . OPs have also been weaponized for use against military and civilian targets, as evidenced by the 2017 chemical attacks in Syria (UN 2017), as well as the assassination attempts of a former intelligence agent in 2018 (Haley 2018) and a Russian opposition leader in 2020 (OPCW 2020). Acute OP intoxication can trigger seizures that rapidly progress to *status epilepticus* and ultimately death (Pope and Brimijoin 2018). Current medical countermeasures for OP-induced cholinergic crisis include atropine to block excessive cholinergic signaling via muscarinic receptors, benzodiazepines to terminate seizures, and pralidoxime (2-PAM) to reactivate AChE (Jett, Sibrizzi et al. 2020). These therapeutics must be administered within minutes after SE initiation to be maximally effective (Jett and Spriggs 2020), but even then, they do not adequately protect against the long-term neurological deficits observed in survivors, including structural brain damage and persistent cognitive deficits (Figueiredo, Apland et al. 2018, Jett, Sibrizzi et al. 2020). There is, therefore, an urgent need to identify more effective medical countermeasures for treating individuals acutely intoxicated with OPs.

In the event of a civilian mass casualty involving OPs, a diverse population varying in age and sex will potentially be affected. However, current preclinical research to develop improved medical countermeasures has almost exclusively used adult male models. This is a troubling gap given a significant literature indicating that children are more susceptible than adults to the neurotoxic effects of environmentally relevant OP levels (Muñoz-Quezada, Lucero et al. 2013, Gonzalez-Alzaga, Lacasana et al. 2014, Sagiv, Bruno et al. 2019), and that neurotoxic outcomes

of OP exposures can be sex-specific (Rauh, Perera et al. 2012, Comfort and Re 2017). A recent preclinical study suggests that juvenile rats at varying stages of neurodevelopment are differentially susceptible to the proconvulsant activity of OP chemical threat agents (Scholl, Miller-Smith et al. 2018). In this study, P28 was found to be the most consistent of the juvenile ages tested. While both sexes were included, sex-specific effects were not directly compared across an identical exposure paradigm, and no long-term endpoints were evaluated. This study sought to address the important question of whether acute OP intoxication during juvenile neurodevelopment has neuropathological consequences, and if so, whether these consequences are sex-specific.

Diisopropylfluorophosphate (DFP) is considered an OP chemical threat agent by the United States Department of Homeland Security (Jett and Spriggs 2020). DFP can induce acute seizures as well as long-term neurological deficits in adult rodent models (Pessah, Rogawski et al. 2016, Putra, Sharma et al. 2019, Guignet, Dhakal et al. 2020). Acute DFP intoxication also is associated with a significant neuroinflammatory response in adult animals (Hobson, Rowland et al. 2019, Rojas, Ganesh et al. 2020). Therefore, the goal of this study was to develop a juvenile model of DFP intoxication and compare effects in males versus females with regard to acute seizure responses and persistent neurological consequences.

Materials and Methods

Animal husbandry

All animals in this study were maintained in facilities fully accredited by AAALAC International. Experimental procedures were performed under protocols approved by the UC Davis Institutional Animal Care and Use Committee (IACUC, protocol #21954) and were

designed to minimize pain or suffering. All studies adhered strictly to the ARRIVE guidelines and the National Institutes of Health guide for the care and use of laboratory animals (NIH publication No. 8023, revised 1978). Juvenile male and female Sprague-Dawley rats (Charles River Laboratories, Hollister, CA, USA) were weaned at postnatal day 21 (P21), at which time they were separated by sex with two animals of the same sex per cage. Animals were housed in standard plastic shoebox cages in an environmentally controlled vivarium (22 ± 2^0C, 40-50% humidity, 12 h light/dark cycle). Food (2018 Tekland global 18% protein rodent diet; Envigo, Huntingdon, UK) and water were provided *ad libitum*.

DFP exposure paradigm

A dose-response assessment was conducted in P28 male and female rats to identify a dose of DFP that caused ≤20% mortality. This study was conducted in accordance with the up-and-down dosing procedure to reduce animal use (Bruce 1985). A starting dose of 6 mg/kg DFP was selected because this dose induces seizure activity in juvenile P28 rats (Scholl, Miller-Smith et al. 2018). The following doses were tested in both sexes: 1.9, 3.4, 6, and 19 mg/kg. A dose of 1.1 mg/kg was also tested in females, but not males because DFP at 1.9 mg/kg had no effect on survival or seizure behavior in males.

DFP (Sigma Chemical Company, St Louis, MO, USA) was prepared in ice-cold sterile phosphate-buffered saline (PBS, 3.6 mM Na_2HPO_4, 1.4 mM NaH_2PO_4, 150 mM NaCl; pH 7.2) within 5 min of injection (*s.c.*). DFP purity was evaluated using previously described ^{1}H, ^{13}C, ^{19}F and ^{31}P-NMR methods (Gao, Naughton et al. 2016) and found to be approximately 90 ± 7% pure. Upon receipt in the laboratory, DFP was aliquoted and stored at –80 °C, a condition under which it retained stability for over 1 year (Heiss, Zehnder et al. 2016). Vehicle (VEH) controls were administered a similar volume (~80 µL) of sterile PBS in place of DFP. One min after DFP

or VEH injection, all animals were administered a combined injection of atropine-sulfate (AS, 0.1 mg/kg; Sigma; >97% purity) and pralidoxime (2-PAM, 25 mg/kg; Sigma; >99% purity). Both compounds increase survival by protecting against peripheral cholinergic toxicity (Pessah, Rogawski et al. 2016). Animals were randomly assigned to groups using a random number generator.

Following DFP or VEH injection, animals were monitored for seizure behavior for 4 h (**Figure 4-1A**) using seizure behavior scale (Deshpande, Carter et al. 2010) as previously described (Guignet, Dhakal et al. 2019). At the end of the observation period, all subjects were injected with 3 mL of 10% w/v dextrose in sterile saline to ensure hydration and then returned to their home cages. Rat food was softened with H_2O until animals were able to resume consumption of solid food, typically within 2-3 days. All subjects were anesthetized using isoflurane (Western Medical Supply, Arcadia, CA, USA) at 1, 7, or 28 d post-intoxication and euthanized by exsanguination to collect brain tissue for further analyses (**Figure 4-1A**).

Electroencephalography (EEG)

A separate cohort of animals not used for biochemical, histological, or behavioral analyses was implanted with cortical electrodes and monitored for EEG activity for ~2 hours post-DFP to confirm whether juvenile females experience electrographic seizures. EEG implants and recordings were performed as previously described (González, Rindy et al. 2020). Briefly, animals were deeply anesthetized with 1-3% isoflurane (MWI Animal Health, Boise, ID, USA) in medical grade oxygen (flow rate=1L/min). Animals were restrained in a stereotaxic platform (Stoelting, Wood Dale, IL, USA), the surgical site was thoroughly cleaned using a betadine scrub (Purdue Products, Stamford, CT, USA) and 70% isopropyl alcohol wipes (Covidien Plc, Dublin, Ireland), and a 1.5-inch incision made from the eyes to the base of the skull. Four stainless steel

head mount screws (P1 Technologies, Roanoke, VA, USA) were implanted into the skull and connected to sterile HD-X02 telemetry devices (Data Sciences International, St. Paul, MN, USA) that were inserted between the skin and muscle layer along the flank of the animal. The incision was sutured (Ethicon, Bridgewater, NJ, USA) and animals allowed to recover for 14 d before being exposed to DFP.

On the day of recordings, animals were placed on PhysioTel Receivers (Data Sciences International) and baseline EEG activity was recorded for ~1 h (Ponemah software, Data Sciences International). Animals were then injected with DFP (3.4 mg/kg, s.c) and recorded for ~2 h post-injection. EEG traces were analyzed using NeuroScore software (Data Sciences International) and a band-pass filter of 20-70 Hz for noise reduction as previously described (Pouliot, Bealer et al. 2016). EEG recordings were qualitatively analyzed for abnormal spike activity that reached >2x baseline amplitude to confirm the presence or absence of seizure activity.

Cholinesterase activity assays

Following euthanasia at each time point, brains were immediately removed, bisected sagittally, and the left hemisphere dissected on ice to remove the cortex. We previously showed that cholinesterase activity in the cortex is representative of cholinesterase activity in multiple major brain regions following acute DFP intoxication in adult rats (González, Rindy et al. 2020). The cortical tissue was snap frozen on dry ice and stored at -80 °C until analyzed. The Ellman assay (Ellman, Courtney et al. 1961, Farahat, Ellison et al. 2011) was used to measure total cholinesterase (ChE), acetylcholinesterase (AChE), and butyrylcholinesterase (BChE) activity as previously described (González, Rindy et al. 2020). Briefly, samples were homogenized in lysis buffer (0.1 M phosphate buffer, pH 8.0 with 0.1% w/v Triton) and centrifuged for 1 min (13,400

x g) at 4 °C. Supernatant was collected, and triplicate samples of each supernatant transferred to a 96-well plate. Samples were equilibrated for 5 min with the colorimetric reagent 5,5'-dithio-bis(2-nitrobenzoicacid) (DTNB, Sigma), and then allowed to react with the AChE substrate acetylthiocholine iodide (ASChI, Sigma). Enzyme activity was quantified by measuring changes in absorbance at 405 nm over 15 min. All samples were run in the absence or presence of 100 µM of the BChE inhibitor, tetraisopropyl pyrophosphoramide (iso-OMPA, Sigma), to determine total ChE and AChE activity, respectively. BChE activity was calculated by subtracting AChE activity from total ChE activity in each sample. Enzyme activity of each sample was normalized by total protein concentration n that sample, as determined using the BCA assay (Pierce, Rockford, IL, USA).

Histologic Analyses

Following euthanasia at each time point, brains were removed and bisected sagittally. The right hemisphere was blocked into 2 mm thick sections using a stainless-steel small rat brain matrix (Kent Scientific, Torrington, CT, USA) and post-fixed in cold 4% paraformaldehyde (Sigma) in PBS (pH 7.2) for 24 h at 4 °C. Tissue slices were then incubated overnight in 30% w/v sucrose (Thermo Fisher, Waltham, MA, USA) in PBS at 4 °C and subsequently embedded in OCT medium (Thermo Fisher) and stored at -80 °C until processing. All brain sections were cryosectioned at -20 °C into 10 µm slices on Superfrost Plus slides (Thermo Fisher). Each histological endpoint was examined in five brain regions using a minimum of 2 slides per region: somatosensory cortex, hippocampus (including the CA1, CA3, and dentate gyrus subregions), thalamus, piriform cortex, and amygdala (**Figure 4-1B**).

Fluoro-Jade C (FJC) staining was performed as previously described (Supasai, González et al. 2020). Briefly, brain sections were stained using 0.06% potassium permanganate w/v (Sigma)

in distilled water, washed in distilled water, and incubated for 10 min in 0.0001% w/v FJC (Cat #AG325; Millipore, Billerica, MA, USA) in 0.1% v/v acetic acid (Acros Organics, Geel, Belgium) in distilled water. DAPI solution (1:50,000; Invitrogen, Carlsbad, CA, USA) was also included to label all cell nuclei. Slides were then cleared in chemical grade xylene (Thermo Fisher) and mounted in 50 µL of Permount (Thermo Fisher).

Immunohistochemistry experiments were performed as previously described (Supasai, González et al. 2020). Briefly, antigen retrieval was performed using 10 mM citrate buffer (pH 6.0) in distilled water at 90 °C for 20 min. To block nonspecific binding, slides were incubated in a blocking buffer comprised of 10% w/v normal goat serum (Vector Laboratories, Burlingame, CA, USA), 1% w/v bovine serum albumin (Sigma), and 0.03% w/v Triton X-100 (Thermo Fisher) in PBS for 1 h at room temperature. Following blocking, slides were incubated overnight at 4 °C with primary antibodies in blocking buffer. The following primary antibodies were used in this study: mouse anti-glial fibrillary acidic protein (GFAP, 1:1000, Cell Signaling Technology, Danvers, MA, USA; RRID:AB_561049), rabbit anti-S100 calcium-binding protein β (S100β, 1:500, Abcam, Cambridge, UK; RRID:AB_2184443), rabbit anti-ionized calcium-binding adapter molecule 1 (IBA-1, 1:1000, Wako Laboratory Chemicals, Richmond, VA, USA; RRID:AB_839504), and mouse anti-CD68 (1:200, Serotec, Hercules, CA, USA; RRID:AB_2291300). Negative controls incubated in blocking buffer in place of a primary antibody were included in each staining batch.

Following primary antibody incubation, slides were washed 3 times in PBS with 0.03% w/v Triton X-100 for 10 min each and subsequently incubated in secondary antibody solution for 90 min at room temperature in the dark. The following secondary antibodies were used in this study: for GFAP, Alexa Fluor 568-conjugated goat anti-mouse IgG_1 (1:1000, Life Technologies,

Carlsbad, CA, USA; RRID:AB_2535766); for S100β, Alexa Fluor 488-conjugated goat anti-rabbit IgG (1:500, Life Technologies; RRID:AB_2576217); for IBA-1, Alexa Fluor 568-conjugated goat anti-rabbit IgG (1:500, Life Technologies; RRID:AB_2535730); and for CD68, Alexa Fluor 488-conjugated goat anti-mouse IgG (1:500, Life Technologies; RRID:AB_2534069). Following incubation, slides were rinsed 3 times in PBS with 0.03% w/v Triton X-100 for 10 min each and cover slipped in 50 µL ProLong Gold Antifade Mountant with DAPI (Invitrogen).

An identical protocol was used to immunostain brain sections for biomarkers of neurogenesis. The following primary antibodies were used: mouse anti-neuronal nuclei (NeuN, 1:500, Millipore; RRID:AB_2298772), guinea pig anti-doublecortin (DCX, 1:500, Millipore; RRID:AB_1586992), and rabbit anti-ki67 (1:750, Abcam; RRID:AB_2756822). The following secondary antibodies were used: for NeuN, Alexa-Fluor 647-conjugated goat anti-mouse IgG (1:500, Life Technologies; RRID:AB_2535809); for DCX, Alexa-Fluor 594-conjugated goat anti-guinea pig IgG (1:1000, Life Technologies; RRID:AB_2534120); and for ki67, Alexa-Fluor 488-conjugated goat anti-rabbit IgG (1:500, Life Technologies; RRID:AB_2576217).

Slides were scanned at 20X magnification using a High-Content ImageXpress XL Imaging System (Molecular Devices, Sunnyvale, CA, USA). Regions of interest were created for the amygdala, piriform cortex, somatosensory cortex, and hippocampus [including the CA1, CA3, and dentate gyrus subregions]) between -3.6 mm to -4.2 mm posterior to bregma, as well as the thalamus between -3.0 mm to -3.6 mm posterior to bregma. Bregma ranges were confirmed using a rat brain atlas (Kruger, Saporta et al. 1995). Fluorescent images were quantified as previously described (Supasai, González et al. 2020). The percent area of positive fluorescence was quantified for each marker and normalized to the total area analyzed, which was held

constant across all animals. Positive staining was defined as fluorescence that reached ≥ 2x background fluorescence intensity observed in negative control images. Percent area was automatically detected on background-subtracted and binarized images using ImageJ analysis software (version 1.48, National Institutes of Health, Bethesda, MD, USA) to eliminate user bias. For neurogenesis analysis, the width of the granular cell layer (GCL) was measured using the measure tool in ImageJ. All image analyses were performed by a single individual with no knowledge of experimental group.

Neurobehavior assays

The open field assay was used to assess general locomotor function prior to learning and memory assays. Subjects were placed into a testing arena (48 cm x 48 cm x 48 cm), allowed 20 minutes of acclimation, and recorded for 10 min under lighting conditions of ~30 lux. A 3x3 grid of equal-sized squares was superimposed over the videos to create nine different movement zones. Locomotor activity was quantified using the number of times an individual crossed a grid line over the 10-minute period. The total number of crossings were quantified and compared across experimental groups.

Learning and memory were assessed using the novel object recognition task performed as previously described (Berg, Pedersen et al. 2020). Briefly, subjects were habituated to an empty testing arena (48 cm x 48 cm x 48 cm) for 30 min prior to testing under lighting conditions of ~45 lux. The following day, subjects were again habituated to the arena followed by an introduction to two identical objects. Subjects were allowed 10 min to interact with these objects followed by an isolation period of 60 min. During the isolation period, the arena and objects were cleaned with 70% ethanol and one object was replaced with a novel object. At the end of the isolation period, subjects were returned to the arena and allowed 5 min to interact with the

familiar and novel objects. The objects used were orange plastic cones and glass bell jars. All phases were video recorded and the time spent sniffing each object was measured by experimenters blinded to experimental group. Data were transformed to calculate % preference for the novel object and an object discrimination index in order to correct for potential differences in exploration time between individuals (Gulinello, Mitchell et al. 2019).

Contextual and cued fear conditioning, performed as previously described (Berg, Pedersen et al. 2020), was used as a second assay of learning and memory. Briefly, subjects were trained to associate a specific context and cue with a foot shock (0.7 mA). The chambers (25 cm h x 32 cm w x 25 cm d) were brightly lit (~100 lux) with floors made of stainless-steel rods placed 1.6 cm apart (Med-Associates Inc., St. Albans, VT, USA). Test chambers were placed into a noise reducing chamber and a front-facing camera was used to record each session. On the first day (training day), subjects were trained in a context that included wire flooring, aluminum walls, and a vanilla scent (1:100 dilution of McCormick Vanilla Extract). The cue was an auditory cue of 80 dB white noise for 30 s. On the second test day (24 h post-training), subjects were placed back into the chambers for 5 min with the identical context but no audio cue or foot shock and the amount of time subject froze was measured. On the third test day (48 h post-training), subjects were placed in chambers in which the context had been altered to a smooth plastic floor, angled black walls, and a lemon scent (1:100 dilution of McCormick Lemon Extract). Subjects were monitored in this environment for 3 min before and 3 min after the auditory cue. The average motion index, a comprehensive measure of overall movement, was automatically quantified by VideoFreeze software (version 2.7; Med-Associates Inc.) to assess the movement of each subject during both the context and cue testing periods.

Statistical analyses

Two different models were considered for the dose response data: 1) 2-parameter log-logistic model; and 2) probit model. For each, we considered a model in which the slope was allowed to differ at LD_{50} for males and females (different shapes) as well as a model in which the slope of the dose response curve at the LD_{50} was constrained to be the same for males and females. Akaike Information Criterion was used to pick the model that best fit the data. Estimates of the LD_{20} and LD_{50} with 95% confidence intervals was determined for each sex using the delta method. The estimated LD_{20} and LD_{50} were compared between the sexes. These analyses were conducted using the *drc* package in R (Ritz and Streibig 2005).

Key outcomes for the histology data included FJC (number of FJC-labeled cells/mm^2), GFAP (% area of immunoreactivity), S100β (% area of immunoreactivity), and IBA-1 (% area of immunoreactivity). Mixed effects models, including animal-specific random effects, were fit to assess differences between exposure groups. Primary factors of interest included exposure (DFP, VEH), brain region (thalamus, piriform cortex, amygdala, hippocampus, cortex), sex (male, female), and time post-exposure (1, 7, 28 d). Interactions between the factors (exposure, brain region, sex, and time point) were considered and the best model was chosen using Akaike Information Criterion. Outcomes were transformed using the natural logarithm after shifting all values by 1 to enable the calculation for samples with no positive staining to better meet the assumptions of the model. Contrasts for exposure group and sex differences were constructed and tested using a Wald test. The Benjamini-Hochberg false discovery rate (FDR) was used within an outcome measure to account for multiple comparisons. Results are presented as geometric mean ratios (GMR) between exposure groups for the log-transformed outcomes. Point estimates of the ratios and 95% confidence intervals are presented in the figures. When the

confidence interval for the GMR includes 1, there is no statistical evidence of a difference between groups. These analyses were performed using SAS software, version 9.4 and alpha was set at 0.05; all reported results remained significant after the FDR procedure.

Key outcomes for neurobehavior included open field (# grid crossings), novel object familiarization (sniff time), novel object test (% novel preference and discrimination index), and fear conditioning (average motion index). Neurogenesis outcomes included ki67 (% positive cells), DCX (% area of immunoreactivity), NeuN (% area of immunoreactivity), and GCL width (μm). These outcomes were analyzed at 28 d and included only brain region. Open field data were analyzed using a Mann-Whitney *U* test, while all other neurobehavior and neurogenesis outcomes were analyzed using a two-way ANOVA with *post-hoc* Holm-Sidak test where applicable. Each of these outcomes are presented as mean ± SE with individual data points representing individual animals. These analyses were conducted in GraphPad Prism, version 8.2.1 with alpha set at 0.05.

Results

DFP was similarly lethal to male and female juvenile rats

Male and female rats were injected with varying doses of DFP and the percent animals surviving at 4 h post-injection was determined (**Figure 4-1C**). The dose-response curve for DFP-induced mortality for females was shifted to the left of that for males (**Figure 4-1D**). Of the statistical models used to fit the data, the best model considered was the 2-parameter log-logistic model with a common slope. The estimated LD_{20} and LD_{50} for males were 4.1 and 6.2 mg/kg, respectively. For females, the estimated LD_{20} and LD_{50} values were 2.9 and 4.4 mg/kg, respectively (**Figure 4-1E**). While there was no statistical difference between these parameters,

there was a trend towards increased susceptibility to lethality following acute DFP intoxication in females ($p = 0.08$). The ratio of effect doses at LD_{20} and LD_{50} for females to males was 0.70 (95% CI: 0.36, 1.03) indicating the dose is 30% lower in females than males at LD_{20} and LD_{50}. However, due to the lack of statistically significant differences between the LD_{20} and LD_{50} values for each sex, DFP was used at a dose of 3.4 mg/kg in both sexes for the remainder of the study.

DFP-induced seizure behavior was more severe in males than females

Seizure behavior were monitored for 4 h following acute DFP intoxication using a scale (**Figure 4-2A**) adapted from an adult rat DFP model (Deshpande, Carter et al. 2010). Seizure scores were plotted over time (**Figure 4-2B**), and the average seizure score over the 4 h period was calculated for each animal (**Figure 4-2C**). Seizure behavior data were also quantified as the total duration of convulsive seizures (scores of ≥3; **Figure 4-2D**). The average seizure scores and convulsive seizure duration were significantly higher in males than females ($p<0.05$) (**Figures 4-2C, 4-2D**). A seizure score of 3 or higher has been demonstrated to correspond with SE in the adult DFP rat (Deshpande, Carter et al. 2010, Phelan, Shwe et al. 2015). The majority of DFP males (86.6%) exhibited a seizure score ≥ 3 at least once during the 4 h post-exposure; whereas, only 53.3% of DFP females reached a score of 3 during the 4 h seizure monitoring period (**Figure 4-2E**).

DFP-induced seizures have been confirmed by EEG in adult male (Guignet, Dhakal et al. 2020) and juvenile male rats (Scholl, Miller-Smith et al. 2018), and a recent publication demonstrated that DFP induced electrographic seizures in adult female rats (Gage, Golden et al. 2020). To determine whether DFP induces electrographic seizures in juvenile females, a small cohort of females was implanted with cortical electrodes 7 d prior to DFP exposure.

Representative EEG traces from a DFP female (**Figure 4-2F**) show a significant increase in electrographic spike activity relative to baseline following DFP intoxication, confirming the ability of DFP to induce robust seizure activity in females.

To assess DFP distribution to the brain of male versus female juveniles, AChE, BChE, and total ChE activity were measured in cortical brain samples at 1 d post-DFP. Baseline cholinesterase levels in VEH animals were comparable between sexes, and AChE was inhibited to the same extent in males and females following DFP exposure (**Figure 4-2G**). The majority of cholinesterase activity in both sexes was driven by AChE, with minimal BChE activity detected in either sex.

DFP caused significant neurodegeneration in male and female brains

Neurodegeneration is a well-documented consequence of acute OP intoxication in adults (reviewed in Chen 2012). Using FJC staining to visualize degenerating neurons (Schmued, Stowers et al. 2005) (**Figure 4-3A)**, we observed significantly increased FJC staining in DFP animals that varied by time post-exposure ($p<.001$), sex ($p<.001$) and by brain region ($p<.001$) (**Figure 4-3B**). In both males and females, DFP-exposed animals had higher FJC staining than VEH animals across days and regions (GMR>2.0, $p<.042$) with the exception of the female cortex at 1 day post-exposure in ($p=.19$). The difference between DFP and VEH animals tended to be higher in males than in females, which was driven by higher FJC staining in male DFP animals compared to female DFP animals (GMR=3.4, 95% CI=2.0-5.8, $p<.001$).

DFP caused sex-specific changes in reactive astrogliosis

Antibodies specific to GFAP and S100β are reported to label unique astrocyte populations in the brain, especially during neurodevelopment (reviewed in Holst, Brochner et al. 2019). GFAP immunoreactivity (**Figure 4-4A**) revealed sex-specific changes in expression following DFP

intoxication. The difference in percent positive GFAP staining area between DFP and VEH animals varied by sex (p=.02) and both time and region (p<.001) (**Figure 4-4B**). Differences in GFAP between DFP and VEH animals were limited at one day post-exposure, with the only significant difference observed in the male hippocampus (GMR=1.4, 95% CI=1.1-1.9, p=.007). By 7 days post-exposure, GFAP levels were significantly elevated in DFP animals compared to VEH animals in all brain regions and both sexes (p<.02) with the exception of the female somatosensory cortex (GMR=1.3, 95% CI=0.9-1.8, p=.1). Elevated GFAP levels in DFP compared to VEH persisted in males at 28 days post-exposure in all brain regions except the somatosensory cortex (GMR=1.4, 95% CI=1.0-2.0, p=.06). In contrast, in females, the only significant difference between DFP and VEH at 28 days post-exposure was in the amygdala (GMR=1.3, 95% CI=1.1-1.5, p=.01).

The difference in S100β immunoreactivity (**Figure 4-5A**) between DFP and VEH animals varied by time (p=.04) and sex (p=.005) with a trend for a difference by region (p=.1) (**Figure 4-5B**). At one day post-exposure, male DFP animals had increased S100β relative to male VEH animals in the piriform cortex (GMR=1.4, 95% CI=1.1-1.7, p=.002) and the thalamus (GMR=1.5, 95% CI=1.1-1.9, p=.003). There were no significant differences between DFP and VEH females at one day post-exposure (p>.3). S100β levels were significantly increased in both male and female DFP animals on day 7 post-exposure in the amygdala (male: GMR=1.8, 95% CI=1.5-2.2, p<.001; female: GMR=1.4, 95% CI=1.1-1.7, p=.004), piriform cortex (male: GMR=1.9, 95% CI=1.6-2.3, p<.001; female: GMR=1.5, 95% CI=1.2-1.8, p<.001) and thalamus (male: GMR=2.0, 95% CI=1.6-2.5, p<.001; female: GMR=1.5, 95% CI=1.2-1.8, p<.001). At 7 da post-exposure, DFP males had elevated S100β expression compared to VEH males in the hippocampus (GMR=1.6, 95% CI=1.3-2.0, p<.001) and cortex (GMR=1.7, 95% CI=1.3-2.1,

p<.001). By day 28 post-exposure, S100β remained elevated in all brain regions for males, but just in the piriform cortex and thalamus for the females. Within the DFP group, there was no significant difference in S100β immunoreactivity between males and females (GMR=1.1, 95% CI=0.9-1.2, p=.4).

DFP-induced microgliosis was delayed in females relative to males

IBA-1 and CD68 immunoreactivity were used to quantify microglia in the brain (**Figure 4-6A**). CD68 was not present at measurable levels in any group and was, therefore, excluded from data analysis. The difference between DFP and VEH animals in percent area of IBA-1 immunostaining varied only by days post-exposure (p=.005) (**Figure 4-6B**). There was no significant difference between groups 1 day post-exposure (GMR=1.1, 95% CI=0.9-1.3, p=.4), but there was significantly higher IBA-1 in DFP animals compared to VEH on days 7 (GMR=1.7, 95% CI=1.4-2.1, p<.001) and 28 (GMR=1.6, 95% CI=1.3-2.0, p<.001) post-exposure.

Neurobehavior assays

The open field assay was used to quantify locomotor function prior to the start of learning and memory testing. Locomotor activity was comparable between VEH and DFP groups in both male (p=0.29) and female (p=0.33) animals (**Figure 4-7A**). Similarly, no differences in locomotor activity were observed between male and female animals of either exposure group.

Novel object recognition was used to test memory function following object familiarization. The familiarization period indicated no preexisting side preference/salience or avoidance in VEH males (p=0.89), DFP males (p=0.7), VEH females (p=0.8), or DFP females (p=0.49) (**Figure 4-7B**). Performance during the test period was analyzed using % novel preference and a discrimination index, two variables commonly used for assessing object preference. DFP males

showed significant deficits by both % novel preference ($p<0.001$) and discrimination index ($p<0.001$) compared to VEH males (**Figure 4-7C**). Similarly, DFP females also showed significant deficits relative to VEH females as determined using both the % novel preference ($p=0.02$) and discrimination index ($p=0.02$) variables (**Figure 4-7C**).

Performance in contextual and cued fear conditioning was used to corroborate learning and memory deficits identified in the novel object recognition task. Freezing behavior in response to a fearful stimulus was quantified using the average motion index, a comprehensive measure of animal movement. No significant differences in movement were detected during the baseline period between the VEH and DFP groups of each sex. During the test periods, DFP males showed significant impairments compared to VEH males during both the context ($p=0.002$) and cue ($p=0.005$) tests (**Figure 4-8A**). DFP females showed a significant impairment compared to VEH females in the context ($p=0.005$) but not cue ($p=0.11$) test (**Figure 4-8B**).

Neurogenesis biomarkers

A period of extensive neurogenesis occurs in the rodent brain during the early perinatal period; however, it continues at a reduced rate in the subgranular zone (SGZ) of postnatal and adult animals (Kempermann, Song et al. 2015, Toda and Gage 2018). Changes in hippocampal neurogenesis following acute DFP intoxication were evaluated by quantifying biomarkers of immature neurons, (DCX immunoreactivity) and proliferating cells (ki67 immunopositive cells), in the SGZ (Kee, Sivalingam et al. 2002, Couillard-Despres, Winner et al. 2005). Structural changes in the dentate gyrus of the hippocampus were evaluated by quantifying NeuN immunoreactivity, a biomarker of mature neurons, and width of the granule cell layer (GCL) (**Figure 4-9A**). DFP males showed a significant increase in the number of $ki67^{+}$ cells in the SGZ compared to their VEH counterparts ($p<0.001$), while there was no difference between female

DFP and VEH animals (p=0.8; **Figure 4-9B**). A similar trend was observed in DCX immunoreactivity, where DFP males had significantly higher levels than VEH males (p=0.005; **Figure 4-9C**), but no differences in DCX immunoreactivity were observed between DFP and VEH females (p=0.13; **Figure 4-9C**). There were no effects of DFP on NeuN immunoreactivity in either male (p=0.83) or female (p=0.079) subjects compared to their VEH counterparts (**Figure 4-9D**). Similarly, DFP did not cause any changes in GCL width in either males (p=0.94) or females (p=0.4) compared to their respective VEH groups (**Figure 4-9E**).

Discussion

Although there are a number of publications evaluating the neurotoxic effects of OP threat agents, the majority of these studies are focused on the adult male brain. To begin to address questions of age and sex in determining neurotoxic outcomes following acute OP intoxication, we examined acute seizure activity and chronic neurological damage in juvenile male and female rats and identified sex-specific neurotoxic effects of DFP. Overall, juvenile males showed more severe seizure behavior immediately following acute DFP intoxication compared to juvenile females, although EEG recordings indicated that DFP induced SE in juvenile females. Both juvenile males and females presented with significant neuropathology following DFP intoxication, although there were sex differences in the extent (number of brain regions involved) and persistence of specific neuropathologic responses. Microglial activation was found to be the most persistent endpoint and did not differ by sex. Both males and females exhibited cognitive deficits but only males had significant changes in neurogenesis. The present findings highlight endpoints of relevance to therapeutic screening and point to microglial activation as a likely

mechanism contributing to the pathogenesis of long-term neurological deficits following acute OP intoxication.

An initial dose-response assessment using increasing doses of DFP revealed comparable mortality curves between male and female animals. The similarities between curves are unsurprising in light of the steep dose-response mortality curves that are well-documented across sex and age in OP threat agent models (Fawcett, Aracava et al. 2009). Regarding seizure behavior, DFP elicited significantly higher seizure behavior scores in males, and while ~25% of males had clear generalized seizures, the most severe seizure observed in a female was forelimb clonus. However, the behavioral seizure response observed in our juvenile DFP model is notably less severe in both males and females than previously published adult DFP models using nearly identical seizure scales (Gage, Golden et al. 2020, Supasai, González et al. 2020), suggesting age-specific effects of DFP on seizure severity. This interpretation is supported by a recent publication that found seizure susceptibility to DFP increased significantly with age, ranging from the early postnatal period into young adulthood (Scholl, Miller-Smith et al. 2018). Although EEG activity was only recorded from a subset of animals, it has been demonstrated that seizure behavior is highly correlated with electrographic seizure activity in both male and female DFP rats (Tanaka, Graham et al. 1996, McDonough and Shih 1997, Gage, Golden et al. 2020). Follow-up studies using more sensitive electrographic techniques are in progress to further elucidate whether the electrographic seizure response in juvenile animals is truly sex-specific following DFP intoxication.

The less severe seizure behavior observed in juvenile animals compared to adults is likely due, at least in part, to immature neural networks that mediate OP-induced seizure activity. Cholinergic receptors play a critical role in seizure induction following acute OP intoxication

(Richardson, Fitsanakis et al. 2019). In the developing brain, there is an increase in muscarinic and nicotinic cholinergic receptor expression between the post-weaning period (~P28) and early adulthood (~P60) (Jett 1998). Similarly, expression levels of the excitatory neurotransmitter acetylcholine also increases in the brain during young adulthood (Jett 1998). These changes can increase susceptibility to chemical-induced seizures. Excitatory glutamate receptors, particularly NMDA receptors, undergo similar increases in expression and significantly upregulate the NR2A and NR2C subunits during postnatal development (Akazawa, Shigemoto et al. 1994, Monyer, Burnashev et al. 1994), which may further contribute to increased seizure susceptibility in older animals by allowing for increased glutamatergic signaling.

The observed sex difference in seizure behavior is consistent with several published seizure models. Adult females have been reported to have less severe SE than males in response to pilocarpine (Scharfman and MacLusky 2014) or DFP (Gage, Golden et al. 2020). While the mechanistic underpinnings of this sex difference are unknown, a few hypotheses have been proposed. One hypothesis is sex hormones (Velíšková and Desantis 2013); however, it is unlikely that sex hormones are driving the differential seizure behavior we observed in this study because P28 rats have yet to experience a large hormonal surge (Bell 2018). Further, it was recently reported that estrous stage has no impact on seizure susceptibility in adult rats acutely intoxicated with DFP (Gage, Golden et al. 2020). Rather, it is more likely that the divergent seizure activity between males and females reflects the sexually dimorphic expression of excitatory and inhibitory receptors throughout the brain. Males and females have differential expression patterns of glutamatergic, cholinergic, and GABAergic receptors in the brain, each of which plays an important role in seizure induction and maintenance (Akman, Moshé et al. 2014, Scharfman and MacLusky 2014). Glutamate receptors, including NR1, NR2A, and GluR1, are

critical for seizure maintenance following OP intoxication and are reported to be expressed at higher levels in males than females during neurodevelopment (Hsu, Hsieh et al. 2000, Bian, Zhu et al. 2012, Damborsky and Winzer-Serhan 2012). Similarly, cholinergic receptor mRNA expression is found at higher levels in males than in females (Potier, Sénécal et al. 2005), increasing the likelihood of excessive cholinergic signaling following the inhibition of AChE by OPs. Lastly, it is well-documented that females have greater expression of $GABA_A$ receptors than males in the brain (by both mRNA and protein) throughout postnatal development (Ravizza, Friedman et al. 2003, Li, Huguenard et al. 2007, Chudomel, Herman et al. 2009). The greater expression of excitatory receptors and reduced expression of inhibitory receptors in males relative to females could potentially explain the greater seizure severity in males versus females that was observed in the present model as well as other chemical-induced seizure models (Scharfman and MacLusky 2014, Gage, Golden et al. 2020).

Despite the difference in acute seizure response, both DFP males and females showed significant neurodegeneration throughout the brain. This may be explained, at least in part, by evidence that DFP can induce brain damage independent of seizure activity in adult rats (González, Rindy et al. 2020), and by the human literature indicating that OPs can cause significant brain damage even at non- or subconvulsive doses (reviewed in Chen 2012). It may also be the case that spontaneous recurrent seizures (SRS), which have been reported in adult male rats following acute DFP intoxication (Guignet, Dhakal et al. 2020, Putra, Sharma et al. 2020), contributed to the sustained neurodegeneration observed in both sexes, but further research is needed to address this hypothesis. Regarding regional damage, the thalamus, piriform cortex, and hippocampus were severely damaged in both male and female juveniles, which is

similar to the regional patterns of brain damage reported in adult animals acutely intoxicated with DFP (Siso, Hobson et al. 2017).

Neurodegeneration is often associated with neuroinflammation, a complex set of cellular and molecular processes triggered in response to insults within the nervous system (Guignet and Lein 2018). The regional effects of DFP on neuroinflammation in the juvenile model mirrored neurodegeneration and were largely comparable to the adult DFP model, with some of the most severe inflammation occurring in the piriform cortex, thalamus, and hippocampus (Siso, Hobson et al. 2017). Two primary neuroimmune cell types, microglia and astrocytes, are known to be activated in the adult brain for months following DFP intoxication (Gage, Golden et al. 2020, Supasai, González et al. 2020). This immune response typically involves overexpression of pro-inflammatory cytokines, sustained neuronal injury, and an aberrant phagocytosis response that may further damage healthy cells (reviewed in Guignet and Lein 2018). In our juvenile model, DFP males exhibited significantly increased immunoreactivity for GFAP and S100β, both biomarkers for astrocytes, throughout the brain at 7 and 28 d post-exposure, with the highest levels of expression in the piriform cortex and thalamus. Juvenile females also showed astrogliosis following DFP, but it was less persistent compared to DFP males. This astrocytic response differs slightly from that of adults, which have shown a significant increase in GFAP immunoreactivity as early as 4 h post-DFP (Liu, Li et al. 2012). The observed sex difference likely reflects the sex differences in the severity of seizure behavior, since it has previously been shown that seizure severity is predictive of the extent of neuroinflammation in DFP models (Kuruba, Wu et al. 2018, Hobson, Rowland et al. 2019). Interestingly, there was no effect of sex on microglial activation, which was increased microglial throughout the brain at 7 and 28 d post-

DFP. This is consistent with observations of the adult DFP model that microglial activation is more persistent than the astrocytic response (Supasai, González et al. 2020).

Acute DFP intoxication impaired cognitive function in both sexes. No differences were observed in locomotor function between DFP and VEH animals of either sex, eliminating a potentially confounding variable on learning and memory assays. DFP males exhibited slightly poorer cognitive performance than DFP females as reflected by significant deficits in both portions of the fear conditioning. Previous literature demonstrated that neuropathology, most notably neuronal degeneration and microglial activation, temporally coincides with behavioral deficits following DFP intoxication in adult rats (Flannery, Bruun et al. 2016, Guignet, Dhakal et al. 2020). Similarly, other models of acute OP intoxication have also reported positive correlations between initial neuropathology and cognitive impairment (de Araujo Furtado, Rossetti et al. 2012, Reddy, Wu et al. 2020). Neuroinflammation has been proposed to be a contributing factor to cognitive dysfunction following chemical-induced seizures (Guignet and Lein 2018). While sex differences in reactive astrogliosis and neurogenesis were observed in our model, both sexes experienced comparable microglial activation and cognitive deficits, both of which were present at 1 mo post-DFP. This relationship, and the congruence between sexes, likely suggests that microglial-mediated neuroinflammation plays a role in learning and memory impairments following acute OP intoxication.

Hippocampal neurogenesis is critical to cognitive function (Lazarov and Hollands 2016) and known to be altered following seizures in the adult brain (reviewed in Jessberger and Parent 2015). Increased neurogenesis is well-documented following chemical-induced seizures, particularly in models of pilocarpine-induced SE (Varodayan, Zhu et al. 2009, Wu, Hu et al. 2019, Velazco-Cercas, Beltran-Parrazal et al. 2020). These findings in adults suggest that

neurogenesis is highly likely to be altered in the juvenile brain following chemical-induced seizures. Our results revealed that DFP males, who experienced prolonged convulsive seizures, exhibited increased hippocampal neurogenesis, but DFP females did not exhibit any significant change in neurogenesis. If females indeed have less severe SE than males, the lack of neurogenic effects in DFP females may be explained by the positive relationship that has been reported between convulsive seizure duration and neurogenesis following chemical-induced SE (Yang, Wang et al. 2008, Hung, Yang et al. 2012). It has also been reported that males are more susceptible to changes in hippocampal signaling and plasticity than females during development (Zitman and Richter-Levin 2013). The increased neurogenesis observed in males may also contribute to the slightly more severe cognitive deficits that males displayed compared to females, as aberrant hippocampal neurogenesis has been shown to directly contribute to cognitive decline following acute seizures (Cho, Lybrand et al. 2015). However, given the presence of cognitive deficits in DFP females independent of neurogenesis changes, it appears more likely that the neurogenic response is simply a function of seizures alone and has minimal relationship to cognition following DFP intoxication. Follow-up studies are required to further elucidate this relationship following postnatal OP intoxication.

To conclude, the present study has developed a juvenile model of acute DFP intoxication that can be used to test novel therapeutics being developed against chemical threats. These data also point to microglial-mediated neuroinflammation as a likely mechanism contributing to long-term neurological deficits following acute OP intoxication. We are the first to report that the long-term effects of DFP on the juvenile brain are sex-specific, a finding with critical implications for therapeutic development. Just as males and females are differentially susceptible to acute DFP intoxication, it may also be the case that their response to medical countermeasures is sex-

specific as well. Importantly, DFP females showed persistent microglial activation and cognitive dysfunction despite the absence of severe convulsions. Should this translate to exposed humans, it reinforces the need to provide medical attention and follow-ups to all exposed individuals, regardless of behavioral response. The temporal relationship between microglial activation and neurobehavioral deficits in both sexes, despite the sex differences observed in other endpoints, highlights the potential for microglia to play a critical role in the long-term neurological consequences of acute OP intoxication. Taken together, these data represent an important step in the development of medical countermeasures that can be used to treat young individuals in the event of a chemical emergency involving OPs.

Acknowledgments

We thank Dr. Suzette Smiley-Jewell (UC Davis CounterACT Center) for her assistance in editing this manuscript and Naomi Saito for her assistance with statistical analyses.

Funding Sources

This work was supported by the CounterACT Program, National Institutes of Health (NIH) Office of the Director and the National Institute of Neurological Disorders and Stroke (NINDS) [grant number U54 NS079202], and predoctoral fellowships to E.A.G from the NINDS [grant number F31 NS110522], the NIH Initiative for Maximizing Student Development [grant number R25 GM5676520], and the ARCS Foundation. This project used core facilities supported by the UC Davis MIND Institute Intellectual and Developmental Disabilities Research Center (U54 HD079125). The sponsors were not involved in the study design, in the collection, analysis, or interpretation of data, in the writing of the report, or in the decision to submit the paper for publication.

Figures and Figure Legends

Figure 4-1

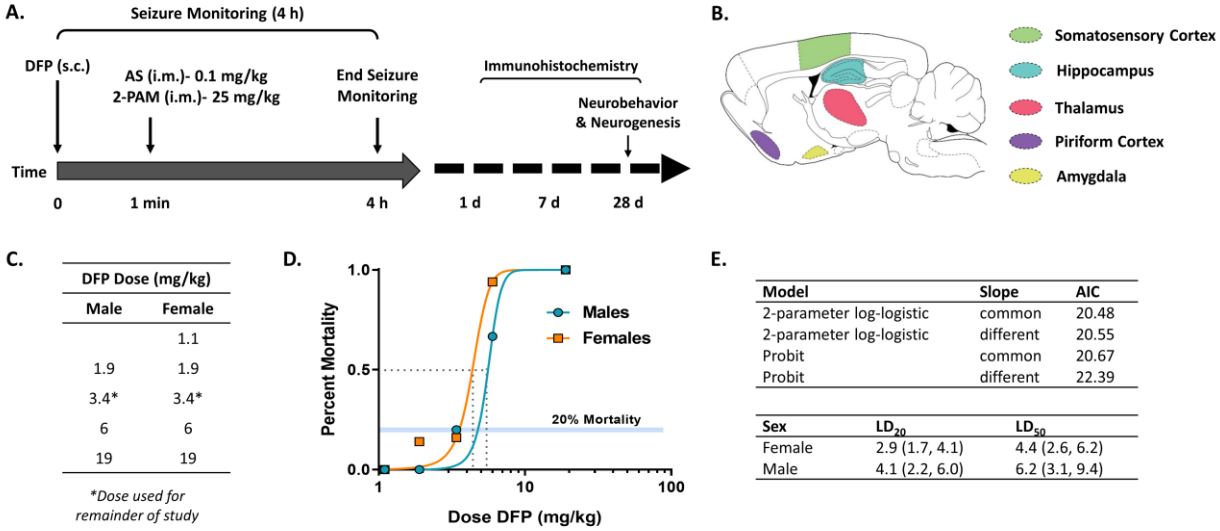

Figure 4-1. DFP exposure paradigm and dose-response assessment. (**A**) Schematic illustrating the dosing paradigm used to intoxicate juvenile male and female P28 Sprague Dawley rats and times post-exposure when other data points were collected. (**B**) Illustration of the five brain regions examined for neuropathology following acute DFP intoxication. (**C**) DFP doses tested and (**D**) mortality dose-response curve using varying doses of DFP. Based on these data, 3.4 mg/kg was selected for all subsequent studies. Sample sizes range from 3-4 at the end doses (1.1, 1.9, and 19 mg/kg) and 6-10 at the middle doses (3.4 and 6 mg/kg). (**E**) Statistical models tested for dose-response analysis. Model with the smallest Akaike Information Criterion (AIC) is the strongest statistical model. Estimated LD_{20} and LD_{50} values by sex (95% confidence interval are included in parentheses). No significant difference between sexes was observed.

Figure 4-2

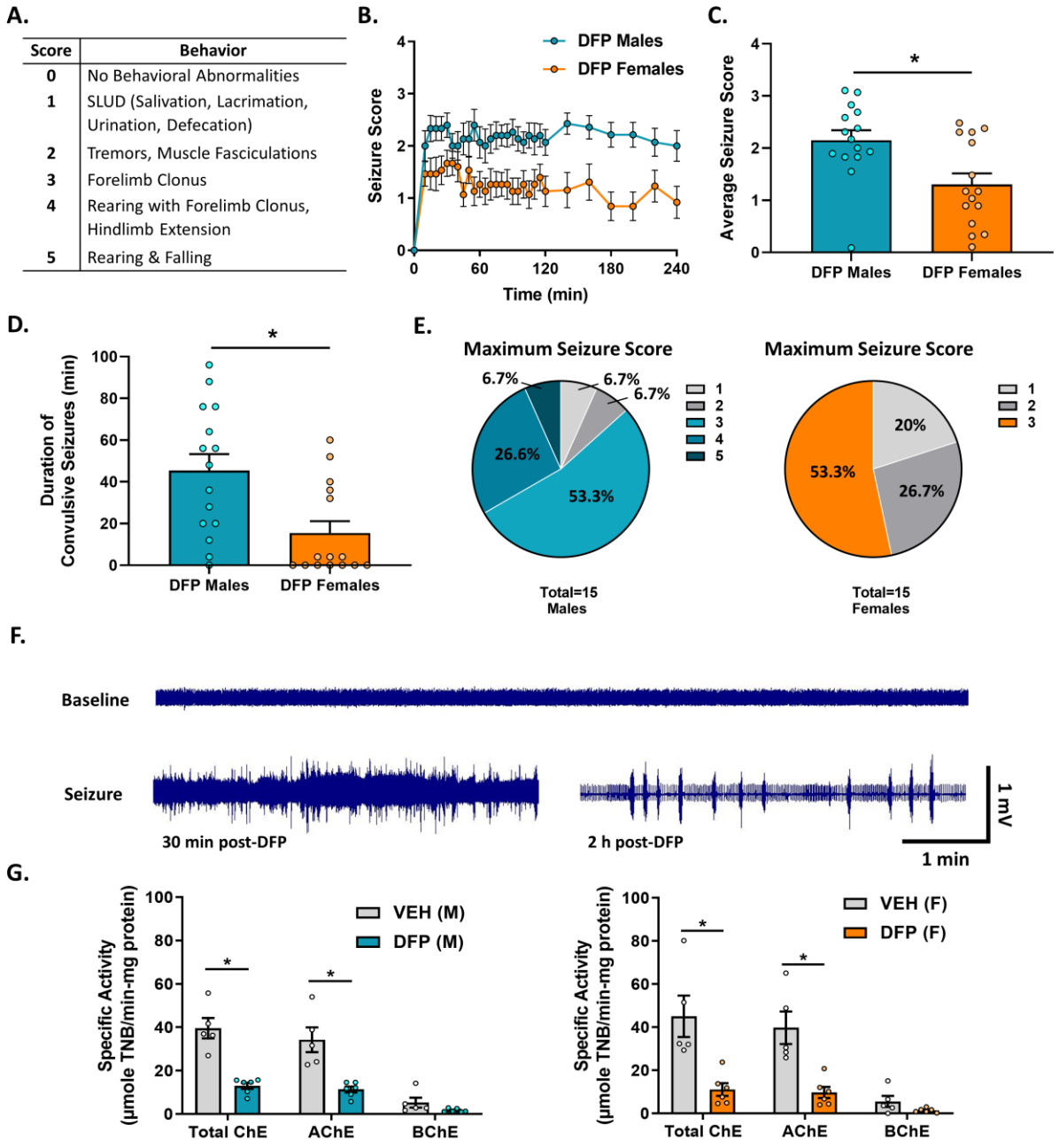
A.
Score | Behavior
0 | No Behavioral Abnormalities
1 | SLUD (Salivation, Lacrimation, Urination, Defecation)
2 | Tremors, Muscle Fasciculations
3 | Forelimb Clonus
4 | Rearing with Forelimb Clonus, Hindlimb Extension
5 | Rearing & Falling
B.
DFP Males
DFP Females
Seizure Score
Time (min)
C.
Average Seizure Score
DFP Males
DFP Females
D.
Duration of Convulsive Seizures (min)
DFP Males
DFP Females
E.
Maximum Seizure Score
6.7%
6.7%
6.7%
26.6%
53.3%
Total=15 Males
Maximum Seizure Score
20%
53.3%
26.7%
Total=15 Females
F.
Baseline
Seizure
30 min post-DFP
2 h post-DFP
1 mV
1 min
G.
Specific Activity (µmole TNB/min-mg protein)
VEH (M)
DFP (M)
Total ChE
AChE
BChE
Specific Activity (µmole TNB/min-mg protein)
VEH (F)
DFP (F)
Total ChE
AChE
BChE

Figure 4-2. Juvenile males exhibited more severe seizure behavior than age-matched females following DFP. (**A**) Seizure behavior scale used to score seizure behavior of juvenile male and female rats following acute intoxication with DFP at 3.4 mg/kg, s.c. (**B**) Temporal profile of seizure scores from males and females during the first 4 h post-DFP exposure. (**C**) Average seizure score and (**D**) average duration of convulsive seizures in DFP-intoxicated males and females. Data presented as mean ± SEM with individual data points per animal (n=15/group); *$p<0.05$ as determined by Mann Whitney test. (**E**) Maximum seizure score reached at any point during the 4 h monitoring period in DFP-intoxicated males (left) and females (right). (**F**) Representative EEG traces confirming electrographic seizure activity in DFP females. (**G**) The enzymatic activity of acetylcholinesterase (AChE) in cortical tissue from males (left) and females (right) at 1 d post-exposure to VEH or DFP. Data presented as mean ± SEM with individual data points per animal (n=5-6 per group); *$p<0.05$ as determined by two-way ANOVA with *post hoc* Holm-Sidak test.

Figure 4-3

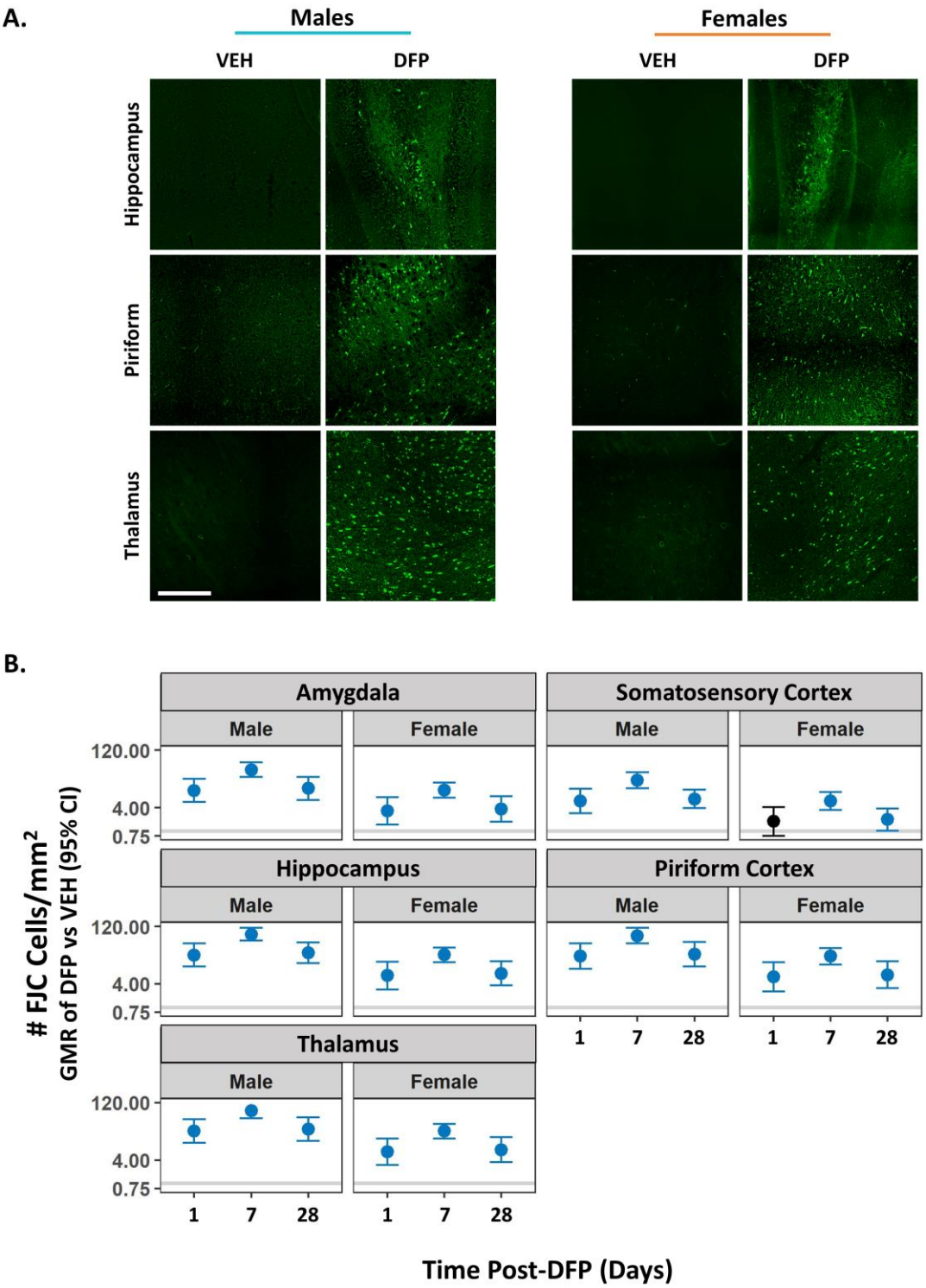
A.
Males
Females
VEH
DFP
VEH
DFP
Hippocampus
Piriform
Thalamus
B.
Amygdala
Somatosensory Cortex
Hippocampus
Piriform Cortex
Thalamus
Male
Female
120.00
4.00
0.75
FJC Cells/mm²
GMR of DFP vs VEH (95% CI)
1
7
28
Time Post-DFP (Days)

Figure 4-3. DFP causes significant neurodegeneration in both male and female rats. (**A**) Representative photomicrographs of Fluoro-Jade C (FJC) staining in the hippocampus, piriform cortex, and thalamus of VEH and DFP intoxicated rats at 7 d post-intoxication. Bar=100 μm. (**B**) The number of FJC-labeled cells was quantified in multiple brain regions of each sex at 1, 7, and 28 d post-DFP injection. Hippocampus includes dentate gyrus, CA1, and CA3 subregions. Data shown as the geometric mean ratio of DFP vs. VEH with 95% confidence intervals. Confidence intervals entirely above or below 1 are colored blue and indicate a significant difference between the two groups being compared at $p < 0.05$ (n=5-7 animals/group).

Figure 4-4

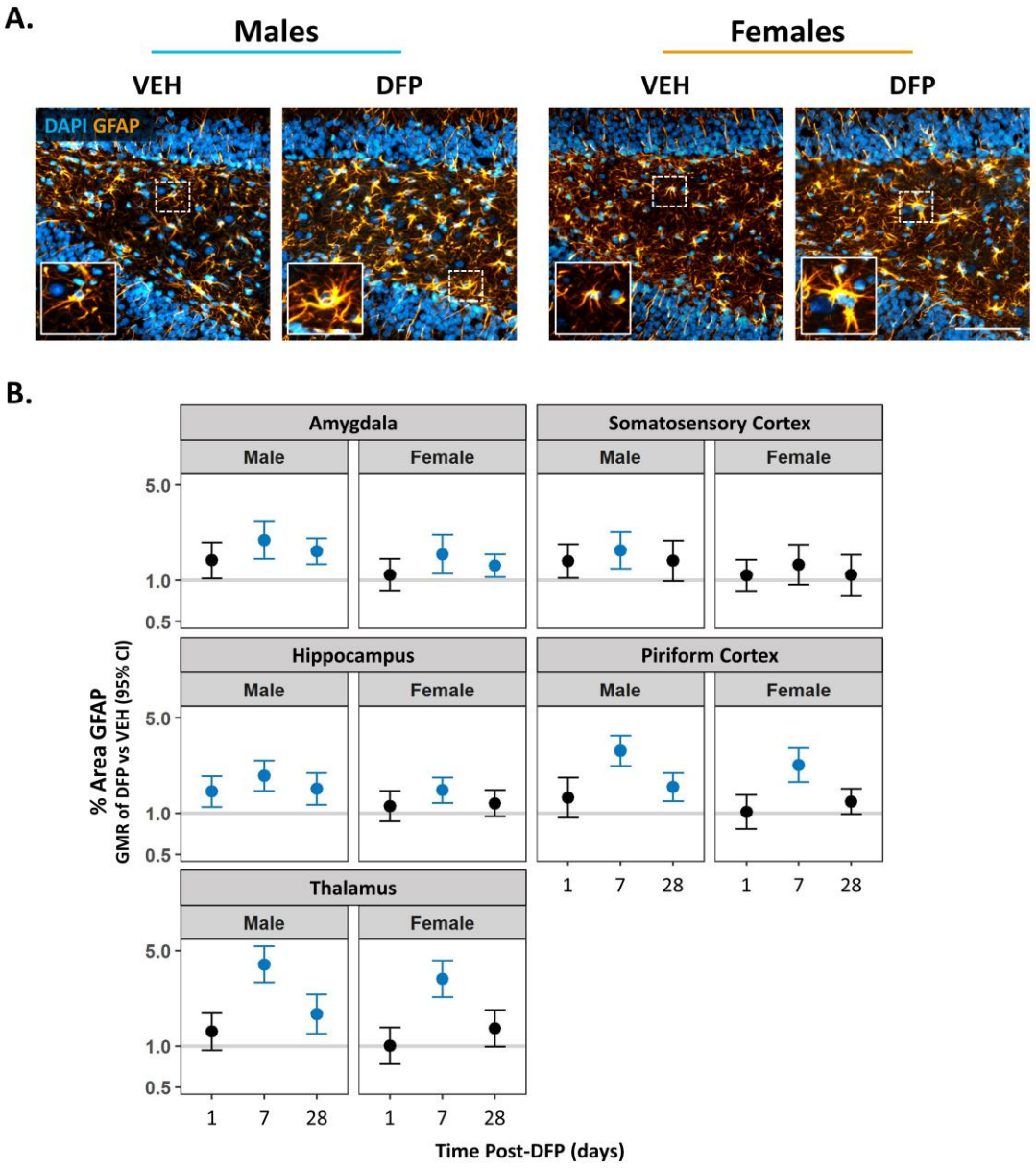
A.
Males
Females
VEH
DFP
VEH
DFP
DAPI GFAP
B.
Amygdala
Somatosensory Cortex
Hippocampus
Piriform Cortex
Thalamus
Male
Female
5.0
1.0
0.5
% Area GFAP
GMR of DFP vs VEH (95% CI)
1
7
28
Time Post-DFP (days)

Figure 4-4. DFP increases GFAP immunoreactivity in a time, region, and sex-dependent manner. (**A**) Representative photomicrographs of GFAP immunostaining (astrocytes and radial glia; orange) in the hippocampus of VEH and DFP rats at 7 d post-intoxication. Blue=DAPI (cell nuclei). Bar=100 μm. (**B**) The % area of GFAP immunoreactivity was quantified in multiple brain regions of each sex at 1, 7, and 28 d post-DFP injection. Hippocampus includes dentate gyrus, CA1, and CA3 subregions. Data shown as the geometric mean ratio of DFP vs. VEH with 95% confidence intervals. Confidence intervals entirely above or below 1 are colored blue and indicate a significant difference between the two groups being compared at $p < 0.05$ (n=5-7 animals/group).

Figure 4-5

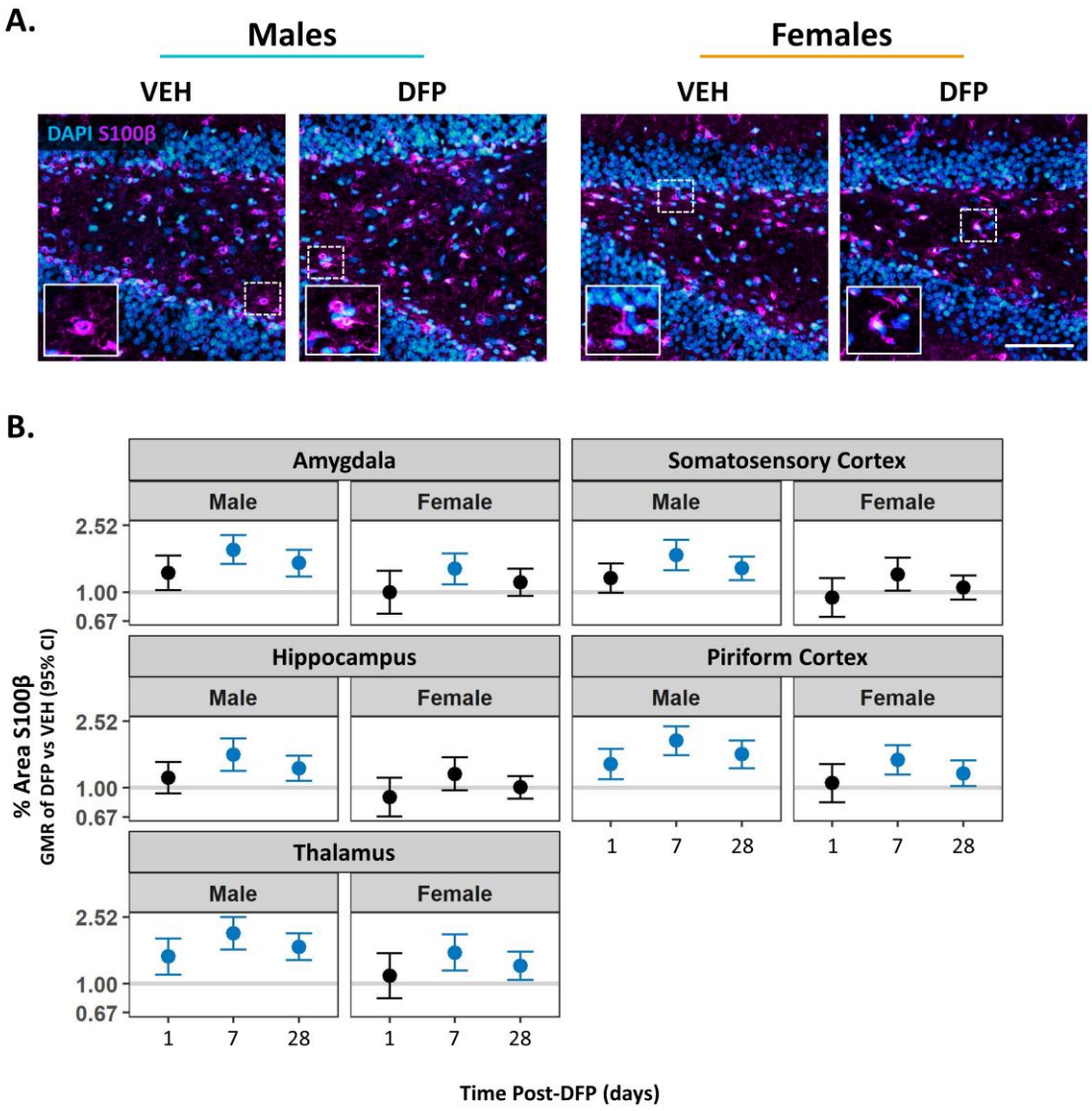
A.
Males
Females
VEH
DFP
VEH
DFP
DAPI S100β
B.
Amygdala
Somatosensory Cortex
Hippocampus
Piriform Cortex
Thalamus
Male
Female
2.52
1.00
0.67
% Area S100β
GMR of DFP vs VEH (95% CI)
1
7
28
Time Post-DFP (days)

Figure 4-5. DFP increases S100β immunoreactivity in a time, region, and sex-specific manner. (**A**) Representative photomicrographs of S100β immunostaining (mature astrocytes; magenta) in the hippocampus of VEH and DFP rats at 7 d post-intoxication. Blue=DAPI (cell nuclei). Bar=100 μm. (**B**) The % area of S100β immunoreactivity was quantified in multiple brain regions of each sex at 1, 7, and 28 d post-DFP injection. Hippocampus includes dentate gyrus, CA1, and CA3 subregions. Data shown as the geometric mean ratio of DFP to VEH with 95% confidence intervals. Confidence intervals entirely above or below 1 are colored blue and indicate a significant difference between the two groups being compared at $p < 0.05$ (n=5-7 animals/group).

Figure 4-6

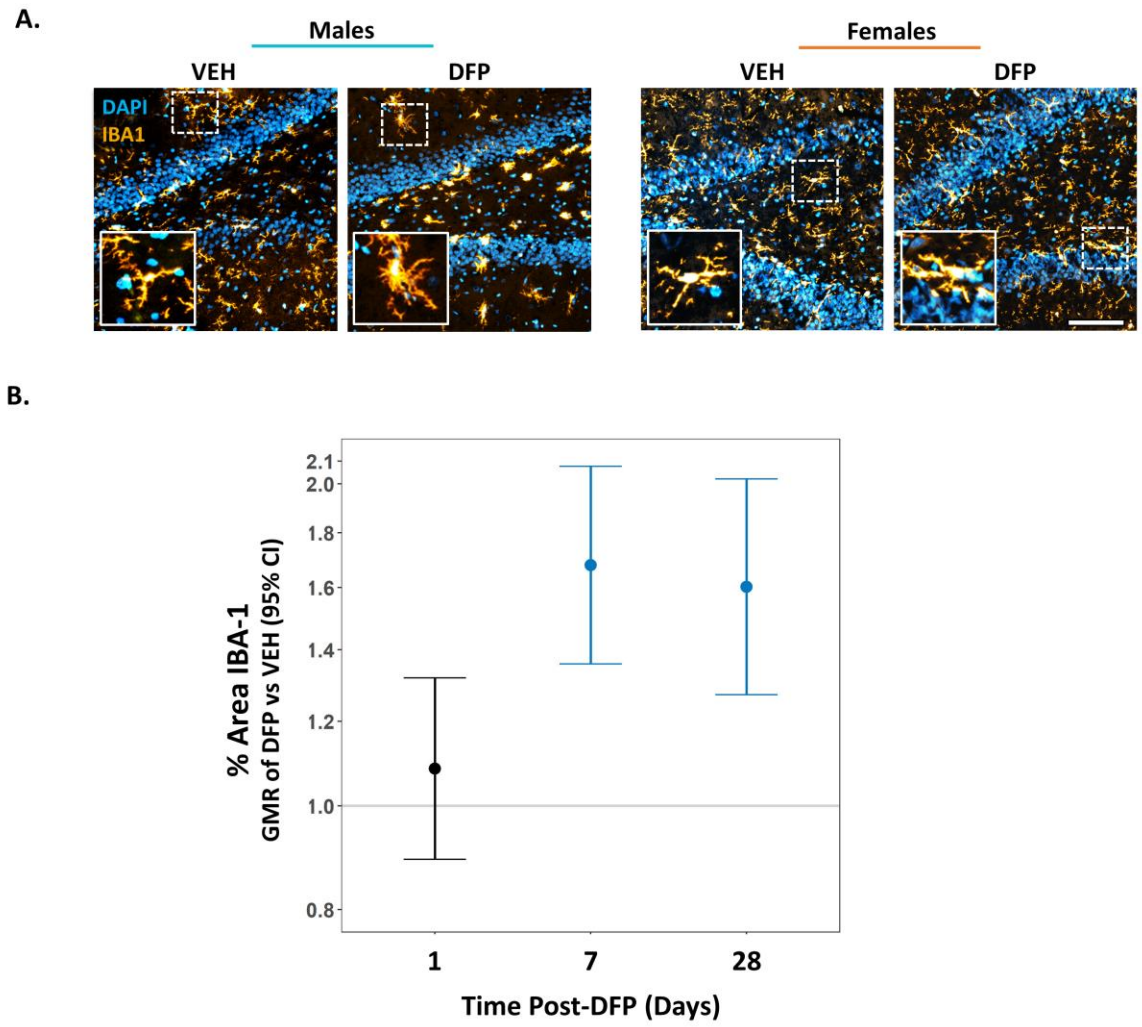
A.
Males
Females
VEH
DFP
VEH
DFP
DAPI
IBA1
B.
% Area IBA-1
GMR of DFP vs VEH (95% CI)
2.1
2.0
1.8
1.6
1.4
1.2
1.0
0.8
1
7
28
Time Post-DFP (Days)

Figure 4-6. DFP-induced persistent microgliosis in both males and females. (**A**) Representative photomicrographs of IBA1 immunostaining (microglia; orange) in the hippocampus of VEH and DFP rats at 7 d post-intoxication. Blue=DAPI (cell nuclei). Bar=100 µm. (**B**) The % area of IBA-1 immunoreactivity was quantified in multiple brain regions of each sex at 1, 7, and 28 d post-DFP injection. No effects of sex or brain region were observed, so data were collapsed across those variables. Data are shown as the geometric mean ratio of DFP to VEH with 95% confidence intervals. Confidence intervals entirely above or below 1 are colored blue and indicate a significant difference between the two groups being compared at $p < 0.05$ (n=5-7 animals/group).

Figure 4-7

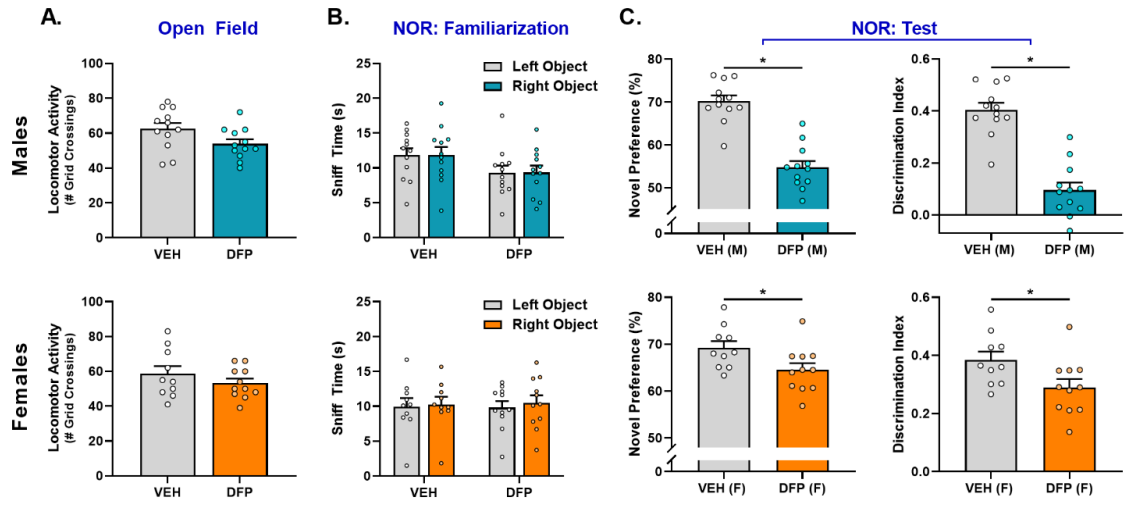
A.
Open Field
B.
NOR: Familiarization
C.
NOR: Test
Males
Females
Locomotor Activity (# Grid Crossings)
Sniff Time (s)
Left Object
Right Object
Novel Preference (%)
Discrimination Index
VEH
DFP
VEH (M)
DFP (M)
VEH (F)
DFP (F)
*

Figure 4-7. Acute DFP intoxication impaired recognition memory in both males and females at 1 month post-exposure. (**A**) Open field data showing locomotor activity in male and female rats as measured by the number of grids crossed in an open arena (48 cm^3) with a 3x3 grid overlay. Novel object recognition data showing sniff time with each object during the familiarization (**B**) and test (**C**) phases of the assay. The familiarization phase compares left vs right objects to ensure there are no inherent biases in object preference. Data from the test phase were analyzed to represent both the novel preference (%) and the discrimination index between VEH and DFP rats of each sex. Data presented as mean ± SEM with individual data points per animal (n=10-12/group); *$p<0.05$ as determined by Mann-Whitney *U* test or two-way ANOVA. NOR=novel object recognition.

Figure 4-8

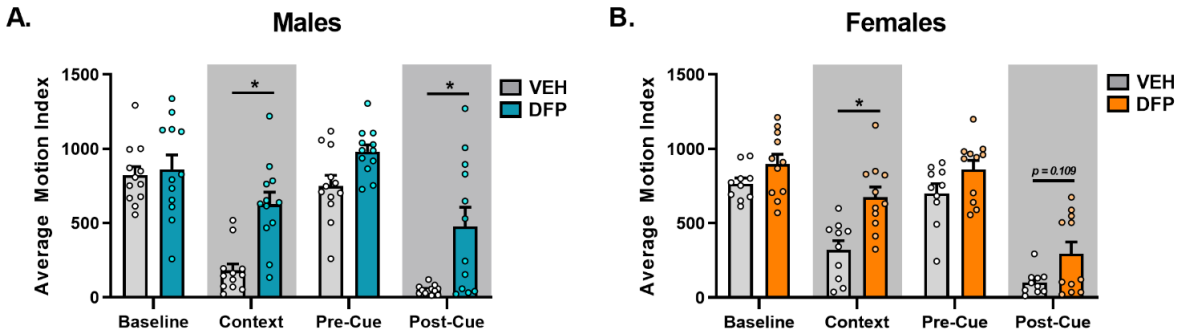
A.
Males
Average Motion Index
1500
1000
500
0
*
*
VEH
DFP
Baseline
Context
Pre-Cue
Post-Cue
B.
Females
Average Motion Index
1500
1000
500
0
*
p = 0.109
VEH
DFP
Baseline
Context
Pre-Cue
Post-Cue

Figure 4-8. DFP males show more pronounced fear-associated memory deficits than DFP females. Movement patterns of VEH and DFP male (**A**) and female (**B**) rats as measured by the average motion index during the baseline, context, and cue periods. Gray shading highlights test periods where subjects were expected to freeze or reduce motion. Data presented as mean ± SEM with individual data points per animal (n=10-12/group); *$p<0.05$ as determined by two-way ANOVA with *post hoc* Holm-Sidak test.

Figure 4-9

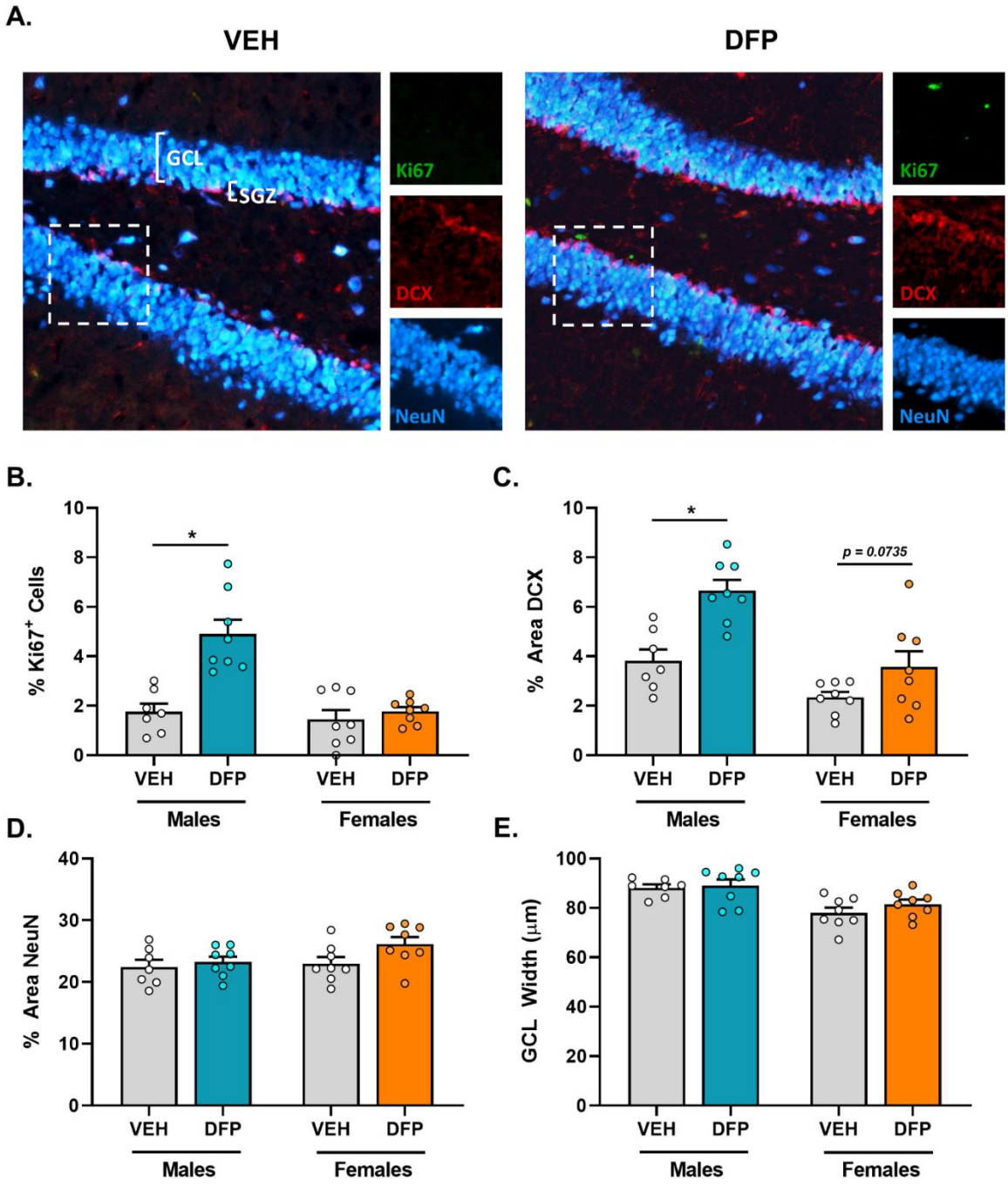
A.
VEH
DFP
GCL
SGZ
Ki67
DCX
NeuN
B.
% Ki67+ Cells
C.
% Area DCX
p = 0.0735
D.
% Area NeuN
E.
GCL Width (μm)
VEH
DFP
Males
Females

Figure 4-9. DFP increases neurogenesis markers in males but shows no evidence of structural changes in the hippocampus at 28 d post-intoxication. (**A**) Representative photomicrographs of ki67 (proliferating cells), doublecortin (DCX; immature neurons), and NeuN (mature neurons) in the hippocampus of VEH vs DFP male rats. No differences between VEH and DFP were observed in female rats. Newly born cells were quantified using the % $ki67^+$ cells (**B**) and the % area of DCX^+ staining (**C**). Mature neurons were quantified using the % area of $NeuN^+$ staining (**D**) and the width of the hippocampal granule cell layer (GCL; **E**). Data presented as mean ± SEM with individual data points per animal (n=6-8/group); *$p<0.05$ as determined by two-way ANOVA with *post hoc* Holm-Sidak test.

References

Akazawa, C., R. Shigemoto, Y. Bessho, S. Nakanishi and N. Mizuno (1994). "Differential expression of five N-methyl-D-aspartate receptor subunit mRNAs in the cerebellum of developing and adult rats." Journal of Comparative Neurology **347**(1): 150-160.

Akman, O., S. L. Moshé and A. S. Galanopoulou (2014). "Sex-specific consequences of early life seizures." Neurobiology of disease **72 Pt B**(Pt B): 153-166.

Bell, M. R. (2018). "Comparing Postnatal Development of Gonadal Hormones and Associated Social Behaviors in Rats, Mice, and Humans." Endocrinology **159**(7): 2596-2613.

Berg, E. L., L. R. Pedersen, M. C. Pride, S. P. Petkova, K. T. Patten, A. E. Valenzuela, C. Wallis, K. J. Bein, A. Wexler, P. J. Lein and J. L. Silverman (2020). "Developmental exposure to near roadway pollution produces behavioral phenotypes relevant to neurodevelopmental disorders in juvenile rats." Transl Psychiatry **10**(1): 289.

Bian, C., K. Zhu, Q. Guo, Y. Xiong, W. Cai and J. Zhang (2012). "Sex differences and synchronous development of steroid receptor coactivator-1 and synaptic proteins in the hippocampus of postnatal female and male C57BL/6 mice." Steroids **77**(1-2): 149-156.

Bruce, R. D. (1985). "An up-and-down procedure for acute toxicity testing." Fundam Appl Toxicol **5**(1): 151-157.

Chen, Y. (2012). "Organophosphate-induced brain damage: mechanisms, neuropsychiatric and neurological consequences, and potential therapeutic strategies." Neurotoxicology **33**(3): 391-400.

Cho, K. O., Z. R. Lybrand, N. Ito, R. Brulet, F. Tafacory, L. Zhang, L. Good, K. Ure, S. G. Kernie, S. G. Birnbaum, H. E. Scharfman, A. J. Eisch and J. Hsieh (2015). "Aberrant hippocampal neurogenesis contributes to epilepsy and associated cognitive decline." Nat Commun **6**: 6606.

Chudomel, O., H. Herman, K. Nair, S. L. Moshé and A. S. Galanopoulou (2009). "Age- and gender-related differences in GABAA receptor-mediated postsynaptic currents in GABAergic neurons of the substantia nigra reticulata in the rat." Neuroscience **163**(1): 155-167.

Comfort, N. and D. B. Re (2017). "Sex-Specific Neurotoxic Effects of Organophosphate Pesticides Across the Life Course." Current environmental health reports **4**(4): 392-404.

Couillard-Despres, S., B. Winner, S. Schaubeck, R. Aigner, M. Vroemen, N. Weidner, U. Bogdahn, J. Winkler, H. G. Kuhn and L. Aigner (2005). "Doublecortin expression levels in adult brain reflect neurogenesis." Eur J Neurosci **21**(1): 1-14.

Damborsky, J. C. and U. H. Winzer-Serhan (2012). "Effects of sex and chronic neonatal nicotine treatment on $Na^{2+}/K^{+}/Cl^{-}$ co-transporter 1, K^{+}/Cl^{-} co-transporter 2, brain-derived neurotrophic factor, NMDA receptor subunit 2A and NMDA receptor subunit 2B mRNA expression in the postnatal rat hippocampus." Neuroscience **225**: 105-117.

de Araujo Furtado, M., F. Rossetti, S. Chanda and D. Yourick (2012). "Exposure to nerve agents: From status epilepticus to neuroinflammation, brain damage, neurogenesis and epilepsy." NeuroToxicology **33**(6): 1476-1490.

Deshpande, L. S., D. S. Carter, R. E. Blair and R. J. DeLorenzo (2010). "Development of a prolonged calcium plateau in hippocampal neurons in rats surviving status epilepticus induced by the organophosphate diisopropylfluorophosphate." Toxicol Sci **116**(2): 623-631.

Ellman, G. L., K. D. Courtney, V. Andres, Jr. and R. M. Feather-Stone (1961). "A new and rapid colorimetric determination of acetylcholinesterase activity." Biochem Pharmacol **7**: 88-95.

Farahat, F. M., C. A. Ellison, M. R. Bonner, B. P. McGarrigle, A. L. Crane, R. A. Fenske, M. R. Lasarev, D. S. Rohlman, W. K. Anger, P. J. Lein and J. R. Olson (2011). "Biomarkers of chlorpyrifos exposure and effect in Egyptian cotton field workers." Environ Health Perspect **119**(6): 801-806.

Fawcett, W. P., Y. Aracava, M. Adler, E. F. Pereira and E. X. Albuquerque (2009). "Acute toxicity of organophosphorus compounds in guinea pigs is sex- and age-dependent and cannot be solely accounted for by acetylcholinesterase inhibition." J Pharmacol Exp Ther **328**(2): 516-524.

Figueiredo, T. H., J. P. Apland, M. F. M. Braga and A. M. Marini (2018). "Acute and long-term consequences of exposure to organophosphate nerve agents in humans." Epilepsia **59 Suppl 2**(Suppl 2): 92-99.

Flannery, B. M., D. A. Bruun, D. J. Rowland, C. N. Banks, A. T. Austin, D. L. Kukis, Y. Li, B. D. Ford, D. J. Tancredi, J. L. Silverman, S. R. Cherry and P. J. Lein (2016). "Persistent neuroinflammation and cognitive impairment in a rat model of acute diisopropylfluorophosphate intoxication." J Neuroinflammation **13**(1): 267.

Gage, M., M. Golden, M. Putra, S. Sharma and T. Thippeswamy (2020). "Sex as a biological variable in the rat model of diisopropylfluorophosphate-induced long-term neurotoxicity." Ann N Y Acad Sci **1479**(1): 44-64.

Gao, J., S. X. Naughton, H. Wulff, V. Singh, W. D. Beck, J. Magrane, B. Thomas, N. A. Kaidery, C. M. Hernandez and A. V. Terry, Jr. (2016). "Diisopropylfluorophosphate Impairs the Transport of Membrane-Bound Organelles in Rat Cortical Axons." J Pharmacol Exp Ther **356**(3): 645-655.

Gonzalez-Alzaga, B., M. Lacasana, C. Aguilar-Garduno, M. Rodriguez-Barranco, F. Ballester, M. Rebagliato and A. F. Hernandez (2014). "A systematic review of neurodevelopmental effects of prenatal and postnatal organophosphate pesticide exposure." Toxicol Lett **230**(2): 104-121.

González, E. A., A. C. Rindy, M. A. Guignet, J. J. Calsbeek, D. A. Bruun, A. Dhir, P. Andrew, N. Saito, D. J. Rowland, D. J. Harvey, M. A. Rogawski and P. J. Lein (2020). "The chemical convulsant diisopropylfluorophosphate (DFP) causes persistent neuropathology in adult male rats independent of seizure activity." Arch Toxicol **94**(6): 2149-2162.

Guignet, M., K. Dhakal, B. M. Flannery, B. A. Hobson, D. Zolkowska, A. Dhir, D. A. Bruun, S. Li, A. Wahab, D. J. Harvey, J. L. Silverman, M. A. Rogawski and P. J. Lein (2019). "Persistent behavior deficits, neuroinflammation, and oxidative stress in a rat model of acute organophosphate intoxication." Neurobiol Dis.

Guignet, M., K. Dhakal, B. M. Flannery, B. A. Hobson, D. Zolkowska, A. Dhir, D. A. Bruun, S. Li, A. Wahab, D. J. Harvey, J. L. Silverman, M. A. Rogawski and P. J. Lein (2020). "Persistent behavior deficits, neuroinflammation, and oxidative stress in a rat model of acute organophosphate intoxication." Neurobiol Dis **133**: 104431.

Guignet, M. and P. J. Lein (2018). Organophosphates. Advances in Neurotoxicology: Role of Inflammation in Environmental Neurotoxicity. M. Aschner and L. G. Costa. Oxford, UK, Elsevier, Ltd. **3:** 35-79.

Gulinello, M., H. A. Mitchell, Q. Chang, W. Timothy O'Brien, Z. Zhou, T. Abel, L. Wang, J. G. Corbin, S. Veeraragavan, R. C. Samaco, N. A. Andrews, M. Fagiolini, T. B. Cole, T. M. Burbacher and J. N. Crawley (2019). "Rigor and reproducibility in rodent behavioral research." Neurobiol Learn Mem **165**: 106780.

Haley, N. (2018). Remarks at an Emergency UN Security Council Briefing on Chemical Weapons Use by Russia in the United Kingdom. United States Mission to the United Nations.

Heiss, D. R., D. W. Zehnder, D. A. Jett, G. E. Platoff, D. T. Yeung and B. N. Brewer (2016). "Synthesis and Storage Stability of Diisopropylfluorophosphate." Journal of Chemistry **2016**: 5.

Hobson, B. A., D. J. Rowland, S. Siso, M. A. Guignet, Z. T. Harmany, S. Bandara, N. Saito, D. J. Harvey, D. A. Bruun, J. R. Garbow, A. J. Chaudhari and P. J. Lein (2019). "TSPO PET Using [18F]PBR111 Reveals Persistent Neuroinflammation Following Acute Diisopropylfluorophosphate Intoxication in the Rat." Toxicol Sci.

Holst, C. B., C. B. Brochner, K. Vitting-Seerup and K. Mollgard (2019). "Astrogliogenesis in human fetal brain: complex spatiotemporal immunoreactivity patterns of GFAP, S100, AQP4 and YKL-40." J Anat.

Hsu, C., Y. L. Hsieh, R. C. Yang and H. K. Hsu (2000). "Blockage of N-methyl-D-aspartate receptors decreases testosterone levels and enhances postnatal neuronal apoptosis in the preoptic area of male rats." Neuroendocrinology **71**(5): 301-307.

Hung, Y.-W., D.-I. Yang, P.-Y. Huang, T.-S. Lee, T. B. J. Kuo, C.-H. Yiu, Y.-H. Shih and Y.-Y. Lin (2012). "The duration of sustained convulsive seizures determines the pattern of hippocampal neurogenesis and the development of spontaneous epilepsy in rats." Epilepsy Research **98**(2): 206-215.

Jessberger, S. and J. M. Parent (2015). "Epilepsy and Adult Neurogenesis." Cold Spring Harb Perspect Biol **7**(12).

Jett, D. A. (1998). Central cholinergic neurobiology. Handbook of Developmental Neurotoxicology, Elsevier**:** 257-274.

Jett, D. A., C. A. Sibrizzi, R. B. Blain, P. A. Hartman, P. J. Lein, K. W. Taylor and A. A. Rooney (2020). "A national toxicology program systematic review of the evidence for long-term effects after acute exposure to sarin nerve agent." Crit Rev Toxicol **50**(6): 474-490.

Jett, D. A. and S. M. Spriggs (2020). "Translational research on chemical nerve agents." Neurobiol Dis **133**: 104335.

Kee, N., S. Sivalingam, R. Boonstra and J. M. Wojtowicz (2002). "The utility of Ki-67 and BrdU as proliferative markers of adult neurogenesis." J Neurosci Methods **115**(1): 97-105.

Kempermann, G., H. Song and F. H. Gage (2015). "Neurogenesis in the Adult Hippocampus." Cold Spring Harb Perspect Biol **7**(9): a018812.

Kruger, L., S. Saporta and L. W. Swanson (1995). Photographic atlas of the rat brain: the cell and fiber architecture illustrated in three planes with stereotaxic coordinates. Cambridge, Cambridge University Press.

Kuruba, R., X. Wu and D. S. Reddy (2018). "Benzodiazepine-refractory status epilepticus, neuroinflammation, and interneuron neurodegeneration after acute organophosphate intoxication." Biochimica et Biophysica Acta (BBA) - Molecular Basis of Disease **1864**(9, Part B): 2845-2858.

Lazarov, O. and C. Hollands (2016). "Hippocampal neurogenesis: Learning to remember." Prog Neurobiol **138-140**: 1-18.

Li, H., J. R. Huguenard and R. S. Fisher (2007). "Gender and age differences in expression of GABAA receptor subunits in rat somatosensory thalamus and cortex in an absence epilepsy model." Neurobiol Dis **25**(3): 623-630.

Liu, C., Y. Li, P. J. Lein and B. D. Ford (2012). "Spatiotemporal patterns of GFAP upregulation in rat brain following acute intoxication with diisopropylfluorophosphate (DFP)." Curr Neurobiol **3**(2): 90-97.

McDonough, J. H., Jr. and T. M. Shih (1997). "Neuropharmacological mechanisms of nerve agent-induced seizure and neuropathology." Neurosci Biobehav Rev **21**(5): 559-579.

Mew, E. J., P. Padmanathan, F. Konradsen, M. Eddleston, S. S. Chang, M. R. Phillips and D. Gunnell (2017). "The global burden of fatal self-poisoning with pesticides 2006-15: Systematic review." J Affect Disord **219**: 93-104.

Monyer, H., N. Burnashev, D. J. Laurie, B. Sakmann and P. H. Seeburg (1994). "Developmental and regional expression in the rat brain and functional properties of four NMDA receptors." Neuron **12**(3): 529-540.

Muñoz-Quezada, M. T., B. A. Lucero, D. B. Barr, K. Steenland, K. Levy, P. B. Ryan, V. Iglesias, S. Alvarado, C. Concha, E. Rojas and C. Vega (2013). "Neurodevelopmental effects in children associated with exposure to organophosphate pesticides: A systematic review." Neurotoxicology **39**: 158-168.

OPCW (2020). "OPCW Issues Report on Technical Assistance Requested by Germany." Organisation for the Prohibition of Chemical Weapons.

Pereira, E. F., Y. Aracava, L. J. DeTolla, Jr., E. J. Beecham, G. W. Basinger, Jr., E. J. Wakayama and E. X. Albuquerque (2014). "Animal models that best reproduce the clinical manifestations of human intoxication with organophosphorus compounds." J Pharmacol Exp Ther **350**(2): 313-321.

Pessah, I. N., M. A. Rogawski, D. J. Tancredi, H. Wulff, D. Zolkowska, D. A. Bruun, B. D. Hammock and P. J. Lein (2016). "Models to identify treatments for the acute and persistent effects of seizure-inducing chemical threat agents." Ann N Y Acad Sci **1378**(1): 124-136.

Phelan, K. D., U. T. Shwe, D. K. Williams, L. J. Greenfield and F. Zheng (2015). "Pilocarpine-induced status epilepticus in mice: A comparison of spectral analysis of electroencephalogram and behavioral grading using the Racine scale." Epilepsy Res **117**: 90-96.

Pope, C. N. and S. Brimijoin (2018). "Cholinesterases and the fine line between poison and remedy." Biochem Pharmacol.

Potier, S., J. Sénécal, J. G. Chabot, C. Psarropoulou and L. Descarries (2005). "A pentylenetetrazole-induced generalized seizure in early life enhances the efficacy of muscarinic receptor coupling to G-protein in hippocampus and neocortex of adult rat." Eur J Neurosci **21**(7): 1828-1836.

Pouliot, W., S. L. Bealer, B. Roach and F. E. Dudek (2016). "A rodent model of human organophosphate exposure producing status epilepticus and neuropathology." Neurotoxicology **56**: 196-203.

Putra, M., S. Sharma, M. Gage, G. Gasser, A. Hinojo-Perez, A. Olson, A. Gregory-Flores, S. Puttachary, C. Wang, V. Anantharam and T. Thippeswamy (2019). "Inducible nitric oxide synthase inhibitor, 1400W, mitigates DFP-induced long-term neurotoxicity in the rat model." Neurobiol Dis.

Putra, M., S. Sharma, M. Gage, G. Gasser, A. Hinojo-Perez, A. Olson, A. Gregory-Flores, S. Puttachary, C. Wang, V. Anantharam and T. Thippeswamy (2020). "Inducible nitric oxide synthase inhibitor, 1400W, mitigates DFP-induced long-term neurotoxicity in the rat model." Neurobiol Dis **133**: 104443.

Rauh, V. A., F. P. Perera, M. K. Horton, R. M. Whyatt, R. Bansal, X. Hao, J. Liu, D. B. Barr, T. A. Slotkin and B. S. Peterson (2012). "Brain anomalies in children exposed prenatally to a common organophosphate pesticide." Proceedings of the National Academy of Sciences of the United States of America **109**(20): 7871-7876.

Ravizza, T., L. K. Friedman, S. L. Moshé and J. Velísková (2003). "Sex differences in GABA(A)ergic system in rat substantia nigra pars reticulata." Int J Dev Neurosci **21**(5): 245-254.

Reddy, S. D., X. Wu, R. Kuruba, V. Sridhar and D. S. Reddy (2020). "Magnetic resonance imaging analysis of long-term neuropathology after exposure to the nerve agent soman:

correlation with histopathology and neurological dysfunction." Ann N Y Acad Sci **1480**(1): 116-135.

Richardson, J. R., V. Fitsanakis, R. H. S. Westerink and A. G. Kanthasamy (2019). "Neurotoxicity of pesticides." Acta neuropathologica **138**(3): 343-362.

Ritz, C. and J. C. Streibig (2005). "Bioassay Analysis Using R." 2005 **12**(5): 22.

Rojas, A., T. Ganesh, W. Wang, J. Wang and R. Dingledine (2020). "A rat model of organophosphate-induced status epilepticus and the beneficial effects of EP2 receptor inhibition." Neurobiol Dis **133**: 104399.

Sagiv, S. K., J. L. Bruno, J. M. Baker, V. Palzes, K. Kogut, S. Rauch, R. Gunier, A. M. Mora, A. L. Reiss and B. Eskenazi (2019). "Prenatal exposure to organophosphate pesticides and functional neuroimaging in adolescents living in proximity to pesticide application." Proc Natl Acad Sci U S A **116**(37): 18347-18356.

Scharfman, H. E. and N. J. MacLusky (2014). "Sex differences in the neurobiology of epilepsy: a preclinical perspective." Neurobiol Dis **72 Pt B**: 180-192.

Schmued, L. C., C. C. Stowers, A. C. Scallet and L. Xu (2005). "Fluoro-Jade C results in ultra high resolution and contrast labeling of degenerating neurons." Brain Res **1035**(1): 24-31.

Scholl, E. A., S. M. Miller-Smith, S. L. Bealer, M. J. Lehmkuhle, J. J. Ekstrand, F. E. Dudek and J. H. McDonough (2018). "Age-dependent behaviors, seizure severity and neuronal damage in response to nerve agents or the organophosphate DFP in immature and adult rats." Neurotoxicology **66**: 10-21.

Siso, S., B. A. Hobson, D. J. Harvey, D. A. Bruun, D. J. Rowland, J. R. Garbow and P. J. Lein (2017). "Editor's Highlight: Spatiotemporal Progression and Remission of Lesions in the Rat Brain Following Acute Intoxication With Diisopropylfluorophosphate." Toxicol Sci **157**(2): 330-341.

Supasai, S., E. A. González, D. J. Rowland, B. Hobson, D. A. Bruun, M. A. Guignet, S. Soares, V. Singh, H. Wulff, N. Saito, D. J. Harvey and P. J. Lein (2020). "Acute administration of diazepam or midazolam minimally alters long-term neuropathological effects in the rat brain following acute intoxication with diisopropylfluorophosphate." Eur J Pharmacol **886**: 173538.

Tanaka, K., S. H. Graham and R. P. Simon (1996). "The role of excitatory neurotransmitters in seizure-induced neuronal injury in rats." Brain Res **737**(1-2): 59-63.

Toda, T. and F. H. Gage (2018). "Review: adult neurogenesis contributes to hippocampal plasticity." Cell Tissue Res **373**(3): 693-709.

UN (2017). Report of the Independent International Commission of Inquiry on the Syrian Arab Republic United Nations General Assembly: Human Rights Council.

Varodayan, F. P., X.-J. Zhu, X.-N. Cui and B. E. Porter (2009). "Seizures increase cell proliferation in the dentate gyrus by shortening progenitor cell-cycle length." Epilepsia **50**(12): 2638-2647.

Velazco-Cercas, E., L. Beltran-Parrazal, C. Morgado-Valle and M. L. López-Meraz (2020). "Status Epilepticus Increases Cell Proliferation and Neurogenesis in the Developing Rat Cerebellum." Cerebellum **19**(1): 48-57.

Velíšková, J. and K. A. Desantis (2013). "Sex and hormonal influences on seizures and epilepsy." Horm Behav **63**(2): 267-277.

Wu, P., Y. Hu, X. J. Li, M. Cheng and L. Jiang (2019). "Sodium valproate suppresses abnormal neurogenesis induced by convulsive status epilepticus." Neural Regen Res **14**(3): 480-484.

Yang, F., J.-C. Wang, J.-L. Han, G. Zhao and W. Jiang (2008). "Different effects of mild and severe seizures on hippocampal neurogenesis in adult rats." Hippocampus **18**(5): 460-468.

Zitman, F. M. P. and G. Richter-Levin (2013). "Age and sex-dependent differences in activity, plasticity and response to stress in the dentate gyrus." Neuroscience **249**: 21-30.

Chapter 5

Conclusion

Based on the historical use of chemical threat agents (Haines and Fox 2014, Bajgar, Fusek et al. 2015, Worek, Wille et al. 2016), recent chemical attacks (Yamasue, Abe et al. 2007, OPCW 2017, UN 2017, Haley 2018) and startlingly high numbers of global poisonings (Dharmani and Jaga 2005, Patel, Ramasundarahettige et al. 2012, Mew, Padmanathan et al. 2017) it is clear that the legacy of chemical weapons is unlikely to change in the near future. In addition to the original organophosphate (OP) nerve agents developed during World War II, a number of similar OPs now pose risks to public health (Jett and Spriggs 2018). For these reasons, there is a worldwide effort to develop more effective medical countermeasures than those currently available to combat chemical threats. The diversity of chemical threats and severity of the resulting health outcomes has made it challenging to identify a universal antidote that is effective against all chemical threats. Even within the context of acute OP intoxication, numerous mechanisms have been implicated in the complex neurological consequences observed in those acutely intoxicated individuals that survive (reviewed in **Figure 5-1**). The current standard of care, which includes atropine to block muscarinic receptors, an oxime to reactivate AChE, and benzodiazepines to terminate seizures, provides protection against lethality and can attenuate acute seizures following acute OP exposures but does not mitigate the chronic neuropathologic, electroencephalographic, or cognitive responses that are known to occur (reviewed in de Araujo Furtado, Rossetti et al. 2012, Figueiredo, Apland et al. 2018). This has led researchers to investigate more efficacious antiseizure therapeutics as well as neuroprotectants that target seizure-independent mechanisms of disease with the goal of improving chronic neurological outcomes.

A currently outstanding question in the field is whether more effective seizure termination following acute OP intoxication will also more effectively mitigate downstream neurological

deficits. The standard of care antiseizure drug, the benzodiazepine diazepam, was recently replaced by the benzodiazepine midazolam due to the latter's superior bioavailability and seizure termination (Silbergleit, Lowenstein et al. 2013, FDA 2018), but whether it also affords increased neuroprotection remains unclear. In particular, prior to the present studies, there was little data available to indicate whether either benzodiazepine protected against chronic neuropathology outcomes. While a relationship between seizure severity and neuropathology has been demonstrated in OP models (McDonough and Shih 1997, Hobson, Siso et al. 2017), it is also known that OPs can cause neurological damage via diverse mechanisms independent of seizures (reviewed in Guignet and Lein 2018, Naughton and Terry 2018). This raises questions as to whether treatment with a single antiseizure medication, either diazepam or midazolam, is sufficient to offer long-term neuroprotection, and whether midazolam is superior to diazepam in providing neuroprotection.

To further address this question, it is helpful to better understand the relative contribution of seizures versus alternative, seizure-independent mechanisms to chronic brain damage. This research question is also relevant in light of the variable human responses that are observed following OP intoxication, which can range from negligible seizure activity to severe SE (Okumura, Takasu et al. 1996, Peter, Sudarsan et al. 2014). This variability was highlighted during the 2005 Tokyo sarin attack, in which humans with roughly equivalent exposures exhibited different susceptibility to seizures and other cholinergic symptoms (Yanagisawa, Morita et al. 2006). Although research has suggested a strong correlation between seizure severity and the extent of subsequent neurological damage (McDonough, Dochterman et al. 1995, Hobson, Rowland et al. 2017), it remains unclear to what extent additional mechanisms are involved.

As therapeutic development against chemical threats advances, it is important to consider which relevant biological variables will be needed to thoroughly evaluate safety and efficacy. To date, much of the preclinical research in this field has focused on the adult male brain. However, even the best therapeutic candidates will have major data gaps if they are not rigorously tested in diverse models. This is especially true given the literature suggesting that chronic exposure to OPs can have both age-specific (Bouchard, Chevrier et al. 2011, Muñoz-Quezada, Lucero et al. 2013, Gonzalez-Alzaga, Lacasana et al. 2014) and sex-specific (Rauh, Perera et al. 2012, Comfort and Re 2017) neurotoxic outcomes. However, the roles of sex and age have not been as rigorously addressed in the context of acute OP intoxication, particularly in terms of chronic neurological outcomes. It has recently been reported that acute DFP intoxication differentially affects juvenile rats in the days post-intoxication (Scholl, Miller-Smith et al. 2018), and that DFP causes sex-specific neurotoxicity in adults for weeks post-intoxication (Gage, Golden et al. 2020). These studies provide the rationale for investigating whether DFP causes persistent neurological damage in developing rats, and whether these effects are sex-specific. The results presented within this dissertation sough to evaluate each of these data gaps and better understand the long-term neurotoxic effects of acute OP intoxication.

Overview of Dissertation Findings

Seizure-independent mechanisms contribute to long-term effects of acute OP intoxication

Each of the data chapters provides evidence that seizure-independent mechanisms contribute to chronic OP-induced neurological outcomes. In chapter 2, both diazepam and midazolam significantly reduced seizure scores below 3, a threshold that is consistent with the induction of *status epilepticus* (SE) (Deshpande, Carter et al. 2010, Phelan, Shwe et al. 2015). However,

neither benzodiazepine was effective at preventing chronic neurodegeneration or neuroinflammation following DFP intoxication. Regarding neuronal degeneration, diazepam had no protective effect and midazolam offered only transient neuroprotection at 3 but not 6 months post-DFP, which emphasizes the need for including late time points in studies of therapeutic efficacy. Treatment with each benzodiazepine partially protected against reactive astrogliosis and mineralization but had no effect on microglial activation. These observations that neither diazepam nor midazolam fully protected against long-term neuropathology, despite significant reductions in seizure activity, suggest that acute SE alone is unlikely the cause of all the adverse consequences observed following DFP intoxication. These data are consistent with the reports of limited neuroprotective efficacy by benzodiazepines in the days following OP intoxication (Kuruba, Wu et al. 2018, Wu, Kuruba et al. 2018, Spampanato, Pouliot et al. 2019), and expand on these studies to suggest that seizure-independent mechanisms are particularly important in the case of chronic neurological outcomes.

Chapter 3 supports this finding in greater detail by taking advantage of a seizure-resistant model to better understand the mechanisms underlying long-term neurological damage. The presence of a subpopulation of rats that did not develop seizures (low responders) in response to a dose of DFP that causes prolonged SE in the majority of rats (high responders) was confirmed by cholinesterase assays and electroencephalogram (EEG) recordings. DFP low responders showed significant neuronal degeneration in multiple brain regions, although it was delayed in onset, less severe, and less persistent than that of high responders. This divergent pattern of neurological damage between populations suggests that seizure severity influences the extent of neurological damage following OP intoxication, which is consistent with prior reports of this relationship (McDonough and Shih 1997, Hobson, Siso et al. 2017). Perhaps more important is

the observation that neuronal degeneration in the piriform cortex and thalamic mineralization at 2 months post-DFP in acute seizure-resistant rats was comparable to that observed in high responders. The presence of such severe phenotypes in the absence of seizures strongly supports the hypothesis that acute DFP intoxication can induce chronic neurotoxicity via seizure-independent mechanisms. In humans, this likely suggests that neuroprotective therapeutics (as opposed to antiseizure therapies) will be even more critical for non- or low-seizing patients.

Lastly, findings from Chapter 4 also support this interpretation. As discussed above, the presence of long-term cognitive deficits in juvenile females despite a muted seizure response compared to males supports the conclusion that chronic neurological outcomes can be triggered by DFP independent of severe or prolonged seizure activity. Taken together, these strong indications of seizure-independent mechanisms have important therapeutic implications for the field of medical countermeasures. The current standard of care consists only of immediate anticholinergic and antiseizure therapies but fails to address other mechanisms that may contribute to the long-term neurologic consequences of acute OP intoxication (Jett and Spriggs 2018). It has been a subject of debate whether enhanced neuroprotection can be achieved using more effective antiseizure therapy alone or whether additional mechanism(s) need to be targeted. The data presented in these chapters strongly suggest that seizure-independent mechanisms play critical roles in the chronic neurological outcomes that are known to occur following acute OP intoxication (Figueiredo, Apland et al. 2018, Guignet and Lein 2018), which likely means that even highly effective antiseizure therapy alone is insufficient to provide complete neuroprotection. With this in mind, preclinical research should focus on the identification of novel targets for neuroprotection and the therapeutic efficacy associated with such targets. A

closer evaluation of the data presented in this thesis can inform therapeutic approaches that may be promising for protecting against chronic outcomes following acute OP intoxication.

Sex and age are biological variables that influence the pathogenesis of acute OP intoxication

Chapter 4 sought to address the lack of diverse models of acute OP intoxication that are available for therapeutic testing and to determine whether sex and/or age influences chronic outcomes following acute OP intoxication. The juvenile DFP model described in Chapter 4 revealed sex-specific effects immediately following DFP injection, with DFP females displaying significantly lower seizure behavior scores than DFP males, although EEG recordings confirmed the presence of seizure activity in females. Both sexes experienced robust neurodegeneration in all brain regions examined (amygdala, hippocampus, piriform cortex, somatosensory cortex, and thalamus), but males had greater raw numbers of degenerating neurons than females. Likewise, males experienced an earlier onset of reactive astrogliosis (1 d post-DFP) compared to females (7 d post-DFP), and had persistent astrogliosis in a greater number of brain regions. As both OPs and seizures have been associated with altered neurogenesis (reviewed in Jessberger and Parent 2015, Rossetti, Stoker et al. 2020), markers of hippocampal neurogenesis were also evaluated at 1 month post-intoxication. DFP males showed increased cellular proliferation and numbers of immature neurons while DFP females did not. Each of the aforementioned outcomes provides evidence that sex is a biological variable influencing both the seizurogenic and long-term pathologic response to acute OP intoxication of the juvenile brain.

In contrast, there were no sex differences in microglial activation. Both sexes showed microglial activation at 7 and 28 d post-DFP, and the persistence of microglial activation in both sexes suggests that it may explain, at least in part, the observation that both DFP males and

females showed significant learning and memory deficits at 1 month post-DFP. Both DFP males and DFP females experienced peak microgliosis at 7 d in several major brain regions, including the hippocampus and piriform cortex. Given the important role of microglia in juvenile cognitive refinement (Hong, Dissing-Olesen et al. 2016, Salter and Stevens 2017), this observed damage is likely a contributing factor to the learning and memory deficits observed in each sex. This hypothesis is supported by preclinical and clinical studies linking persistent microglial activation and cytokine expression to cognitive decline during aging (reviewed in Simen, Bordner et al. 2011). A perhaps surprising finding was that DFP females show clear cognitive deficits relative to their VEH counterparts at 1 month post-DFP but do not show corresponding changes in hippocampal neurogenesis. If seizure activity in males is confirmed to be more severe than females as our data have suggested, it may suggest that DFP-induced neurogenesis changes are primarily a function of seizure severity, as it has been well-established that seizures can promote increased neuronal growth within the hippocampus (Varodayan, Zhu et al. 2009, Wu, Hu et al. 2019, Velazco-Cercas, Beltran-Parrazal et al. 2020).

The data presented in Chapter 4 also provides evidence that age is an important biological variable to consider following acute OP intoxication. The seizure response of juveniles to DFP is less severe than that reported in adults (Guignet, Dhakal et al. 2019), which may have important implications for the use of antiseizure medications, many of which have adverse side effects (Uzun, Kozumplik et al. 2010, Choi, Kim et al. 2020). This suggests that caution should be used in younger animals, and that the use of lower doses than adults may be more appropriate. Juveniles may also be uniquely susceptible to adverse cognitive outcomes following acute OP intoxication, as both sexes were shown to develop significant learning and memory deficits despite having lower seizure behavior scores than previously published adult models (Gage,

Golden et al. 2020, Guignet, Dhakal et al. 2020). However, a direct comparison of juvenile and adult animals is needed to determine whether developing animals are indeed more susceptible to cognitive deficits. Another important distinction is that juveniles show almost no neuroinflammation at 1 d post-DFP, which is in contrast to the pronounced inflammation, evidenced as robust microgliosis and astrogliosis, that has been reported in adult rats at 1 d after acute DFP intoxication (Li, Lein et al. 2015, Flannery, Bruun et al. 2016). The causal relationship between neuroinflammation and neurodegeneration following acute OP intoxication has been a subject of debate in recent years (Guignet and Lein 2018). The earlier onset of neuronal degeneration compared to microglial activation and reactive astrogliosis suggest that neurodegeneration may be a trigger of neuroinflammation in the juvenile brain. Optimal therapeutic strategies following acute OP intoxication may differ between young and adult individuals, particularly in the case of neuroinflammation. If microglia are indeed playing a significant role in cognitive deficits, a more detailed temporal pattern of activation within the hours and immediate days following intoxication will likely inform therapeutic windows of administration that will be most effective. Should the juvenile pattern of microglial activation be significantly delayed compared to adults, later administration of anti-inflammatory therapies may be more beneficial for younger populations.

Insights regarding novel targets for neuroprotection

Several therapeutic targets are currently being researched for efficacy against OP chemical threats (**Figure 5-2**). Our findings suggest that neuroinflammatory responses, particularly those mediated by microglia, represent promising therapeutic targets for mitigating long-term neurological consequences of acute OP intoxication. In the comparative study of diazepam vs. midazolam (Chapter 2), microglial activation was found to be more severe and resistant to

treatment than the astrocytic response, which was significantly mitigated by each benzodiazepine. This observation that microglial activation is relatively unaffected by antiseizure therapy may suggest a relationship with cognitive function, as this endpoint has also been reported to persist despite standard of care treatment in both humans (Chen 2012, Figueiredo, Apland et al. 2018) and animal models (de Araujo Furtado, Rossetti et al. 2012, Guignet and Lein 2018). Persistent microglial activation has also been linked to cognitive decline in non-pathological aging models (Simen, Bordner et al. 2011). A similar parallel between microglial activation and cognitive deficits was observed in the juvenile DFP model (Chapter 4). DFP females did not experience prolonged seizures, and by 1 month post-DFP, they showed little to no alterations in reactive astrogliosis or hippocampal neurogenesis. However, DFP females did exhibit persistent microglial activation that preceded and coincided with cognitive deficits. While it is possible that early pathological changes may have triggered cognitive dysfunction later in life, the persistence of microglial activation and temporal relationship to cognitive outcomes increases the likelihood that the two are related.

This interpretation is supported by, and expands on, prior literature that has demonstrated reduced microglial activation, reduced cytokine mRNA expression, and increased neuronal survival following anti-inflammatory administration in OP-induced seizure models (Finkelstein, Kunis et al. 2012, Li, Lein et al. 2015). However, none of these studies evaluated therapeutic efficacy at late time points (>1 month post-intoxication) or neuroprotection against long-term cognitive deficits. Only recently has it been reported that administration of an anti-inflammatory EP2 antagonist, TG6-10-1, provided neuroprotection against DFP-induced memory deficits in the novel object recognition task (Rojas, Ganesh et al. 2020). However, only a single task of learning and memory was evaluated, and the precise mechanisms driving the cognitive deficits

remain unknown. Nonetheless, our findings have contributed important long-term data to a growing body of literature suggesting a possible relationship between neuroinflammation and cognitive impairment following acute OP intoxication (Guignet and Lein 2018). Our findings also provide evidence that microglia may be more critical drivers of chronic OP-induced neurological damage than other cell types.

Micro-CT data revealed persistent mineral deposits, likely comprised largely of calcium (Valdes Hernandez Mdel, Maconick et al. 2012), in the thalamus of both high and low seizing animals (Chapter 3), and data from Chapter 2 indicated that these mineral deposits were resistant to benzodiazepine treatment. While the functional consequences of such deposits are largely unknown, calcium dysregulation is associated with altered connectivity in the brain and impaired cognition (Kirkland, Sarlo et al. 2018, Lerdkrai, Asavapanumas et al. 2018, Muller, Ahumada-Castro et al. 2018). As calcium is known to be dysregulated following OP intoxication (Deshpande, Blair et al. 2016), it may be the case that stabilizing calcium signaling confers neuroprotection in acute OP models. Pharmacological inhibition of excess calcium release using dantrolene, a ryanodine receptor antagonist, protected against paraoxon-induced neuronal degeneration at 2 d post-intoxication (Deshpande, Blair et al. 2016). A rat model of repeated, low-dose DFP exposure revealed that treatment with levetiracetam, which blocks intracellular calcium release through RyR and IP_3R receptors, reversed excess intracellular calcium release and hippocampal neuronal damage at 6 months post-exposure (Phillips and Deshpande 2018), suggesting therapeutic potential for calcium stabilizing compounds. However, further research is needed to determine whether compounds of this nature protect against cognitive deficits following acute OP intoxication.

Future Directions and Concluding Remarks

Outstanding research questions

The presented data strongly suggest that there is a dynamic response to acute OP intoxication that differs in severity over the weeks to months post-intoxication. This has important treatment implications, highlighting the distinction between early treatment during SE and long-term treatment that may offer improved neuroprotection once the pathologies underlying chronic neurological damage have been triggered. The data across each chapter support the need to broaden the therapeutic windows following acute OP intoxication and consider ongoing therapies in patients.

In addition to contributing novel data to the field, the data presented in this dissertation have raised important questions. Follow-up studies on chapter 2 would be beneficial to identify whether early antiseizure treatment has any impact on long-term cognitive function. The seizure-resistant model in chapter 3 can be further studied to better understand whether differences in neurotransmission-related endpoints, such as ACh release, glutamate neurotransmission, or calcium buffering, explain the divergent seizure responses. The precise mechanisms underlying the sex-specific seizurogenic and neuropathologic responses to acute OP intoxication observed in chapter 4 remain unknown. The question of whether these mechanisms change throughout neurodevelopment also requires further research. Additionally, it is unknown whether males and females, or juveniles and adults, differ in their response to treatment for acute OP intoxication. Elucidation of the mechanisms underlying these differences will likely aid in developing appropriate therapeutic strategies for different subpopulations.

A better understanding of the role of microglial-mediated neuroinflammation in the pathogenesis of long-term cognitive outcomes is warranted. Follow-up studies further detailing the inflammatory profile of microglia following acute OP intoxication will likely reveal novel therapeutic targets. Relevant endpoints to investigate include the temporal patterns of microglial polarization, cytokine release profiles, or changes in receptor/ion channel expression following injury. The identification of increased hippocampal neurogenesis following acute DFP intoxication of juvenile males raises questions as to the functional consequences of such changes. Given the suggested relationship between seizure severity and aberrant neurogenesis in chemical-induced seizure models (Hung, Yang et al. 2012, Wu, Hu et al. 2019, Velazco-Cercas, Beltran-Parrazal et al. 2020), it would also be beneficial to understand whether adults experience the same neurogenic changes following acute OP intoxication.

Concluding Remarks

The data presented in this dissertation suggest that antiseizure therapy alone is largely insufficient to protect against chronic OP-induced neuropathology, and that inflammation mediated by microglia represents a promising therapeutic target. Given the urgent need for improved therapies, these results will aid in the prioritization of therapeutic candidates for further studies. These data have also identified the important role of both sex and age as biological variables that influence OP-induced neuropathology, particularly at late time points post-intoxication. The development of a juvenile DFP model using both males and females will allow for more comprehensive therapeutic testing and better representation of the diverse human populations affected by chemical threats.

Figures and Figure Legends

Figure 5-1

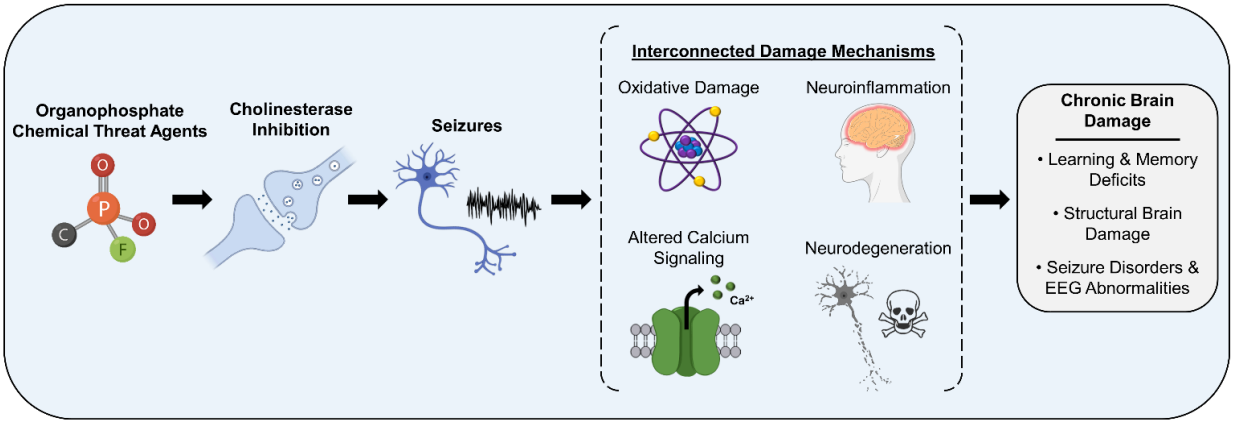

Figure 5-1. Schematic outlining the general pathway leading from acute organophosphate intoxication to long-term neurological damage, including learning & memory deficits, structural brain damage, and seizure disorders.

Figure 5-2.

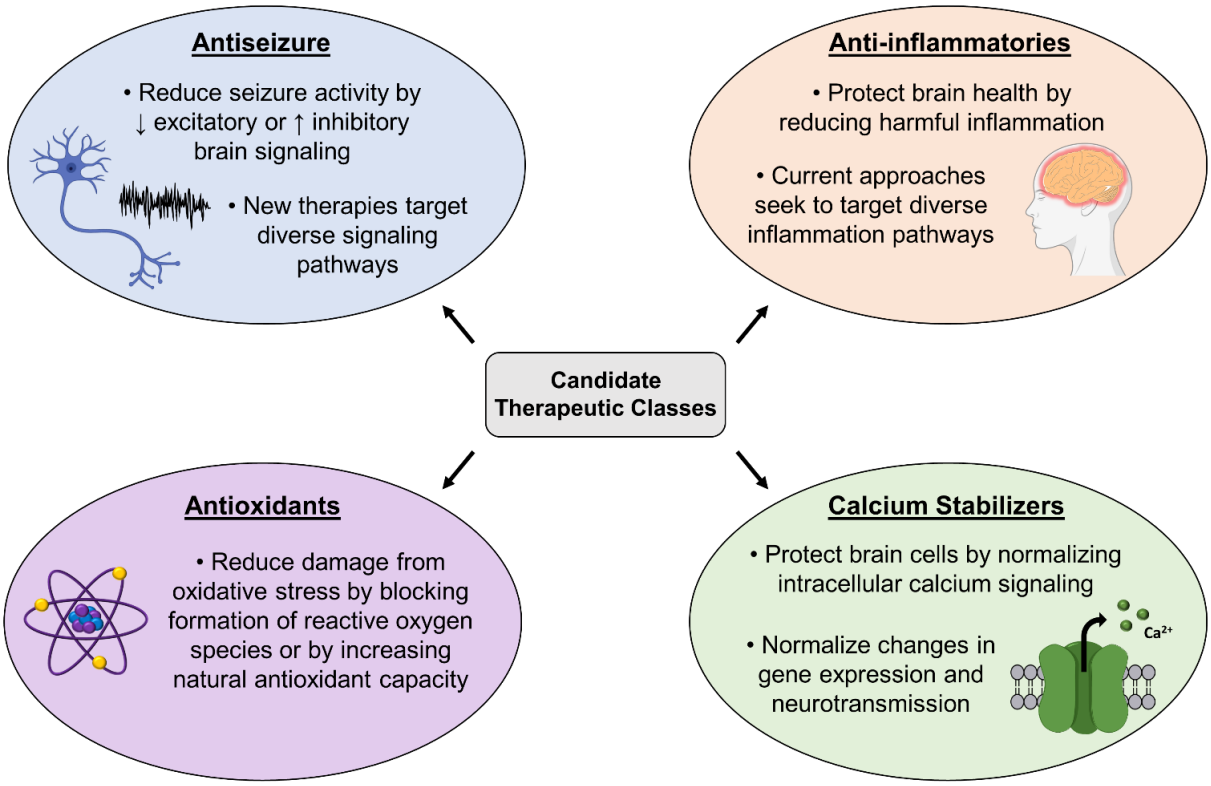
Antiseizure
• Reduce seizure activity by ↓ excitatory or ↑ inhibitory brain signaling
• New therapies target diverse signaling pathways
Anti-inflammatories
• Protect brain health by reducing harmful inflammation
• Current approaches seek to target diverse inflammation pathways
Candidate Therapeutic Classes
Antioxidants
• Reduce damage from oxidative stress by blocking formation of reactive oxygen species or by increasing natural antioxidant capacity
Calcium Stabilizers
• Protect brain cells by normalizing intracellular calcium signaling
• Normalize changes in gene expression and neurotransmission
Ca2+

Figure 5-2. Diagram summarizing four major therapeutic classes (antiseizure, anti-inflammatories, antioxidants, and calcium stabilizers) currently being researched to combat chemical threat agents.

References

Bajgar, J., J. Fusek, J. Kassa, K. Kuca and D. Jun (2015). Chapter 3 - Global Impact of Chemical Warfare Agents Used Before and After 1945. Handbook of Toxicology of Chemical Warfare Agents (Second Edition). R. C. Gupta. Boston, Academic Press**:** 17-25.

Bouchard, M. F., J. Chevrier, K. G. Harley, K. Kogut, M. Vedar, N. Calderon, C. Trujillo, C. Johnson, A. Bradman, D. B. Barr and B. Eskenazi (2011). "Prenatal exposure to organophosphate pesticides and IQ in 7-year-old children." Environ Health Perspect **119**(8): 1189-1195.

Chen, Y. (2012). "Organophosphate-induced brain damage: Mechanisms, neuropsychiatric and neurological consequences, and potential therapeutic strategies." NeuroToxicology **33**(3): 391-400.

Choi, S. A., H. Kim, S. Kim, S. Yoo, S. Yi, Y. Jeon, H. Hwang and K. J. Kim (2020). "Analysis of antiseizure drug-related adverse reactions from the electronic health record using the common data model." Epilepsia **61**(4): 610-616.

Comfort, N. and D. B. Re (2017). "Sex-Specific Neurotoxic Effects of Organophosphate Pesticides Across the Life Course." Current environmental health reports **4**(4): 392-404.

de Araujo Furtado, M., F. Rossetti, S. Chanda and D. Yourick (2012). "Exposure to nerve agents: from status epilepticus to neuroinflammation, brain damage, neurogenesis and epilepsy." Neurotoxicology **33**(6): 1476-1490.

de Araujo Furtado, M., F. Rossetti, S. Chanda and D. Yourick (2012). "Exposure to nerve agents: From status epilepticus to neuroinflammation, brain damage, neurogenesis and epilepsy." NeuroToxicology **33**(6): 1476-1490.

Deshpande, L. S., R. E. Blair, B. A. Huang, K. F. Phillips and R. J. DeLorenzo (2016). "Pharmacological blockade of the calcium plateau provides neuroprotection following organophosphate paraoxon induced status epilepticus in rats." Neurotoxicology and teratology **56**: 81-86.

Deshpande, L. S., R. E. Blair, K. F. Phillips and R. J. DeLorenzo (2016). "Role of the calcium plateau in neuronal injury and behavioral morbidities following organophosphate intoxication." Annals of the New York Academy of Sciences **1374**(1): 176-183.

Deshpande, L. S., D. S. Carter, R. E. Blair and R. J. DeLorenzo (2010). "Development of a prolonged calcium plateau in hippocampal neurons in rats surviving status epilepticus induced by the organophosphate diisopropylfluorophosphate." Toxicol Sci **116**(2): 623-631.

Dharmani, C. and K. Jaga (2005). "Epidemiology of acute organophosphate poisoning in hospital emergency room patients." Rev Environ Health **20**(3): 215-232.

FDA (2018). "Center For Drug Evalutaion And Research- Midazolam Review." Food and Drug Administration **Application 209566Orig1s000**.

Figueiredo, T. H., J. P. Apland, M. F. M. Braga and A. M. Marini (2018). "Acute and long-term consequences of exposure to organophosphate nerve agents in humans." Epilepsia **59**(S2): 92-99.

Finkelstein, A., G. Kunis, T. Berkutzki, A. Ronen, A. Krivoy, E. Yoles, D. Last, Y. Mardor, K. Van Shura, E. McFarland, B. A. Capacio, C. Eisner, M. Gonzales, D. Gregorowicz, A. Eisenkraft, J. H. McDonough and M. Schwartz (2012). "Immunomodulation by poly-YE reduces organophosphate-induced brain damage." Brain, Behavior, and Immunity **26**(1): 159-169.

Flannery, B. M., D. A. Bruun, D. J. Rowland, C. N. Banks, A. T. Austin, D. L. Kukis, Y. Li, B. D. Ford, D. J. Tancredi, J. L. Silverman, S. R. Cherry and P. J. Lein (2016). "Persistent neuroinflammation and cognitive impairment in a rat model of acute diisopropylfluorophosphate intoxication." J Neuroinflammation **13**(1): 267.

Gage, M., M. Golden, M. Putra, S. Sharma and T. Thippeswamy (2020). "Sex as a biological variable in the rat model of diisopropylfluorophosphate-induced long-term neurotoxicity." Ann N Y Acad Sci **1479**(1): 44-64.

Gonzalez-Alzaga, B., M. Lacasana, C. Aguilar-Garduno, M. Rodriguez-Barranco, F. Ballester, M. Rebagliato and A. F. Hernandez (2014). "A systematic review of neurodevelopmental effects of prenatal and postnatal organophosphate pesticide exposure." Toxicol Lett **230**(2): 104-121.

Guignet, M., K. Dhakal, B. M. Flannery, B. A. Hobson, D. Zolkowska, A. Dhir, D. A. Bruun, S. Li, A. Wahab, D. J. Harvey, J. L. Silverman, M. A. Rogawski and P. J. Lein (2019). "Persistent behavior deficits, neuroinflammation, and oxidative stress in a rat model of acute organophosphate intoxication." Neurobiol Dis.

Guignet, M., K. Dhakal, B. M. Flannery, B. A. Hobson, D. Zolkowska, A. Dhir, D. A. Bruun, S. Li, A. Wahab, D. J. Harvey, J. L. Silverman, M. A. Rogawski and P. J. Lein (2020). "Persistent behavior deficits, neuroinflammation, and oxidative stress in a rat model of acute organophosphate intoxication." Neurobiology of disease **133**: 104431-104431.

Guignet, M. and P. J. Lein (2018). Organophosphates. Advances in Neurotoxicology: Role of Inflammation in Environmental Neurotoxicity. M. Aschner and L. G. Costa. Oxford, UK, Elsevier, Ltd. **3:** 35-79.

Guignet, M. and P. J. Lein (2018). Organophosphates. Advances in Neurotoxicology: Role of Inflammation in Environmental Neurotoxicity. M. Aschner and L. G. Costa. Oxford, UK, Elsevier**:** 35-79.

Haines, D. D. and S. C. Fox (2014). "Acute and Long-Term Impact of Chemical Weapons: Lessons from the Iran-Iraq War." Forensic Sci Rev **26**(2): 97-114.

Haley, N. (2018). Remarks at an Emergency UN Security Council Briefing on Chemical Weapons Use by Russia in the United Kingdom. United States Mission to the United Nations.

Hobson, B. A., D. J. Rowland, S. Supasai, D. J. Harvey, P. J. Lein and J. R. Garbow (2017). "A magnetic resonance imaging study of early brain injury in a rat model of acute DFP intoxication." Neurotoxicology.

Hobson, B. A., S. Siso, D. J. Rowland, D. J. Harvey, D. A. Bruun, J. R. Garbow and P. J. Lein (2017). "From the Cover: MagneticResonance Imaging Reveals Progressive Brain Injury in Rats Acutely Intoxicated With Diisopropylfluorophosphate." Toxicol Sci **157**(2): 342-353.

Hong, S., L. Dissing-Olesen and B. Stevens (2016). "New insights on the role of microglia in synaptic pruning in health and disease." Curr Opin Neurobiol **36**: 128-134.

Hung, Y.-W., D.-I. Yang, P.-Y. Huang, T.-S. Lee, T. B. J. Kuo, C.-H. Yiu, Y.-H. Shih and Y.-Y. Lin (2012). "The duration of sustained convulsive seizures determines the pattern of hippocampal neurogenesis and the development of spontaneous epilepsy in rats." Epilepsy Research **98**(2): 206-215.

Jessberger, S. and J. M. Parent (2015). "Epilepsy and Adult Neurogenesis." Cold Spring Harb Perspect Biol **7**(12).

Jett, D. A. and S. M. Spriggs (2018). "Translational research on chemical nerve agents." Neurobiol Dis.

Kirkland, A. E., G. L. Sarlo and K. F. Holton (2018). "The Role of Magnesium in Neurological Disorders." Nutrients **10**(6): 730.

Kuruba, R., X. Wu and D. S. Reddy (2018). "Benzodiazepine-refractory status epilepticus, neuroinflammation, and interneuron neurodegeneration after acute organophosphate intoxication." Biochimica et Biophysica Acta (BBA) - Molecular Basis of Disease **1864**(9, Part B): 2845-2858.

Lerdkrai, C., N. Asavapanumas, B. Brawek, Y. Kovalchuk, N. Mojtahedi, M. Olmedillas Del Moral and O. Garaschuk (2018). "Intracellular Ca(2+) stores control in vivo neuronal hyperactivity in a mouse model of Alzheimer's disease." Proc Natl Acad Sci U S A **115**(6): E1279-e1288.

Li, Y., P. J. Lein, G. D. Ford, C. Liu, K. C. Stovall, T. E. White, D. A. Bruun, T. Tewolde, A. S. Gates, T. J. Distel, M. C. Surles-Zeigler and B. D. Ford (2015). "Neuregulin-1 inhibits neuroinflammatory responses in a rat model of organophosphate-nerve agent-induced delayed neuronal injury." J Neuroinflammation **12**: 64.

McDonough, J. H., Jr., L. W. Dochterman, C. D. Smith and T. M. Shih (1995). "Protection against nerve agent-induced neuropathology, but not cardiac pathology, is associated with the anticonvulsant action of drug treatment." Neurotoxicology **16**(1): 123-132.

McDonough, J. H., Jr. and T. M. Shih (1997). "Neuropharmacological mechanisms of nerve agent-induced seizure and neuropathology." Neurosci Biobehav Rev **21**(5): 559-579.

Mew, E. J., P. Padmanathan, F. Konradsen, M. Eddleston, S. S. Chang, M. R. Phillips and D. Gunnell (2017). "The global burden of fatal self-poisoning with pesticides 2006-15: Systematic review." J Affect Disord **219**: 93-104.

Muller, M., U. Ahumada-Castro, M. Sanhueza, C. Gonzalez-Billault, F. A. Court and C. Cardenas (2018). "Mitochondria and Calcium Regulation as Basis of Neurodegeneration Associated With Aging." Front Neurosci **12**: 470.

Muñoz-Quezada, M. T., B. A. Lucero, D. B. Barr, K. Steenland, K. Levy, P. B. Ryan, V. Iglesias, S. Alvarado, C. Concha, E. Rojas and C. Vega (2013). "Neurodevelopmental effects in children associated with exposure to organophosphate pesticides: A systematic review." Neurotoxicology **39**: 158-168.

Naughton, S. X. and A. V. Terry (2018). "Neurotoxicity in acute and repeated organophosphate exposure." Toxicology **408**: 101-112.

Okumura, T., N. Takasu, S. Ishimatsu, S. Miyanoki, A. Mitsuhashi, K. Kumada, K. Tanaka and S. Hinohara (1996). "Report on 640 Victims of the Tokyo Subway Sarin Attack." Annals of Emergency Medicine **28**(2): 129-135.

OPCW (2017). "Report on the use of a chemical weapon in the death of a DPRK National. ." Organisation for the Prohibition of Chemical Weapons.

Patel, V., C. Ramasundarahettige, L. Vijayakumar, J. S. Thakur, V. Gajalakshmi, G. Gururaj, W. Suraweera and P. Jha (2012). "Suicide mortality in India: a nationally representative survey." Lancet **379**(9834): 2343-2351.

Peter, J. V., T. I. Sudarsan and J. L. Moran (2014). "Clinical features of organophosphate poisoning: A review of different classification systems and approaches." Indian J Crit Care Med **18**(11): 735-745.

Phelan, K. D., U. T. Shwe, D. K. Williams, L. J. Greenfield and F. Zheng (2015). "Pilocarpine-induced status epilepticus in mice: A comparison of spectral analysis of electroencephalogram and behavioral grading using the Racine scale." Epilepsy Res **117**: 90-96.

Phillips, K. F. and L. S. Deshpande (2018). "Chronic Neurological Morbidities and Elevated Hippocampal Calcium Levels in a DFP-Based Rat Model of Gulf War Illness." Mil Med **183**(suppl_1): 552-555.

Rauh, V. A., F. P. Perera, M. K. Horton, R. M. Whyatt, R. Bansal, X. Hao, J. Liu, D. B. Barr, T. A. Slotkin and B. S. Peterson (2012). "Brain anomalies in children exposed prenatally to a common organophosphate pesticide." Proceedings of the National Academy of Sciences of the United States of America **109**(20): 7871-7876.

Rojas, A., T. Ganesh, W. Wang, J. Wang and R. Dingledine (2020). "A rat model of organophosphate-induced status epilepticus and the beneficial effects of EP2 receptor inhibition." Neurobiol Dis **133**: 104399.

Rossetti, M. F., C. Stoker and J. G. Ramos (2020). "Agrochemicals and neurogenesis." Mol Cell Endocrinol **510**: 110820.

Salter, M. W. and B. Stevens (2017). "Microglia emerge as central players in brain disease." Nat Med **23**(9): 1018-1027.

Scholl, E. A., S. M. Miller-Smith, S. L. Bealer, M. J. Lehmkuhle, J. J. Ekstrand, F. E. Dudek and J. H. McDonough (2018). "Age-dependent behaviors, seizure severity and neuronal damage in response to nerve agents or the organophosphate DFP in immature and adult rats." Neurotoxicology **66**: 10-21.

Silbergleit, R., D. Lowenstein, V. Durkalski and R. Conwit (2013). "Lessons from the RAMPART study--and which is the best route of administration of benzodiazepines in status epilepticus." Epilepsia **54 Suppl 6**: 74-77.

Simen, A. A., K. A. Bordner, M. P. Martin, L. A. Moy and L. C. Barry (2011). "Cognitive dysfunction with aging and the role of inflammation." Therapeutic advances in chronic disease **2**(3): 175-195.

Spampanato, J., W. Pouliot, S. L. Bealer, B. Roach and F. E. Dudek (2019). "Antiseizure and neuroprotective effects of delayed treatment with midazolam in a rodent model of organophosphate exposure." Epilepsia **60**(7): 1387-1398.

UN (2017). Report of the Independent International Commission of Inquiry on the Syrian Arab Republic United Nations General Assembly: Human Rights Council.

Uzun, S., O. Kozumplik, M. Jakovljević and B. Sedić (2010). "Side effects of treatment with benzodiazepines." Psychiatr Danub **22**(1): 90-93.

Valdes Hernandez Mdel, C., L. C. Maconick, E. M. Tan and J. M. Wardlaw (2012). "Identification of mineral deposits in the brain on radiological images: a systematic review." Eur Radiol **22**(11): 2371-2381.

Varodayan, F. P., X.-J. Zhu, X.-N. Cui and B. E. Porter (2009). "Seizures increase cell proliferation in the dentate gyrus by shortening progenitor cell-cycle length." Epilepsia **50**(12): 2638-2647.

Velazco-Cercas, E., L. Beltran-Parrazal, C. Morgado-Valle and M. L. López-Meraz (2020). "Status Epilepticus Increases Cell Proliferation and Neurogenesis in the Developing Rat Cerebellum." Cerebellum **19**(1): 48-57.

Worek, F., T. Wille, M. Koller and H. Thiermann (2016). "Toxicology of organophosphorus compounds in view of an increasing terrorist threat." Archives of Toxicology **90**(9): 2131-2145.

Wu, P., Y. Hu, X. J. Li, M. Cheng and L. Jiang (2019). "Sodium valproate suppresses abnormal neurogenesis induced by convulsive status epilepticus." Neural Regen Res **14**(3): 480-484.

Wu, X., R. Kuruba and D. S. Reddy (2018). "Midazolam-Resistant Seizures and Brain Injury after Acute Intoxication of Diisopropylfluorophosphate, an Organophosphate Pesticide and Surrogate for Nerve Agents." J Pharmacol Exp Ther **367**(2): 302-321.

Yamasue, H., O. Abe, K. Kasai, M. Suga, A. Iwanami, H. Yamada, M. Tochigi, T. Ohtani, M. A. Rogers, T. Sasaki, S. Aoki, T. Kato and N. Kato (2007). "Human brain structural change related to acute single exposure to sarin." Annals of Neurology **61**(1): 37-46.

Yanagisawa, N., H. Morita and T. Nakajima (2006). "Sarin experiences in Japan: Acute toxicity and long-term effects." Journal of the Neurological Sciences **249**(1): 76-85.